INVESTIGATING PHENOLIC-MEDIATED PROTEIN MATRIX DEVELOPMENT FOR POTENTIAL CONTROL OF CEREAL STARCH DIGESTION

by

Leigh Christine R. Schmidt

A Dissertation

Submitted to the Faculty of Purdue University

In Partial Fulfillment of the Requirements for the degree of

Doctor of Philosophy

Department of Food Science

West Lafayette, Indiana

August 2019

THE PURDUE UNIVERSITY GRADUATE SCHOOL
STATEMENT OF COMMITTEE APPROVAL

Dr. Bruce R. Hamaker, Chair
Department of Food Science
Dr. Osvaldo Campanella
Department of Food Science and Technology
The Ohio State University
Dr. Mario Ferruzzi
Department of Food, Bioprocessing and Nutrition
North Carolina State University
Dr. Owen Jones
Department of Food Science

Approved by:

Dr. Arun K. Bhunia
Head of the Graduate Program

To my husband Wes, and to my family.

All my love.

ACKNOWLEDGMENTS

Fellowship support and project funding was provided by a USDA National Needs Fellowship for Foods and Health and the Whistler Center for Carbohydrate Research.

I would like to extend my sincere appreciation to my major professor, Dr. Bruce Hamaker, for his patience, encouragement, mentorship, and insights over the last several years. I appreciate your support and guidance in growing personally and professionally.

I also thank my advisory committee, Dr. Osvaldo Campanella, Dr. Mario Ferruzzi, and Dr. Owen Jones, for their support and knowledge while pursuing my PhD. Thank you also to Dr. Min Li and Zulfiqar Mohamedshah of Dr. Ferruzzi's lab for chromatography and analytical assistance and Dennis Cladis for technical assistance. My thanks as well to the Purdue Food Science Department for the encouragement and support they provide to the students, as your passion to see us thrive makes a difference.

Without an enormous support network, I would not be where I am today. To former lab members and friends, I appreciate you taking the time to welcome me and the support, personal and professional, you provided along the way. I am especially grateful for the friendship and assistance of Dr. Like Y. Hasek, Dr. Byung-hoo Lee, Dr. Elizabeth Pletsch, and Dr. Bin Zhang. To current lab members, thank you also for your encouragement, help, support, and friendship, especially Anna Hayes, Dr. Marwa El Hindawy, Pablo Torres Aguilar, Jongbin Lim, and Dr. Xiaowei Zhang.

Over the years many friends have walked with me on my journey, and I would like to express my deepest gratitude for you, near and far. To Purdue friends who provided welcome distractions, Dennis and Dr. Mary Ann Cladis, Matthew and Beth Treibe, and Dr. Simran Kaur, they were appreciated. To my Davis Ladies, Dr. Claudia Delgado, Dr. Tyann Blessington, Dr. Patchanee "Tik" Yasurin, and Dr. Carol D'Lima, my thanks for the years of friendship and support. My California Framily, especially, Aileen and Nick Harter, the fauxlings, Trent Schmidt and Lauren Jones, and Michael Kinder, I appreciate your care for Wes and I during this time. Misty Price, Lizzy and Kacy Pierce, you always have my love. My cousin Dr. Kitty Campbell, for so many things over the last years, thank you. And to my housemates and family, Stephen and

Deborah Belter, thank you for everything over a lifetime, and for giving me a place to call home the last few years.

Without my family, I am diminished. To my extended family, whom I've had the chance to see more often during this time, my love and appreciation for your support. To all my in-laws, thank you for your support, help, and love of us both. To my sisters and their families, I've treasured this opportunity to be miles closer again, for a while, and spend time with your littles, and watch some of them grow into bigs.

Thank you to my parents, Charles and Leslie Robison, for their unconditional love and encouragement, always. I appreciate your faith in me and how you live your faith in God. I hope I can continue to make you proud. Thank you as well to my parents-in-law, Thomas and Karla Schmidt, for being part of my life and for your love and support. To all my family and friends, thank you for believing in me.

Last of all, I would like to thank my husband Wes. I appreciate your patience as things took longer than expected, your handiness in fixing my house, your humor and gamesmanship, your dedication, and most of all your love. Thank you for being with me every step, no matter how far. I am blessed, and I love you.

In all things, God's will.

TABLE OF CONTENTS

LIST OF TABLES

LIST OF FIGURES

LIST OF ABBREVIATIONS

AE	Apigeninidin Equivalents
APG1	Yellow corn with apigeninidin at sorghum endosperm content
APG2	Yellow corn porridge with twice the apigeninidin as APG1
Cys	Cysteine
DAD	Diode Array Detector
DNS	Dinitrosalicylic Acid
E_a	Activation Energy of complex formation
f_a	Fraction of Tryptophan accessible to quencher
GAE	Gallic Acid Equivalents
K_A	Association Constant
K_D	Dissociation Constant
K_q	Stern-Volmer Quenching Constant
K_{SV}	Stern-Volmer Constant
MGAM	Maltase Glucoamylase
MOPS	3-(N-morpholino)propanesulfonic acid
MS	Mass Spectrometer
n	Number of binding sites
SDS-PAGE	Sodium Dodecyl Sulfate Polyacrylamide Gel Electrophoresis
SI	Sucrase Isomaltase
SPE	Solid Phase Extraction
TE	Trolox Equivalents
TEAC	Trolox Equivalent Antioxidant Capacity
Tg	Glass Transition Temperature
Tm	Melting Temperature
Trolox	6-hydroxy-2,5,7,8-tetramethylchroman-2-carboxylic acid
Trp	Tryptophan
UPLC	Ultra High Pressure Liquid Chromatography
YC	Yellow corn untreated control

ABSTRACT

Author: R. Schmidt, Leigh, C. PhD
Institution: Purdue University
Degree Received: August 2019
Title: Investigating Phenolic-Mediated Protein Matrix Development for Potential Control of Cereal Starch Digestion
Committee Chair: Bruce R. Hamaker

Shifts in the human diet to more refined foods and ingredients have contributed to the rise in metabolic disease rates associated with long-term consumption of foods causing swift rises in blood glucose response. Foods which result in a more moderate blood glucose curve are considered healthier by increasing satiety and reducing oxidative stress. Sorghum products contain naturally slowly digested starch. The matrix of sorghum porridges contains kafirin protein bodies which cross link around gelatinizing starch molecules, while similar nascent matrices in other cereals aggregate and collapse. The 3-deoxyanthocyanidin pigments unique to sorghum may be accountable for the difference in matrix stability. The density of the starch entrapped in the matrices is thought to partially inhibit α-amylase access to the starch, reducing overall starch digestion and thereby mitigating glucose response. The purpose of this work was to increase our understanding of how phenolic compounds in sorghum interact with endosperm proteins to create a stable matrix, and to explore if the knowledge might be translated to other starchy cereal products. In the first study, phenolic extracts from flours (sorghum, corn masa, white rice) were characterized for phenolic content, antioxidant activity, phenolic components, and their ability to interact with a model protein system (ovalbumin) in order to examine protein polymerization. While neither phenolic content nor antioxidant activity were found to predict polymerization, sorghum extracts demonstrated more diverse molecular weight (MW) products than masa or rice. In the second study, specific phenolic compounds in sorghums (*p*-coumaric, sinapic, and gallic acids; (+)-catechin; and apigeninidin, a 3-deoxyanthocyanidin found in sorghums) were interacted in the model protein system at different concentrations to observe extent and type of protein polymerization, and promising compounds subjected to fluorescence quenching spectroscopy to examine the nature of the interactions. Apigeninidin produced a wide range of MW products linked by disulfide bonds, while gallic acid stimulated oxidation-driven polymerization with disulfide and other non-amide peptide linkages. Catechin, gallic acid, and apigeninidin quenching of

ovalbumin native tryptophan fluorescence intensified as concentration (0-50 μM) and temperature (25-95°C) increased. At higher concentrations (25-50 μM), apigeninidin had the greatest effect on protein structure, indicated as a red shift (+6 ±1 nm) in peak emission wavelength due to increased hydrogen bond formation. The number of binding sites per ovalbumin tended to rise with temperature for apigeninidin and catechin, as did the binding affinity, but temperature had less effect on gallic acid binding. With the polymerization and binding data, apigeninidin was determined as a prospective molecule for increasing protein matrix stability in foods without causing excessive oxidation-driven aggregation. The final study explored the effects of apigeninidin addition to a yellow corn flour and naturally present anthocyanin (blue corn) on starch digestion and microstructure of porridges by utilizing an *in vitro* α-amylase assay and confocal microscopy. Notably, apigeninidin was not found to inhibit α-amylase at the levels used and would not have contributed to slower digestion. Porridges with apigeninidin evinced a reduction of initial starch digestion rate through 20 min digestion, and increased protein matrix formation and stability compared to an untreated control. Enhanced matrix remained more stable through 60 min α-amylase digestion. Blue corn protein microstructure was less extensive and less stable than apigeninidin-treated samples but improved compared to the untreated yellow corn. In conclusion, the slow digestion of starch in cooked sorghum products can be attributed to the 3-deoxyanthocyanidin compounds present in the grain participating in sulfhydryl-disulfide interchanges which results in extensive kafirin cross-linking surrounding starch granules. While other phenolic and redox-active components may affect matrix formation and stability, 3-deoxyanthocyanidins appear to have the most direct influence, and their ability to modify food protein matrices appears to have a direct result on starch digestion *in vitro*.

CHAPTER 1. INTRODUCTION

A variety of metabolic disorders, including obesity, type 2 diabetes mellitus (T2DM), and heart diseases, have been linked to changes in ingestive behaviors, particularly general overconsumption, as well as increased carbohydrate and lipid bioavailability (Blaak and others 2012; Roumen and others 2008). Many highly refined ingredients and food products become, in essence, too readily digestible, leading to an abundance of caloric availability from foods. Swift increases of postprandial blood glucose activate oxidative stress and inflammatory signaling pathways, which can progress to metabolic disease states over time (Blaak and others 2012). The "Western" style diet tends to lack fundamental food components, such as dietary fiber (Cordain and others 2005), and alterations of intrinsic food properties can lead to changes in matrices and matrix formation which would otherwise assist to control digestion and absorption rates of macronutrients (Aguilera 2018; Parada and Aguilera 2007).

Sorghum flour porridges, while a staple food in many parts of Africa and Asia, are considered nutritionally poorer (MacLean Jr and others 1981) when compared to corn or rice porridges (consumed mainly in the Americas and Asia, respectively). The starch component of sorghum porridges digests slowly, and protein digestion is also slow and incomplete (Axtell and others 1981). Kafirin (prolamin) protein bodies in the endosperm form dense cross-links surrounding the starch granules during the cooking process, as the starch gelatinizes. Previous work in our laboratory (Bugusu 2004; Cholewinski 2010) suggested that a phenolic component or components specific to sorghum grains was likely responsible for the high degree of disulfide bond development amongst the starch-associated protein bodies of the endosperm. Additionally, the denser protein matrix is thought to contribute to the apparent slow starch digestion of sorghum porridges (Bugusu 2004; Ezeogu and others 2008) by limiting carbohydrase access to portions of the starch. As sorghums are the only cereal grains commonly containing the 3-deoxyanthocyanidin pigments, one or more of these anthocyanin derivatives was hypothesized as the causative agent leading to stable protein matrix formation.

1.1 Purpose and Research Hypothesis

The overarching purpose of this research was to increase our understanding of the contributions of cereal flour phenolic compounds to the development of the protein component of starch-protein matrices in cooked cereal products. In addition, we endeavored to discover how changes to the protein matrix may lead to deviations in the digestion rate of starch. Properties which promote slow starch digestion may influence a number of factors (including gastric emptying rate, glycemic response, and satiety) which may ultimately lead to improved health outcomes.

It was previously hypothesized that, as 3-deoxyanthocyanidin compounds remain fairly molecularly stable at near-neutral pH (5-7), they may participate in oxidation/reduction (redox) reactions through sulfhydryl-disulfide interchanges to form highly cross-linked protein matrices around starch granules in the endosperm, which occur naturally in cooked sorghum. Indeed, changing the redox state during cooking of sorghum porridge alters the digestion rate of starch (Bugusu 2004; Choi and others 2008).

Thus, we hypothesized that phenolic-protein interactions might be modeled for protein-phenolic binding leading to polymerization, and further, that addition of phenolic compounds which aid construction of more durable, non-aggregative protein matrices may be utilized to yield designed food products with slower glucose release from starch.

1.2 Specific Objectives

In the first study, the objective was to examine interactions between a model protein and endosperm phenolic extracts (containing a mixture of natively occurring phenolic components) to better characterize the aspects which may lead to formation of stable protein matrices. The second study aimed to better understand how specific phenolic compounds interact with the model protein system and how the compounds may individually affect protein matrix formation. The objective of the final study was to assess addition of a 3-deoxyanthocyanidin to a corn flour porridge by evaluating changes in starch digestion and protein matrix formation.

1.3 Significance of the Work

The food matrix is often mentioned in food science as an important component of foods and their quality through processing, storage, and digestion. Various aspects of food matrices have been studied and reviewed (Singh and others 2010; Aguilera 2018), yet the influence of food matrices on the physiological impacts of macronutrient release are not well defined. Deepening our understanding of matrix formation increases the potential to manipulate construction of matrices to slow starch digestion. This work adds to the science of matrix formation by contributing knowledge of how a food protein interacts with individual phenolic compounds, affecting their potential to construct stable, non-aggregating protein matrices.

Modifying macronutrient release and thus location of absorption in the small intestine has the potential to alter physiological outcomes. The research presented here demonstrates the capability to slow the digestion of starch with improved matrix stability. The increase in stability may create digestive hindrances, slowing the effective rates of digestion and absorption, allowing for extended energy release from the food matrix, and also improving the possibility of triggering physiological feedback mechanisms such as the ileal brake.

1.4 Thesis Organization

Chapter 1 is an introduction to the work performed and presented herein, including an overview of the most relevant background information and explanation of the research.

Chapter 2 functions as a literature review and also introduces the food matrix and proposes the concept of its manipulation specifically to alter the digestive properties of a food in order to alter biological response outcomes. An introduction of the experimental work presented in further chapters is also provided.

Chapter 3 is an experimental chapter characterizing the phenolic extracts of cereal endosperm flours and their potential to polymerize a model protein system.

Chapter 4 is a second experimental chapter studying the interactions of individual low molecular weight phenolic compounds found widely in sorghum varieties with a model protein. The effects across a several log concentration differential on protein polymerization were clarified. Phenolics which demonstrated significant polymerization differences were further examined

utilizing native tryptophan fluorescence quenching to better understand the nature of interactions between the selected phenolics and the model protein.

Chapter 5 is a final experimental chapter focusing on the outcomes of *in vitro* starch digestion and protein matrix formation in a corn flour system from the presence of anthocyanins (blue corn flour or 3-deoxyanthocyanidin added to a yellow corn). Protein matrix was observed using confocal microscopy.

Finally, Chapter 6 presents a summation of the findings and conclusions from the thesis, as well as observations regarding future work to further advance the research.

References

Aguilera JM. 2018. The food matrix: implications in processing, nutrition and health. Critical Reviews in Food Science and Nutrition:1-18.

Axtell JD, Kirleis AW, Hassen MM, Mason NDC. 1981. Digestibility of sorghum proteins. Proceedings of the National Academy of Sciences of the United States of America 78(3):1333-5.

Blaak EE, Antoine JM, Benton D, Björck I, Bozzetto L, Brouns F, Diamant M, Dye L, Hulshof T, Holst JJ, Lamport DJ, Laville M, Lawton CL, Meheust A, Nilson A, Normand S, Rivellese AA, Theis S, Torekov SS, Vinoy S. 2012. Impact of postprandial glycaemia on health and prevention of disease. Obesity Reviews 13(10):923-84.

Bugusu BA. 2004. Understanding the basis of the slow starch digestion characteristic of sorghum porridges and how to manipulate starch digestion rate [Doctoral Dissertation]. West Lafayette, IN, USA: Purdue University.

Choi S, Woo H, Ko S, Moon T. 2008. Confocal Laser Scanning Microscopy to Investigate the Effect of Cooking and Sodium Bisulfite on In Vitro Digestibility of Waxy Sorghum Flour. Cereal Chemistry 85(1):65-9.

Cholewinski JL. 2010. Sorghum endosperm components responsible for promoting protein polymerization through sulfhydryl-disulfide interchange. [M.S.]: Purdue University. 137 p. Available from: 1490634.

Cordain L, Eaton SB, Sebastian A, Mann N, Lindeberg S, Watkins BA, O'Keefe JH, Brand-Miller J. 2005. Origins and evolution of the Western diet: Health implications for the 21st century. The American Journal of Clinical Nutrition 81(2):341-54.

Ezeogu LI, Duodu KG, Emmambux MN, Taylor JRN. 2008. Influence of Cooking Conditions on the Protein Matrix of Sorghum and Maize Endosperm Flours. Cereal Chemistry 85(3):397-402.

MacLean Jr WC, Lopez De Romana G, Placko RP, Graham GG. 1981. Protein quality and digestibility of sorghum in preschool children: Balance studies and plasma free amino acids. Journal of Nutrition 111(11):1928-36.

Parada J, Aguilera JM. 2007. Food Microstructure Affects the Bioavailability of Several Nutrients. Journal of Food Science 72(2):R21-R32.

Roumen C, Corpeleijn E, Feskens EJM, Mensink M, Saris WHM, Blaak EE. 2008. Impact of 3-year lifestyle intervention on postprandial glucose metabolism: the SLIM study. Diabetic Medicine 25(5):597-605.

Singh J, Dartois A, Kaur L. 2010. Starch digestibility in food matrix: a review. Trends in Food Science & Technology 21(4):168-80.

CHAPTER 2. LITERATURE REVIEW & CONCEPT INTRODUCTION: MANIPULATION OF THE FOOD MATRIX TO CONTROL STARCH DIGESTION RATE & POTENTIALLY AFFECT HEALTH OUTCOMES

2.1 Cereal Grains and Carbohydrate Digestion

Cereal grains (monocot grass species) are the foremost source of carbohydrate intake globally, with approximately 50% of total calories estimated to originate from cereals. The 8 major cereals worldwide are corn (maize), wheat, rice, oat, sorghum, rye, barley, and millet. Basic cereal grain structure is comprised by the endosperm, containing mainly starch; the germ, including the grain embryo; the aleurone or outermost layer of the endosperm; and the seedcoat and other pericarp layers, consisting predominantly of fiber. Cereals may be consumed in a variety of forms, including dehulled whole seeds, grits, flour, debranned or decorticated, degermed, or some combination thereof. In the presence of water and high heat, endosperm starches gelatinize, melting starch structures and facilitating digestion by carbohydrases.

A variety of factors determine the digestibility of starch, including the degree of gelatinization and retrogradation, presence and activity of carbohydrases (mainly salivary and pancreatic α-amylases and the brush border α-glucosidases maltase-glucoamylase [MGAM] and sucrase-isomaltase [SI]), presence and concentration of carbohydrase inhibitors including some phenolic compounds (Flores, Singh, Kerr, Pegg, & Kong, 2013; Lee et al., 2012), the fine structure of the starch, and matrices which impede enzymatic access and thus starch bioaccessibility (Singh, Dartois, & Kaur, 2010). Some of the cereal grains have a slowly digestible carbohydrate characteristic, even when processed to remove much of the bran (containing the highest concentration of fiber) which may contain phenolic and anti-nutritive factors slowing the digestion and absorption of starch. Sorghums are generally considered to have slow or incompletely digested macronutrients (Axtell, Kirleis, Hassen, & Mason, 1981), whether in the form of whole grain or decorticated flour products, with both the starch and protein fractions having reduced digestibility (Hamaker, Kirleis, Mertz, & Axtell, 1986).

2.2 Sorghum

Sorghum is the fifth most produced cereal grain in the world, and is especially important to subtropical and sub-arid zones due to its ability to grow and yield in hotter and drier regions (Hariprasanna & Rakshit, 2016), and it is commonly consumed in these areas as a thick porridge made from decorticated flour. Decortication is the process of abrasively removing much of the bran portion from the grain, and it also tends to remove aleurone, a portion of floury endosperm, and some anti-nutritional factors.

As with other cereals, the principle parts of the sorghum grain are the pericarp, aleurone, endosperm, and germ. The endosperm is made up of floury and vitreous regions with different microstructures, with cells of both chiefly containing starch granules, protein bodies, cellular matrix components, and cell wall material. Floury endosperm contains loosely packed cells with discontinuity between the components, allowing for air gaps within cells. Vitreous endosperm cells are tightly packed and consist of a continuous matrix of starch granules, tightly bound kafirin protein bodies, and desiccated cytoplasmic proteins.

Normal sorghum starch contains approximately 24-33% amylose (Beta, Obilana, & Corke, 2001). When isolated, cooked sorghum starches digest similarly to other cereal starches (Zhang & Hamaker, 1998). However, when consumed as an integral part of a sorghum flour product, the rate of starch glycolysis was reduced, with starch digestion of cooked whole flours generally less than decorticated flours (Bugusu, 2004).

2.3 Cereal Storage Proteins

Cereals are important nutrient sources of protein in the human diet, even though proteins only make up approximately 10-12% of the dry weight of the seed (Shewry & Halford, 2002). In the endosperm, prolamin and glutelin proteins predominate, as storage proteins to provide nutrients for the seedling upon germination. Prolamins are the main storage proteins of sorghum and corn, while for rice it is the glutelins. The amino acid composition of prolamins is high amounts of glutamine and hydrophobic amino acids, but low in essential amino acids.

Kafirins, the prolamin storage proteins of sorghum, are more readily digested in their raw, native state than after cooking (with the exception of some highly digestible mutants), and pre-

digestion with pepsin before cooking sorghum flours increases starch digestion, as does addition of reducing compounds to the cooking water (Choi, Woo, Ko, & Moon, 2008). Kafirin proteins are stored in the endosperm as tightly bound starch-associated protein bodies. The principle α-kafirin and β-kafirin make up the core, surrounded on the exterior by γ-kafirins, which are high in cysteine. The cysteine residues of γ-kafirins are highly susceptible to forming disulfide bridges during cooking (Xu, 2008) above the glass transition (Tg) and melting temperatures (Tm) of the proteins, forming intermolecular cross-links and resulting in expanded web-like structures of protein around the gelatinized starch granules (Bugusu, 2004).

Zeins, the prolamin storage proteins of corn, though similar in amino acid composition, sequence homology, sub-classes, and structure to kafirins (Altschul et al., 2005; DeRose, Ma, Kwon, Hasnain, Klassy, & Hall, 1989), do not tend to form the stable starch-associated matrix found in sorghums. The lower Tm of zeins compared to sorghums may provide a portion of the disparity in behavior.

The thiol groups on the amino acid cysteine have the potential to form intra- and inter-molecular disulfide bonds which can stabilize protein secondary and tertiary structures and polymerize disparate protein molecules, and can also lead to aggregate development. Above the Tm, sulfhydryl residues of cysteines which may be located in the hydrophobic pocket can become available for disulfide bond formation. The sulfhydryl-disulfide interchange reaction involves the formation of disulfide bonds from free thiol groups and the disruption of disulfide bonds to re-form free thiols. The interchange is responsible for the kafirin matrices of sorghums growing with gelatinizing starch granules (Cholewinski, 2010) rather than remaining fixed after their initial formation.

The densely cross-linked, stable kafirin matrix resists pepsin digestion (Oria, Hamaker, & Shull, 1995) and may have a role in the slow digestion of starch in sorghum products (Hamaker & Bugusu, 2003). Similar matrices in other cereals (corn, rice) collapse and aggregate during the cooking process (Bugusu, 2004), indicating a factor or factors unique to sorghums are responsible for the formation of the matrix rather than resulting in aggregation.

2.4 3-Deoxyanthocyanidins

The color pigmentation of sorghums is mainly due to the presence of 3-deoxyanthocyanidin compounds, anthocyanin derivatives found in all sorghum varieties but that are rare in other foods. As naturally-occurring phytoalexins, they are synthesized in response to UV light and fungal exposure. Apigeninidin (a pelargonidin derivative) and luteolinidin (a cyanidin derivative) are the major 3-deoxyanthocyanidins present in sorghums. The absence of the highly reactive hydroxyl group at the C-3 position enhances the stability of the molecules to oxidation and changes in pH (Awika, Rooney, & Waniska, 2004; Mazza & Brouillard, 1987), and also shifts the absorbance in the visible spectrum to yellow/orange from red/blue. As the flavylium cation is neutralized with increasing pH, pigmentations alter towards red as the molecular form shifts to neutral quinoidal bases.

Although the aglycone forms are the most abundant, derivatives of apigeninidin and luteolinidin have also been identified in sorghums. Both C-7 and C-5 substitutions occur, with C-7 substitutions more common, mainly as O-methylation and O-glucosidation (Wu & Prior, 2005). The 3-deoxyanthocyanidin compounds can be found throughout the sorghum plant (including stalks, leaves, and grains) and are present in other plant species, including some used in food products (e.g., some varieties of red, blue, purple, and black grains; black teas), though in lesser amounts than sorghums (Awika, 2011).

Anthocyanin compounds have been found to inhibit carbohydrases and appear to be more efficient inhibitors of the brush border α-glucosidases than the α-amylases (Flores, Singh, Kerr, Pegg, & Kong, 2013). Total phenolic concentrations may reach high μM to low mM concentrations in the intestinal lumen (Scalbert & Williamson, 2000), but the levels of individual components would be far lower.

2.5 Oxidation of Phenolic Compounds

Hydroxyl groups on phenolic compounds allow hydrogen bond formation to occur, allowing interactions between molecules, including proteins and other phenolic compounds. Multiple hydroxyls may provide multiple sites for interaction, with the number and positions of hydroxyl groups and substitutions on the ring structure determining the susceptibility of a hydroxyl

for oxidation (Afanas'ev, Dcrozhko, Brodskii, Kostyuk, & Potapovitch, 1989). During oxidative degradation, hydroxyl groups of phenolic antioxidants donate an electron to a free radical. The aromatic ring structure of phenolics produces a resonance effect, allowing phenolic radicals to partially stabilize. Radicals can be terminated with an antioxidant to re-form the phenolic compound; with another radical to form a neutral phenolic adduction; or it may oxidize further by loss of another electron to form a hydroxybenzene and/or quinone at the radicalized position. When two phenolic radicals neutralize, the result is a neutral diphenol (Nguyen, Kryachko, & Vanquickenborne, 2003). In the presence of proteins, phenolic radicals may form cross-links at susceptible amino acid residues, causing the proteins to polymerize (Haslam, 1974).

2.6 Cereal Starch

Cereal starches are comprised of amylose and amylopectin, with branching frequency (occurrence of α-1,6 glucosidic bonds), fine structure, and amylose/amylopectin ratio differing by botanical species as well as specific variety (Srichuwong, Curti, Austin, King, Lamothe, & Gloria-Hernandez, 2017). Waxy varieties, for example, may contain nearly 100% amylopectin and negligible amylose. Salivary and pancreatic α-amylases are often considered the major starch digesting enzymes in humans, with the main products as maltose, malto-oligosaccharides, and α-limit dextrins. Maltose and malto-oligosaccharides readily reduce to glucose when digested by the brush-border α-glucosidases MGAM and SI, but the α-limit dextrins digest more slowly due to the α-1,6 branching points which restrict production of short malto-oligosaccharides from α-amylase.

Native starch is densely packed into granules, with amylopectin packaged into blocklets that are arranged into semi-crystalline concentric ring structures. In the presence of α-amylase, glucose oligomers are released slowly, as double-helical strands and crystalline regions preclude easy conformation to the active site for hydrolysis. Some native starches are therefore sources of slowly digestible carbohydrate. Before and during gelatinization, water is absorbed by the granules, causing swelling and plasticizing of the starch strands and finally melting of double-helical structures. As gelatinized starch pastes and gels cool, retrogradation, or partial reassociation of linear portions of the strands, transpires which also reduces digestion of the starch. Starch retrogradation is not thought to contribute significantly to the reduced starch digestion rate of

sorghum porridge products as amylopectin retrogradation occurs slowly (Wang, Li, Copeland, Niu, & Wang, 2015).

2.7 Starch Digestion and Health

Starch makes up the largest proportion of caloric carbohydrates in the diet. The digestion of starch and release of glucose are dependent on several physicochemical properties, including particle size (Mahasukhonthachat, Sopade, & Gidley, 2010), granular and fine molecular structure (Singh, Dartois, & Kaur, 2010), physical form and the food matrix, modification of the starch (Han & BeMiller, 2007), and the presence of inhibitory compounds.

Rapidly digestible starch, classified by the Englyst method (Englyst, Kingman, & Cummings, 1992) as starch digested within 20 min and absorption in the proximal small intestine, has been associated with swift peaks in postprandial blood glucose concentration, which activates a variety of oxidative biochemical pathways (Rolo & Palmeira, 2006), contributing to metabolic disease onsets over time. Slowly digestible starch, releasing glucose between 20-120 min, has been associated with reduced glucose and insulin responses curves and extending the glucose response (Péronnet, Meynier, Sauvinet, Normand, Bourdon, Mignault, et al., 2015; Vinoy, Normand, Meynier, Sothier, Louche-Pelissier, Peyrat, et al., 2013).

Slowing glucose release into the ileum triggers the ileal brake (van Avesaat, Troost, Ripken, Hendriks, & Masclee, 2014), a feedback mechanism wherein enteroendocrine L-cells release hormones such as GLP-1 and PYY, which control gastric emptying rate and release of food particles to the small intestine for final digestion and absorption. Consumption of slowly digestible starch has been shown to prolong gastric emptying in humans (Cisse, Pletsch, Erickson, Chegeni, Hayes, & Hamaker, 2017).

Predicting the *in vivo* digestion and glucose response of starchy food products from *in vitro* data remains difficult, and speculating on further biochemical mechanisms and health effects based on *in vitro* information is even more imprecise. While these classifications of starch based on relative *in vitro* digestibility rate are useful, only data based on *in vivo* studies can depict physiological impact.

2.8 Concept: Manipulation of the Food Matrix to Control Starch Digestion Rate & Potentially Affect Health Outcomes

2.8.1 Introduction & Background

Human diets long ago evolved from a mainly hunter-gatherer lifestyle high in complex fibers to a high carbohydrate and animal protein based one due to the establishment of farms cultivating foodstuffs and husbanding animals. Since the Industrial Revolution, higher fat foods and faster food processing methods (e.g., frying, extrusion), as well as the introduction of prepared foods and readily available refined ingredients, have further shifted food intake. The "Western" diet developed from these changes to also encompass reduced nutritional quality from increased high glycemic carbohydrate intake, lack of fiber, purported negative changes in fatty acid composition and increased fat content, and micronutrient loss (mitigated in some products by enrichment or fortification) (Cordain, Eaton, Sebastian, Mann, Lindeberg, Watkins, et al., 2005). Even more recent alterations to modern diets incorporate aspects of convenience and variations in eating habits, such as differences in meal number or eating events and portion sizes.

Taken together, these changes to human ingestive behaviors are thought to contribute to growing rates of chronic metabolic diseases (Popkin, 2006). Regarding dietary carbohydrates, instances of obesity, cardiovascular diseases, and Type 2 diabetes mellitus are associated with long-term consumption of foods which generate a swift rise in post-prandial blood glucose response and trigger oxidative stress and inflammatory signaling pathways (Blaak, Antoine, Benton, Björck, Bozzetto, Brouns, et al., 2012; Ceriello, 2005). In the United States, more than 1 in 3 adults (36.5%) is considered obese (Ogden, Carroll, Fryar, & Flegal, 2015). A significant portion of the population (11.5%) have been diagnosed with a variety of heart diseases (Blackwell & Villarroel, 2018) and approximately 8.5% with Type 2 diabetes mellitus,[(A)] with an additional estimated 33.9% having prediabetes (Centers for Disease Control and Prevention, 2017). The factors implicated in disease onset are complex and varied (including sex, age, genetics, lifestyle and dietary habits (Grau, Tetens, Bjørnsbo, & Heitman, 2011; Roumen, Corpeleijn, Feskens, Mensink, Saris, & Blaak, 2008), and although pharmaceutical interventions can mitigate disease progress, they are considered more effective in combination with dietary and/or lifestyle changes[(B)] (American Diabetes Association, 2015; Nigro, Luon, & Baker, 2013). While the contribution of

diet to disease onset and progression is inconstant (being both individual and inadequately understood), it cannot be ignored.

(A) Based on the estimate that, of the 9.4% of the US population diagnosed with diabetes, 5-10% are T1 diabetic

(B) In some cases, bariatric surgery may be recommended, which swiftly and severely alters the body's digestive and absorptive capabilities to improve health outcomes.

For consumers, cost, flavor, and convenience still occupy major roles in modern purchasing intents, but consumer behavior can be influenced by other factors including company ethics and health effects of the product. While for some, "healthy" foods may be perceived as more tasty, (Jo & Lusk, 2018) other consumers may consider them as less flavorful (Raghunathan, Naylor, & Hoyer, 2006). "Better for you," "clean label," and "natural" food products, fresh and minimally processed or prepared foods, and whole grain foods have gained popularity in recent years (Aschemann-Witzel, Varela, & Peschel, 2019; Mattucci, 2018; Román, Sánchez-Siles, & Siegrist, 2017). Additionally, the "value" of a calorie, in the simple concept of "calories in, calories out", is being reconsidered by consumers due to recognition that the way calories are delivered to the body and a variety of other individual food properties affect health, though consumer interpretations of food label claims may also stretch beyond the intended statements (Labiner-Wolfe, Jordan Lin, & Verrill, 2010), replacing healthier eating objectives for less beneficial actions.

Delving further, a variety of physiological feedback mechanisms contribute to food intake and ingestive behaviors, ultimately influencing health outcomes. Many of these mechanisms—including gastric emptying rate, ileal and colonic brakes, and other hormonal gut-brain axis responses—are affected by both nutrient type and location of absorption in the intestines (Dockray, 2013; Sclafani & Ackroff, 2012). Chyme viscosity and molecular mobility affect nutrient absorption rate, which can be affected by the presence of gelling and thickening hydrocolloids and fibers, such as β-glucans found in oats and psyllium (McRorie & McKeown, 2017). As well, the presence of factors governing nutrient release from food particles–including the particle size and diffusion rates, activity of enzymes, presence of inhibitors, and the structure of the food matrix–contribute to digestion and nutrient release rates, ultimately affecting rate and location of absorption (Aguilera, 2018; Parada & Aguilera, 2007).

While the food science community speaks frequently on the influence of food matrix, specific effectual contributions to nutrient release and absorption (rates of permeability, particle degradation, steric effects) are poorly understood due to the diverse nature of foodstuffs and limitations of available models (Guerra, Etienne-Mesmin, Livrelli, Denis, Blanquet-Diot, & Alric, 2012). There is a need for more investigation into the formation and breakdown of various food matrices and the resulting bio-accessibility and -availability of macro- and micronutrients. Additionally, little information is available on the intentional modification of these matrices to control bioavailability of specific nutrients. The development, during processing, of defined matrices with unique digestion properties has the potential to transform designed foods to directly impact human health. Moreover, such knowledge may be useful in the development of targeted gastrointestinal delivery of pharmaceutical agents. In this manuscript, the concept of manipulating the formation of food matrices—particularly of grain-based products—with the aim of controlling glycemic carbohydrate digestion will be expounded.

2.8.2 Defining "Food Matrix"

Modifying the definition of "food matrix" as stated in the USDA National Agricultural Library Glossary (2015) (retrieved April 2019 from http://lod.nal.usda.gov/nalt/17238) to incorporate aspects of digestion provides a fairly comprehensive definition as: The influence of physical structure and molecular relationships between both nutrient and non-nutrient components of foods on the bioaccessibility and release (digestion), absorption, and utilization of nutrients.

2.8.3 The Importance of Food Matrices

In their native forms, plant and animal products have naturally occurring matrices to maintain the shape and integrity of organelles, cells, and macrostructure or physical form. Structural elements can entirely sequester, partially segregate, or impede access to nutritional components of ingested foods due to the presence of intact cell walls or organelles, components undigestible by upper GI enzymes (including dietary fiber) or which hinder enzyme access, or presence of other molecules causing resistance to digestion, such as chelating agents, phytic acids, or enzyme inhibitors (Kato, Saito, Kashimura, Shinohara, Kurahashi, & Taniguchi, 2002).

Processing may weaken or break native matrices as structures swell, diminish, stretch, or shear apart, altering the access to cellular contents (Altan, McCarthy, Tikekar, McCarthy, & Nitin, 2011; Faltermaier, Zarnkow, Becker, Gastl, & Arendt, 2015; Zarnkow, Mauch, Back, Arendt, & Kreisz, 2007). Changes in molecular formations may also occur with processing which can increase (or decrease) the availability and digestibility of macro- and micronutrients.

A classic example within carbohydrates for processing causing changes to matrices and increasing digestibility is observed with starch. In the presence of α-amylase, native starch granules slowly release glucose oligomers (low turnover number, k_{cat}) (Sarikaya, Higasa, Adachi, & Mikami, 2000) due to the molecular structure of double-helices and semi-crystalline regions limiting the correct stereochemical presentation of the substrate (α-1,4 linked glucose polymers) to the enzyme. Upon gelatinization, compact granular structures expand as water is absorbed, double-helices and crystalline regions melt, and amylose leaches from the granule, all of which permit greater steric access to the polysaccharide strands in an environment more conducive to molecular mobility—increasing the probability of conformational arrangements favoring enzyme-substrate interactions.

Matrices can also be created during processing, and may lead to slower nutrient release as multiple barriers decrease bioaccessibility and thus bioavailability (Rein, Renouf, Cruz-Hernandez, Actis-Goretta, Thakkar, & da Silva Pinto, 2013). Examples of formation within grain-based foods include the development of viscoelastic gluten networks of cross-linking gliadin (a prolamin) and glutenin (a glutelin) proteins in wheat-based doughs and batters, also enmeshing starch granules. Corn starch pastes and gels develop matrices (Han & Hamaker, 2000) as the amylose and amylopectin polymers, granules, and remnants interact and additionally bind water within the structures. Less known are sorghum flour porridges which form highly cross-linked semi-rigid prolamin complexes during cooking as kafirins (prolamins) in protein bodies form disulfide linkages with adjoining protein bodies around gelatinizing starch granules (Bugusu, 2004). Transglutaminase enzymes have been utilized in a variety of food systems to increase protein cross-linking, including research into modifying gluten-free bread batters (Renzetti, Dal Bello, & Arendt, 2008). By modifying the protein network structure (forming ϵ-(γ-glutamyl)lysine isopeptide bonds), the bread microstructure, baking, and texture properties change. While a variety of matrices are found in food systems, the concept of manipulating matrix construction in order to produce a defined physiological response upon consumption of a food product is fairly new.

The physical processes of digestion (chewing and stomach grinding, incorporation of saliva and gastric juices) are meant to break down native and formed matrices to provide access for digestive enzymes (α-amylase, pepsin and other proteases, lipases, and small intestine brush-border enzymes) to release nutrients for absorption. Both the macrostructure and microstructure of foods contribute to physical and rheological behaviors. However, because macrostructure is purposefully damaged by physical digestion, it is the microstructural elements that dictate transport phenomena and enzymatic access to nutrients (Parada & Aguilera, 2007). Therefore, changes to the microstructure have the potential to alter said access and may shift physiological responses due to the modified system presented for digestion (Rein, Renouf, Cruz-Hernandez, Actis-Goretta, Thakkar, & da Silva Pinto, 2013). The starch granule-associated protein matrix in cereal products becomes an ideal subject for modification with the purpose of slowing glucose release in order to produce a protracted blood glucose response and attempt to induce ileal brake feedback mechanisms, as L-cells release satiety-inducing hormones (such as GLP-1) in the ileum triggered by the presence of nutrients (Maljaars, Peters, Mela, & Masclee, 2008).

2.8.4 Matrices in Cereal Products

Mature cereal grains mainly consist of endosperm composed of starch granules and surrounding protein bodies in a continuous matrix found in maize, sorghum, the millets, and perhaps rice; and a continuous matrix only in wheat, rye, barley, and oats (Shewry & Halford, 2002), which is largely maintained after milling to flours, though much reduced in size. In maize, sorghum, and the millets, prolamins are the storage proteins contained in protein bodies; and, in wheat and similar cereals, prolamins and glutelins are dispersed in the continuous protein matrix. (Zein, gliadin, hordein, kafirin, and secalin are the prolamins for corn, wheat, barley, sorghum, and rye, respectively.) The glass transition (Tg) and melting temperatures (Tm) of prolamins vary by grain and are also influenced by the presence and type of plasticizers. In more concentrated systems (e.g., extrusion), Tg may have greater impact, while in high water systems (e.g., porridge) Tm would be considered. Proteins with lower Tg or Tm can expose interior side chains at lower temperatures during heat processing, which increases the potential for interactions compared to proteins with higher Tg or Tm. Cereal starches,[(C)] though differing in fine structure, granule size,

and amylose/amylopectin ratios, tend to have a fairly narrow overall range of gelatinization peak temperatures.

(C) Starch gelatinization temperatures are mainly dependent on: botanical source, which determines fine structure, granule size, and amylose/amylopectin ratios (Srichuwong et al., 2017); water content; and the presence of other compounds (e.g., salts) which can shift gelatinization temperatures of cereal flours (Ubwa, Abah, Asemave, & Shambe, 2012).

One of the most studied food matrices is that of wheat bread. The matrix of wheat-based bread dough and bread mainly consists of a protein (gluten) network embedded with starch granules. Flour is hydrated with water, which plasticizes gliadin and glutenin and reduces their Tg to below room temperature (Cocero & Kokini, 1991; de Graaf, Madeka, Cocero, & Kokini, 1993), allowing freer molecular movement and interactions leading to hydrogen bond associations and disulfide cross-linking and gluten formation. Commercial wheat bread processing utilizes several methods to manipulate gluten formation, including flour protein content, hydration percentage, and mixing conditions, as well as the addition of dough conditioners(D) in order to reduce processing time and control product consistency and sensory properties (Wieser, 2003). While formation of the dough matrix is specifically directed by utilizing these methods, it is mainly to produce a bread loaf in minimal time and with particular characteristics of texture.

(D) Oxidizers increase disulfide bonding between free cysteines in the proteins, forming a stronger gluten network, increasing gas retention and reducing processing times. Reducing agents break disulfide bonds, increasing dough extensibility and weakening the dough, while emulsifiers (with effects dependent on chemical nature) may slow starch retrogradation and staling, increase loaf volume, or improve dough tolerance (Wieser, 2003).

In pasta making, similar to bread dough, a starch-enmeshed gluten protein network is formed. However, pastas are considered medium glycemic index(E) (GI) food products (white spaghetti 49 ±2; whole meal spaghetti 48 ±5), while wheat breads are high GI foods (white wheat bread 75 ±2; whole meal bread 74 ±2) (Atkinson, Foster-Powell, & Brand-Miller, 2008). Of major difference in pasta noodles when compared to bread, the protein network is exceedingly dense, providing a physically inhibiting barrier to starch access by digestive enzymes and limiting growth of starch granules, even with complete gelatinization. Enzymatic removal of the gluten proteins

has been shown to increase the rate of initial starch hydrolysis (Colonna, Barry, Cloarec, Bornet, Gouilloud, & Galmiche, 1990). Entrapment of the starch granules within the gluten network can also limit water uptake, granule swelling, and gelatinization in dense internal portions of the pasta strands (Zou, Sissons, Gidley, Gilbert, & Warren, 2015). The matrix of pasta is not designed specifically to slow the digestion of starch, but it serves as an example of an industrially produced food product where differences in food matrices consisting of the same principle materials directly affect glucose release.

(E) While there is controversy regarding the usefulness of the glycemic index on an individual physiological basis, GI can act as a reference tool for relative apparent starch digestibility.

A variety of "low carb" wheat bread and cereal products are commercially produced, but their dough matrices are not developed with the intent of altering digestive properties of the bread or pasta. Many of these utilize added fiber and wheat gluten in their formulations, which correspondingly reduces the amount of flour (and thus, starch) consumed per serving. However, by further examining and exploiting the known effects of various ingredients and processes on the formation of dough matrices, it may be possible to increase the slowly digestible starch portion of wheat breads and pastas, while still manufacturing a sensorily acceptable product. Increasing the amount of slowly digestible starch or reducing the rate of glucose release for absorption may have potential health benefits (Blaak, et al., 2012; Péronnet, et al., 2015; Vinoy, et al., 2013).

2.8.5 Release of Macronutrients from the Matrix

Particle size of digesta has been shown previously to affect rates of digestion and absorption in both human and animal studies (Edwards, Vasilopoulou, Grundy, Butterworth, Berry, Grassby, et al., 2015; Owsley, Knabe, & Tanksley, 1981). Gastric sieving, where smaller particles exit the stomach through the pyloric valve and effect a larger average size of remaining particles, and gastric emptying rate control the dimensions of chyme entering the small intestine for further digestive degradation and nutrient absorption. This indicates that a significant portion of nutrient release for absorption occurs from particles of increasing initial size distribution over time. Larger particles will consequently encompass a greater mass which may act as a barrier to digestion, temporarily slowing total nutrient release as outer material is digested first, dependent

upon penetration / diffusion rates and removal of nutrients via digestion, to permit access to particulate core materials by digestive enzymes.

Starches contain a single monomer (glucose) and two bond types (α-1,4 and α-1,6), with primary digestion occurring by α-amylase acting in the oral cavity and bolus on the α-1,4 bonds until gastric juices penetrate sufficiently to inhibit amylolytic activity via pH inactivation. However, starch partially protects α-amylase from pH inactivation, which may allow salivary amylase to continue cleavage of malto-oligosaccharides for longer periods (Rosenblum, Irwin, & Alpers, 1988). The majority of starch digestion occurs in the small intestine, with primary digestion by pancreatic α-amylase and final digestion by the brush border α-glucosidases SI and MGAM. (Any starch remnants which enter the colon are considered resistant starch and are classified as dietary fiber.) Triacylglycerides in fats and oils contain a variety of fatty acids with assorted chain lengths and degrees of unsaturation, however, all have two bond types for primary digestion by lipases in the small intestine, the glycerol bonds at n-1/3 and 2. Proteins are the most complex macronutrient to digest due to the diversity in monomers forming the peptide bonds, altering the specific chemical ecosystem and spatial access for enzymatic associations.

The amino acid chains of proteins determine both the physicochemical nature of the bonds and the structural conformation presented for digestion. There are several proteases and peptidases in the human digestive tract (including pepsin, trypsin, chymotrypsin, elastases, and carboxypeptidases) which hydrolyze proteins to peptides to amino acids for absorption. Exotic peptide linkages (e.g., tyrosine-tyrosine crosslinks, transglutaminase catalyzed lysine-glutamine isopeptide bonds) and disulfide bonds introduce further complexity to protein digestion (Erbersdobler, 1989). A high degree of cross-linking introduces a hurdle for enzymatic protein digestion, as portions of the structure become more compact and rigid, and less able to conform to the active site (Öste, 1991). Disulfide bonds form the majority of non-peptide linkages in gluten systems, followed by tyrosine crosslinks. Per gram of flour, approximately 10 mmol disulfide bonds and 1 nmol tyrosine crosslinks form (Wieser, 2003).

2.8.6 Introducing the Research Presented

As has already been mentioned, sorghum protein bodies form stable disulfide cross-linked matrices around starch granules during cooking, while similar nascent matrices in other cereals

aggregate and collapse (Bugusu, 2004). The stability of the matrix is thought to contribute to the slow starch digestion characteristic of sorghum products. Specific attributes affecting construction of the food matrix have been studied, but exact contributions to matrix assembly are poorly understood. Many proteins and protein-based matrices incorporate disulfide bonding in the structure, adding rigidity and decreasing flexibility, and also reducing digestibility, as noted previously. By studying the interaction of individual compounds with a model for a matrix-forming system, in our case modeling cereal prolamin proteins, the role of each material in matrix construction can be better defined.

Chicken egg white ovalbumin was utilized in our laboratory as a model protein for grain storage proteins. Ovalbumin was deemed a suitable model due to having a high melting temperature (Tm) akin to sorghum kafirins; containing several cysteine residues as do γ-kafirins, including in the hydrophobic pocket, which may become available for disulfide linkages above the Tm; being water soluble, which permits close examination of material-protein interactions in an environment utilized for many food processing systems,(F) and exhibiting oxidation-driven polymerization upon heating and in the presence of a strong food grade oxidizer (potassium bromate).

(F) The physico-chemical properties of kafirins preclude use of a water-based system for close examination of protein interactions as they are insoluble in water, and extraction significantly alters the protein conformations (Wang, Tilley, Bean, Sun, & Wang, 2009).

Previous work in our laboratory suggested the 3-deoxyanthocyanidins, anthocyanin pigment derivatives lacking the hydroxyl group at the 3-position on the C-ring and unique to sorghum amongst the cereal grains, may be responsible for the stable disulfide-linked kafirin networks in cooked sorghum porridges (Bugusu, 2004; Cholewinski, 2010). The 3-deoxyanthocyanidin compounds are more structurally stable at elevated pH (5-7) and less reactive antioxidants than anthocyanidins specifically because they lack the hydroxyl at the 3-position (Mazza & Brouillard, 1987). By decreasing the probability of irreversible oxidation products, 3-deoxyanthocyanidins have a greater potential to act in oxidation/reduction reactions multiple times per molecule.

To better understand how these compounds interact with protein to facilitate disulfide bonding without high occurrence of aggregate formations, flour extracts, apigeninidin (a 3-

deoxyanthocyanidin common to sorghums), and other individual phenolic compounds (gallic, *p*-coumaric, and sinapic acids, catechin) found in sorghums were observed in the model for their ability to facilitate interprotein linkages above the Tm of ovalbumin, distinguished using SDS-PAGE. Utilizing this system, we were able to discern differences in degree of polymerization (disulfide bonding and exotic inter-protein linkages) by compound and concentration, as described further in Chapter 4. Specifics of binding associations between phenolics and ovalbumin were also elucidated utilizing fluorescence quenching spectroscopy. Lastly, investigations of apigeninidin addition to corn flour porridges were examined for changes to protein matrix stability and starch digestion.

2.8.7 Possible Negative Consequences of Matrix Alterations

While undigestible structures are undesirable, producing a slight resistance to digestion in order to delay nutrient release as particles travel further down the small intestine is the goal of matrix manipulation for improved health outcomes. Along with the expected health benefits from slowing the digestion of rapidly digestible carbohydrates, several concerns must also be addressed as a result of manipulating food matrices.

Perhaps the most obvious is the aspect of slowing digestion to an extent which produces "colonic dumping," or the introduction of nutrients which would normally have been digested and absorbed prior to the proximal large intestine. Gut microbiota communities are altered in response to the changed nutrient sources, and gastrointestinal discomfort would be a likely side effect in portions of the populace. The implications of causing deviations in colonic bacterial and fungal populations have increasingly been noted as essential to long-term health (Bliss & Whiteside, 2018; Wahlström, Sayin, Marschall, & Bäckhed, 2016) and would be important to characterize in order to prevent unintended negative consequences, and positive benefits may occur due to the presence of resistant starch.

There is an exchange between altered protein digestibility and availability of amino acids. In the US, a very low percentage of the population experiences protein insufficiency or amino acid deficiencies, however, in other areas of the world, purposefully reducing protein digestibility by any manner could lead to total protein or essential amino acid malnutrition. Cereal grains, while major sources of dietary macronutrients and energy, are often deficient in essential amino acids

(Shewry & Halford, 2002), suggesting cereal grain products utilizing designed matrices may have a more minimal impact on whole-body amino acid pools and associated health aspects. Major protein sources and sources of essential amino acids (such as protein isolate ingredients, legumes, nuts, seeds, animal proteins, etc.) attempting to apply protein matrix manipulation to food products may require increased scrutiny of protein digestibility (e.g., protein digestibility corrected amino acid score or digestible indispensable amino acid score testing) in order to ascertain whether protein- or essential amino acid-based health outcomes might be affected.

Finally, a partial resistance to digestion is common to many allergenic food proteins. Therefore, the possibility exists for proteins designed to partially withstand digestion to enhance sensitivity or allergic responses in a small population of consumers. However, as digestive resistance is not a definitive factor in food allergies (Bøgh & Madsen, 2016), it is also possible there would be no increase in experienced sensitivity or allergenicity. As well, known allergens could potentially be utilized in formed matrices with little impact on consumer behavior due to consumers with such food allergies already avoiding foodstuffs containing the products to which they are allergic.

2.8.8 Conclusions

Greater understanding of specific food matrix effects on nutrient bioavailability are necessary in order to further the cause of “better for you” foods and the ideal of designed foods to implement improvements to human health and metabolic disease outcomes. The focus of this review has been on protein-based matrices in cereal foods, but other components also have the potential to participate in matrix construction and its manipulation. Lipids, carbohydrates, hydrocolloids, and surfactants also frame portions of food matrices in different products and have the capability to be utilized specifically in regard to altering the digestive properties of the food materials into which they are incorporated. Reproducing natural phenomena (such as the kafirin matrices of sorghum) to better constrain the digestion of glycemic carbohydrates may emerge as a feasible method to augment other diet, exercise, and pharmaceutical interventions to decrease rates and consequences of metabolic diseases.

References

Afanas'ev, I. B., Dcrozhko, A. I., Brodskii, A. V., Kostyuk, V. A., & Potapovitch, A. I. (1989). Chelating and free radical scavenging mechanisms of inhibitory action of rutin and quercetin in lipid peroxidation. Biochemical Pharmacology, 38(11), 1763-1769. https://doi.org/https://doi.org/10.1016/0006-2952(89)90410-3.

Aguilera, J. M. (2018). The food matrix: implications in processing, nutrition and health. Critical Reviews in Food Science and Nutrition, 1-18. https://doi.org/10.1080/10408398.2018.1502743.

Altan, A., McCarthy, K. L., Tikekar, R., McCarthy, M. J., & Nitin, N. (2011). Image Analysis of Microstructural Changes in Almond Cotyledon as a Result of Processing. Journal of Food Science, 76(2), E212-E221. https://doi.org/doi:10.1111/j.1750-3841.2010.01994.x.

Altschul, S. F., Wootton, J. C., Gertz, E. M., Agarwala, R., Morgulis, A., Schäffer, A. A., & Yu, Y. K. (2005). Protein database searches using compositionally adjusted substitution matrices. FEBS Journal, 272(20), 5101-5109. https://doi.org/10.1111/j.1742-4658.2005.04945.x.

American Diabetes Association. (2015). Standards of Medical Care in Diabetes—2015 Abridged for Primary Care Providers. Clinical Diabetes : A Publication of the American Diabetes Association, 33(2), 97-111. https://doi.org/10.2337/diaclin.33.2.97.

Aschemann-Witzel, J., Varela, P., & Peschel, A. O. (2019). Consumers' categorization of food ingredients: Do consumers perceive them as 'clean label' producers expect? An exploration with projective mapping. Food Quality and Preference, 71, 117-128. https://doi.org/https://doi.org/10.1016/j.foodqual.2018.06.003.

Atkinson, F. S., Foster-Powell, K., & Brand-Miller, J. C. (2008). International Tables of Glycemic Index and Glycemic Load Values: 2008. Diabetes Care, 31(12), 2281-2283. https://doi.org/10.2337/dc08-1239.

Awika, J. M. (2011). Sorghum Flavonoids: Unusual Compounds with Promising Implications for Health. In Advances in Cereal Science: Implications to Food Processing and Health Promotion (pp. 171-200): American Chemical Society.

Awika, J. M., Rooney, L. W., & Waniska, R. D. (2004). Properties of 3-deoxyanthocyanins from sorghum. Journal of Agricultural and Food Chemistry, 52(14), 4388. https://doi.org/10.1021/jf049653f.

Axtell, J. D., Kirleis, A. W., Hassen, M. M., & Mason, N. D. C. (1981). Digestibility of sorghum proteins. Proceedings of the National Academy of Sciences of the United States of America, 78(3), 1333-1335. https://doi.org/10.1073/pnas.78.3.1333.

Beta, T., Obilana, A. B., & Corke, H. (2001). Genetic Diversity in Properties of Starch from Zimbabwean Sorghum Landraces. Cereal Chemistry, 78(5), 583-589. https://doi.org/10.1094/CCHEM.2001.78.5.583.

Blaak, E. E., Antoine, J. M., Benton, D., Björck, I., Bozzetto, L., Brouns, F., Vinoy, S. (2012). Impact of postprandial glycaemia on health and prevention of disease. Obesity Reviews, 13(10), 923-984. https://doi.org/10.1111/j.1467-789X.2012.01011.x.

Blackwell, D. L., & Villarroel, M. A. (2018). Tables of Summary Health Statistics for U.S. Adults: 2016 National Health Interview Survey. National Center for Health Statistics. Available from: http://www.cdc.gov/nchs/nhis/SHS/tables.htm.

Bliss, E. S., & Whiteside, E. (2018). The Gut-Brain Axis, the Human Gut Microbiota and Their Integration in the Development of Obesity. Frontiers in Physiology, 9, 900.

Bugusu, B. A. 2004. Understanding the basis of the slow starch digestion characteristic of sorghum porridges and how to manipulate starch digestion rate [Doctoral Dissertation]. West Lafayette, IN, USA: Purdue University.

Bøgh, K. L., & Madsen, C. B. (2016). Food Allergens: Is There a Correlation between Stability to Digestion and Allergenicity? Critical Reviews in Food Science and Nutrition, 56(9), 1545-1567. https://doi.org/10.1080/10408398.2013.779569.

Centers for Disease Control and Prevention. (2017). National Diabetes Statistics Report, 2017. Atlanta, GA: Centers for Disease Control and Prevention, US Department of Health and Human Services.

Ceriello, A. (2005). Postprandial Hyperglycemia and Diabetes Complications. Diabetes, 54(1), 1-7. https://doi.org/10.2337/diabetes.54.1.1.

Choi, S., Woo, H., Ko, S., & Moon, T. (2008). Confocal Laser Scanning Microscopy to Investigate the Effect of Cooking and Sodium Bisulfite on In Vitro Digestibility of Waxy Sorghum Flour. Cereal Chemistry, 85(1), 65-69. https://doi.org/10.1094/CCHEM-85-1-0065.

Cholewinski, J. L. (2010). Sorghum endosperm components responsible for promoting protein polymerization through sulfhydryl-disulfide interchange. Food Science (Vol. M.S., p. 137): Purdue University.

Cisse, F., Pletsch, E. A., Erickson, D. P., Chegeni, M., Hayes, A. M. R., & Hamaker, B. R. (2017). Preload of slowly digestible carbohydrate microspheres decreases gastric emptying rate of subsequent meal in humans. Nutrition Research, 45, 46-51. https://doi.org/https://doi.org/10.1016/j.nutres.2017.06.009.

Cocero, A. M., & Kokini, J. L. (1991). The study of the glass transition of glutenin using small amplitude oscillatory rheological measurements and differential scanning calorimetry. Journal of Rheology, 35(2), 257-270. https://doi.org/10.1122/1.550255.

Colonna, P., Barry, J. L., Cloarec, D., Bornet, F., Gouilloud, S., & Galmiche, J. P. (1990). Enzymic susceptibility of starch from pasta. Journal of Cereal Science, 11(1), 59-70. https://doi.org/https://doi.org/10.1016/S0733-5210(09)80181-1.

Cordain, L., Eaton, S. B., Sebastian, A., Mann, N., Lindeberg, S., Watkins, B. A., Brand-Miller, J. (2005). Origins and evolution of the Western diet: Health implications for the 21st century. The American Journal of Clinical Nutrition, 81(2), 341-354.

de Graaf, E. M., Madeka, H., Cocero, A. M., & Kokini, J. L. (1993). Determination of the Effect of Moisture on Gliadin Glass Transition Using Mechanical Spectrometry and Differential Scanning Calorimetry. Biotechnology Progress, 9(2), 210-213. https://doi.org/10.1021/bp00020a015.

DeRose, R. T., Ma, D. P., Kwon, I. S., Hasnain, S. E., Klassy, R. C., & Hall, T. C. (1989). Characterization of the kafirin gene family from sorghum reveals extensive homology with zein from maize. Plant Molecular Biology, 12(3), 245-256. https://doi.org/10.1007/BF00043202.

Dockray, G. J. (2013). Enteroendocrine cell signalling via the vagus nerve. Current Opinion in Pharmacology, 13(6), 954-958. https://doi.org/https://doi.org/10.1016/j.coph.2013.09.007.

Edwards, C. H., Vasilopoulou, D., Grundy, M. M. L., Butterworth, P. J., Berry, S. E. E., Grassby, T., . . . Frost, G. S. (2015). Manipulation of starch bioaccessibility in wheat endosperm to regulate starch digestion, postprandial glycemia, insulinemia, and gut hormone responses: a randomized controlled trial in healthy ileostomy participants. The American Journal of Clinical Nutrition, 102(4), 791-800. https://doi.org/10.3945/ajcn.114.106203.

Englyst, H. N., Kingman, S. M., & Cummings, J. H. (1992). Classification and measurement of nutritionally important starch fractions. European Journal of Clinical Nutrition, 46(0954-3007 (Print)), S33-50.

Erbersdobler, H. F. (1989). Protein Reactions during Food Processing and Storage — Their Relevance to Human Nutrition. In J. C. Somogyi & H. R. Müller (Eds.), Nutritional Impact of Food Processing (pp. 140-155). Basel: Karger.

Faltermaier, A., Zarnkow, M., Becker, T., Gastl, M., & Arendt, E. K. (2015). Common wheat (Triticum aestivum L.): evaluating microstructural changes during the malting process by using confocal laser scanning microscopy and scanning electron microscopy. European Food Research and Technology, 241(2), 239-252. https://doi.org/10.1007/s00217-015-2450-x.

Flores, F. P., Singh, R. K., Kerr, W. L., Pegg, R. B., & Kong, F. (2013). Antioxidant and Enzyme Inhibitory Activities of Blueberry Anthocyanins Prepared Using Different Solvents. Journal of Agricultural and Food Chemistry, 61(18), 4441-4447. https://doi.org/10.1021/jf400429f.

Grau, K., Tetens, I., Bjørnsbo, K. S., & Heitman, B. L. (2011). Overall glycaemic index and glycaemic load of habitual diet and risk of heart disease. Public Health Nutrition, 14(1), 109-118. https://doi.org/10.1017/S136898001000176X.

Guerra, A., Etienne-Mesmin, L., Livrelli, V., Denis, S., Blanquet-Diot, S., & Alric, M. (2012). Relevance and challenges in modeling human gastric and small intestinal digestion. Trends in Biotechnology, 30(11), 591-600. https://doi.org/https://doi.org/10.1016/j.tibtech.2012.08.001.

Hamaker, B. R., & Bugusu, B. A. (2003). Overview: Sorghum proteins and food quality. In P. S. Belton & J. R. N. Taylor (Eds.), Afripro Workshop on the Proteins of Sorghum and Millets. Pretoria, South Africa.

Hamaker, B. R., Kirleis, A. W., Mertz, E. T., & Axtell, J. D. (1986). Effect of Cooking on the Protein Profiles and in Vitro Digestibility of Sorghum and Maize. Journal of Agricultural and Food Chemistry, 34(4), 647-649. https://doi.org/10.1021/jf00070a014.

Han, J.-A., & BeMiller, J. N. (2007). Preparation and physical characteristics of slowly digesting modified food starches. Carbohydrate Polymers, 67(3), 366-374. https://doi.org/https://doi.org/10.1016/j.carbpol.2006.06.011.

Han, X. Z., & Hamaker, B. R. (2000). Functional and Microstructural Aspects of Soluble Corn Starch in Pastes and Gels. Starch - Stärke, 52(2-3), 76-80. https://doi.org/doi:10.1002/(SICI)1521-379X(200004)52:2/3<76::AID-STAR76>3.0.CO;2-B.

Hariprasanna, K., & Rakshit, S. (2016). Economic Importance of Sorghum. In S. Rakshit & Y.-H. Wang (Eds.), The Sorghum Genome (pp. 1-25). Cham: Springer International Publishing.

Haslam, E. (1974). Polyphenol–protein interactions. Biochemical Journal, 139(1), 285-288. https://doi.org/10.1042/bj1390285.

Jo, J., & Lusk, J. L. (2018). If it's healthy, it's tasty and expensive: Effects of nutritional labels on price and taste expectations. Food Quality and Preference, 68, 332-341. https://doi.org/https://doi.org/10.1016/j.foodqual.2018.04.002.

Kato, T., Saito, N., Kashimura, K., Shinohara, M., Kurahashi, T., & Taniguchi, K. (2002). Germination and Growth Inhibitors from Wheat (Triticum aestivum L.) Husks. Journal of Agricultural and Food Chemistry, 50(22), 6307-6312. https://doi.org/10.1021/jf0204755.

Labiner-Wolfe, J., Jordan Lin, C.-T., & Verrill, L. (2010). Effect of Low-carbohydrate Claims on Consumer Perceptions about Food Products' Healthfulness and Helpfulness for Weight Management. Journal of Nutrition Education and Behavior, 42(5), 315-320. https://doi.org/https://doi.org/10.1016/j.jneb.2009.08.002.

Lee, B.-H., Eskandari, R., Jones, K., Reddy, K. R., Quezada-Calvillo, R., Nichols, B. L., Pinto, B. M. (2012). Modulation of Starch Digestion for Slow Glucose Release through "Toggling" of Activities of Mucosal α-Glucosidases. Journal of Biological Chemistry, 287(38), 31929-31938. https://doi.org/10.1074/jbc.M112.351858.

Mahasukhonthachat, K., Sopade, P. A., & Gidley, M. J. (2010). Kinetics of starch digestion in sorghum as affected by particle size. Journal of Food Engineering, 96(1), 18-28. https://doi.org/https://doi.org/10.1016/j.jfoodeng.2009.06.051.

Maljaars, P. W. J., Peters, H. P. F., Mela, D. J., & Masclee, A. A. M. (2008). Ileal brake: A sensible food target for appetite control. A review. Physiology & Behavior, 95(3), 271-281. https://doi.org/https://doi.org/10.1016/j.physbeh.2008.07.018.

Mattucci, S. (2018). Is "Clean" the New Healthy? (Vol. 2018, pp. Mintel Purchase Intelligence 2017 US Better-for-You Food and Drink Trends Market Report): Mintel Group, Ltd.

Mazza, G., & Brouillard, R. (1987). Color stability and structural transformations of cyanidin 3,5-diglucoside and four 3-deoxyanthocyanins in aqueous solutions. Journal of Agricultural and Food Chemistry, 35(3), 422-426. https://doi.org/10.1021/jf00075a034.

McRorie, J. W., & McKeown, N. M. (2017). Understanding the Physics of Functional Fibers in the Gastrointestinal Tract: An Evidence-Based Approach to Resolving Enduring Misconceptions about Insoluble and Soluble Fiber. Journal of the Academy of Nutrition and Dietetics, 117(2), 251-264. https://doi.org/https://doi.org/10.1016/j.jand.2016.09.021.

Nguyen, M. T., Kryachko, E. S., & Vanquickenborne, L. G. (2003). General and Theoretical Aspects of Phenols. The Chemistry of Phenols, 1-198. https://doi.org/doi:10.1002/0470857277.ch1

10.1002/0470857277.ch1.

Nigro, S. C., Luon, D., & Baker, W. L. (2013). Lorcaserin: A novel serotonin 2C agonist for the treatment of obesity. Current Medical Research and Opinion, 29(7), 839-848. https://doi.org/10.1185/03007995.2013.794776.

Ogden, C. L., Carroll, M. D., Fryar, C. D., & Flegal, K. M. (2015). Prevalence of Obesity Among Adults and Youth: United States, 2011-2014. NCHS Data Brief(219), 1-8.

Oria, M. P., Hamaker, B. R., & Shull, J. M. (1995). Resistance of sorghum α-, β-, and γ-kafirins to pepsin digestion. Journal of Agricultural and Food Chemistry, 43(8), 2148-2153. https://doi.org/10.1021/jf00056a036.

Owsley, W. F., Knabe, D. A., & Tanksley, T. D. (1981). Effect of sorghum particle size on digestibility of nutrients at the terminal ileum and over the total digestive tract of growing-finishing pigs. J Anim Sci, 52(3), 557-566.

Parada, J., & Aguilera, J. M. (2007). Food Microstructure Affects the Bioavailability of Several Nutrients. Journal of Food Science, 72(2), R21-R32. https://doi.org/doi:10.1111/j.1750-3841.2007.00274.x.

Popkin, B. M. (2006). Global nutrition dynamics: the world is shifting rapidly toward a diet linked with noncommunicable diseases. The American Journal of Clinical Nutrition, 84(2), 289-298. https://doi.org/10.1093/ajcn/84.2.289.

Péronnet, F., Meynier, A., Sauvinet, V., Normand, S., Bourdon, E., Mignault, D., Vinoy, S. (2015). Plasma glucose kinetics and response of insulin and GIP following a cereal breakfast in female subjects: effect of starch digestibility. European Journal of Clinical Nutrition, 69, 740. https://doi.org/10.1038/ejcn.2015.50.

Raghunathan, R., Naylor, R. W., & Hoyer, W. D. (2006). The Unhealthy = Tasty Intuition and Its Effects on Taste Inferences, Enjoyment, and Choice of Food Products. Journal of Marketing, 70(4), 170-184. https://doi.org/10.1509/jmkg.70.4.170.

Rein, M. J., Renouf, M., Cruz-Hernandez, C., Actis-Goretta, L., Thakkar, S. K., & da Silva Pinto, M. (2013). Bioavailability of bioactive food compounds: A challenging journey to bioefficacy. British journal of clinical pharmacology, 75(3), 588-602. https://doi.org/10.1111/j.1365-2125.2012.04425.x.

Renzetti, S., Dal Bello, F., & Arendt, E. K. (2008). Microstructure, fundamental rheology and baking characteristics of batters and breads from different gluten-free flours treated with a microbial transglutaminase. Journal of Cereal Science, 48(1), 33-45. https://doi.org/https://doi.org/10.1016/j.jcs.2007.07.011.

Rolo, A. P., & Palmeira, C. M. (2006). Diabetes and mitochondrial function: Role of hyperglycemia and oxidative stress. Toxicology and Applied Pharmacology, 212(2), 167-178. https://doi.org/https://doi.org/10.1016/j.taap.2006.01.003.

Román, S., Sánchez-Siles, L. M., & Siegrist, M. (2017). The importance of food naturalness for consumers: Results of a systematic review. Trends in Food Science & Technology, 67, 44-57. https://doi.org/https://doi.org/10.1016/j.tifs.2017.06.010.

Rosenblum, J. L., Irwin, C. L., & Alpers, D. H. (1988). Starch and glucose oligosaccharides protect salivary-type amylase activity at acid pH. American Journal of Physiology-Gastrointestinal and Liver Physiology, 254(5), G775-G780. https://doi.org/10.1152/ajpgi.1988.254.5.G775.

Roumen, C., Corpeleijn, E., Feskens, E. J. M., Mensink, M., Saris, W. H. M., & Blaak, E. E. (2008). Impact of 3-year lifestyle intervention on postprandial glucose metabolism: the SLIM study. Diabetic Medicine, 25(5), 597-605. https://doi.org/10.1111/j.1464-5491.2008.02417.x.

Sarikaya, E., Higasa, T., Adachi, M., & Mikami, B. (2000). Comparison of degradation abilities of α- and β-amylases on raw starch granules. Process Biochemistry, 35(7), 711-715. https://doi.org/https://doi.org/10.1016/S0032-9592(99)00133-8.

Scalbert, A., & Williamson, G. (2000). Dietary Intake and Bioavailability of Polyphenols. The Journal of Nutrition, 130(8), 2073S-2085S. https://doi.org/10.1093/jn/130.8.2073S.

Sclafani, A., & Ackroff, K. (2012). Role of gut nutrient sensing in stimulating appetite and conditioning food preferences. American Journal of Physiology-Regulatory, Integrative and Comparative Physiology, 302(10), R1119-R1133. https://doi.org/10.1152/ajpregu.00038.2012.

Shewry, P. R., & Halford, N. G. (2002). Cereal seed storage proteins: structures, properties and role in grain utilization. Journal of Experimental Botany, 53(370), 947-958. https://doi.org/10.1093/jexbot/53.370.947.

Singh, J., Dartois, A., & Kaur, L. (2010). Starch digestibility in food matrix: a review. Trends in Food Science & Technology, 21(4), 168-180. https://doi.org/https://doi.org/10.1016/j.tifs.2009.12.001.

Srichuwong, S., Curti, D., Austin, S., King, R., Lamothe, L., & Gloria-Hernandez, H. (2017). Physicochemical properties and starch digestibility of whole grain sorghums, millet, quinoa and amaranth flours, as affected by starch and non-starch constituents. Food Chemistry, 233, 1-10. https://doi.org/https://doi.org/10.1016/j.foodchem.2017.04.019.

Ubwa, S., Abah, J., Asemave, K., & Shambe, T. (2012). Studies on the Gelatinization Temperature of Some Cereal Starches. International Journal of Chemistry, 4(6), 22-28. https://doi.org/10.5539/ijc.v4n6p22.

van Avesaat, M., Troost, F. J., Ripken, D., Hendriks, H. F., & Masclee, A. A. M. (2014). Ileal brake activation: macronutrient-specific effects on eating behavior? International Journal of Obesity, 39, 235. https://doi.org/10.1038/ijo.2014.112

https://www.nature.com/articles/ijo2014112#supplementary-information.

Vinoy, S., Normand, S., Meynier, A., Sothier, M., Louche-Pelissier, C., Peyrat, J., Laville, M. (2013). Cereal Processing Influences Postprandial Glucose Metabolism as Well as the GI Effect. Journal of the American College of Nutrition, 32(2), 79-91. https://doi.org/10.1080/07315724.2013.789336.

Wahlström, A., Sayin, S. I., Marschall, H.-U., & Bäckhed, F. (2016). Intestinal Crosstalk between Bile Acids and Microbiota and Its Impact on Host Metabolism. Cell Metabolism, 24(1), 41-50. https://doi.org/10.1016/j.cmet.2016.05.005.

Wang, S., Li, C., Copeland, L., Niu, Q., & Wang, S. (2015). Starch Retrogradation: A Comprehensive Review. Comprehensive Reviews in Food Science and Food Safety, 14(5), 568-585. https://doi.org/10.1111/1541-4337.12143.

Wang, Y., Tilley, M., Bean, S., Sun, X. S., & Wang, D. (2009). Comparison of Methods for Extracting Kafirin Proteins from Sorghum Distillers Dried Grains with Solubles. Journal of Agricultural and Food Chemistry, 57(18), 8366-8372. https://doi.org/10.1021/jf901713w.

Wieser, H. (2003). 20 - The use of redox agents. In S. P. Cauvain (Ed.), Bread Making (pp. 424-446): Woodhead Publishing.

Wu, X., & Prior, R. L. (2005). Identification and characterization of anthocyanins by high-performance liquid chromatography-electrospray ionization-tandem mass spectrometry in common foods in the United States: vegetables, nuts, and grains. Journal of agricultural and food chemistry, 53(8), 3101-3113. https://doi.org/10.1021/jf0478861.

Xu, X. (2008). In vitro digestibility of starch in sorghum differing in endosperm hardness and flour particle size. Department of Grain Science and Industry. Manhattan, KS: Kansas State University.

Zarnkow, M., Mauch, A., Back, W., Arendt, E. K., & Kreisz, S. (2007). Proso millet (Panicum miliaceum L.): An Evaluation of the Microstructural Changes in the Endosperm during the Malting Process by Using Scanning-Electron and Confocal Laser Microscopy. Journal of the Institute of Brewing, 113(4), 355-364. https://doi.org/doi:10.1002/j.2050-0416.2007.tb00762.x.

Zhang, G., & Hamaker, B. R. (1998). Low α-Amylase Starch Digestibility of Cooked Sorghum Flours and the Effect of Protein. Cereal Chemistry, 75(5), 710-713. https://doi.org/10.1094/CCHEM.1998.75.5.710.

Zou, W., Sissons, M., Gidley, M. J., Gilbert, R. G., & Warren, F. J. (2015). Combined techniques for characterising pasta structure reveals how the gluten network slows enzymic digestion rate. Food Chemistry, 188, 559-568. https://doi.org/https://doi.org/10.1016/j.foodchem.2015.05.032.

Öste, R. E. (1991). Digestibility of Processed Food Protein. In M. Friedman (Ed.), Nutritional and Toxicological Consequences of Food Processing (pp. 371-388). Boston, MA: Springer US.

CHAPTER 3. INVESTIGATING CEREAL ENDOSPERM PHENOLICS AS POTENTIAL DISULFIDE INTERCHANGE MEDIATORS

3.1 Abstract

Cooked sorghum porridge starch digests comparatively poorly compared to other cereals, with kafirin proteins in starch-associated protein bodies implicated with the reduced digestibility. During cooking, γ-kafirin towards the exterior of the protein bodies polymerize, forming complex three-dimensional protein structures, which surround gelatinizing starch granules. In sorghums, a stable and expanded matrix is formed, while rice and maize protein matrices collapse during cooking. The stability of the matrix possibly limits the action of α-amylases, leading to the slow starch digestion characteristic of sorghum. Phenolic compounds were examined as potential factors responsible for promoting these structures via sulfhydryl-disulfide interchanges. Aqueous alcohol extracts (with and without acidification) of decorticated normal tan sorghum, corn masa, and white rice flours were analyzed for soluble phenolic content, antioxidant activity, and characterized for free phenolic compounds by UPLC. Finally, the ability of the extracts to polymerize a model protein (chicken egg white ovalbumin) was observed using SDS-PAGE. Solvent affected the extracted phenolic contents and antioxidant activities, which was increased with acidified solvents. The extraction of sorghum 3-deoxyanthocyanidins was also higher using acidified solvents. Sorghum extracts produced higher and greater ranges in protein molecular weight compared to corn and rice, which appeared more aggregative, indicating phenolics present in sorghum may promote protein disulfide bonds. Elucidating the role phenolics play in protein matrix formation could allow construction of similar matrices in food and cereal products to slow starch digestion and locationally move it towards the ileum, where physiological feedback via the gut-brain axis could be triggered.

3.2 Introduction

Sorghum nutritional quality is considered to be poor in comparison to other cereal grains, due to a lack of macronutrient bioavailability (MacLean Jr and others, 1981). Both the protein and starch fractions of prepared sorghum porridges are less digestible when compared to other cereal

porridges (Axtell and others 1981), resulting in adverse nutritional implications for areas of Africa and Asia where sorghum is a staple grain. Comparatively, maize flour porridges are highly digestible (Hamaker and others 1986; MacLean Jr and others 1981), though maize and sorghum contain similar proportions of macronutrients (U.S. Department of Agriculture, 2013) and similar kernel protein profiles, including γ-prolamin amino acid sequences (Altschul and others 1997; Altschul and others 2005) and structures (Bietz 1982; DeRose and others 1989) that have been implicated in the poor digestibility trait. (Maize Q548E9 compared to sorghum C5XDL2: BLASTP 2.8.0 return 77% identity, 79% positive, E-value 1e-33; Needleman-Wunsch alignment of two sequences return 63.2% global alignment with 67.1% similarity.)

The deficiency of sorghum protein digestibility has been linked to extensive disulfide cross-linking that occurs on cooking of γ-kafirin proteins, which surround the major α-kafirin seed storage protein (Oria and others 1995) in sorghum protein bodies. Bugusu (2004) found the protein fraction of sorghum flour is likely also responsible for the reduced cooked starch digestion. Microscopy observations of cooked sorghum flour pastes illustrated the development of an expanded three-dimensional web-like structure surrounding the gelatinized starch granules. Similar images of corn and rice flour pastes demonstrate aggregation and collapse of the protein. Access of carbohydrases to the gelatinized granules is thought to be more restricted through the denser protein matrix surrounding the starch granules, slowing the digestion of starch (Bugusu 2004; Ezeogu and others 2008), and contributing to sorghum's slowly digestible carbohydrate characteristic. The polymerized protein matrix originates from the tightly bound protein bodies surrounded by desiccated cytoplasmic proteins that are associated with starch granules in the vitreous endosperm.

Sulfhydryl-disulfide bond interchange reactions are involved in formation of the protein matrix surrounding the starch granules (Bugusu 2004; Choi and others 2008; Cholewinski 2010). As the cooking environments for maize and sorghum flours generally are highly similar, a compound or compounds found natively in sorghum was speculated to create an environment favoring formation of the stable protein network observed in sorghum. Understanding the mechanism for development of this network would potentially allow for the manipulation of stable matrix formation, and thereby starch digestibility, in order to improve sorghum nutritional value and also to possibly constrain starch digestion in other cereal products.

Sorghums contain a diverse range of phenolic compounds (Awika and Rooney 2004; Dykes and Rooney 2007; N'Dri and others 2013; Wu and Prior 2005) and are commonly consumed in areas of Africa and Asia as thick porridges. Corn products, also containing various phenolic components (de la Parra and others 2007; Siyuan and others 2018), are often consumed as masa products in the Americas. White rice, while low in free phenolic content (Min and others 2012; Zhou and others 2004), is a staple food to much of Asia and is also commonly consumed globally. Many phenolic compounds are redox active, potentially participating as either electron donors or acceptors in disulfide bond formation. However, few compounds likely maintain the stability to act as both donor and acceptor in disparate reactions to promote the sulfhydryl-disulfide interchange across a significant time period during heat processing. Extensive dynamic polymerization leads to the observed three-dimensional protein structures in sorghum, with the protein network growing as the starch granule swells and gelatinizes. The addition of phenolic-specific extracts from sorghum, corn masa, and rice flours to a model protein was used to investigate the occurrence of dynamic protein polymerization.

3.3 Materials

All solvents were of HPLC or ACS grade and obtained from Fisher Scientific (Chicago, IL, USA). Purified water (17.0 MΩ) was produced using a Barnstead E-pure system (Dubuque, IA, USA). Assay reagents were purchased from Millipore-Sigma (St. Louis, MO, USA). Precast polyacrylamide 8-16% Mini-PROTEAN® TGX gels, protein Broad Range Standard, Tris-glycine-SDS buffer (10x), and Coomassie Brilliant Blue R250 for SDS-PAGE analysis were acquired from Bio-Rad (Hercules, CA, USA).

Spectrophotometric determinations were made using a Beckman DU 530 UV/Vis spectrophotometer. Solid phase extraction (SPE) columns were purchased from Waters Corporation (Milford, MA, USA). Ultra-high performance liquid chromatography (UPLC) analyses were performed using a Waters Acquity H Class UPLC system equipped with a diode array detector (DAD) and QDa mass detector for mass spectra (Waters Corporation, Milford, MA, USA). All mobile phases were filtered and degassed prior to use. Phenolic standards (gallic, vanillic, caffeic, *p*-coumaric, ferulic, and sinapic acids, catechin, and epicatechin) were obtained

from Millipore-Sigma (St. Louis, MO, USA) and apigeninidin (chloride) from ChromaDex (Irvine, CA, USA).

3.4 Methods

3.4.1 Grain Samples and Sample Preparation

A whole grain normal white sorghum variety (P721N) was obtained from the Purdue Agronomy Farm and frozen at -20°C until use. The grains were decorticated and milled using a Tangential Abrasive Dehulling Device (TADD, Venables Machine Works Ltd., Saskatoon, Canada) according to the method of (Reichert and others 1986). Briefly, grain was tempered at room temperature for 24 hours in the container used for frozen storage, 40 g whole sorghum was placed in each of the 5 cups, and the TADD was run to remove 20% of the original weight. Decorticated samples were milled through a 0.5 mm mesh screen with a cyclone mill (FOSS North America, Eden Prairie, MN, USA).

Commercial corn masa flour (“Maseca” brand) and white rice flour (“Bob’s Red Mill” brand) were obtained from a local grocery store and used without additional preparation.

3.4.2 Extraction of Free Phenolic Compounds

Free phenolics from the different grain flours were extracted (adapted from Adom and Liu 2002) by mixing 12.5 g flour with 25 mL chilled 80% (v/v) aqueous ethanol or methanol, both with and without 0.2% (v/v) glacial acetic acid, for 10 min at room temperature in a circular shaker at 120 rpm. Three replicates of each flour were extracted. Mixtures were centrifuged at 2500 g for 10 min (Beckman Avanti J25-I, Beckman Coulter, Indianapolis, IN) and supernatants collected, and the extraction was repeated on the pellet. Supernatants for each sample were pooled and filtered through a Whatman No. 3 (GE Healthcare, Pittsburgh, PA) cellulose filter prior to evaporation under vacuum at 45°C to 5 mL (Labconco RapidVap, Kansas City, MO, USA). Extracts were reconstituted to a final volume of 25 mL using purified water and stored at -40°C until use.

Extracts were subjected to a SPE procedure (modified from Song and others 2013) for purification prior to UPLC and SDS-PAGE analyses. Waters Oasis HLB 1cc cartridges (Milford, MA) were conditioned with methanol followed by water. Extracts (1 mL) were loaded, washed with 2% (v/v) formic acid and eluent collected for phenolic content assay correction, washed with 5% (v/v) methanol and eluent discarded, before partially purified phenolic samples were collected by eluting with 2% (v/v) formic acid in methanol. Samples were dried under a nitrogen stream and resolubilized in either 0.5 mL 2% (v/v) formic acid for UPLC analysis or 0.5 mL 50 mM phosphate buffer (pH 6.8) for SDS-PAGE before storing at -80°C until use.

3.4.3 Total Phenolic Content (TPC)

TPC of the grain extracts were determined by the Folin-Ciocalteu method (Waterhouse 2005) using gallic acid as a standard, and TPC expressed as mg gallic acid equivalents (GAE) per gram of grain flour. The correction factor eluent from SPE was analyzed to adjust for free reducing compounds (especially sugars and vitamin C) which may be present in crude extracts.

3.4.4 Trolox Equivalent Antioxidant Capacity Assay

Antioxidant capacity of the extracts was obtained using a Trolox (6-hydroxy-2,5,7,8-tetramethylchroman-2-carboxylic acid) Equivalent Antioxidant Capacity (TEAC) assay (Ferruzzi and others 2002). Crude grain extracts were diluted 1:10 with distilled water to fit the curve linear range. Absorbance values were read at 515 nm at 0 and 10 min and the rate used to determine antioxidant capacity was determined based on the standard curve. TEAC values were expressed as μmoles Trolox Equivalents (TE) per gram flour.

3.4.5 UPLC-UV/Vis-MS

The SPE extracts (2% formic acid) were thawed at room temperature, centrifuged at 14,000 rpm for 10 min at 4°C in a microcentrifuge, and filtered through 0.45 μm PTFE syringe filters prior to injection (10 μL) and separation on a UPLC-DAD-MS system according to the method by Li and others (2016, modified). Elution profiles were examined at 280 nm for benzoic acid

derivatives and catechins (gallic and vanillic acids, catechin, and epicatechin), 320 nm for cinnamic acid derivatives (caffeic, *p*-coumaric, ferulic, and sinapic acids), and at 470 nm for 3-deoxyanthocyanidins. Phenolic compounds were identified by comparing retention time, spectra, and molecular mass of sample peaks to standards according to calibration curves (0.1-50 μg/mL), and reported as μg per gram flour. The 3-deoxyanthocyanidin components were calculated based on DAD spectra only and expressed as apigeninidin equivalents (AE) based on an apigeninidin standard curve from 0.1-100 μg/mL.

Phenolic compounds were separated on a UPLC-DAD-MS system with a BEH C18 column (2.1 mm id × 100 mm) at a flow rate of 0.5 mL/min. A gradient elution was utilized, of 0.2% formic acid in acetonitrile (solvent A) and 0.2% formic acid in water : acetonitrile (95:5) (solvent B), following a program of 0 min, 100% B; 0–7 min, 100–68% B; 7–8 min, 100% B; 8–9 min, 100% B. Conditions for MS utilized ESI- ionization mode and mass to charge ratio (m/z) scanned from 100-1000 m/z, capillary voltage 0.8 kV, cone voltage 20 V; probe temperature 150 °C, source temperature 600°C, and gas pressure 100 psi.

3.4.6 Gel Electrophoresis

A 0.2% (w/v) ovalbumin solution was prepared in 50 mM phosphate buffer (pH 6.8). In microcentrifuge tubes, 100 μL protein solution was combined with a 10 μL aliquot of treatment solution (buffer, negative control; 1% potassium bromate, positive control; or crude or SPE extract) and vortexed. Capped tubes were heated at 95°C in a dry thermal cycler (Eppendorf ThermoMixer C, Fisher Scientific, Chicago, IL, USA) for 10 min at 300 rpm and cooled on ice. Laemmli buffer (2x) was added to each tube (1:1) and vortexed. Tubes were returned to the thermal unit for 5 min under the same conditions, removed, and cooled. Samples were centrifuged at 10,000 rpm for 1 min (Beckman-Coulter microcentrifuge, Indianapolis, IN) before gel loading. Non-reducing conditions were utilized for preparation and gel separation of proteins.

Broad Range Standard (200 to 7 kDa), negative and positive controls, and sample solutions were loaded onto pre-cast Mini-PROTEAN TGX gels (10-20%) and run at constant voltage using the Mini-PROTEAN Tetra Cell system (Bio-Rad, Hercules, CA) according to manufacturer instructions. Voltage initially was low to allow sample to move through the loading comb in a single band before increasing to 120V. Lane 1 always contained the Broad Range Standard, Lane

2 the negative control, and Lane 3 the positive control. Gels were removed and stained overnight with Coomassie Blue before multiple washes of destaining solution. Destained gels were stored in a 7% glacial acetic acid solution prior to imaging on a light pad. Gel analyses were performed based on relative differences within each gel to negative and positive controls, with significance determined visually.

3.4.7 Statistical Analysis

Quantitative results performed on triplicate samples are reported as mean ± standard deviation. One-way and two-way analysis of variance tests were used to test for significant differences within and between grain and solvent types and Tukey's Multiple Comparison test was used to discriminate among differences using SAS software version 9.4 (SAS Institute, Inc., Cary, NC, USA) using a significance level of $p < 0.05$.

3.5 Results

3.5.1 Total Phenolic Contents and Antioxidant Activities of Extracts

The TPC of each grain differed ($p<0.001$), with Sorghum > Corn Masa > Rice, as shown in Table 3.1. Extraction solvent also affected TPC, with ethanol being less efficient ($p<0.001$). No significant difference in extraction efficacy occurred between the remaining solvents, though a general trend of increasing average TPC ensued with methanol < acidified ethanol < acidified methanol. Both the sorghum and corn masa flour extracts contained similar amounts of total phenolics with variances due to extraction solvent ($p<0.001$). Only the ethanol extracts resulted in lower TPC ($p<0.01$), for sorghum and corn (1.22±0.06 and 1.06±0.11 mg GAE/g flour, respectively, compared to 1.82±0.16 and 1.46±0.16 mg GAE/g for acidified methanol extracts). Rice contained lower free phenolics than the other grains analyzed ($p<0.001$), with no significant difference occurring due to solvent.

The antioxidant activity of sorghum and corn extracts were comparable overall while the TEAC of rice was lower than both other grains ($p<0.001$) (Table 3.1). Solvent and acidification affected TEAC, with acidified methanol > acidified ethanol > methanol > ethanol ($p<0.05$). Rice

antioxidant activity was not significantly affected by solvent. Sorghum and corn antioxidant activity were lowest in ethanol extracts (3.24±0.06 and 3.18±0.25 μmol TE/g grain, respectively) and highest in acidified methanol extracts (5.88±0.34 and 5.04±0.36 μmol TE/g grain, respectively).

3.5.2 Extract Component Identification by UPLC/DAD/MS

Sample chromatograms for acidified methanolic extracts of the 3 flours are presented in Figure 3.1 (280 nm) and Figure 3.2 (320 nm), with standards of phenolic acids and catechins identified, and sorghum extract at 470 nm for 3-deoxyanthocyanidin compounds (Figure 3.3). Mass fragments (M^{-1}) were utilized to confirm standard peaks for acids and catechins. Calculated values for phenolics confirmed by standards are found in Table 3.2, with sorghum 3-deoxyanthocyanidins in Table 3.3. Sorghum contained all 9 of the phenolics identified by standards, while corn masa was found to include caffeic, vanillic, *p*-coumaric, and ferulic acids, catechin, and epicatechin. Only caffeic, vanillic, *p*-coumaric, and ferulic acids were measured from rice extracts, and only vanillic and ferulic acids were present in quantifiable amounts.

The number of peaks observed at both 280 and 320 nm was highest for sorghum, indicating greater diversity in phenolic components. Several seemingly significant peaks were undetermined. Corn masa also contained several peaks at both wavelengths, with a number of compounds remaining undetermined. Rice exhibited the fewest peaks with the lowest absorbances, signifying an overall lack of phenolic components and minimal phenolic content, as expected from the TPC analysis.

While anthocyanins absorb well and can be identified at 520 nm (Wrolstad and others 2005), the absence of the 3-hydroxyl shifts the maximum absorbance of 3-deoxyanthocyanidins to 470-480 nm. Five peaks were detected in sorghum at 470 nm and assumed as 3-deoxyanthocyanidin compounds (Figure 3.3), with apigeninidin and luteolinidin the major contributors to total 3-deoxyanthocyanidins. The remaining peaks may be methoxy- and/or glucoside derivatives which have previously been identified (7-methoxyapigeninidin-5-glucoside, 5-methoxyluteolinidin-7-glucoside, and apigeninidin-5-glucoside, (Nip and Burns 1971; Awika and others 2004; Wu and Prior 2005)). Mass fragments could not be utilized for identification as anthocyanins (flavylium cation) are not detected in negative ion mode.

3.5.3 Effects of Different Grain Extracts on Polymerization

The effect of the crude extracts from sorghum, corn masa, and rice on ovalbumin polymerization (SDS-PAGE) are shown in Figure 3.4. The oxidative crosslinking potential of ovalbumin, as the model protein used, is shown in Lanes 2 and 3, where addition of the potassium bromate, as food grade oxidizing agent, resulted in almost complete polymerization of ovalbumin as indicated by the high molecular weight band in Lane 3. None of the bands present on the gel were discrete and sharp, indicating the presence of many products with varying degrees of polymerization.

Heating ovalbumin in the presence of sorghum extracts (Figure 3.4, Lanes 4-7) produced greater variation in molecular weight (MW) products in comparison to the masa or rice extracts. The banding patterns around 200 kDa were broader, signifying a wider range of polymer sizes (denoted within the green box), and appear fainter overall, indicating less protein was present at each differing MW compared to the large bands visible >200 kDa in masa and rice. Of the ethanolic extracts, the sorghum extracts also appeared to have more protein present between 66-115 kDa, as well as more remaining monomers (43 kDa). Taken together, this suggests sulfhydryl-disulfide interchanges may have occurred in the system.

Free phenolics in the masa (Figure 3.4, Lanes 8-11) and rice (Figure 3.4, Lanes 12-15) flours appeared to produce mainly high MW polymers, with the ethanolic extracts seeming to induce greater polymerization than methanolic extracts (Lanes 10-11, 14-15) but few products of differing MW, including very low residual monomers. While all 3 flours demonstrated differences in MW products compared to the negative control, corn masa and rice extracts yielded greater concentrations of MW bands ≥200 kDa and slightly lower residual monomers, with the ethanolic extracts more similar to the positive control, which may indicate aggregative polymerization and a lack of sulfhydryl-disulfide interchanges.

When the partially purified extracts were examined for their effects on polymerization in the model (Figure 3.5), inconsistent results occurred. This presumably was due to lingering acid from the SPE procedure that acidified several of the extracts beyond the buffering capacity of the solutions. Lower pH (<5, indicated after Laemmli buffer addition to some sample tubes turned the bromophenol blue from blue to green and yellow) resulted in gelling and precipitation of some

proteins. Higher proportion of monomers and less polymerization than the negative control resulted for these samples (most notably in Lanes 4, 9, 11, and 14), highlighting the inconsistent results between solvents and cereal grains.

3.6 Discussion

Redox reaction capacity of phenolic compounds is related to their oxidative state. pH can affect the charge and oxidative stability of phenolic compounds, which can also affect their ability to promote redox reactions (Castañeda-Ovando and others 2009; Zhou and Elias 2013). As observed in Table 3.1, acidification of the solvent increased TEAC, likely through improved stability of the samples due to the lower pH during extraction.

Sorghum grain is known to contain a diverse range of phenolic compounds (Awika and Rooney 2004; Wu and Prior 2005) and is the only cereal to natively produce 3-deoxyanthocyanidins, especially apigeninidin and luteolinidin, in all varieties. The difference in total free phenolic content between sorghum and corn extracts was statistically insignificant overall and amount alone did not account for the observed large difference in ability to polymerize protein, indicating the variations observed are not due to a difference in phenolic content. Similarly, only slight differences in antioxidant activity for the same solvent occurred. Levels of free phenolic compounds in unpigmented rices are generally low compared to other cereal grains, (Dykes and Rooney 2007; Zhou and others 2004; Min and others 2012) as observed in this work, as was the corresponding antioxidant activity. As the amount of phenolic compounds present and the antioxidant activity of the extracts, especially between sorghum and corn masa, were not deemed sufficiently disparate to provide the basis for the variations observed in polymerizing ability, differences in specific phenolic components of the extracts were expected to be the cause.

Ferulic acid, sinapic acid, and *p*-coumaric acid are the major phenolic acids found in cereal grains (Awika and Rooney 2004; Wu and Prior 2005). Ferulic and *p*-coumaric acids, while abundant, are primarily bound to cell wall components rather than freely extracted. The commonality of these compounds make them unlikely to be the main factor producing dynamic polymerization interchanges. All 8 of the phenolic acids and catechin compounds used as standards were found in the endosperm of several cereal grains in their free forms. Of the phenolic components examined, only the 3-deoxyanthocyanidins are unique to sorghum, and as they are

known to be redox active (Awika and others 2004), these compounds become candidates for further study of dynamic sulfhydryl-disulfide mediated protein polymerization through redox reactions.

Protein polymerization through the sulfhydryl-disulfide interchange reaction using gel electrophoresis has been demonstrated previously (Damodaran and Anand 1997). Only the sorghum extracts of these three flours seem to have the ability to consistently induce protein polymerization that does not appear aggregative and generates wide ranges of MW products. The presence of 3-deoxyanthocyanidins in sorghums is notable as they are highly redox active compounds (Awika and others 2004) and may act in the sulfhydryl-disulfide interchange as both antioxidants which reduce exposed disulfide bonds and subsequently as oxidizers to facilitate disulfide bond formation from free sulfhydryl groups. The interchange reaction can result in varying degrees of polymerization on the SDS-PAGE gels, as shown in Figure 3.4 for the sorghum extracts.

Anthocyanins have been shown to have higher antioxidant capacities than many other classes of flavonoids (Pietta 2000), but tend to lose stability as pH increases, initially forming semi-quinone and quinone products, followed by further oxidative degradation. The 3-deoxyanthocyanidin compounds have greater inherent stability due to the lack of the hydroxyl at the 3-position, which may permit these molecules to retain redox activity for longer periods of time and at higher pH ranges (including the near-neutral conditions utilized in the model system, pH 6.8). Above pH 4, apigeninidin has been found to occur in neutral forms (semi-quinone, quinone) dependent on pH, and to maintain stability for up to several hours (Mazza and Brouillard 1987). As the polymerization reactions were performed at near-neutral conditions, the 3-deoxyanthocyanidin structures would be likely to occur mainly as neutral (lacking the positive charge of the flavylium cation) forms. The neutral structures may enhance some types of interaction with proteins, such as π-stacking, which could increase the opportunity for these compounds to act as redox mediators in sulfhydryl-disulfide reactions by temporarily augmenting the stability of the protein-phenolic association.

3.7 Conclusions

Phenolic extracts from cereal grain endosperms are capable of polymerizing proteins through disulfide bond formation, with components in sorghum appearing to do so in a dynamic manner, while those in corn masa and white rice tend to form mainly higher MW products, which appear to favor aggregation via disulfide polymerization, rather than disulfide interchanges. The 3-deoxyanthocyanidin compounds in sorghum flour are likely responsible for the seemingly dynamic polymerizing ability of the sorghum extracts. The extent to which individual components are able to cause polymerization, and the underlying mechanism, are the subject of the subsequent chapters. Additionally, whether other anthocyanin compounds would be capable of similar reactivity is of interest.

Extensive disulfide bond formation during cooking has been shown previously to reduce the digestibility of sorghum protein to a level that has caused concern regarding its nutritional value. Furthermore, studies indicate the lower starch digestibility of sorghum food products is impacted by its protein fraction (Bugusu 2004). A better understanding of the sorghum 3-deoxyanthocyanidins that promote dynamic protein polymerization may afford the opportunity for plant scientists to improve sorghum grain nutritional quality, as well as pursue ways to slow the rate of starch digestion in other cereal grains and products for health benefits.

References

Adom K, Liu RH. 2002. Antioxidant activity of grains. Journal of Agricultural and Food Chemistry 50(21):6182-7.

Altschul SF, Madden TL, Schaffer AA, Zhang JH, Zhang Z, Miller W, Lipman DJ. 1997. Gapped BLAST and PSI-BLAST: A new generation of protein database search programs. Nucleic acids research 25(17):3389-402.

Altschul SF, Wootton JC, Gertz EM, Agarwala R, Morgulis A, Schäffer AA, Yu YK. 2005. Protein database searches using compositionally adjusted substitution matrices. FEBS Journal 272(20):5101-9.

Awika JM, Rooney LW. 2004. Sorghum phytochemicals and their potential impact on human health. Phytochemistry 65(9):1199-221.

Awika JM, Rooney LW, Waniska RD. 2004. Properties of 3-deoxyanthocyanins from sorghum. Journal of Agricultural and Food Chemistry 52(14):4388.

Axtell JD, Kirleis AW, Hassen MM, Mason NDC. 1981. Digestibility of sorghum proteins. Proceedings of the National Academy of Sciences of the United States of America 78(3):1333-5.

Bietz J. 1982. Cereal prolamin evolution and homology revealed by sequence analysis. Biochemical Genetics 20(11):1039-53.

Bugusu, B. A. 2004. Understanding the basis of the slow starch digestion characteristic of sorghum porridges and how to manipulate starch digestion rate [Doctoral Dissertation]. West Lafayette, IN, USA: Purdue University.

Castañeda-Ovando A, Pacheco-Hernández MdL, Páez-Hernández ME, Rodríguez JA, Galán-Vidal CA. 2009. Chemical studies of anthocyanins: A review. Food Chemistry 113(4):859-71.

Choi S, Woo H, Ko S, Moon T. 2008. Confocal Laser Scanning Microscopy to Investigate the Effect of Cooking and Sodium Bisulfite on In Vitro Digestibility of Waxy Sorghum Flour. Cereal Chemistry 85(1):65-9.

Cholewinski JL. 2010. Sorghum endosperm components responsible for promoting protein polymerization through sulfhydryl-disulfide interchange. [M.S.]: Purdue University. 137 p. Available from: 1490634.

Damodaran S, Anand K. 1997. Sulfhydryl−Disulfide Interchange-Induced Interparticle Protein Polymerization in Whey Protein-Stabilized Emulsions and Its Relation to Emulsion Stability. Journal of Agricultural and Food Chemistry 45(10):3813-20.

de la Parra C, Serna Saldivar SO, Liu RH. 2007. Effect of Processing on the Phytochemical Profiles and Antioxidant Activity of Corn for Production of Masa, Tortillas, and Tortilla Chips. Journal of Agricultural and Food Chemistry 55(10):4177-83.

DeRose RT, Ma DP, Kwon IS, Hasnain SE, Klassy RC, Hall TC. 1989. Characterization of the kafirin gene family from sorghum reveals extensive homology with zein from maize. Plant Molecular Biology 12(3):245-56.

Dykes L, Rooney L. 2007. Phenolic Compounds in Cereal Grains and Their Health Benefits. Cereal Foods World 52(3):105-11.

Ezeogu LI, Duodu KG, Emmambux MN, Taylor JRN. 2008. Influence of Cooking Conditions on the Protein Matrix of Sorghum and Maize Endosperm Flours. Cereal Chemistry 85(3):397-402.

Ferruzzi MG, Böhm V, Courtney PD, Schwartz SJ. 2002. Antioxidant and Antimutagenic Activity of Dietary Chlorophyll Derivatives Determined by Radical Scavenging and Bacterial Reverse Mutagenesis Assays. Journal of Food Science 67(7):2589-95.

Hamaker BR, Kirleis AW, Mertz ET, Axtell JD. 1986. Effect of Cooking on the Protein Profiles and in Vitro Digestibility of Sorghum and Maize. Journal of Agricultural and Food Chemistry 34(4):647-9.

Li M, Koecher K, Hansen L, Ferruzzi MG. 2016. Phenolic recovery and bioaccessibility from milled and finished whole grain oat products. Food & Function 7(8):3370-81.

MacLean Jr WC, Lopez De Romana G, Placko RP, Graham GG. 1981. Protein quality and digestibility of sorghum in preschool children: Balance studies and plasma free amino acids. Journal of Nutrition 111(11):1928-36.

Mazza G, Brouillard R. 1987. Color stability and structural transformations of cyanidin 3,5-diglucoside and four 3-deoxyanthocyanins in aqueous solutions. Journal of Agricultural and Food Chemistry 35(3):422-6.

Min B, Gu L, McClung AM, Bergman CJ, Chen M-H. 2012. Free and bound total phenolic concentrations, antioxidant capacities, and profiles of proanthocyanidins and anthocyanins in whole grain rice (Oryza sativa L.) of different bran colours. Food Chemistry 133(3):715-22.

N'Dri D, Mazzeo T, Zaupa M, Ferracane R, Fogliano V, Pellegrini N. 2013. Effect of cooking on the total antioxidant capacity and phenolic profile of some whole-meal African cereals. Journal of the Science of Food and Agriculture 93(1):29-36.

Nip WK, Burns EE. 1971. Pigment characterization in grain sorghum. II. White varieties. Cereal Chemistry Jan(1):74-80.

Oria MP, Hamaker BR, Shull JM. 1995. Resistance of sorghum α-, β-, and γ-kafirins to pepsin digestion. Journal of Agricultural and Food Chemistry 43(8):2148-53.

Pietta P-G. 2000. Flavonoids as Antioxidants. Journal of Natural Products 63(7):1035-42.

Reichert RD, Tyler RT, York AE, Schwab DJ, Tatarynovich JE, Mwasaru MA. 1986. Description of a production model of the tangential abrasive dehulling device and its application to breeders' samples. Cereal chemistry (3):201-7.

Siyuan S, Tong L, Liu R. 2018. Corn phytochemicals and their health benefits. Food Science and Human Wellness 7(3):185-95.

Song BJ, Sapper TN, Burtch CE, Brimmer K, Goldschmidt M, Ferruzzi MG. 2013. Photo- and Thermodegradation of Anthocyanins from Grape and Purple Sweet Potato in Model Beverage Systems. Journal of Agricultural and Food Chemistry 61(6):1364-72.

Waterhouse AL. 2005. Determination of Total Phenolics. In: Wrolstad RE, Acree TE, Decker EA, Penner MH, Reid DS, Schwartz SJ, Shoemaker CF, Smith D, Sporns P, editors. Handbook of Food Analytical Chemistry: John Wiley and Sons, Inc. p. 463-70.

Wrolstad RE, Durst RW, Lee J. 2005. Tracking color and pigment changes in anthocyanin products. Trends in Food Science & Technology 16(9):423-8.

Wu X, Prior RL. 2005. Identification and characterization of anthocyanins by high-performance liquid chromatography-electrospray ionization-tandem mass spectrometry in common foods in the United States: vegetables, nuts, and grains. Journal of agricultural and food chemistry 53(8):3101-13.

Zhou L, Elias RJ. 2013. Antioxidant and pro-oxidant activity of (−)-epigallocatechin-3-gallate in food emulsions: Influence of pH and phenolic concentration. Food Chemistry 138(2-3):1503-9.

Zhou Z, Robards K, Helliwell S, Blanchard C. 2004. The distribution of phenolic acids in rice. Food Chemistry 87(3):401-6.

Table 3.1 Total phenolic content and antioxidant activity of crude extracts from white sorghum, corn masa, and white rice endosperm flours. [#]

	White Sorghum				**Corn Masa**				**White Rice**			
	Ethanol	Acidified Ethanol	Methanol	Acidified Methanol	Ethanol	Acidified Ethanol	Methanol	Acidified Methanol	Ethanol	Acidified Ethanol	Methanol	Acidified Methanol
Phenolic Content [1]	1.22 ±0.06 AEFGH	1.88 ±0.23 BCD	1.66 ±0.19 BCDFGH	1.82 ±0.16 BCDF	1.06 ±0.11 AEKL	1.50 ±0.11 ACDFGH	1.41 ±0.20 ACFGH	1.46 ±0.16 ACFGH	0.57 ±0.09 IJKL	0.64 ±0.08 IJKL	0.75 ±0.10 EIJKL	0.74 ±0.03 EIJKL
Antioxidant Activity [2]	3.24 ±0.06 aceg	4.27 ±0.30 bfg	3.22 ±0.44 ace	5.88 ±0.34 d	3.18 ±0.25 ace	4.85 ±0.43 bfh	3.91 ±0.32 abg	5.04 ±0.36 fh	0.65 ±0.05 i	1.12 ±0.06 i	0.86 ±0.07 i	1.12 ±0.08 i

[1] TPC reported as mg GAE per gram flour
[2] TEAC reported as μmol TE per gram flour
[#] Values with the same letter are NOT significantly different ($p<0.05$)

Table 3.2 Phenolic acids and catechins identified from extracts of white sorghum, corn masa, and white rice endosperm flours. [1,#]

	R_t (min)	White Sorghum				Corn Masa				White Rice			
		Ethanol	Acidified Ethanol	Methanol	Acidified Methanol	Ethanol	Acidified Ethanol	Methanol	Acidified Methanol	Ethanol	Acidified Ethanol	Methanol	Acidified Methanol
Gallic Acid	0.50	1.65 ±0.01 a	0.63 ±0.01 a	0.81 ±0.05 b	0.76 ±0.07 b	nd [2]	nd	nd	nd	nd	nd	nd	nd
Catechin	2.32	0.93 ±0.04 acdfh	0.74 ±0.02 bef	1.05 ±0.04 acdh	1.03 ±0.07 acdfh	0.65 ±0.03 beg	0.87 ±0.12 abdf	0.55 ±0.07 eg	1.05 ±0.02 acdh	nd	nd	nd	nd
Caffeic Acid	2.6	1.34 ±0.09 a	1.04 ±0.05 b	1.93 ±0.07 c	1.29 ±0.11 a	1.03 ±0.04 b	1.25 ±0.04 a	0.98 ±0.01 b	1.23 ±0.01 a	Detected [3]	Detected	Detected	Detected
Vanillic Acid	2.7	1.23 ±0.04 aceg	2.48 ±0.14 b	1.32 ±0.07 acg	2.60 ±0.06 b	1.71 ±0.19 d	0.99 ±0.07 aefghjk	0.97 ±0.01 efghjk	1.17 ±0.14 aceg	0.91 ±0.03 efhijk	0.70 ±0.03 hijk	0.88 ±0.03 efhijk	0.74 ±0.10 efhijk
Epicatechin	3.05	0.34 ±0.01 a	0.63 ±0.04 b	0.57 ±0.03 b	1.43 ±0.10 c	0.94 ±0.04 d	0.97 ±0.08 d	0.72 ±0.03 b	0.91 ±0.06 d	nd	nd	nd	nd
p-Coumaric Acid	3.5	2.04 ±0.14 a	8.06 ±0.56 b	3.22 ±0.10 c	8.03 ±0.32 b	0.03 ±0.00 d	0.02 ±0.00 d	0.08 ±0.00 d	1.23 ±0.16 e	Detected	Detected	Detected	Detected
Ferulic Acid	4.05	5.47 ±0.37 a	20.14 ±1.14 befh	8.19 ±0.80 c	22.56 ±1.42 dfh	19.62 ±1.39 befh	21.97 ±1.30 bdefh	26.22 ±1.13 g	21.22 ±1.36 bdefh	0.97 ±0.02 i	1.53 ±0.15 i	1.32 ±0.01 i	2.21 ±0.23 i
Sinapic Acid	4.15	1.47 ±0.05 a	1.26 ±0.05 b	1.58 ±0.10 c	1.59 ±0.01 c	nd	nd	nd	nd	nd	nd	nd	nd

[1] Reported as μg phenolic per gram flour

[2] nd, not detected

[3] Detected, detected at unquantifiable amounts using the standard curve

Values with the same letter are NOT significantly different (p<0.05) for each phenolic compound

Table 3.3 The contents of 3-deoxyanthocyanidins[1] from white sorghum flour extracts.[#]

	R_t (min)	Ethanol	Acidified Ethanol	Methanol	Acidified Methanol
Apigeninidin	4.2	5.75±0.12 a	22.9±1.73 b	12.1±1.01 c	22.5±2.01 b
Luteolinidin	4.85	2.51±0.18 a	6.96±0.26 b	4.54±0.43 c	6.54±0.55 b
Total 3-Deoxyanthocyanidins		9.86±0.12 a	32.3±2.88 b	19.5±2.37 c	30.2±2.82 b

[1] Reported as μg Apigeninidin Equivalents per gram flour

[#] Values within the same row with the same letter are NOT significantly different ($p<0.05$)

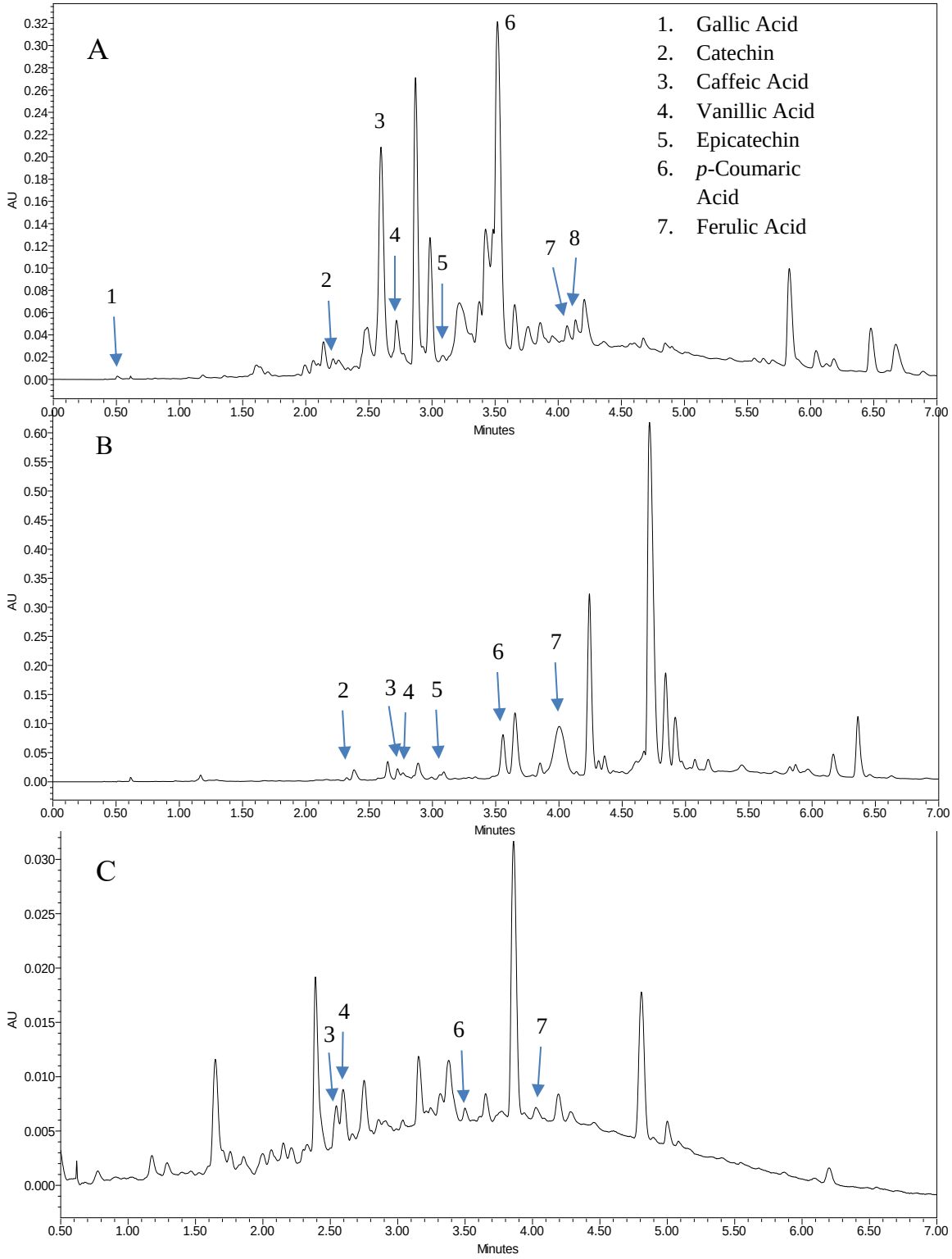

Figure 3.1 Chromatograms of partially purified acidified methanol extracts from A) white sorghum, B) corn masa, and C) white rice endosperm flours at 280 nm.

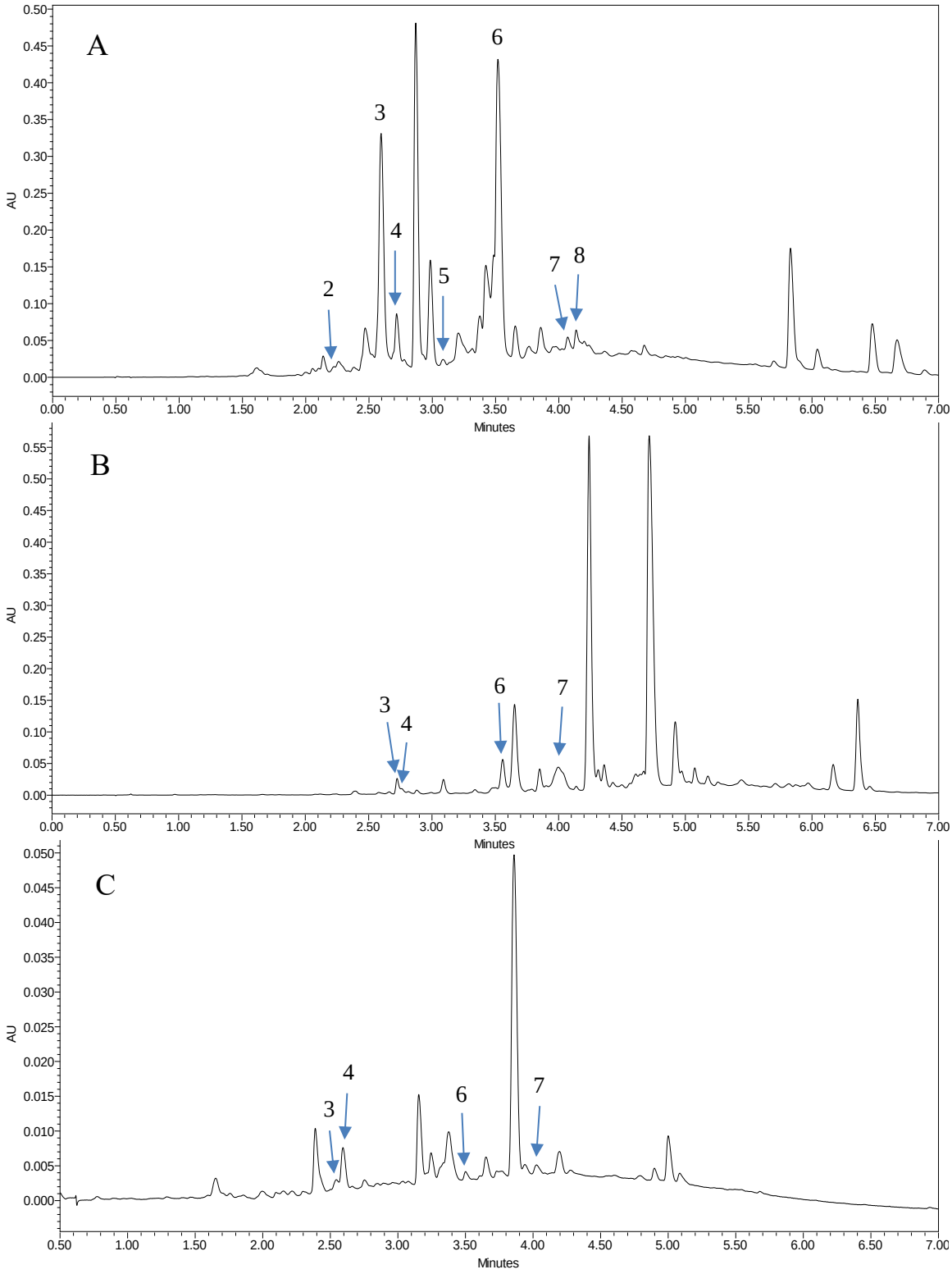

Figure 3.2 Chromatograms of partially purified acidified methanol extracts from A) white sorghum, B) corn masa, and C) white rice endosperm flours at 320 nm.
(Peak identification as for Fig. 3.1.)

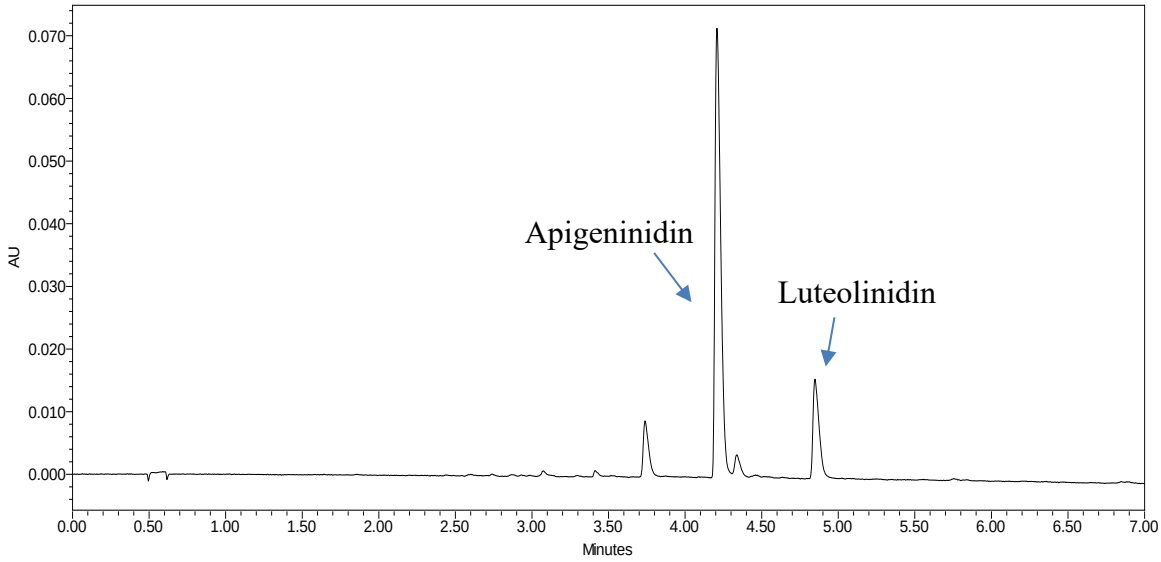

Figure 3.3 Chromatograms of partially purified acidified methanol extracts from white sorghum at 470 nm depicting 3-deoxyanthocyanidin compounds.

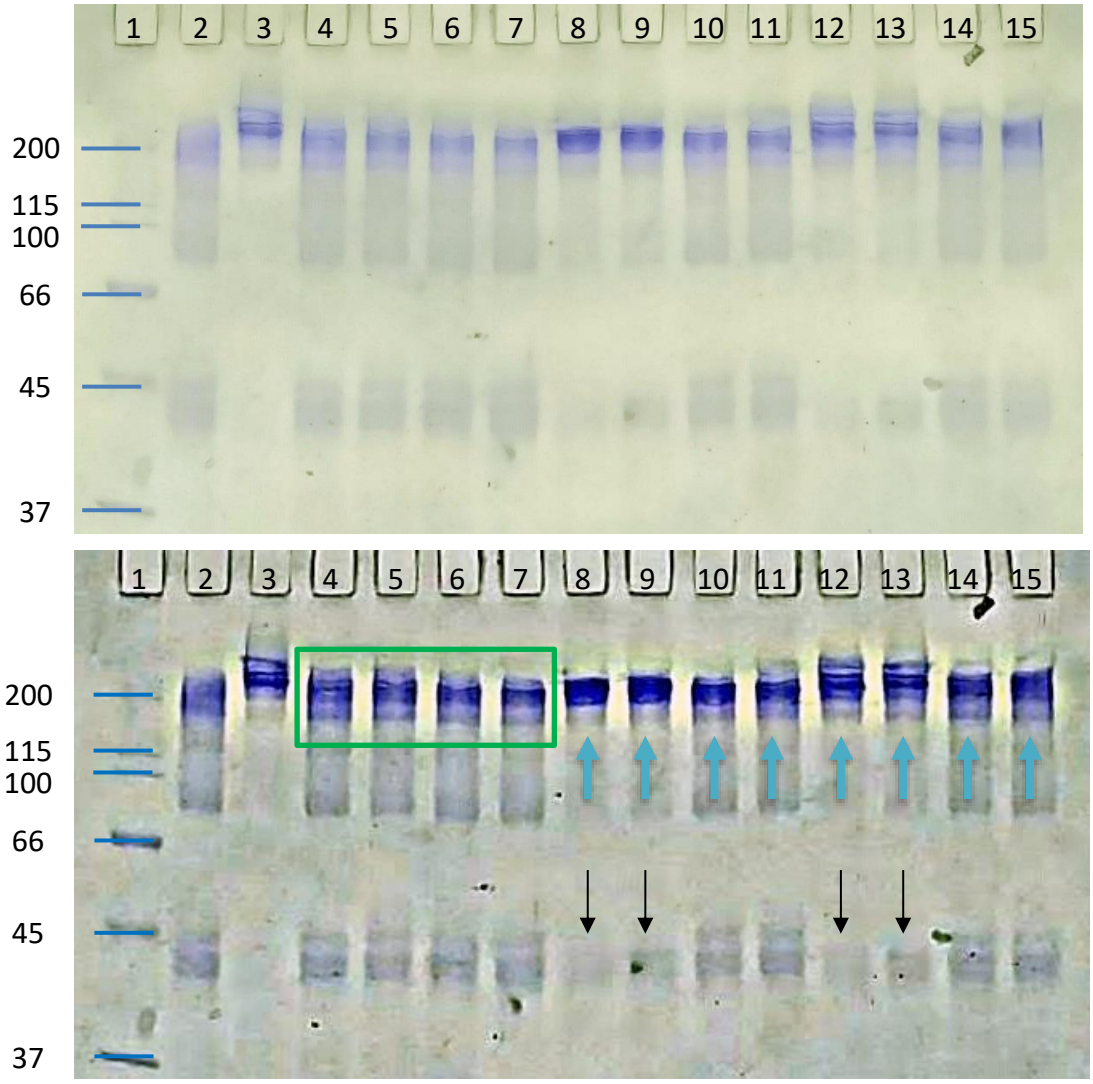

Figure 3.4 SDS-PAGE gel of 0.2% ovalbumin with crude cereal flour phenolic extracts. Top: original image. Bottom: subject to "HDR" filter to enhance band differences.

Lane 1: Broad Range Standard (200-37 kDa, gel cropped)
Lane 2: Negative control, buffer (50 mM phosphate buffer, pH 6.8)
Lane 3: Positive control, 1% potassium bromate
Lane 4: Sorghum 80% ethanol extract
Lane 5: Sorghum 80% acidified ethanol extract
Lane 6: Sorghum 80% methanol extract
Lane 7: Sorghum 80% acidified methanol extract
Lane 8: Corn Masa 80% ethanol extract
Lane 9: Corn Masa 80% acidified ethanol extract
Lane 10: Corn Masa 80% methanol extract
Lane 11: Corn Masa 80% acidified methanol extract
Lane 12: Rice 80% ethanol extract
Lane 13: Rice 80% acidified ethanol extract
Lane 14: Rice 80% methanol extract
Lane 15: Rice 80% acidified methanol extract

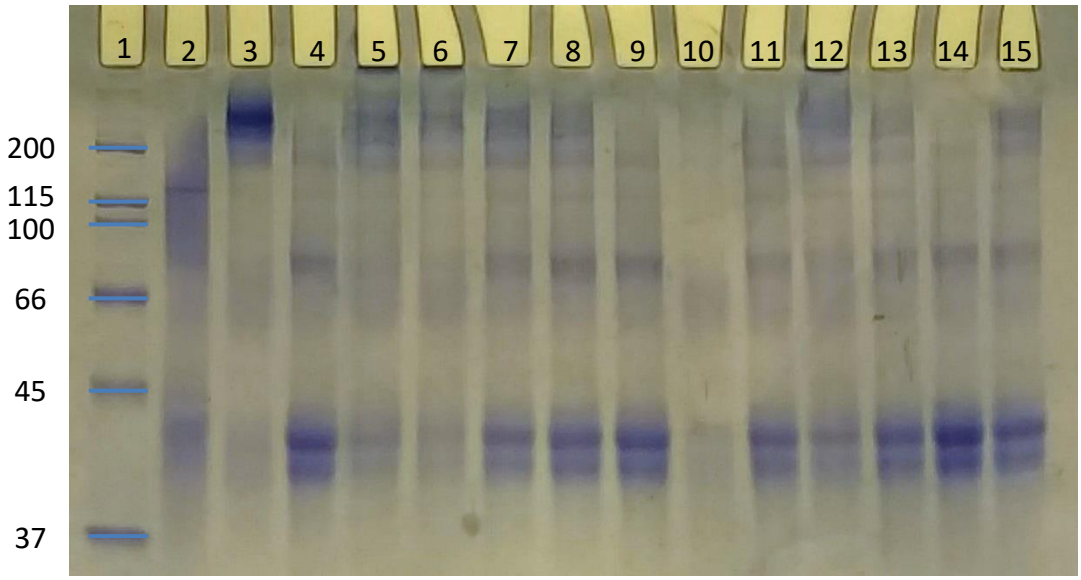

Figure 3.5 SDS-PAGE of 0.2% ovalbumin with cereal flour partially purified phenolic (SPE) extracts.

Lane 1: Broad Range Standard (200-37 kDa, gel cropped)
Lane 2: Negative control, buffer (50 mM phosphate buffer, pH 6.8)
Lane 3: Positive control, 1% potassium bromate
Lane 4: Sorghum 80% ethanol extract
Lane 5: Sorghum 80% acidified ethanol extract
Lane 6: Sorghum 80% methanol extract
Lane 7: Sorghum 80% acidified methanol extract
Lane 8: Corn Masa 80% ethanol extract
Lane 9: Corn Masa 80% acidified ethanol extract
Lane 10: Corn Masa 80% methanol extract
Lane 11: Corn Masa 80% acidified methanol extract
Lane 12: Rice 80% ethanol extract
Lane 13: Rice 80% acidified ethanol extract
Lane 14: Rice 80% methanol extract
Lane 15: Rice 80% acidified methanol extract

CHAPTER 4. INTERACTIONS OF PHENOLIC COMPOUNDS WITH OVALBUMIN AND IMPLICATIONS FOR FOOD MATRIX FORMATION

4.1 Abstract

The development of cereal food protein matrices is heavily dependent on the formation environment during processing. By changing the physico-chemical properties, modifications to the matrix can be made which may allow manipulation of the food to alter starch digestive properties for improved health benefits. Sorghum grains contain 3-deoxyanthocyanidins, phenolic pigments which appear to contribute to the high degree of kafirin protein body cross-linking around gelatinizing starch granules, forming stable matrices which slows the starch digestion. Protein-phenolic interactions may therefore be a target for manipulating food matrix formation. Ovalbumin was utilized as a model protein to study protein-phenolic interactions, above denaturation temperature and at near-neutral conditions (pH 6.8), with apigeninidin (a 3-deoxyanthocyanidin), gallic acid, *p*-coumaric acid, sinapic acid, and catechin, all phenolic compounds common to sorghums, at different concentrations using SDS-PAGE. Compounds demonstrating wider variations of molecular weight products were further investigated. Protein-phenolic binding interactions were examined using tryptophan (Trp) quenching by fluorescence spectroscopy at different temperatures. Apigeninidin and gallic acid exhibited the highest increases in polymerization, with interactions dose-dependent, though catechin at low concentrations produced a greater range of high molecular weight (MW) products. The remaining two phenolic acids produced little difference in polymerization and did not undergo fluorescence spectroscopy analysis. Apigeninidin quenched Trp most efficiently and had the largest apparent effect on protein conformation based on peak shift, though catechin had the highest binding site number, binding affinity, and lowest estimated interaction complex activation energy based on fit to a Stern-Volmer equation model. 3-Deoxyanthocyanidins promoted protein-phenolic interactions and polymerization of the model ovalbumin protein and are suggested to be involved in protein matrix enlargement around gelatinizing starch in sorghum flour, which may be associated with reduced starch digestion rate.

4.2 Introduction

Food matrices are complex microstructures providing the physical structure and chemical properties affecting the release of nutrients for absorption (Aguilera, 2018; Parada & Aguilera, 2007; Singh, Dartois, & Kaur, 2010). By changing the structure and/or associated properties, digestion of the macronutrients can be altered (Choi, Woo, Ko, & Moon, 2008; Ezeogu, Duodu, Emmambux, & Taylor, 2008; McClements, Decker, Park, & Weiss, 2008; Renzetti, Dal Bello, & Arendt, 2008), yet relatively little is known about protein matrix formation, particularly in regards to changing digestion rate kinetics of entrapped gelatinized starch in foods. Phenolic compounds are secondary plant metabolites which can act as biochemical antioxidants, maintaining redox environments in plant cells, but the phenolic components can incorporate with other constituents to affect the redox environment or micro-environment during processing and modify the resulting food matrix (Moser, Chegeni, Jones, Liceaga, & Ferruzzi, 2014; Zhou & Elias, 2013).

Improving our understanding of protein-phenolic interactions, which affect food matrix construction, may instigate further research into food products with matrices specifically modified to provide health benefits, such as slowed starch digestion for moderated blood glucose response and prolonged energy release. Towards this end, in the present study a model protein system utilizing ovalbumin that was previously shown to polymerize in the presence of oxidizing compounds (Cholewinski, 2010) was combined with phenolic compounds to examine the outcome of protein-phenolic interaction.

Egg white ovalbumin (Figure 4.1; Stein, Leslie, Finch, & Carrell, 1991) is a 385 residue globular glycoprotein of the serpin (serine protease inhibitor) superfamily without protease activity, containing 4 cysteine (Cys) residues (Cys11, Cys30, Cys367, Cys382) and one native disulfide bond (Cys73-Cys120). The protein contains 3 locationally different tryptophan (Trp) residues: Trp 148 is accessible to solvent and located on the F helical strand; Trp 184, in the hydrophobic pocket, initiates an anti-parallel β-sheet strand; and Trp 267 is partially solvent exposed on the H helical strand (Wright, Qian, & Huber, 1990).

We previously demonstrated utilizing ovalbumin to assess protein polymerization via sulfhydryl-disulfide interchanges affected by phenolic extracts from grain flours (Chapter 3, Cholewinski, 2010), which differ from oxidation-driven polymerization by oxidizing agents such as potassium bromate. Following up from this work, in the present study the interactions of ovalbumin with phenolic compounds were assessed to better determine the phenolic structures,

concentrations, and resulting types of formed inter-molecular bonds which may lead to stable protein matrix formation. Individual phenolics present in sorghum (apigeninidin, *p*-coumaric acid, sinapic acid, (+)-catechin, and gallic acid) were introduced to the ovalbumin model system, and promising compounds were further subjected to fluorescence quenching spectroscopy to examine the nature of the interactions. Structures of the phenolics utilized are presented in Figure 4.2.

Previous studies have also shown ovalbumin interactions with phenolic compounds that were measured using fluorescence spectroscopy (Ognjenović, Stojadinović, Milčić, Apostolović, Vesić, Stambolić, et al., 2014; Xie, Wehling, Ciftci, & Zhang, 2017). Fluorescence quenching refers to the decrease in measurable fluorescence yield from a protein fluorophore generated by molecular interaction with the introduced quencher molecules (Joseph R. Lakowicz, Gryczynski, Gryczynski, & Dattelbaum, 1999). Quenching of native tryptophan fluorescence was used to investigate binding interactions between ovalbumin and phenolics at different temperatures while maintaining pH, and consequently preserving relatively constant initial phenolic structures and redox states. Thus, in this chapter candidate phenolic compounds present in sorghum were evaluated for their protein polymerization potential through sulfhydryl-disulfide interchange and direct binding to the polymer, which provides guidance for directing protein matrix formation in food products to alter digestive properties.

4.3 Materials

Ovalbumin, phenolic acids (gallic, *p*-coumaric, sinapic), and (+)-catechin hydrate were obtained from Millipore Sigma (St. Louis, MO, USA). Apigeninidin (chloride) was procured from ChromaDex (Irvine, CA, USA). Chemical reagents and solvents were purchased from Fisher Scientific (Chicago, IL) and were at least ACS grade. Precast polyacrylamide 8-16% Mini-PROTEAN® TGX gels, 10x running buffer, Laemmli buffer, and Broad Range Standard (10-250 kDa) were acquired from Bio Rad (Hercules, CA). Purified water (at least 12 MΩ) was produced using a Millipore Elix 7 water system (Millipore Sigma, St. Louis, MO, USA).

4.4 Methods

4.4.1 Polymerization Interactions of Phenolic Compounds with a Model Protein

For polymerization interaction assessments, a 100 μL solution of 0.2% (w/v) ovalbumin in 50 mM phosphate buffer (pH 6.8) was mixed 10:1 with phenolic solutions ranging from 2 ng/mL – 200 μg/mL in the same buffer. Final concentrations ranged from 0.1 ng to 10 μg phenolic/mg ovalbumin. Buffer was used as the negative control and 1% potassium bromate as the positive control to promote ovalbumin polymerization, and treated in the same manner. Protein solutions were heated and stirred at 95°C using a ThermoBlock dry bath (ThermoFisher Scientific, Chicago, IL, USA) for 10 min and immediately cooled on ice. Solutions were diluted with 2x Laemmli buffer and heated a further 5 min before cooling on ice. The samples, molecular weight (MW) standard, and controls were loaded (10 μL each) into 15-well precast polyacrylamide 8-16% Mini-PROTEAN® TGX gels. Non-reducing conditions were utilized for preparation and gel separation.

Lane 1 always contained the Broad Range Standard with molecular weight (MW) markers ranging from 10-250 kDa. The negative control (buffer and ovalbumin) and positive control (1% potassium bromate and ovalbumin) were Lanes 2 and 3, respectively, and were treated in the same manner as the samples. Protein-phenolic interaction mixtures were in Lanes 4-15, from highest (Lane 4) to lowest (Lane 15) concentration of phenolic compound. The gels were run using a Mini-Protean TETRA-cell system (Bio-Rad, Hercules, CA) and Basic PowerPac at constant voltage. A low voltage was used initially to allow the samples to enter the gel from the comb in a tighter band before increasing the voltage to 120 V and running to the end of the gels. Gels were stained overnight using Coomassie Blue before several changes of destaining solution to remove excess dye. Imaging took place using a backlit white light pad using a camera phone.

4.4.2 Determination of Polymerization Type

Phenolic compounds which demonstrated distinct interactions with ovalbumin in the system (gallic acid, apigeninidin) were then subjected to reduction of disulfide bonds following the 10 min interaction at 95°C. β-Mercaptoethanol was added to the Laemmli buffer used to dilute the samples prior to the 5 min heating at 95°C, and samples were loaded, run, dyed, and destained as described in Section 4.4.1.

4.4.3 Gel Analysis

Gels were analyzed using ImageJ software (Schneider, Rasband, & Eliceiri, 2012). All images were first subjected to rolling ball background subtraction and changed to 8-bit images. Areas of MW groupings (monomers, 75-150, 150-250, and >250 kDa), rather than individual peak areas, were determined using drop-down to a common baseline per gel lane. Baseline was determined as the signal detected between the 15 and 25 kDa MW markers. Differences were determined using the standard error of each peak group mean for individual gels.

4.4.4 Fluorescence Spectroscopy of Protein-Phenolic Interactions

A stock solution of ovalbumin in 20 mM sodium phosphate buffer (pH 6.8) was prepared and kept on ice. Solutions of gallic acid, (+)-catechin hydrate, and apigeninidin chloride were freshly prepared in the same buffer, blanketed with nitrogen gas, and kept on ice. The concentration of ovalbumin was fixed at 5 μM, while final concentrations of the phenolic compounds were added at different ratios just prior to heating to achieve 0, 1, 5, 10, 25, and 50 μM in the sample.

Triplicate samples of protein + phenolic at each concentration were stirred and heated on a ThermoBlock dry bath (ThermoFisher, Chicago, IL, USA) for 10 min at 25, 45, 65, 75, 85, or 95°C, then rapidly cooled to room temperature. Fluorescence quenching measurements for the ovalbumin-phenolic mixtures were obtained using a Perkin Elmer LS-55 Fluorescence Spectrometer (Woodbridge, ON, Canada). Spectra were recorded in a 1 cm (1.4 mL) quartz cuvette cell at room temperature using an excitation wavelength (λ_{ex}) = 285 nm with the slit width set to 10 nm. Fluorescence emission spectra were collected between (λ_{em}) 290-500 nm using a slit width of 2.5 nm and scanning at 100 nm/min, with intensity at 340 nm (Trp) recorded. All experiments were corrected against a blank containing the buffer with corresponding phenolic concentration (0-50 μM) heated under the same conditions, with the blank spectra automatically subtracted.

4.4.5 Fluorescence Quenching Analysis

Quenching of native Trp fluorescence was analyzed using fluorescence intensity at 340 nm and performed using the Stern-Volmer equation (Eq. 1) described by Lakowicz (1999). The Stern-Volmer model was selected as it is suitable for examining either collisional or static quenching, allows determination of the main quenching method (static or dynamic), and has been commonly utilized and published in studies involving quenching of fluorescence from food proteins by phenolic compounds.

$$F_0 / F = 1 + K_q \hat{0}_0 [Q] = 1 + K_{SV} [Q] \quad \text{Equation 1}$$

Where F_0 and F were the fluorescence intensity in the absence and presence, respectively, of quencher compounds (phenolics) at concentration [Q]. K_{SV} was the Stern-Volmer quenching constant, also equal to $K_q \tau_o$, where K_q was the fluorescence quenching rate constant and τ_o the fluorophore half-life without quencher (10 ns). Stern-Volmer plots in the linear range were utilized to obtain K_{SV}, with K_q also calculated from K_{SV} and τ_o. These values represent the strength of interaction between ovalbumin and the phenolic compound.

When the calculated K_q was approximately 100 times greater than the limiting diffusion rate constant of biomolecules (2×10^{10} M^{-1} s^{-1}), static quenching, not dynamic, was indicated as the main quenching mechanism between the molecules. The binding constant (K_A) and binding sites (n) for the interactions were then estimated from the double logarithmic Stern-Volmer equation (Eq. 2).

$$\log[(F_0 - F) / F] = \log K_A + n^* \log[Q] \quad \text{Equation 2}$$

The approximate fraction (f_a) of the fluorophore (Trp) accessible to the quencher molecules was calculated using a modified Stern-Volmer equation (Eq. 3).

$$F_0 / (F_0 - F) = 1/f_a + 1/(f_a K_q)\ 1/[Q] \quad \text{Equation 3}$$

The activation energy (E_a) of phenolic-ovalbumin interaction between 75-95°C was estimated using a modified Arrhenius equation (Eq. 4), where ΔG is the free energy, K_q is the calculated Stern-Volmer equation quenching constant, A is the Arrenhius factor, E_a the estimated activation energy, R is the gas constant, and T the temperature in Kelvin.

$$\Delta G = \ln(K_q) = \ln A - E_a/R\ (1/T) \quad \text{Equation 4}$$

Peak shift data from fluorescence quenching analyses are presented as means ± standard deviations. Values from the Stern-Volmer equation, modified Stern-Volmer equation, double-log

plots, accessible fraction, and estimated activation energy are presented as calculated regression values.

4.5 Results

4.5.1 Protein-Phenolic Polymerization

The addition of apigeninidin from 2 ng-2 μg/mg ovalbumin (Figure 4.3) resulted in higher residual monomer concentrations at 2.1 and 0.71 μg/mg ovalbumin (Lanes 4-7, indicated by arrows) compared to the negative control (Lane 2). As apigeninidin to ovalbumin ratio increased, a greater diversity of compounds >250 kDa were produced, seen as a broadening of the band towards the comb. Lower amounts of apigeninidin developed fewer polymers >250 kDa (Lanes 8-15), with the 2 ng level (Lanes 14-15) appearing similar to the negative control. None of the treatment levels produced polymerization which appeared similar to the positive control (Lane 3) or to primarily occupy a single high molecular weight banding area. Though difficult to perceive visually, computer analysis (Image J) discerned slight differences in the 75-150 kDa range were dose-dependent, with higher amounts of apigeninidin producing more products in this range, but fewer of these residues were present at all levels compared to negative control.

Interactions between ovalbumin and *p*-coumaric acid (Figure 4.4) were more subtle. Large differences in MW products did not occur across the 5 log concentration differential from 10 μg-0.1 ng/mg ovalbumin. Products below 150 kDa, including monomers, were comparable between all samples and negative control. The highest treatment concentration (10-5 μg/mg OVA, Lanes 4-5) demonstrates a broadening of products from below the comb >250 kDa and in the 150-250 kDa area. To 1 μg/mg OVA (Lane 6), the products >250 kDa continue to exhibit a minor broadening in MW compared to negative control.

Similar to *p*-coumaric acid, very few differences were observed following sinapic acid interaction with ovalbumin (Figure 4.5) across all concentrations examined. No changes in monomer amounts were evident, while the main difference between negative control and all sample concentrations was a slight decrease in 75-150 kDa and corresponding increase in 150-250 kDa products for sinapic acid samples. While evident there is an effect due to the presence of sinapic acid, none of the levels investigated appear to distinguish any particular treatment level.

Catechin addition (Figure 4.6) again demonstrated only subtle differences in polymerization. No appreciable differences in monomer content were visible, and high concentrations (Lanes 4-8, 10-0.5 μg/mg) resulted in highly similar banding patterns. As the concentration of catechin reduced further, the >250 band spread towards the comb, indicating the formation of higher MW products, and may signify sulfhydryl-disulfide exchanges occurred at lower concentrations.

Treatment with gallic acid (Figure 4.7) produced the most significant differences in polymerization. With 10 μg gallic acid (Lane 4), ovalbumin polymerization was similar to the positive control (Lane 3), and 5 μg (Lane 5) was also highly similar. Evidence for incomplete polymerization became clearer from Lane 6 (1 μg gallic acid), with more defined monomer bands and products from 75-250 kDa visible. Levels ≤0.1 μg (Lanes 9-15) had similar residual monomers to the negative control, and polymers between 150-250 kDa had relative amounts similar to or less than negative control.

The multimers of 75-150 kDa increased as gallic acid concentration decreased to 10 ng (Lane 11, Figure 4.7), with Lanes 11-13 (10-1 ng) showing no difference from the negative control. Fewer polymers were evident in the lowest concentrations (Lanes 14-15) compared to negative control. Residual monomer concentrations increased as gallic acid decreased until Lane 9, where levels comparable to the negative control persisted. As gallic acid content decreased, the very high MW products (>250 kDa) at the top of the gel reduced slightly in MW, evinced by the emergence of space under the comb for Lanes 7-11. Further decreases in concentration once again produced higher MW products, observed as loss of the space under the comb in Lanes 12-15, but at a reduced intensity compared to positive control or higher levels of gallic acid.

4.5.2 Determination of Polymerization Type

After reducing disulfide bonds, the apigeninidin gel (Figure 4.8) across a 1 ng-10 μg/mg ovalbumin concentration differential showed that the polymerization was due almost entirely to formation of disulfide bridges, as the monomer bands predominated and no differences were observed between treatments and either negative or positive controls. Very small amounts of other types of bonding may have occurred (seen as faint bands at higher MW), these also occurred in negative and positive controls.

Reducing gallic acid-ovalbumin interaction products (Figure 4.9) demonstrated the presence of non-disulfide polymerization, as several high MW products remained on the gel. The intensities of the bands followed gallic acid concentration, with more products remaining at higher gallic acid treatment concentrations. The approximate range of gallic acid found in many cereal grains (1-10 ng/mg protein, Lanes 11-13) produced low amounts of these exotic linkages, indicating the majority of polymerization at these concentrations would be due to disulfide bond formation. At the lowest amounts of gallic acid (Lanes 14-15, 0.1-0.5 ng/mg ovalbumin), no appreciable difference from the negative control (Lane 2) was observed.

4.5.3 Fluorescence Quenching of Ovalbumin Native Tryptophan Residues

4.5.3.1 Fluorescence Spectra of Ovalbumin with Phenolics Following Heat Treatment

Ovalbumin fluorescence spectra were dominated by Trp fluorescence, with a maximum emission at approximately 340 nm. Increasing amounts of the 3 phenolics examined (apigeninidin, catechin, gallic acid) exhibited greater quenching of fluorescence (Figure 4.10) between 300-500 nm, as did increases in temperature. At 0 μM phenolics (5 μM ovalbumin only), a decrease in fluorescence was also observed, especially above denaturation onset, implying unfolding and/or polymerization shielded a portion of the exposed Trp residues. However, the increase in K_{SV} in the presence of phenolic components would indicate Trp accessibility improved. Accordingly, it may be more likely fluorescence of ovalbumin alone was reduced by an increase in collisional quenching with temperature.

A red shift could also be observed in the emission maxima with each of the phenolics as the concentration (0-50 μM) and temperature (25-95°C) increased (Table 4.1), signifying enhanced hydrogen bond formation from increased accessibility of the Trp fluorophores to solvent and quencher molecules. Protein without phenolic added (0 μM) also exhibited a slight red shift of ~0.5-1 nm with heat treatment as ovalbumin denatured.

Ovalbumin maxima in the presence of catechin and gallic acid shifted as much as 2-3 nm as both temperature and phenolic concentration increased. For catechin, the most significant shift appeared around the denaturation onset and peak temperatures (75-85°C), while the gallic acid shift mainly occurred at and above denaturation temperature (85-95°C). The shifts caused by

apigeninidin were more dramatic with escalating temperature and concentration. The maximum emission shift due to 25 μM apigeninidin after 95°C treatment was approximately 3 nm above ovalbumin without phenolic at 25°C, while the 50 μM treatment exhibited shifts of 6 nm ≥65°C.

4.5.3.2 Fluorescence Quenching Mechanism and Binding Parameters

For all 3 of the phenolic compounds studied, static quenching was determined to be the main mechanism of fluorescence quenching, as the obtained bimolecular quenching constant values (Table 4.2) were higher than the rate of diffusion-limited quenching (2×10^{10} M^{-1} s^{-1}, Gudgin, Lopez-Delgado, & Ware, 1983). The Stern-Volmer equation plots used to calculate K_q (Figure 4.11) were linear up to 50 μM catechin and gallic acid. However, the 50 μM apigeninidin data had to be excluded as it exhibited an exponential change in F_0 / F in comparison to lower apigeninidin concentrations, and may denote the occurrence of multi-site or multi-mechanism binding at high apigeninidin concentrations, particularly with further Trp exposure due to denaturation.

Binding parameters obtained from the double logarithmic Stern-Volmer equation plots including K_A and n (Table 4.2) show the binding sites per ovalbumin molecule generally increased with temperature for apigeninidin and catechin, but gallic acid binding decreased slightly approaching the denaturation temperature of ovalbumin. The number of apigeninidin and catechin molecules binding per ovalbumin molecule approximately doubled as temperature increased from 25-95°C. The K_A values for apigeninidin and catechin increased with temperature, and the strongest binding for all 3 of the phenolics studied occurred at 95°C.

The accessible fraction (f_a) of Trp to the quenching molecules at each treatment temperature was calculated across several concentrations for the 3 phenolics and presented in Table 4.2. Fraction can change based on the conformation of the protein (exposing or shielding Trp residues) as well as the micro-environment surrounding Trp, altering access to the fluorophore (Alston, Lasagna, Grimsley, Scholtz, Reinhart, & Pace, 2008). Below onset of denaturation, only catechin significantly altered the accessibility of Trp, with fraction accessible to apigeninidin increasing above denaturation onset (0.37 at 65°C to 0.50 at 75°C). Accessibility to gallic acid remained low until denaturation of ovalbumin. Estimated activation energy (E_a) of the interactions

(Table 4.3) was lowest for catechin at approximately 0.145 kJ/mol and highest for gallic acid (0.807 kJ/mol).

4.6 Discussion

4.6.1 Polymerization of Ovalbumin

Ovalbumin denaturation peak temperature, under aqueous conditions and at neutral pH (7.5), has been established as 85°C, with transition onset near 72°C (Photchanachai, Mehta, & Kitabatake, 2002). Weijers et al. (2003) found, within the transition range at 80°C and at pH 7, a denaturation half-time of approximately 1 min for Sigma ovalbumin, independent of protein concentration and ionic strength. Thus, heating at 95°C allowed swift denaturation of the proteins to expose cysteine and cystine groups of the hydrophobic interior for interaction with phenolic compounds and polymerization reactions. A hydrophobic environment would assist sulfhydryl-disulfide interchanges by lowering the energy required for the reactions to take place (Fernandes & Ramos, 2004).

In the Weijers et al. (2003) study, residual monomers were observed to decrease with heating temperature and time. Yet, even after extended heating (>1000 min), a small percentage of monomers remained unpolymerized. The presence of monomers in the negative control and many treatment samples in the protein-phenolic interaction gels was observed in this work also (Figures 4.3-4.7).

4.6.2 Fluorescence Quenching of Ovalbumin Tryptophan Residues

Tryptophan exhibits more sensitivity to the microcosm of its environment (Pierce & Boxer, 1995) than other fluorescing aromatic amino acid residues (phenylalanine and tyrosine), allowing for improved interpretation of spectral shifts. The nature of interactions between a quenching molecule, such as a phenolic compound, and a protein can be measured using fluorescence quenching spectroscopy (van de Weert & Stella, 2011). Static quenching refers to the formation of a complex between the fluorophore (Trp) and the quencher, whereas dynamic quenching indicates the occurrence of molecular collisions. As static quenching was determined to be the

main mechanism for each of the phenolics studied, temporarily stable, non-covalent molecular complexes were formed between the ovalbumin Trp residues and the 3 phenolics studied.

Photoexcitation of egg white lysozyme (Wu, Sheng, Xie, & Wang, 2008) and human α-lactalbumin (Permyakov, Permyakov, Deikus, Morozova-Roche, Grishchenko, Kalinichenko, et al., 2003) have been shown to reduce disulfide bonds in the near-UV wavelength range upon extended exposure. Though not studied in this work, conformational changes due to the exposure of ovalbumin to 290 nm could potentially alter the data collected in the longer-term. The maximum exposure of each sample was no more than 10 min, far below the maximal induced shifts in fluorescence intensity observed in the studies.

Of the phenolic compounds examined, only catechin emitted significant fluorescence at 340 nm, which increased with concentration and temperature treatment (data not shown). Due to the background subtraction of the treated phenolic solutions, minimal impact on the fluorescence data was expected, though increased inner filter effect, where the quencher absorbs fluorescence emitted by the Trp (Chen, Yu, & Wang, 2018), would be most likely to occur for catechin treatments. As the difference in the correction factor which would be applied (van de Weert & Stella, 2011) was less than 1% for all treatments, and no improvement to R^2 values was observed, no inner filter correction to the data was employed.

The strength of the associations, K_A (Table 4.2), indicate fairly weak binding occurred between ovalbumin and both apigeninidin and gallic acid, whereas the catechin-ovalbumin complex was likely to be slightly more stable due to higher K_A values. Increasing temperature increased K_A for catechin and apigeninidin, signifying stability of the complex rose with temperature, while gallic acid association with ovalbumin was less dependent on temperature. Higher K_A values may be a consequence of increased viscosity as ovalbumin proteins form partial gels, or due to protein unfolding and changes to protein structure rather than increased direct interaction with Trp. However, differentiation is not possible with the given data. Further studies utilizing isothermal titration calorimetry and rheology studies of protein-phenolic mixtures may provide greater clarity. The estimated activation energy, E_a, of the interactions (Table 4.3) was <1 kJ for each phenolic, signifying non-covalent interactions were responsible for phenolic-Trp complex formation.

The most stable complexes were formed at 95°C for all 3 phenolics. The spectral red shifts revealed the ovalbumin structure and conformation were opened compared to the native state,

allowing for improved hydrophobic and hydrogen bond formation. The enhanced interactions likely also contributed to further unfolding of the protein. At 340 nm, apigeninidin had the highest UV-light absorption of the phenolics (Figure 4.12), and the absorption also shifted slightly towards red light with increasing temperature (95°C). While difficult to quantify, the absorption shift may have contributed slightly to the apparent significant red shift of apigeninidin-treated ovalbumin at high concentrations (25-50 μM) and at higher temperature (≥65°C).

Binding site number for ovalbumin (Table 4.2) was dependent on temperature for both apigeninidin and catechin, but less so for gallic acid. As temperature increased, the number of binding sites rose, approximately doubling for catechin (0.685 vs 1.346) and apigeninidin (0.585 vs 0.907) from 25°C to 95°C, respectively. Gallic acid binding site number seemed to remain stable from 25-65°C at approximately 0.85, but then fell slightly upon denaturation to ~0.76. Changes in binding number, both increases and loss, could be due to slight conformational changes of the protein molecule as Trp becomes more exposed to the solvent. For apigeninidin and catechin, unfolding of the hydrophobic pocket may enhance binding to aromatic amino acid residues (including the hydrophobic pocket located Trp). The reduction in gallic acid binding number may be due to changes in its oxidative state or structure, or a nearby residue altering the specific environment near one or more Trp residues.

4.6.3 Ovalbumin Interactions with Apigeninidin

The formation of sulfhydryl-disulfide interchange products of various MW due to the presence of apigeninidin (Figure 4.3) occurred mainly as substantial band spreading ≥250 kDa (Lanes 4-9) which extended into the comb, as well as higher residual monomers compared to the negative control (Lane 2). An increase in monomer concentration would indicate more efficient reduction of some formed polymers back to monomers. This, together with the lack of significant high MW aggregation compared to the positive control (Lane 3), suggested interchanges, rather than extensive oxidation-driven polymerization, were responsible for the ensuing MW ranges. Sulfhydryl-disulfide interchanges are characterized by the reduction of a disulfide bond by a sulfhydryl group, with the subsequent formation of another disulfide bond between the original sulfhydryl and one of the newly reduced groups (Jensen, 1959), whereas cysteine oxidation by other means produces disulfide bonds or thiyl radicals without generating a sulfhydryl unit.

Polymerization of ovalbumin by inter-molecular disulfide formation was confirmed by addition of a reducing compound (β-mercaptoethanol) and subsequent polymer loss (Figure 4.8).

The 3-deoxyanthocyanidin content of sorghum endosperm (Chapter 3) is approximately 0.2-0.4 μg/mg protein (assuming a normal range of endosperm protein, ~9-12%, (Hulse, Laing, & Pearson, 1980)), corresponding most closely to Figure 4.3 Lanes 8-9. Due to the near-neutral conditions, apigeninidin (Figure 4.2a) would be present in one or more neutral forms (semi-quinone, quinone (Figure 4.2b)) rather than the flavylium cation form (Mazza & Brouillard, 1987) which could enhance π-stacking and/or hydrogen bonding to form more stable temporary interactions with amino acid residues on the protein. The high redox activity and stability of 3-deoxyanthocyanidins (Awika, Rooney, & Waniska, 2004) may allow these compounds to participate in sulfhydryl-disulfide interchanges without forming irreversible oxidation products, or formation may occur at a slow rate, allowing extensive disulfide formation to occur.

4.6.4 Interactions of Ovalbumin with *p*-Coumaric and Sinapic Acids.

Very few differences in the polymer state of ovalbumin were observed across the 5-log difference in phenolic concentration for *p*-coumaric acid (Figure 4.4) and sinapic acid (Figure 4.5). Both *p*-coumaric and sinapic acids (Figure 4.2c and 4.2d, respectively) are hydroxy-cinnamic acid derivatives, with pK_A values of 4.34 and 4.25, respectively, therefore the acids were in deprotonated form when interacting with the protein. As the pI of ovalbumin is 4.54, there may have been sufficient negative charges to repel many potential molecular interactions with the acids. Fluorescence analysis of proteins has demonstrated reduced Trp quenching by negatively charged molecules when the Trp residue is adjacent to negative charges, as electrostatic stabilization alters the electron charge transfer state (Alston, Lasagna, Grimsley, Scholtz, Reinhart, & Pace, 2008). Hydrogen bond formation would also be reduced in comparison to gallic acid, catechin, or apigeninidin.

4.6.5 Catechin Interaction with Ovalbumin

Whisked egg whites (composed primarily of ovalbumin) have been used as a “fining” agent in winemaking to remove tannins (mainly comprised of polymeric catechin, epi-catechin, and their

derivatives), but reduction of monomeric catechin concentration also occurs (Balík, Kyseláková, Tříska, Vrchotová, Veverka, Híc, et al., 2017). Catechin (Figure 4.2e), a neutral compound, also exhibited a low impact on polymerization, as shown in Figure 4.6. The disulfide bond formation and sulfhydryl-disulfide interchange reactions rely on oxidation of the cysteine thiol residues. The oxidizability of catechin, even at neutral pH, is considered low (Roginsky & Alegria, 2005), and catechins tend to dimerize (Waterhouse, 2002) when oxidized, perhaps limiting their ability to oxidize thiol groups. The apparent dynamic interchange at low catechin concentrations may then be explained by reduced opportunities for catechin to dimerize with other catechin molecules, allowing oxidized catechins to participate in the interchanges. Alternatively, because the Trp fraction accessible to catechin rose with temperature (Table 4.2), and above denaturation temperature, catechin exhibited the lowest complex-forming activation energy (Table 4.3), a simpler explanation may suffice. Greater aggregation of the protein may have occurred in the presence of catechin, leading to partial loss of these interaction products during the centrifugation step for SDS-PAGE and resulting in the lack of observed polymerization compared to the negative control.

4.6.6 Interactions Between Gallic Acid and Ovalbumin

The pK_A of gallic acid (Figure 4.2f), a benzoic acid derivative, is 4.4, indicating the deprotonated (negatively charged) form was present in the interaction system. However, unlike *p*-coumaric and sinapic acids, considerable polymerization was observed (Figure 4.7) and found to be highly dose-dependent with regard to the MW products of formed polymers. The difference in molecular interactions was likely due to the tendency of gallic acid to radicalize when deprotonated, forming a highly reactive species. The rate constant of gallic acid + ·OH reactions at pH 6.8 has been reported as 1.1×10^{10} M^{-1} s^{-1} (Dwibedy, 1999), with the hydroxyl at the *para*-position most susceptible to oxidation. The thiol (cysteine) groups of proteins are targets of radical species (Nauser, Pelling, & Schöneich, 2004), inducing oxidative conversion of the thiol groups to thiyl (cysteinyl) radicals, which readily form disulfide bonds. Other residues may also be subject to radicalization, such as tyrosine (Tyr) forming tyrosyl radicals (Nauser, Koppenol, & Schöneich, 2015).

The association constants (K_A) for gallic acid were fairly low and did not demonstrate extensive change with temperature (Table 4.2), while the Trp available to gallic as a quencher was highly dependent on temperature. Combined with a high estimated E_a for complexation (Table 4.3), it may be more likely for the gallic acid forms (deprotonated and/or radical) in the system to interact more commonly with other residues which lead to intermolecular bond formation.

The highest concentrations of gallic acid yielded pronounced amounts of extensively polymerized products (Figure 4.7, Lanes 4-6), yet the lowest concentrations also resulted in very high MW products (Lanes 14-15), albeit in much lower quantities (observed as lighter blue due to the presence of less Coomassie Blue dye). This may be indicative that an acute effect was responsible for differences in polymerization at low gallic acid amounts, rather than any dynamic sulfhydryl-disulfide bond interchanges. However, due to the highly volatile reactivity observed, gallic acid may be important to protein matrix formation as a polymerizing stimulus.

4.6.7 Contributions of Non-Amide Peptide Bonds to Polymerization

Though not examined in this study, phenolic compounds may also interact with other amino acid residues, including tyrosine (Tyr). Radicalization of Tyr promotes the formation of non-amide peptide bonds, including disulfide and dityrosine linkages (Bhattacharjee, Deterding, Jiang, Bonini, Tomer, Ramirez, et al., 2007), with proximity of Cys residues to Tyr facilitating radical transfer. It is consequently worth noting the ovalbumin Tyr29 residue is Cα-adjacent to the Cys30 residue (Stein, Leslie, Finch, & Carrell, 1991), and phenolic interactions with Tyr29 may potentially augment disulfide formation or exchanges between Cys30 and other Cys residues. Examination of treated ovalbumin (e.g., by protease digestion and mass spectrometry) would allow for better discernment of specific residues involved in disulfide bond formation (Na, Paek, Choi, Kim, Lee, & Kwon, 2015; Wu, Sheng, Xie, & Wang, 2008).

The formation of dityrosine (and possibly tyrosine-lysine, lysine-lysine, or other lysine isopeptide linkages due to reactive ϵ-amino groups of lysine residues) was implicated and could have contributed to non-amide peptide bond formation observed in the presence of gallic acid (Figure 4.9). Dityrosine and other isopeptide bonds are oxidative covalent cross-links between the side chains of amino acid residues, away from the main peptide (Cα) chain, and are resistant to reduction by β-mercaptoethanol. The appearance on a reduced gel of bands of higher MW would

indicate the presence of one or more types of non-reducible intermolecular bonds, observed mainly in Figure 4.9 (gallic acid) Lanes 4-8 as dimers, trimers, tetramers, and higher polymers.

Addition of these bond types to the polymer conformation would likely increase resistance to protein digestion by increasing rigidity of the structure and also modifying the precise chemical nature of the structure presented to proteases (Erbersdobler, 1989). Dityrosine linkages have been considered in biomaterial development (Partlow, Applegate, Omenetto, & Kaplan, 2016) and would supplement matrix design by adding further complexity to the structure. However, administration of foods containing high amounts of dityrosine may have negative health effects, demonstrating impaired glucose tolerance and insulin production in mice (Ding, Cheng, Li, Wu, Yang, Shi, et al., 2017; Ding, Li, Cheng, Ran, Wu, Shi, et al., 2017; Ding, Tang, Cheng, Wang, Li, Wu, et al., 2017).

4.7 Conclusions

The interactions between ovalbumin and phenolic compounds are dependent on the form of the phenolic, temperature, and the accessibility of reactive amino acid residues. Disulfide bond formation is the main mode of polymerization arising from interactions of phenolics and ovalbumin above the denaturation temperature, though other intermolecular non-amide peptide bond formation occurred, especially due to the presence of gallic acid at near-neutral pH, which may be an important polymerization stimulus. While the 3 phenolics all produced a red spectral shift, apigeninidin caused the most significant change in ovalbumin conformation approaching and above the denaturation temperature. Combined with increased accessible Trp fraction, apigeninidin appears to have had the greatest effect on the micro-environment surrounding the Trp residues while catechin complexations were easier to form and transpired at lower temperatures. These data seem to confirm apigeninidin (and possibly other 3-deoxyanthocyanidins) interacts with proteins in seemingly unique fashion compared to more common phenolic compounds, leading to non-aggregative protein polymerization which results in the extensive disulfide cross-linked kafirin matrices around starch granules found in sorghum products. The 3-deoxyanthocyanidins therefore emerge as prospective molecules for enhancing protein matrix stability in other cereal food products to slow starch digestion.

References

Aguilera, J. M. (2018). The food matrix: implications in processing, nutrition and health. Critical Reviews in Food Science and Nutrition, 1-18.

Alston, R. W., Lasagna, M., Grimsley, G. R., Scholtz, J. M., Reinhart, G. D., & Pace, C. N. (2008). Peptide Sequence and Conformation Strongly Influence Tryptophan Fluorescence. Biophysical Journal, 94(6), 2280-2287.

Awika, J. M., Rooney, L. W., & Waniska, R. D. (2004). Properties of 3-deoxyanthocyanins from sorghum. Journal of Agricultural and Food Chemistry, 52(14), 4388.

Balík, J., Kyseláková, M., Tříska, J., Vrchotová, N., Veverka, J., Híc, P., Totušek, J., & Lefnerová, D. (2017). The changes of selected phenolic substances in wine technology. Czech Journal of Food Sciences, 26, S3-S12.

Bhattacharjee, S., Deterding, L. J., Jiang, J., Bonini, M. G., Tomer, K. B., Ramirez, D. C., & Mason, R. P. (2007). Electron Transfer between a Tyrosyl Radical and a Cysteine Residue in Hemoproteins: Spin Trapping Analysis. Journal of the American Chemical Society, 129(44), 13493-13501.

Chen, S., Yu, Y.-L., & Wang, J.-H. (2018). Inner filter effect-based fluorescent sensing systems: A review. Analytica Chimica Acta, 999, 13-26.

Choi, S., Woo, H., Ko, S., & Moon, T. (2008). Confocal Laser Scanning Microscopy to Investigate the Effect of Cooking and Sodium Bisulfite on In Vitro Digestibility of Waxy Sorghum Flour. Cereal Chemistry, 85(1), 65-69.

Cholewinski, J. L. (2010). Sorghum endosperm components responsible for promoting protein polymerization through sulfhydryl-disulfide interchange. Purdue University.

Ding, Y.-Y., Cheng, X.-R., Li, Z.-Q., Wu, S.-J., Yang, Y., Shi, Y.-H., & Le, G.-W. (2017). Effect of dietary oxidized tyrosine products on insulin secretion via the oxidative stress-induced mitochondria damage in mice pancreas. RSC Advances, 7(43), 26809-26826.

Ding, Y.-Y., Li, Z.-Q., Cheng, X.-R., Ran, Y.-M., Wu, S.-J., Shi, Y., & Le, G. (2017). Dityrosine administration induces dysfunction of insulin secretion accompanied by diminished thyroid hormones T3 function in pancreas of mice. Amino Acids, 49(8), 1401-1414.

Ding, Y.-Y., Tang, X., Cheng, X.-R., Wang, F.-F., Li, Z.-Q., Wu, S.-J., Kou, X.-R., Shi, Y., & Le, G. (2017). Effects of dietary oxidized tyrosine products on insulin secretion via the thyroid hormone T3-regulated TRβ1–Akt–mTOR pathway in the pancreas. RSC Advances, 7(86), 54610-54625.

Dwibedy, P. (1999). Pulse Radiolysis Studies on Redox Reactions of Gallic Acid: One Electron Oxidation of Gallic Acid by Gallic Acid-OH Adduct. Physical Chemistry Chemical Physics, 1, 1915-1918.

Erbersdobler, H. F. (1989). Protein Reactions during Food Processing and Storage — Their Relevance to Human Nutrition. In J. C. Somogyi & H. R. Müller (Eds.), Nutritional Impact of Food Processing, (pp. 140-155). Basel: Karger.

Ezeogu, L. I., Duodu, K. G., Emmambux, M. N., & Taylor, J. R. N. (2008). Influence of Cooking Conditions on the Protein Matrix of Sorghum and Maize Endosperm Flours. Cereal Chemistry, 85(3), 397-402.

Fernandes, P. A., & Ramos, M. J. (2004). Theoretical Insights into the Mechanism for Thiol/Disulfide Exchange. Chemistry – A European Journal, 10(1), 257-266.

Gudgin, E., Lopez-Delgado, R., & Ware, W. R. (1983). Photophysics of tryptophan in water, deuterium oxide and in nonaqueous solvents. The Journal of Physical Chemistry, 87(9), 1559-1565.

Hulse, J. H., Laing, E. M., & Pearson, O. E. (1980). Sorghum and the Millets: Their Composition and Nutritive Value. London: Academic Press.

Jensen, E. V. (1959). Sulfhydryl-Disulfide Interchange. Science, 130(3385), 1319-1323.

Lakowicz, J. R. (1999). Principles of Fluorescence Spectroscopy (2nd ed.). Boston, MA: Springer.

Lakowicz, J. R., Gryczynski, I., Gryczynski, Z., & Dattelbaum, J. D. (1999). Anisotropy-Based Sensing with Reference Fluorophores. Analytical Biochemistry, 267(2), 397-405.

Mazza, G., & Brouillard, R. (1987). Color stability and structural transformations of cyanidin 3,5-diglucoside and four 3-deoxyanthocyanins in aqueous solutions. Journal of Agricultural and Food Chemistry, 35(3), 422-426.

McClements, D. J., Decker, E. A., Park, Y., & Weiss, J. (2008). Designing Food Structure to Control Stability, Digestion, Release and Absorption of Lipophilic Food Components. Food Biophysics, 3(2), 219-228.

Moser, S., Chegeni, M., Jones, O. G., Liceaga, A., & Ferruzzi, M. G. (2014). The effect of milk proteins on the bioaccessibility of green tea flavan-3-ols. Food Research International, 66(Supplement C), 297-305.

Na, S., Paek, E., Choi, J.-S., Kim, D., Lee, S. J., & Kwon, J. (2015). Characterization of disulfide bonds by planned digestion and tandem mass spectrometry. Molecular BioSystems, 11(4), 1156-1164.

Nauser, T., Koppenol, W. H., & Schöneich, C. (2015). Protein thiyl radical reactions and product formation: a kinetic simulation. Free Radical Biology and Medicine, 80, 158-163.

Nauser, T., Pelling, J., & Schöneich, C. (2004). Thiyl Radical Reaction with Amino Acid Side Chains: Rate Constants for Hydrogen Transfer and Relevance for Posttranslational Protein Modification. Chemical Research in Toxicology, 17(10), 1323-1328.

Ognjenović, J., Stojadinović, M., Milčić, M., Apostolović, D., Vesić, J., Stambolić, I., Atanasković-Marković, M., Simonović, M., & Velickovic, T. C. (2014). Interactions of epigallo-catechin 3-gallate and ovalbumin, the major allergen of egg white. Food Chemistry, 164, 36-43.

Parada, J., & Aguilera, J. M. (2007). Food Microstructure Affects the Bioavailability of Several Nutrients. Journal of Food Science, 72(2), R21-R32.

Partlow, B. P., Applegate, M. B., Omenetto, F. G., & Kaplan, D. L. (2016). Dityrosine Cross-Linking in Designing Biomaterials. ACS Biomaterials Science & Engineering, 2(12), 2108-2121.

Permyakov, E. A., Permyakov, S. E., Deikus, G. Y., Morozova-Roche, L. A., Grishchenko, V. M., Kalinichenko, L. P., & Uversky, V. N. (2003). Ultraviolet illumination-induced reduction of α-lactalbumin disulfide bridges. Proteins: Structure, Function, and Bioinformatics, 51(4), 498-503.

Photchanachai, S., Mehta, A., & Kitabatake, N. (2002). Heating of an Ovalbumin Solution at Neutral pH and High Temperature. Bioscience, Biotechnology, and Biochemistry, 66(8), 1635-1640.

Pierce, D. W., & Boxer, S. G. (1995). Stark effect spectroscopy of tryptophan. Biophysical Journal, 68(4), 1583-1591.

Renzetti, S., Dal Bello, F., & Arendt, E. K. (2008). Microstructure, fundamental rheology and baking characteristics of batters and breads from different gluten-free flours treated with a microbial transglutaminase. Journal of Cereal Science, 48(1), 33-45.

Roginsky, V., & Alegria, A. E. (2005). Oxidation of Tea Extracts and Tea Catechins by Molecular Oxygen. Journal of Agricultural and Food Chemistry, 53(11), 4529-4535.

Schneider, C. A., Rasband, W. S., & Eliceiri, K. W. (2012). NIH Image to ImageJ: 25 years of image analysis. Nature Methods, 9, 671-675.

Singh, J., Dartois, A., & Kaur, L. (2010). Starch digestibility in food matrix: a review. Trends in Food Science & Technology, 21(4), 168-180.

Stein, P. E., Leslie, A. G. W., Finch, J. T., & Carrell, R. W. (1991). Crystal structure of uncleaved ovalbumin at 1·95 Å resolution. Journal of Molecular Biology, 221(3), 941-959.

van de Weert, M., & Stella, L. (2011). Fluorescence quenching and ligand binding: A critical discussion of a popular methodology. Journal of Molecular Structure, 998(1), 144-150.

Waterhouse, A. L. (2002). Wine Phenolics. Annals of the New York Academy of Sciences, 957(1), 21-36.

Weijers, M., Barneveld, P. A., Cohen Stuart, M. A., & Visschers, R. W. (2003). Heat-induced denaturation and aggregation of ovalbumin at neutral pH described by irreversible first-order kinetics. Protein Science, 12(12), 2693-2703.

Wright, T. H., Qian, H. X., & Huber, R. (1990). Crystal structure of plakalbumin, a proteolytically nicked form of ovalbumin: Its relationship to the structure of cleaved α-1-proteinase inhibitor. Journal of Molecular Biology, 213(3), 513-528.

Wu, L.-Z., Sheng, Y.-B., Xie, J.-B., & Wang, W. (2008). Photoexcitation of tryptophan groups induced reduction of disulfide bonds in hen egg white lysozyme. Journal of Molecular Structure, 882(1), 101-106.

Xie, L., Wehling, R. L., Ciftci, O., & Zhang, Y. (2017). Formation of complexes between tannic acid with bovine serum albumin, egg ovalbumin and bovine beta-lactoglobulin. Food Research International, 102, 195-202.

Zhou, L., & Elias, R. J. (2013). Antioxidant and pro-oxidant activity of (−)-epigallocatechin-3-gallate in food emulsions: Influence of pH and phenolic concentration. Food Chemistry, 138(2-3), 1503-1509.

A)

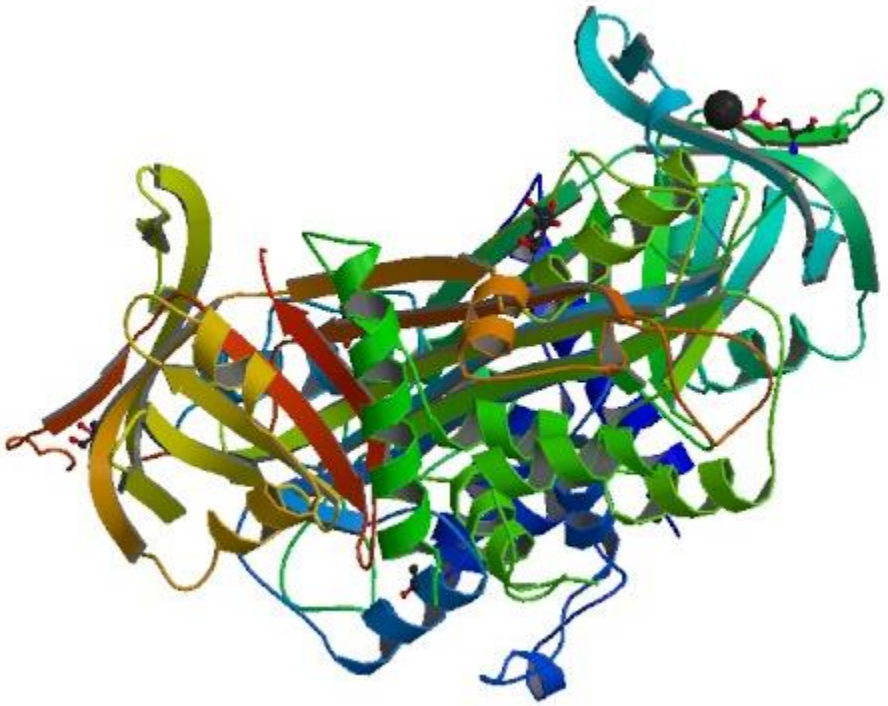

B)

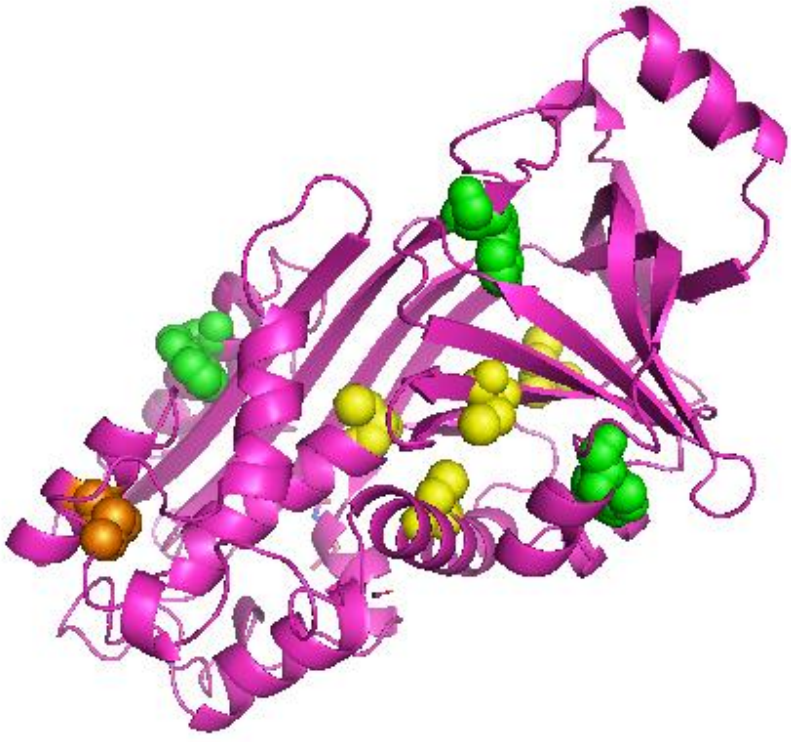

Figure 4.1 Structure of ovalbumin A) as cartoon backbone from PDB, B) as PyMOL cartoon image emphasizing presence of Trp residues (green), Cys residues (yellow), and the native disulfide bond (orange).

A)

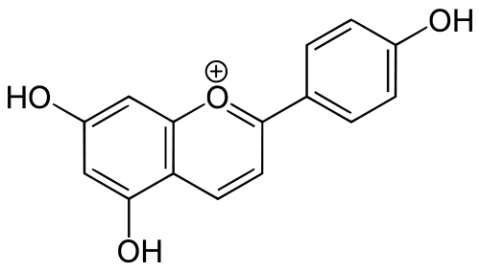

B)

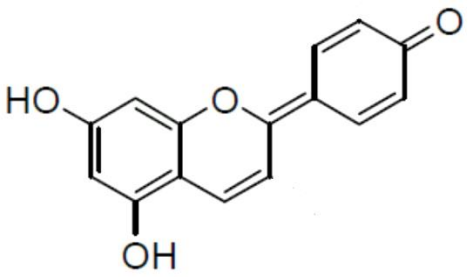

C)

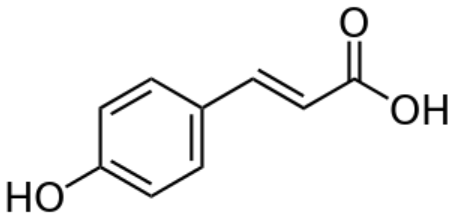

D)

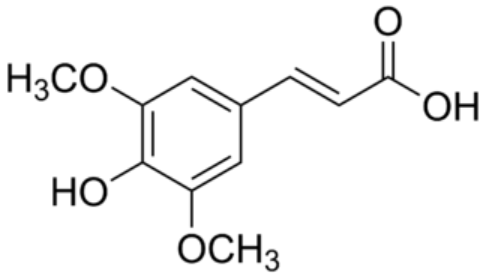

E)

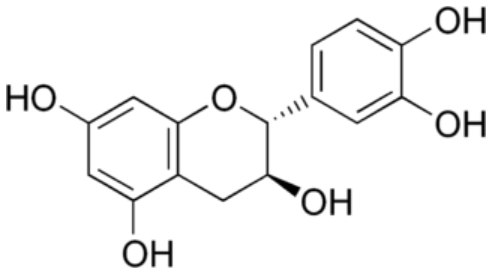

F)

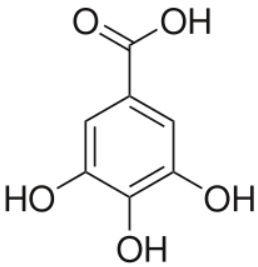

Figure 4.2 Structures of phenolic compounds utilized in phenolic-ovalbumin interaction studies. A) Apigeninidin flavylium cation form and B) Apgeninidin quinone form, C) *p*-Coumaric Acid, D) Sinapic Acid, E) (+)-Catechin, F) Gallic Acid

Images obtained through public domain files on Wikimedia Commons.

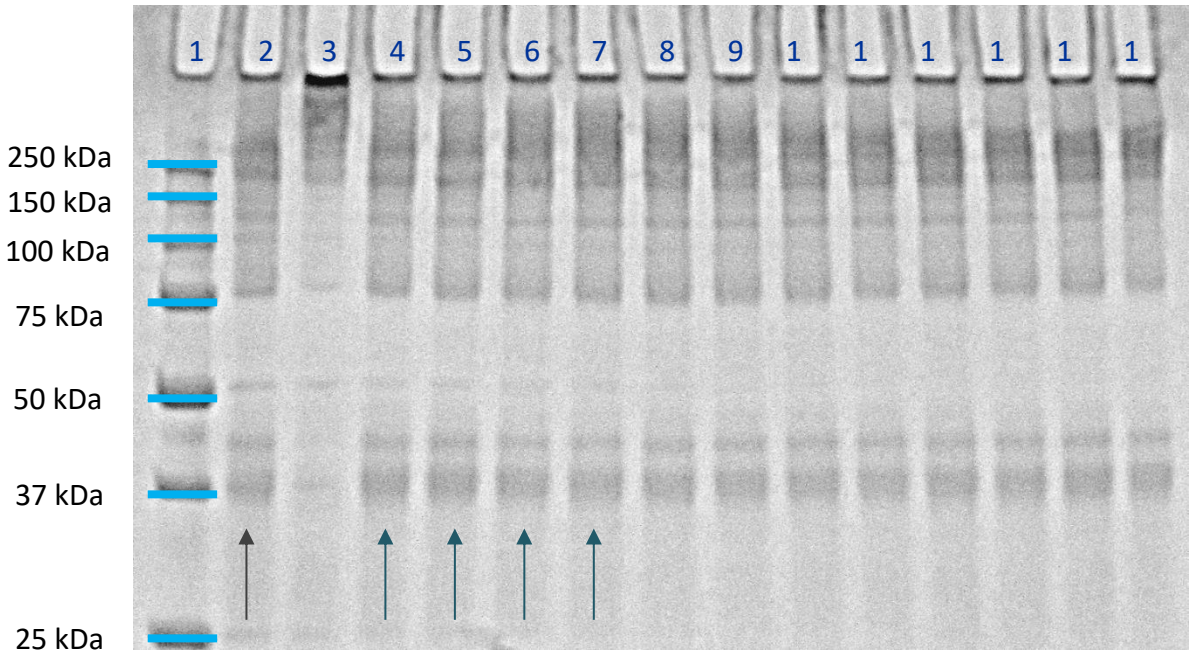

Figure 4.3 SDS-PAGE gel demonstrating polymerizing interactions of apigeninidin with ovalbumin.

Lane 1: Broad Range Standard (250-25 kDa, gel cropped)
Lane 2: Negative Control (ovalbumin + buffer)
Lane 3: Positive Control (ovalbumin + 1% potassium bromate)
Lane 4: 2.1 µg Apigeninidin / mg Ovalbumin
Lane 5: 2.1 µg Apigeninidin / mg Ovalbumin
Lane 6: 0.71 µg Apigeninidin / mg Ovalbumin
Lane 7: 0.71 µg Apigeninidin / mg Ovalbumin
Lane 8: 0.21 µg Apigeninidin / mg Ovalbumin
Lane 9: 0.21 µg Apigeninidin / mg Ovalbumin
Lane 10: 71 ng Apigeninidin / mg Ovalbumin
Lane 11: 71 ng Apigeninidin / mg Ovalbumin
Lane 12: 21 ng Apigeninidin / mg Ovalbumin
Lane 13: 21 ng Apigeninidin / mg Ovalbumin
Lane 14: 2.1 ng Apigeninidin / mg Ovalbumin
Lane 15: 2.1 ng Apigeninidin / mg Ovalbumin

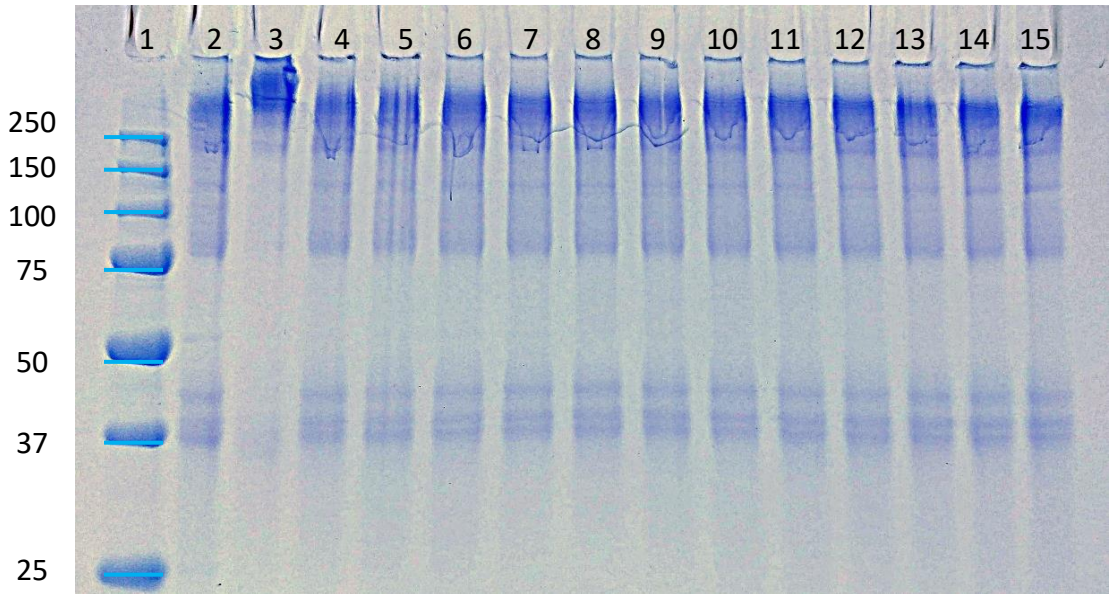

Figure 4.4 SDS-PAGE gel demonstrating polymerizing interactions of *p*-coumaric acid with ovalbumin.

Lane 1: Broad Range Standard (250-25 kDa, gel cropped)
Lane 2: Negative Control (ovalbumin + buffer)
Lane 3: Positive Control (ovalbumin + 1% potassium bromate)
Lane 4: 10 µg *p*-Coumaric Acid / mg Ovalbumin
Lane 5: 5 µg2 *p*-Coumaric Acid / mg Ovalbumin
Lane 6: 2.5 µg *p*-Coumaric Acid / mg Ovalbumin
Lane 7: 1 µg *p*-Coumaric Acid / mg Ovalbumin
Lane 8: 0.5 µg *p*-Coumaric Acid / mg Ovalbumin
Lane 9: 0.1 µg *p*-Coumaric Acid / mg Ovalbumin
Lane 10: 50 ng *p*-Coumaric Acid / mg Ovalbumin
Lane 11: 10 ng *p*-Coumaric Acid / mg Ovalbumin
Lane 12: 5 ng *p*-Coumaric Acid / mg Ovalbumin
Lane 13: 1 ng *p*-Coumaric Acid / mg Ovalbumin
Lane 14: 0.5 ng *p*-Coumaric Acid / mg Ovalbumin
Lane 15: 0.1 ng *p*-Coumaric Acid / mg Ovalbumin

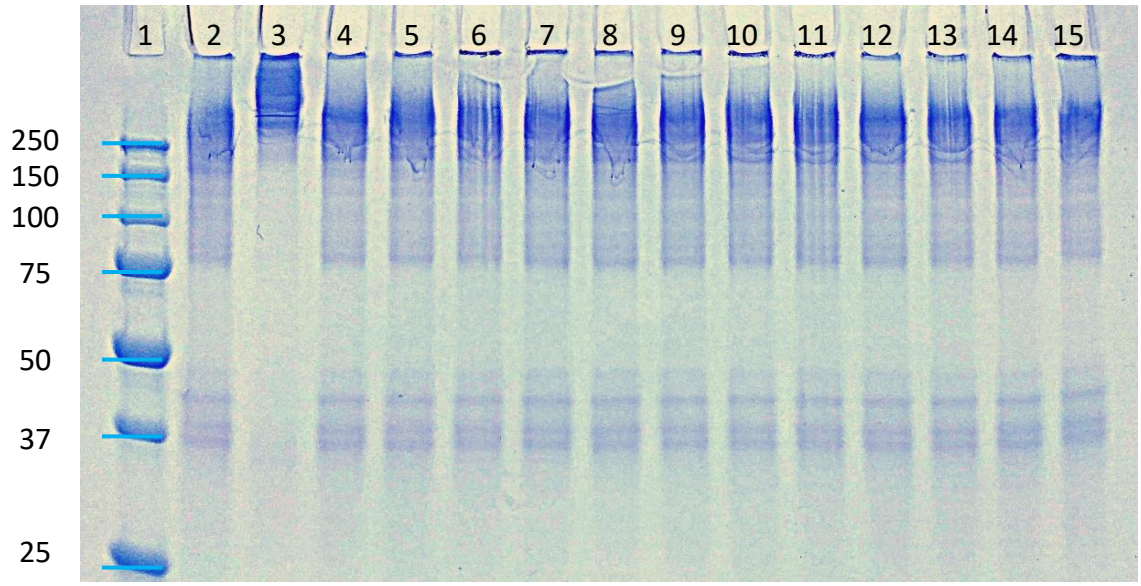

Figure 4.5 SDS-PAGE gel demonstrating polymerizing interactions of sinapic acid with ovalbumin.

Lane 1: Broad Range Standard (250-25 kDa, gel cropped)
Lane 2: Negative Control (ovalbumin + buffer)
Lane 3: Positive Control (ovalbumin + 1% potassium bromate)
Lane 4: 10 µg Sinapic Acid / mg Ovalbumin
Lane 5: 5 µg2 Sinapic Acid / mg Ovalbumin
Lane 6: 2.5 µg Sinapic Acid / mg Ovalbumin
Lane 7: 1 µg Sinapic Acid / mg Ovalbumin
Lane 8: 0.5 µg Sinapic Acid / mg Ovalbumin
Lane 9: 0.1 µg Sinapic Acid / mg Ovalbumin
Lane 10: 50 ng Sinapic Acid / mg Ovalbumin
Lane 11: 10 ng Sinapic Acid / mg Ovalbumin
Lane 12: 5 ng Sinapic Acid / mg Ovalbumin
Lane 13: 1 ng Sinapic Acid / mg Ovalbumin
Lane 14: 0.5 ng Sinapic Acid / mg Ovalbumin
Lane 15: 0.1 ng Sinapic Acid / mg Ovalbumin

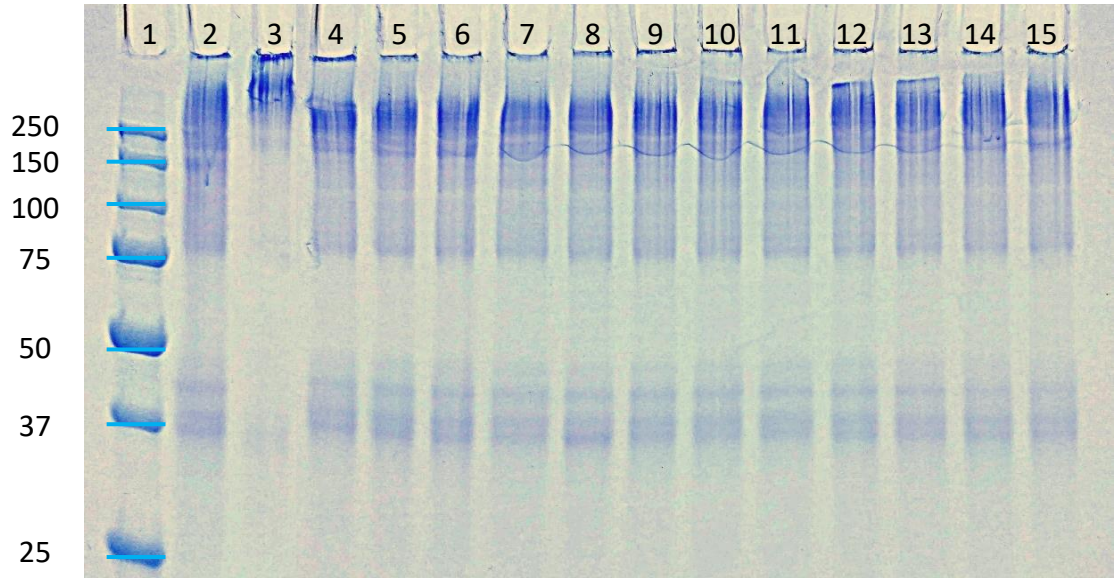

Figure 4.6 SDS-PAGE gel demonstrating polymerizing interactions of catechin with ovalbumin.

Lane 1: Broad Range Standard (250-25 kDa, gel cropped)
Lane 2: Negative Control (ovalbumin + buffer)
Lane 3: Positive Control (ovalbumin + 1% potassium bromate)
Lane 4: 10 µg Catechin / mg Ovalbumin
Lane 5: 5 µg2 Catechin / mg Ovalbumin
Lane 6: 2.5 µg Catechin / mg Ovalbumin
Lane 7: 1 µg Catechin / mg Ovalbumin
Lane 8: 0.5 µg Catechin / mg Ovalbumin
Lane 9: 0.1 µg Catechin / mg Ovalbumin
Lane 10: 50 ng Catechin / mg Ovalbumin
Lane 11: 10 ng Catechin / mg Ovalbumin
Lane 12: 5 ng Catechin / mg Ovalbumin
Lane 13: 1 ng Catechin / mg Ovalbumin
Lane 14: 0.5 ng Catechin / mg Ovalbumin
Lane 15: 0.1 ng Catechin / mg Ovalbumin

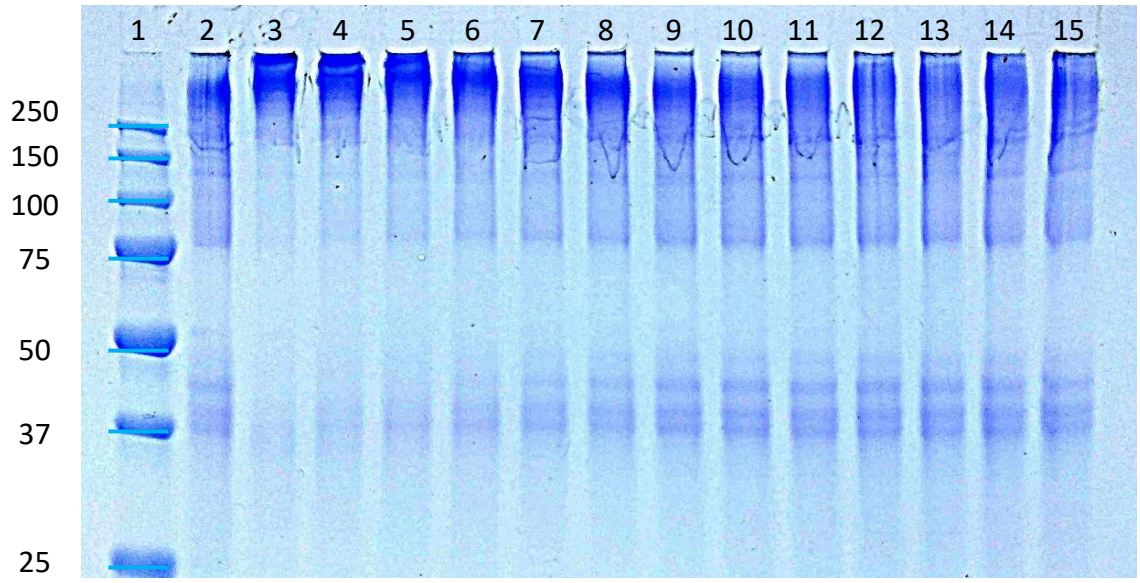

Figure 4.7 SDS-PAGE gel demonstrating polymerizing interactions of gallic acid with ovalbumin.

Lane 1: Broad Range Standard (250-25 kDa, gel cropped)
Lane 2: Negative Control (ovalbumin + buffer)
Lane 3: Positive Control (ovalbumin + 1% potassium bromate)
Lane 4: 10 µg Gallic Acid / mg Ovalbumin
Lane 5: 5 µg2 Gallic Acid / mg Ovalbumin
Lane 6: 2.5 µg Gallic Acid / mg Ovalbumin
Lane 7: 1 µg Gallic Acid / mg Ovalbumin
Lane 8: 0.5 µg Gallic Acid / mg Ovalbumin
Lane 9: 0.1 µg Gallic Acid / mg Ovalbumin
Lane 10: 50 ng Gallic Acid / mg Ovalbumin
Lane 11: 10 ng Gallic Acid / mg Ovalbumin
Lane 12: 5 ng Gallic Acid / mg Ovalbumin
Lane 13: 1 ng Gallic Acid / mg Ovalbumin
Lane 14: 0.5 ng Gallic Acid / mg Ovalbumin
Lane 15: 0.1 ng Gallic Acid / mg Ovalbumin

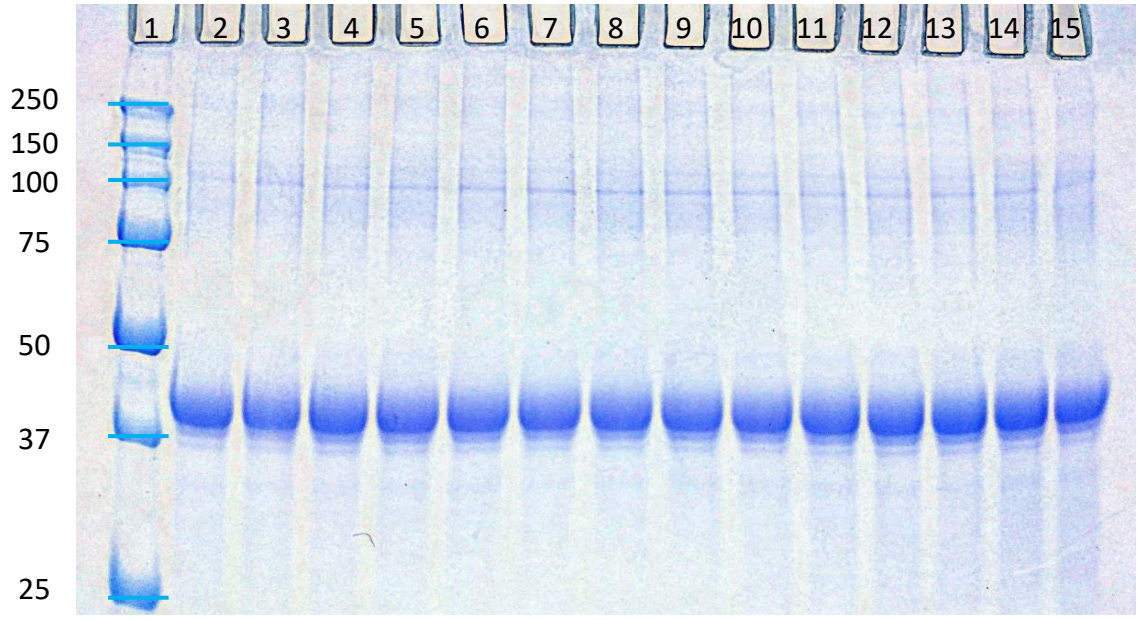

Figure 4.8 SDS-PAGE gel demonstrating remaining polymerizing interactions from apigeninidin with ovalbumin following disulfide bond reduction.

Lane 1: Broad Range Standard (250-25 kDa, gel cropped)
Lane 2: Negative Control (ovalbumin + buffer)
Lane 3: Positive Control (ovalbumin + 1% potassium bromate)
Lane 4: 10 µg Apigeninidin / mg Ovalbumin
Lane 5: 5 µg2 Apigeninidin / mg Ovalbumin
Lane 6: 2.5 µg Apigeninidin / mg Ovalbumin
Lane 7: 1 µg Apigeninidin / mg Ovalbumin
Lane 8: 0.5 µg Apigeninidin / mg Ovalbumin
Lane 9: 0.1 µg Apigeninidin / mg Ovalbumin
Lane 10: 50 ng Apigeninidin / mg Ovalbumin
Lane 11: 10 ng Apigeninidin / mg Ovalbumin
Lane 12: 5 ng Apigeninidin / mg Ovalbumin
Lane 13: 1 ng Apigeninidin / mg Ovalbumin
Lane 14: 0.5 ng Apigeninidin / mg Ovalbumin
Lane 15: 0.1 ng Apigeninidin Catechin / mg Ovalbumin

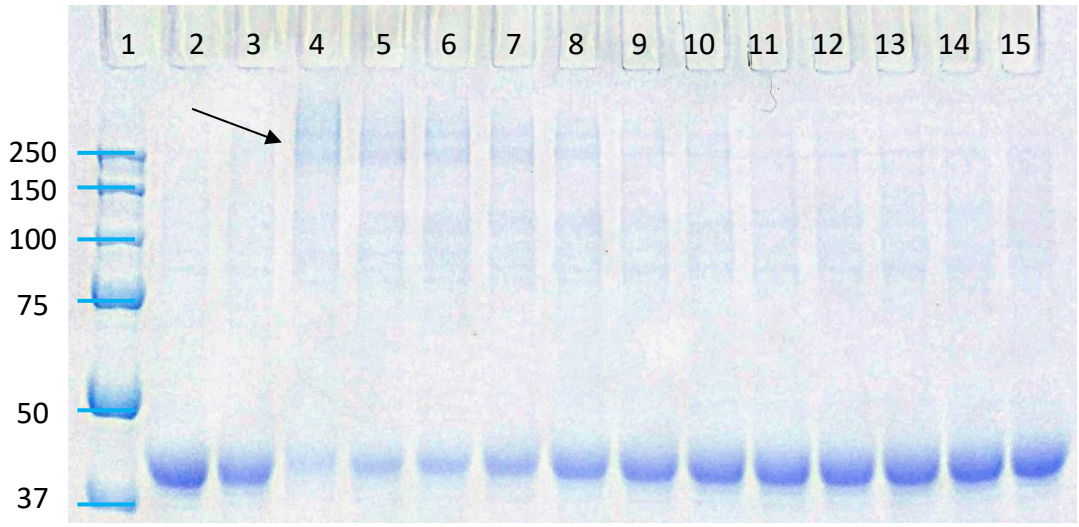

Figure 4.9 SDS-PAGE gel demonstrating remaining polymerizing interactions from gallic acid with ovalbumin following disulfide bond reduction.
Arrow indicates presence of non-reducing polymers.

Lane 1: Broad Range Standard (250-37 kDa, gel cropped)
Lane 2: Negative Control (ovalbumin + buffer)
Lane 3: Positive Control (ovalbumin + 1% potassium bromate)
Lane 4: 10 µg Gallic Acid / mg Ovalbumin
Lane 5: 5 µg2 Gallic Acid / mg Ovalbumin
Lane 6: 2.5 µg Gallic Acid / mg Ovalbumin
Lane 7: 1 µg Gallic Acid / mg Ovalbumin
Lane 8: 0.5 µg Gallic Acid / mg Ovalbumin
Lane 9: 0.1 µg Gallic Acid / mg Ovalbumin
Lane 10: 50 ng Gallic Acid / mg Ovalbumin
Lane 11: 10 ng Gallic Acid / mg Ovalbumin
Lane 12: 5 ng Gallic Acid / mg Ovalbumin
Lane 13: 1 ng Gallic Acid / mg Ovalbumin
Lane 14: 0.5 ng Gallic Acid / mg Ovalbumin
Lane 15: 0.1 ng Gallic Acid / mg Ovalbumin

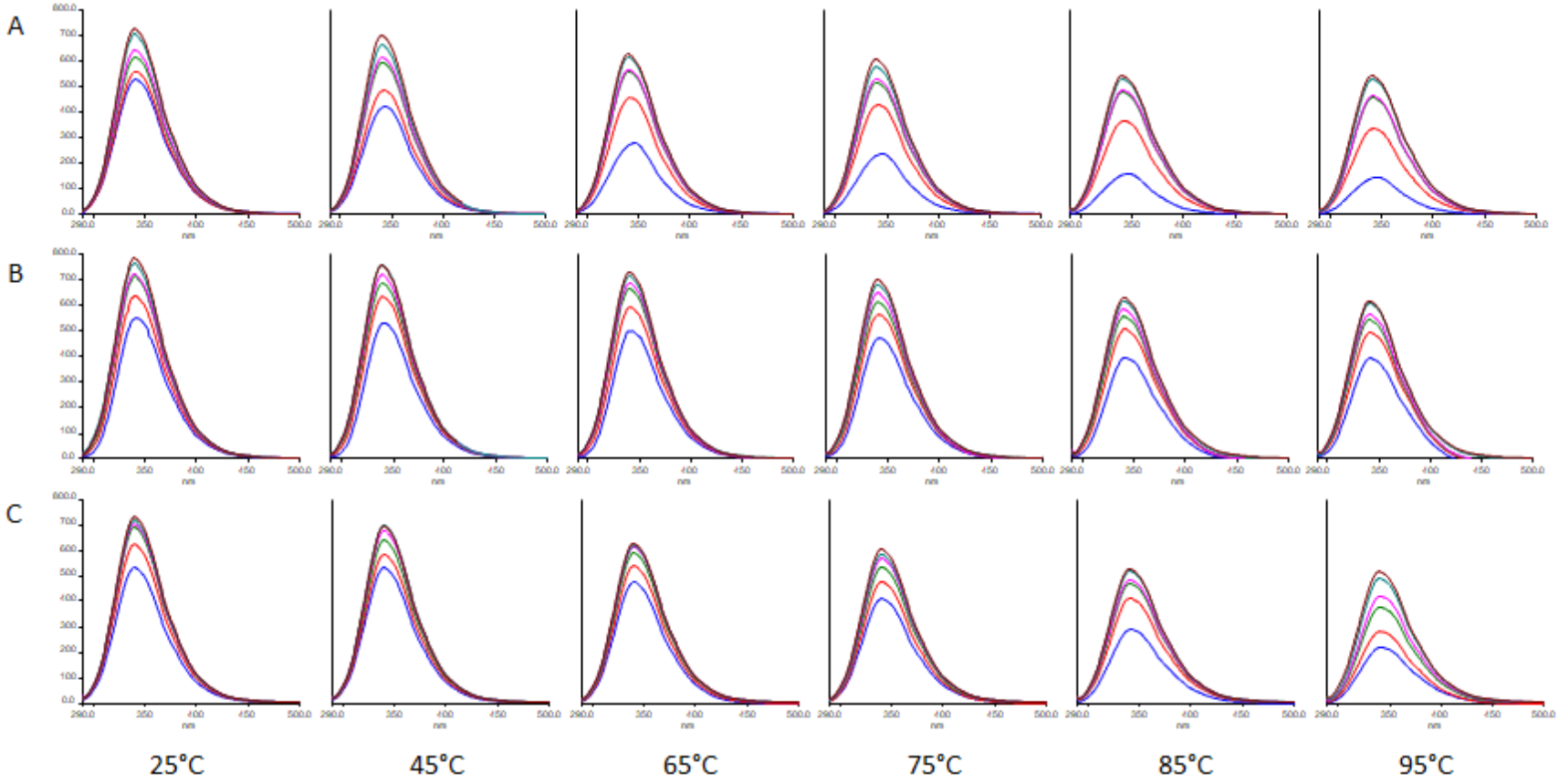

Figure 4.10 The effect of A) Apigeninidin, B) Catechin, and C) Gallic Acid (0-50 μM) on the tryptophan quenching of 5 μM ovalbumin at different temperatures.

Table 4.1 Shift in ovalbumin maximum fluorescence emission intensity wavelength (nm) due to changes in phenolic concentration (0-50 μM) and temperature (25-95°C).

Apigeninidin	25°C	±SD[1]	45°C	±SD	65°C	±SD	75°C	±SD	85°C	±SD	95°C	±SD
0	339.33	0.94	340.33	0.24	340.13	0.41	340.70	0.68	340.42	0.34	340.77	0.58
1	339.67	0.47	340.25	0.90	340.60	0.58	340.75	0.63	340.89	0.51	341.05	0.32
5	340.67	0.62	340.40	0.37	341.17	0.47	341.50	0.65	341.95	0.72	341.50	0.63
10	340.33	0.85	340.83	0.47	341.42	0.45	341.50	0.61	341.79	0.69	341.80	0.40
25	341.33	0.85	342.90	0.73	342.33	0.75	342.67	0.75	343.21	0.52	343.00	0.71
50	340.67	0.24	342.90	0.86	346.00	0.45	346.25	0.95	346.31	1.03	346.20	1.08
Catechin	**25°C**	**±SD**	**45°C**	**±SD**	**65°C**	**±SD**	**75°C**	**±SD**	**85°C**	**±SD**	**95°C**	**±SD**
0	340.00	0.41	340.50	1.26	340.50	0.35	340.83	1.49	340.88	0.41	340.63	0.65
1	340.50	0.41	340.20	0.24	340.00	0.00	339.70	0.81	341.00	0.71	340.83	0.62
5	340.80	0.24	340.08	0.61	340.50	0.41	340.83	1.11	340.80	0.51	341.25	0.83
10	340.33	0.47	340.67	0.69	340.10	0.58	340.92	0.34	341.58	0.84	340.93	0.44
25	341.17	0.24	341.00	0.71	341.10	0.92	342.50	1.30	341.83	0.62	340.33	0.47
50	341.67	0.24	341.50	0.84	341.25	1.95	342.00	0.00	342.93	1.80	340.95	0.37
Gallic Acid	**25°C**	**±SD**	**45°C**	**±SD**	**65°C**	**±SD**	**75°C**	**±SD**	**85°C**	**±SD**	**95°C**	**±SD**
0	339.33	0.94	340.33	0.24	340.13	0.41	340.70	0.68	340.50	0.82	340.77	0.58
1	340.67	0.24	340.67	0.69	340.67	0.69	340.42	0.45	341.10	0.58	341.34	0.65
5	340.25	0.75	340.80	0.24	340.80	0.24	341.08	0.53	341.39	0.66	342.00	0.58
10	340.13	0.41	340.25	0.25	340.25	0.25	340.83	0.47	341.17	0.24	341.64	0.35
25	339.83	0.24	340.80	0.40	340.80	0.40	340.67	0.69	341.53	0.62	341.88	0.41
50	340.38	0.54	340.50	0.65	340.50	0.65	340.92	0.53	342.70	0.56	341.17	0.37

[1] SD, Standard Deviation

Table 4.2 Parameters of the quenching constant (K_q), binding constant (K_A), binding site number (n), dissociation constant (K_D), and fraction of Trp available to the quencher molecules (f_a) between ovalbumin and apigeninidin, catechin, and gallic acid under different temperature conditions.

	Phenolic	**25°C**	**45°C**	**65°C**	**75°C**	**85°C**	**95°C**
K_q (M^{-1} s^{-1})	Apigeninidin	1.38E+12	1.87E+12	1.51E+12	1.67E+12	1.89E+12	2.41E+12
	R^2	0.94	0.98	0.98	0.96	0.97	0.97
	Catechin	1.10E+12	8.40E+11	8.91E+11	9.16E+11	1.07E+12	1.10E+12
	R^2	0.97	0.99	0.99	0.99	0.99	0.99
	Gallic Acid	6.88E+11	6.66E+11	6.79E+11	1.02E+12	1.76E+12	2.90E+12
	R^2	0.99	0.99	0.99	0.99	0.99	0.98
n	Apigeninidin	0.585	0.687	0.645	0.659	0.732	0.907
	Catechin	0.685	0.884	0.940	0.951	0.938	1.346
	Gallic Acid	0.845	0.850	0.854	0.772	0.741	0.763
K_A (M^{-1})	Apigeninidin	1.60E+02	6.03E+02	2.85E+02	3.91E+02	8.56E+02	8.12E+03
	Catechin	3.54E+02	2.72E+03	4.84E+03	5.62E+03	5.88E+03	4.67E+05
	Gallic Acid	1.32E+03	1.47E+03	1.31E+03	9.56E+02	1.11E+03	2.58E+03
K_D (mM)	Apigeninidin	6.23	1.66	3.507	2.555	1.168	0.123
	Catechin	2.83	0.367	0.207	0.178	0.170	2.14E-03
	Gallic Acid	0.755	0.682	0.763	1.05	0.898	0.388
R^2 values for fitting n, K_A, and K_D	Apigeninidin	0.99	0.99	0.95	0.96	0.92	0.96
	Catechin	0.99	0.99	0.99	0.99	0.99	0.94
	Gallic Acid	0.99	0.99	0.94	0.99	0.98	0.99
f_a	Apigeninidin	0.31	0.36	0.37	0.50	0.77	1.08
	R^2	0.99	0.98	0.96	0.99	0.99	0.99
	Catechin	0.26	0.43	0.60	0.71	0.98	0.98
	R^2	0.97	0.98	1.00	0.99	0.99	0.99
	Gallic Acid	0.23	0.26	0.23	0.26	0.36	0.56
	R^2	0.99	0.99	1.00	0.99	0.96	0.97

Table 4.3 Estimated activation energy for phenolic-Trp complex formation between 75-95°C.

Apigeninidin	0.283 kJ/mol	$R^2 = 0.96$
Catechin	0.145 kJ/mol	$R^2 = 0.89$
Gallic Acid	0.807 kJ/mol	$R^2 = 0.99$

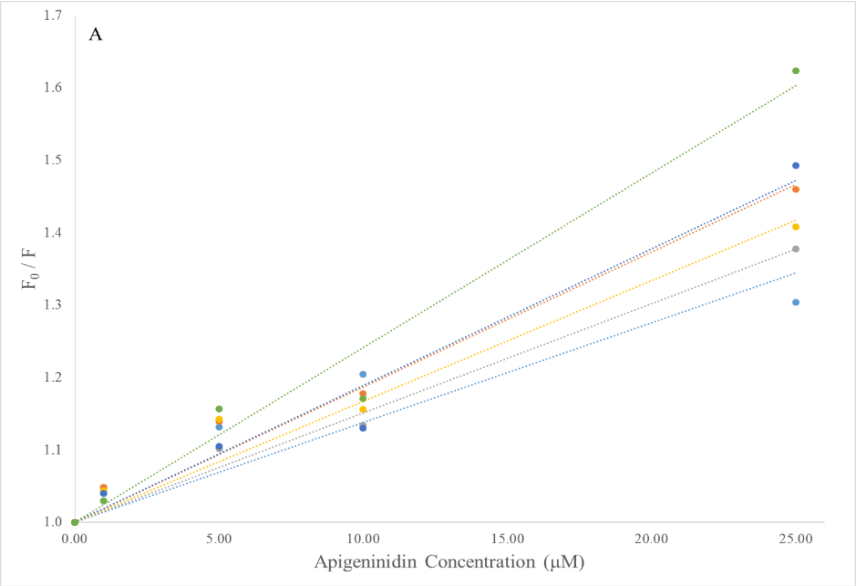

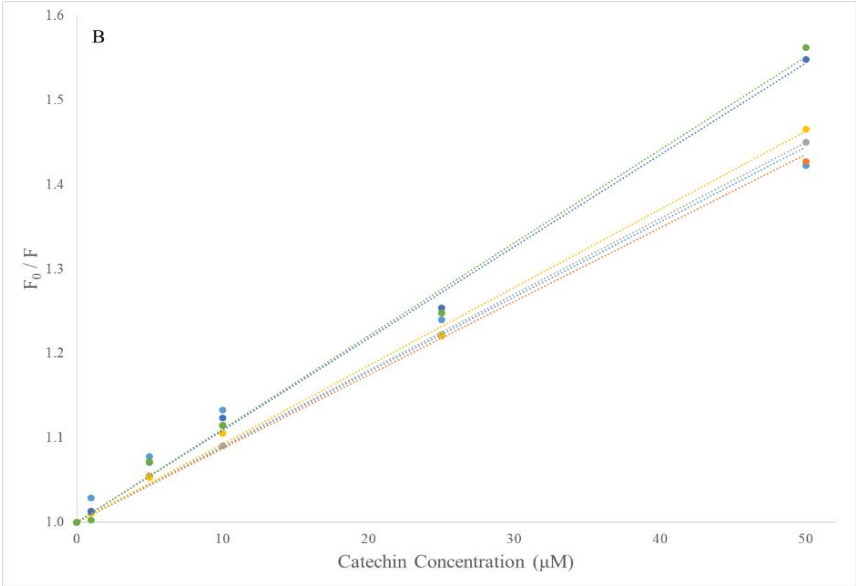

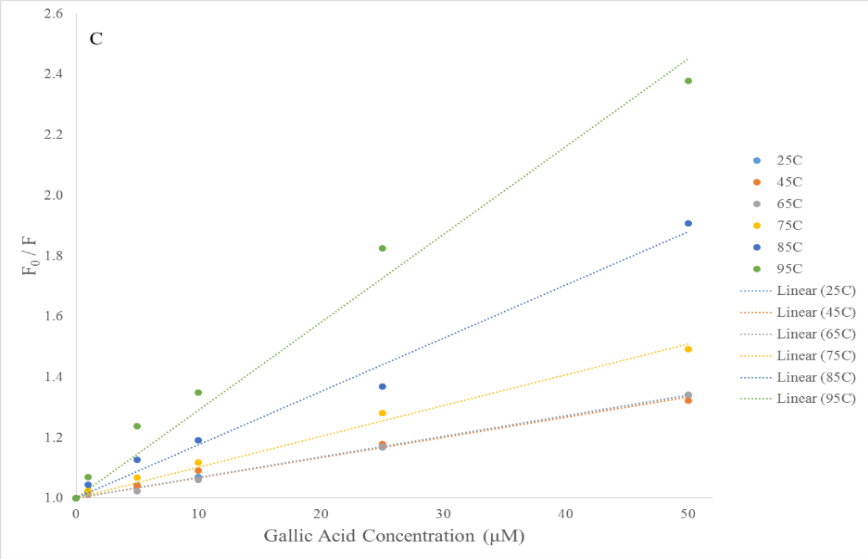

Figure 4.11 Stern-Volmer equation plots for determining the quenching constants of A) Apigeninidin, B) Catechin, and C) Gallic Acid for ovalbumin under different temperature conditions.
(Legend key shown in C.)

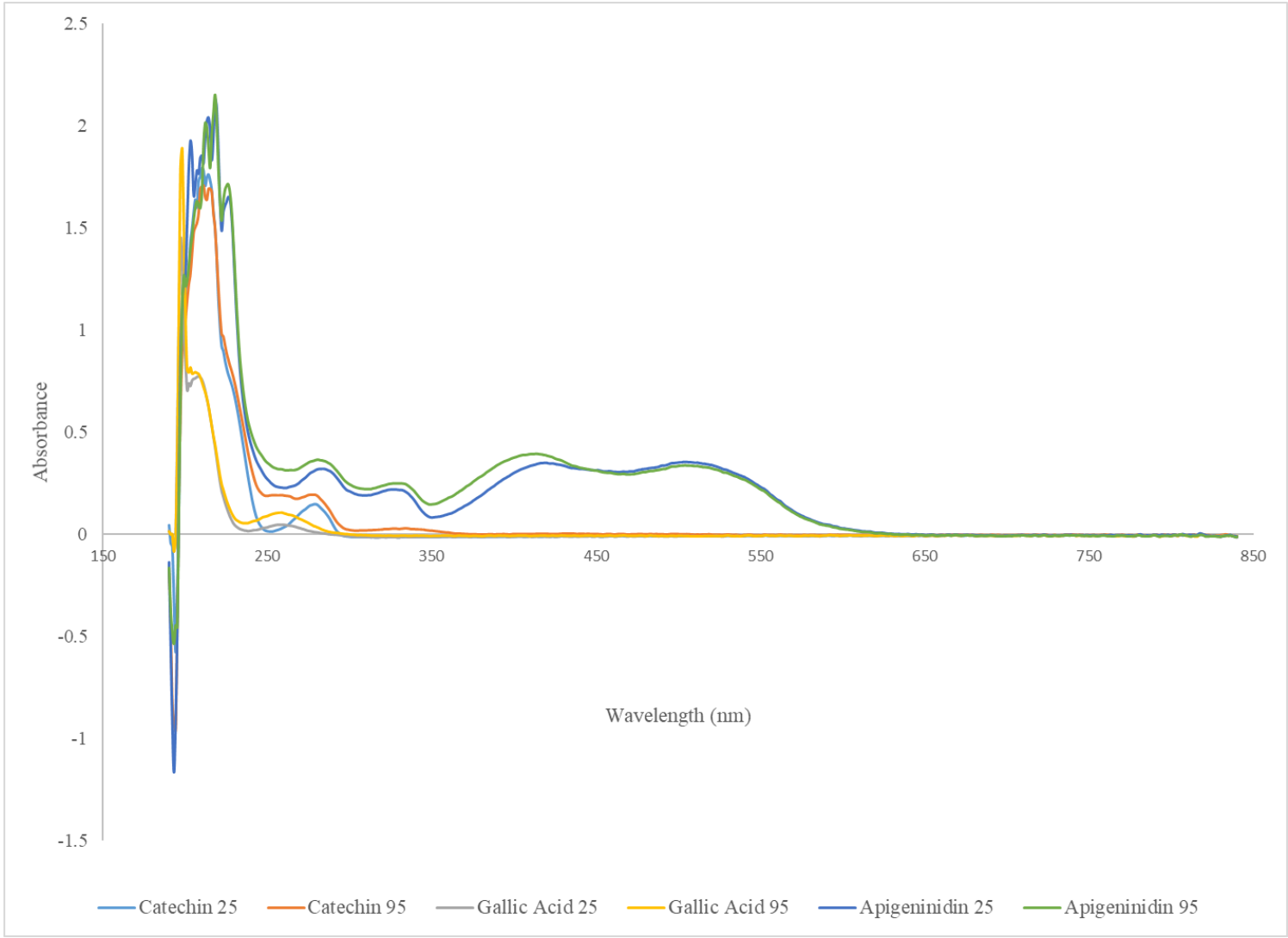

Figure 4.12 UV-Vis absorbance spectra of 50 μM catechin, gallic acid, and apigeninidin at 25°C and after 10 min at 95°C.

CHAPTER 5. EFFECTS OF ANTHOCYANIN COMPOUNDS ON COOKED STARCH-ASSOCIATED PROTEIN MATRIX FORMATION AND STARCH DIGESTION

5.1 Abstract

The human diet has shifted to more refined foods and ingredients and long-term consumption of foods causing swift blood glucose response, which has been associated with rising metabolic disease rates. Anthocyanin compounds are directly related to a number of health benefits, but the physicochemical effects of their presence on processed food microstructure have not been elucidated. As redox active compounds, anthocyanins and other phenolics may participate in a variety of reactions, including sulfhydryl-disulfide interchanges between proteins that can affect the structure and function of protein-based food matrices. Sorghums, which have a slow starch digestion characteristic, are the only cereal to natively contain 3-deoxyanthocyanidins, anthocyanin derivatives which lack the hydroxyl group at the C-3 position Other grains have anthocyanin-containing varieties (blue and purple corns, black rice), some of which have also been found to digest starch more slowly than similar non-anthocyanin products. Because anthocyanins poorly inhibit α-amylase, differences in microstructure were hypothesized, in particular the formation of expanded protein networks around gelatinized starch that could slow its digestion. A yellow corn flour porridge was produced without and with addition of apigeninidin, a 3-deoxyanthocyanidin present in sorghums, and tested for differences in starch digestion and of the microstructure using confocal microscopy. A commercial blue corn and sorghum porridges were also examined. Apigeninidin attenuated initial starch digestion rate, and improved the stability of the protein matrix. The microstructure of the corn flour porridge was significantly altered, as the zein-containing protein bodies demonstrated areas of extensive web-like structures and less protein aggregation throughout a 60 min α-amylase digestion. Blue corn matrices, while more structured than untreated yellow corn, were less stable than those formed by apigeninidin addition and collapsed following starch removal. Sorghum microstructure exhibited the highest protein network stability. Formation of strong protein web-like structures surrounding starch may allow for the design of foods to with attenuated starch digestion for a modulated glycemic response.

5.2 Introduction

The health benefits associated with consumption of anthocyanin compounds have been expounded upon (Badshah, Ullah, Kim, Kim, Lee, & Kim, 2013; Khoo, Azlan, Tang, & Lim, 2017), yet are often poorly understood. Additionally, the physicochemical effects of anthocyanins on the microstructure of processed food matrices are not well defined, though as redox active compounds (Kähkönen & Heinonen, 2003) they have the potential to participate in reactions including protein sulfhydryl-disulfide interchanges. Amongst the cereals, sorghum varieties are the only grains which natively contain 3-deoxyanthocyanidin compounds, which may be the factor contributing to the unique formation of physically stable protein networks or matrices surrounding gelatinized starch in sorghum endosperm porridge through sulfhydryl-disulfide interchange reactions (Bugusu, 2004; Hamaker & Bugusu, 2003; Oria, Hamaker, & Shull, 1995).

The starch component of sorghum porridges digests more slowly than other similar cereal porridges (such as corn or rice), with the protein portion of the matrix implicated in the protracted breakdown of starch by α-amylase (Duodu, Taylor, Belton, & Hamaker, 2003). As shown in Chapter 4, apigeninidin, a 3-deoxyanthocyanidin of sorghums, appears to promote sulfhydryl-disulfide interchanges in denatured protein (ovalbumin). The structural stability of 3-deoxyanthocyanidins to oxidation (Awika, Rooney, & Waniska, 2004; Mazza & Brouillard, 1987), due to the lack of the hydroxyl group at the C-3 position, may enable the compounds to facilitate multiple sulfhydryl-disulfide interchange reactions before encountering an irreversible molecular change, whilst anthocyanin and anthocyanidin compounds are more labile (Castañeda-Ovando, Pacheco-Hernández, Páez-Hernández, Rodríguez, & Galán-Vidal, 2009; Friedman & Jurgens, 2000).

Anthocyanin-containing grain-based foods such as blue corn tortillas have also shown a tendency to digest more slowly than similar yellow or white corn products (Hernández-Uribe, Agama-Acevedo, Islas-Hernández, Tovar, & Bello-Pérez, 2007). Although many phenolic compounds affect glucosidic enzyme activities, anthocyanins appear to inhibit the brush border associated α-glucosidases of the small intestine more strongly than α-amylases (Flores, Singh, Kerr, Pegg, & Kong, 2013; McDougall & Stewart, 2005; Ng, Gu, Zhang, Yusolf Putri, & Ng, 2015). Additionally, while naturally present anthocyanins have been implicated in slowing glucose release from cereal foods (Camelo-Méndez, Agama-Acevedo, Tovar, & Bello-Pérez, 2017; Camelo-Méndez, Flores-Silva, Agama-Acevedo, Tovar, & Bello-Pérez, 2018; Hernández-Uribe,

Agama-Acevedo, Islas-Hernández, Tovar, & Bello-Pérez, 2007), the effect of intrinsic anthocyanins (having the C3-hydroxyl) on food matrix formation and associated macronutrient release has not been studied.

Sorghum kafirins, prolamin storage proteins, stored in the endosperm as tightly bound starch-associated protein bodies, occur as the principle α-kafirin with β-kafirin found in the core and exterior, and surrounded by concentrated γ-kafirins on the exterior. The γ-kafirins, high in cysteine, tend to readily form disulfide bridges during cooking (Xu, 2008) above the melting temperature (Tm), forming intermolecular cross-links in expanded web-like structures around gelatinized starch (Bugusu, 2004; Hamaker et al., 2003), and are resistant to pepsin digestion. (Oria et al., 1995) Zeins, the prolamin storage proteins of maize, though similar in amino acid composition, sequence homology, sub-classes, and structure to kafirins (Altschul et al., 2005; DeRose, Ma, Kwon, Hasnain, Klassy, & Hall, 1989), do not tend to form the stable starch-associated matrix found in sorghum.

In sorghums, 3-deoxyanthocyanidins are hypothesized to stabilize the kafirin protein portion of the cooked product starch-protein matrix and sterically inhibit starch digestion, and this is tested in the present study by assessing whether 3-deoxyanthocyanidin addition to yellow corn has a similar effect with regard to matrix formation and starch digestion. Furthermore, the microstructure of traditional anthocyanin-containing grains has not been well characterized, leading to an investigation of naturally-present anthocyanin compounds in blue corn and the associated effects on protein (zein) matrix and starch digestion.

5.3 Materials

Dehulled, degermed yellow corn meal was kindly provided by Troy Tonner, MS ABE (Tonner, 2018), and was donated to his research by Agricor Inc. (Marion, IN). A commercial whole blue corn meal was obtained locally (medium grind, stone ground Bob's Red Mill brand). The corn meals were kept at 4°C until tempering to room temperature prior to milling. Both blue and yellow corn meals were milled through a 0.5 mm mesh screen using a cyclone mill (FOSS North America, Eden Prairie, MN, USA) to a fine flour. The whole grain normal white sorghum (P721N) used previously (Chapter 2) was decorticated (20%, according to (Reichert, Tyler, York, Schwab, Tatarynovich, & Mwasaru, 1986) followed by milling in the same manner.

All solvents except those utilized for chromatography were at least reagent grade, and those used for chromatography were HPLC grade. All chemical reagents, standards, and solvents were obtained from Fisher Scientific (Chicago, IL, USA) or Millipore Sigma (St. Louis, MO, USA). Total Starch Assay kit was purchased from Megazyme (Bray, Ireland). Purified water (at least 12 MΩ) was produced using an Elix Advantage water system (Millipore Sigma, St. Louis, MO, USA).

A Waters Acquity I class ultra-high performance liquid chromatography (UPLC) system equipped with a XEVO triple-quadripole mass spectrometer (MS) detector for MS/MS analysis (Waters Corporation, Milford, MA, USA) was utilized for chromatographic separation and identification of phenolic compounds (courtesy of M. Ferruzzi). All mobile phases were filtered and degassed prior to use. Standards used for identification of compounds were *p*-coumaric acid, caffeic acid, ferulic acid, syringic acid, quercetin, and cyanidin-3-glucoside.

5.4 Methods

5.4.1 Phenolic Extraction and Characterization of Cereal Flours

The free phenolic components of the yellow and blue corns were extracted as described previously (Chapter 3) using 80% (v/v) methanol acidified with 0.2% glacial acetic acid. Briefly, 5 g flour was shaken with 10 mL solvent for 10 min, centrifuged and supernatant removed, extraction and centrifugation repeated on the pellet, and supernatants pooled. After filtering to remove particulates, solvent was removed under a nitrogen gas stream to dryness and residue resolubilized in water. A SPE method was used to partially purify the crude extracts (Song, Sapper, Burtch, Brimmer, Goldschmidt, & Ferruzzi, 2013). Cartridges (Waters Oasis HLB 1 cc cartridges, Milford, MA, USA) were activated with methanol, rinsed with water, and extracts loaded. After clean-up elutions of 2% (v/v) formic acid followed by 5% (v/v) methanol, the phenolic samples were eluted with 2% (v/v) formic acid in methanol, dried under a nitrogen stream, and resolubilized in 2% (v/v) formic acid. The samples were then filtered through 0.45 μm PTFE syringe filters before freezing at -40°C until chromatographic separation.

Phenolic acids were separated with an Acquity UPLC BEH C18 1.7 μM (2.1 x 50 mm) column at a flow rate of 0.5 mL/min utilizing a gradient elution of 0.1% formic acid in acetonitrile (solvent A) and 0.1% formic acid in water (solvent B). The 6 min separation followed a program

of 0 min, 100% B; 0-0.5 min 100-94% B; 0.5-2 min 94-91% B; 2-3 min 91-87% B; 3-4.5 min 87-65% B; 4.5-5.5 min 65-100% B; 5.5-6 min, 100% B. Conditions for MS utilized ESI– ionization mode with capillary voltage 3 kV, cone voltage 32 V; desolvation temperature 600°C; desolvation gas flow 650 L/hr; and collision energy 20 V.

The separation and detection were similar for anthocyanin compounds, using the same gradient program except solvent B was 2% formic acid in water, and ESI+ ionization mode was utilized with the following conditions: capillary voltage 3 kV, cone voltage 30 V; desolvation temperature 600°C; desolvation gas flow 1000 L/hr; and collision energy 20 V.

5.4.2 Determination of Total Starch in Cereal Flours

Total starch content of the flours was determined using the Megazyme Total Starch Assay Kit (Megazyme, Bray, Ireland) according to the manufacturer instructions. Briefly, 100 mg each flour was dispersed in ethanol and dissolved in a 2 M solution of potassium hydroxide. A thermostable α-amylase and amyloglucosidase were added and allowed to digest the samples for 30 min at 50°C. The released glucose was colorimetrically determined using the glucose oxidase/peroxidase (GOPOD) method using a conversion factor of 0.9.

5.4.3 Activity of Porcine α-Amylase Enzyme

The porcine pancreatic α-amylase powder (Millipore Sigma, St. Louis, MO, USA) Type IV-B (1 g) was gently mixed with 10 mL of a cold 50 mM 3-(N-morpholino)propanesulfonic acid (MOPS) buffer (pH 7). The mixture was allowed to set at 4°C for 30 min prior to centrifuging at 4°C (8,000 *g*) for 15 min. The supernatant was collected and re-centrifuged for further purification of the enzyme. A slurry of 1% (w/v) corn starch in the same MOPS buffer was heated with continuous stirring in a boiling water bath for 15 min, cooled, and aliquots reacted with the α-amylase solution (50 μL) for 3 minutes. The liberated maltose was quantified using the 3,5-dinitrosalicylic acid (DNS) reducing sugars assay and compared to a maltose standard curve (0-1 mg/mL), with samples diluted to fit the linear range. Absorbance readings at 540 nm were taken using a SpectraMax 190 microplate reader (SoftMax Pro software; Molecular Devices, San Jose,

CA, USA). One unit (U) of enzyme activity was defined as the amount of enzyme that catalyzes the release of 1 mg maltose from starch in three minutes.

5.4.4 Preparation of Cereal Porridges

For each cereal flour, 5 mL deionized water (pH ~6) was added to 0.5 g starch weight flour, mixed, and allowed to set at room temperature for 5 min with stirring. For yellow corn porridges treated with 3-deoxyanthocyanidin, apigeninidin in ethanol was added to the water and the total volume of liquid maintained at 5 mL. (No more than 20 μL ethanol solution was added.) Two levels of addition were used, approximately imitating the level of free 3-deoxyanthocyanidins in sorghum endosperm (APG1), and also approximately twice that level (APG2). Slurries were cooked in a boiling water bath with continuous stirring for 20 min, vortexed to break up the starch paste, and cooled at room temperature for 10 min. The entire portion of porridge was used for starch digestion assays. Triplicate samples of all porridges were prepared for *in vitro* assay.

5.4.5 *In Vitro* Starch Digestion Using Porcine α-Amylase

A modified version of an *in vitro* digestion of starch by α-amylase (Zhang, Dhital, Flanagan, Luckman, Halley, & Gidley, 2015) was utilized. MOPS buffer (50 mM, pH 7, containing 5 mM calcium chloride) was added to each tube of porridge, vortexed, and equilibrated at 37°C with stirring. Aliquots were removed to measure endogenous reducing sugars. The α-amylase enzyme solution was added (3.4U) to each tube and aliquots removed at specific time points over a 2-h period to measure reducing sugars released. Removed aliquots were immediately added to an equal volume of ice-cold calcium carbonate solution (0.3 M) and vortexed to prevent further enzymatic action, and the tubes kept on ice. Tubes were centrifuged (16,000*g*, 5 min) to remove undigested particulates, and the supernatants (300 μL) measured for reducing sugar content with an equal volume of DNS solution. The DNS and sample supernatants were boiled for 10 min and immediately cooled on ice. Reducing sugars were determined colorimetrically by absorbance at 540 nm using a SpectraMax 190 microplate reader (SoftMax Pro software; Molecular Devices, San Jose, CA, USA). Maltose (1 mg/mL) in the MOPS buffer was used to prepare standard curves. Samples were diluted to fit the linear range.

Porridge samples were prepared in the same manner (5.4.4) for observation of the microstructure using confocal microscopy. Cooked porridge samples (approximately 50 mg porridge) were removed following the cooling period, frozen, and freeze-dried. The remaining porridge was subjected to α-amylase digestion. Larger aliquots (5 mL) of each partially digested porridge were removed after 30 and 60 min starch digestion and the reaction halted as previously described. Samples were centrifuged, washed twice with purified water, and the residue freeze-dried before fluorescent labeling.

5.4.6 Inhibition of Porcine α-Amylase by Apigeninidin

A method similar to the determination of α-amylase activity was used to determine if any change in apparent activity occurred due to the presence of apigeninidin in the buffer. Enzyme, apigeninidin, and starch were prepared in a phosphate buffer (50 mM, pH 6.8). Apigeninidin was diluted to final assay concentrations from 0-300 μM (triplicate samples) in the buffer fraction while starch and enzyme concentrations were maintained. To the apigeninidin in buffer, starch was added and allowed to set for 5 min before the enzyme was added to begin catalysis. Maltose equivalents were quantified using DNS and compared to a maltose standard curve (0-1 mg/mL).

Additionally, a selection of apigeninidin concentrations were chosen to ensure the presence of apigeninidin would not alter the absorbance at 540 nm for DNS, interfering with the assay. Buffer and apigeninidin solution (no starch or enzyme) were treated with DNS, heated, cooled, and measured as described. Apigeninidin in buffer samples were measured with and without further dilution.

5.4.7 Sample Preparation and Visualization using Confocal Microscopy

Raw flours, cooked porridges, and partially digested porridges underwent a double-labeling procedure modified from Bugusu (2004), which was based on methods by Bantan-Polak et al. (2001) and Vodovotz & Chinachoti (1998). Raw flours were dehydrated overnight in absolute ethanol, while cooked and partially digested porridges were freeze dried. Samples were treated in opaque microtubes in a dark room. First, carbohydrates (mainly starch) were labeled using a

periodic acid-Schiff reaction, followed by protein labeling with fluorescamine. Approximately 5-10 mg each sample was labeled.

Samples were oxidized with 0.5% (w/v) periodic acid for 5 min, rinsed 3 times with purified water, stained with Schiff reagent for 10 min, rinsed twice with 0.5% (w/v) potassium sulfite, and finally rinsed 5 times with purified water. Fluorescamine (200 μL, 0.1% w/v in acetonitrile) and 0.1M sodium (tetra)borate (300 μL, pH 8.0) were added and allowed to react for 5 min, and the labeled samples rinsed 5 times with purified water. A 75% (v/v) glycine solution was added to the tubes and 10 μL aliquots removed to glass microscope slides. Cover slips were adhered using clear nail varnish.

Images were acquired on a Nikon A1R-MP inverted multiphoton confocal microscope equipped with PlanApo 20x, 40x, and 60x objectives and an argon laser, using NIS-Elements software. (Nikon, Tokyo, Japan). Carbohydrates were excited at 561 nm, with laser power held at 1.96 for all samples. Emission was detected in channel 3 at 600/50 nm. Protein excitation occurred at 405 nm. Laser power was held constant at 1.08, and detection occurred in channel 1 at 450/50 nm. Pinhole size was automatically set at 1.2 for all samples. The pixel brightness was attenuated to approximately 2000-3000 by altering the high voltage (HV) setting in order to maintain appropriate brightness and visibility of observable components, limit pixel oversaturation, and produce images of high quality.

For all sample observations, starch and protein were imaged separately to prevent emission spectral overlay. Z-stacks were acquired incorporating the visible range of each sample (usually ~15-30 μm) using 1.6-2 μm steps and processed with ImageJ software (Schneider, Rasband, & Eliceiri, 2012) to produce 3D images using at least 6 images from each (starch or protein) stack. Protein images were pseudo-colored green, and background removed using rolling-ball method as needed, to allow for better visuals.

5.4.8 Statistical Analysis

Quantitative results were expressed as means ± standard deviations of triplicate measurements. One- or two-way analysis of variance tests were used in SAS software version 9.4 (SAS Institute, Inc., Cary, NC, USA) using a significance level of $p < 0.05$.

5.5 Results

5.5.1 Free Phenolic Components of Blue and Yellow Corn Flours

Content of the identified phenolics and retention times are presented in Table 5.1. The 4 phenolic acids utilized as standards (*p*-coumaric, caffeic, ferulic, and syringic acids) were present in the extracts of both corn flours. Additionally, protocatechuic, sinapic, and feruleyolquinic acids were identified. Only the blue corn contained quercetin and cyanidin-3-glucoside, as well as quercetin-3-glucoside and other identified anthocyanin compounds. Of the similar components, syringic acid was higher in yellow corn (13.3±3.4 μg/g compared to 0.30±0.056 μg/g), while other phenolic acids were present at similar levels. In blue corn, cyanidin-3-glucoside was the major anthocyanidin at 89.5±19.4 μg/g, with other anthocyanidin compounds, including arabinoside and *p*-coumaryl variants of cyanidin and peonidin, present below 1 μg/g.

5.5.2 Starch Digestion of Cereal Porridges with and without Anthocyanin Compounds

Overall, the addition of apigeninidin slowed initial starch digestion rate but did not reduce total starch digestion (Figure 5.1). Blue corn exhibited very high starch digestion in the first 5 min, higher even than the control yellow corn, followed by a swift tapering of maltose equivalent release. After 20 min digestion, the treated and control yellow corn porridges demonstrated no differences in maltose equivalent release at each time point. Blue corn and sorghum were similarly undifferentiated after 40 min digestion. Sorghum exhibited the slowest starch digestion curve, and both blue corn and sorghum achieved ~70% total starch digestion after 2 hours, while corn porridges released ~80% of starch as reducing sugars.

The control yellow corn (YC) porridge without apigeninidin treatment exhibited a rapid initial starch digestion rate, with 50% digestion occurring between 10-20 min. (Extrapolation provides a time point for 50% starch digestion prior to 15 min.) The starch in YC achieved ~80% digestion within 60 min, with little further change by the end of two hours.

The addition of apigeninidin into the slurry prior to cooking had a significant effect on the initial rate of yellow corn starch digestion ($p<0.05$). For samples approximating sorghum 3-deoxyanthocyanidin content (APG1), after 5 and 10 min, relative maltose release had been attenuated by 7% and 12%, respectively. However, at 20 min α-amylase digestion and beyond, no

further significant differences in reducing sugars were detected compared to YC at the same time point. At 20 min, 50% of the starch had been digested, with approximately 80% digestion occurring by 60 min. Adding twice the content of 3-deoxyanthocyanidins in sorghum endosperm to the yellow corn slurry (APG2) also diminished initial starch digestion compared to the YC control, but it was not significantly different from APG1.

5.5.3 Apigeninidin Inhibition of α-Amylase and Determination of Assay Interference

With starch and enzyme concentration kept constant, no evidence of α-amylase inhibition by apigeninidin was found across a 300 μM range, as shown in Figure 5.2. Apparent activity of α-amylase remained stable at approximately 6.2 (±0.12) U.

When apigeninidin in buffer (treated with DNS) at 50, 200, or 250 μM was diluted to the same level as samples treated with starch and enzyme to fit the linear range of the standard curve, absorbance was the same as empty microplate wells. (Data not shown.) The undiluted 200 and 250 μM solutions (treated with DNS) demonstrated increases in absorption at 540 nm compared to the blank solution (buffer + DNS), however absorbance of the undiluted 50 μM solution was not different from the blank. (Data not shown.) From these results, the conclusion was made that apigeninidin ≤ 300 μM did not affect the DNS assay when samples were diluted to remain within the linear range of the standard curve used for quantitation.

5.5.4 Visualization of Endosperm Microstructure with Confocal Microscopy

The starch granules of raw flours appeared polygonal, with portions surrounded by protein bodies. Visual differences between yellow corn (Figure 5.3), blue corn (Figure 5.4), and sorghum (Figure 5.5) starch granules were minimal, though sorghum and blue corn flours were evident more often as particulate clumps. Granule clumping did, however, allow improved visibility of intrinsic protein body association with starch granules in the flour matrix. Some particulates exhibit such tight packing of granules as to nearly prevent the ingress of the fluorescamine dye to the protein.

Cooked porridges mainly showed a frame of gelatinized starch, but differences in protein structure became evident. YC porridge (Figures 5.6) protein existed mainly as aggregates–small

clumpy areas of protein–within or as thin filaments through the gelatinized starch, though some areas also appeared to develop more stable protein formations (Figure 5.7). With apigeninidin addition to the yellow corn porridge, enhanced configurations of proteins were observed (APG1, Figure 5.8; APG2, Figure 5.9) compared to YC. In some areas, extensively connected (cross-linked) arrangements of proteins occurred, appearing web-like, and can be more readily viewed with the protein alone (Figures 5.10 and 5.11, respectively). Although areas of irregular matrix construction and aggregation were apparent, APG1 and APG2 exhibited evidence of extensive web-like matrix formation and improved matrix stability compared to the YC cooked porridge, with more structures noticeable in APG2.

The blue corn porridge (Figures 5.12-13) protein matrices revealed areas of extensive web-like connected structures surrounding the starch granules, indicating cross-linking. However, the prevalence of this cross-linking was less than observed in sorghum or APG2-treated samples, as the protein filaments appeared thin and wispy through the starch, more comparable to the areas of more stable protein in YC or some areas of APG1. Protein matrix structures in cooked sorghum (Figures 5.14-15) were more similar to apigeninidin treated porridges overall, with some areas of widespread cross-linking as well as areas of sporadic formation and aggregation. Partial constriction of starch granules growth was most recognizable in sorghum.

Following partial α-amylase digestion, starch remnants remained primarily associated with protein. After 30 min, protein in YC (Figures 5.16-5.18) more clearly lacked interaction with starch, leading to matrix collapse and aggregation, with little defined structure. Partial collapse of matrix occurred in APG1, but starch-protein association could be observed by the yellowing from overlapping pixels in the combined image (Figure 5.19) and starch structures (Figure 5.20) outlining portions of the protein matrix (Figure 5.21). Enhanced association between starch and protein was also discerned in APG2 samples (Figure 5.22), with remaining starch after initial digestion (Figure 5.23) again tending to follow the shape of protein matrix structures (Figure 5.24). Most notable may be the small protein particulate in the upper left corner of Figure 5.24 which appears empty of starch yet retained the conformation established during cooking.

Blue corn particles (Figure 5.25) displayed more starch-protein affiliation than APG1 or APG2, with higher levels of overlapped pixels, though the protein matrix (Figure 5.27) appeared to collapse to a greater extent around the starch (Figure 5.26). Sorghum emerged with the most dramatic correlation between starch and the protein network as starch digestion resulted in

hollowed areas of the particles (Figure 5.28). Examining the starch (Figure 5.29) and protein (Figure 5.30) separately, showed that extensive starch remained which seemed intrinsically associated with the protein.

An hour of α-amylase digestion produced few differences in microstructure of corn porridges compared to 30 min. Less starch was present, and starch particulates tended to be smaller, but remnants were principally surrounded by protein, as observed with YC (Figures 5.31-5.33) which experienced almost complete collapse of protein matrix structure onto the starch, as well as areas of aggregation (Figure 5.33). Both APG1 and APG2 (Figures 5.34 and 5.37, respectively) again exhibited areas of closely associated starch and protein, with starch structure mirroring that of the protein (Figures 5.35 and 5.38, respectively). In each, portions of the protein matrices collapsed (Figures 5.36 and 5.39, respectively), but both also maintained regions of protein structure, with APG2 displaying greater stability. The protein matrix of blue corn porridge mainly collapsed around starch remnants by 60 min digestion, with areas of protein aggregation (Figures 5.40-5.42). Sorghum microstructure (Figures 5.43-5.45) remained unique compared to the corn samples, with protein matrices and starch remnants apparently conjoined.

5.6 Discussion

Levels of total phenolics in the intestinal lumen can reach high μM to low mM concentrations (Scalbert & Williamson, 2000), however amounts of individual phenolic components, including anthocyanins, released from the food matrix and available for enzymatic interaction and inhibition are much lower. A 10% (w/v) decorticated normal white sorghum flour porridge would contain approximately 15 μM 3-deoxyanthocyanidins (prior to further dilution with digestive juices), which would not be immediately released from the food matrix for potential enzymatic inhibition. Lack of α-amylase inhibition by apigeninidin ≤300 μM indicates that 3-deoxyanthocyanidins are unlikely to contribute to α-amylase inhibition at physiologically relevant concentrations, though niche environments within the food particles and/or digestive tract may experience locationally higher concentrations during digestion and absorption.

A cook time of 20 min in boiling water has been shown previously to completely gelatinize porridges of 10% (w/v) starch basis flour using DSC (Bugusu, 2004; Pletsch, 2018), though in some cereal products (such as sorghum porridges and pasta), growth of the starch granules may be

restricted by the protein matrix (Colonna, Barry, Cloarec, Bornet, Gouilloud, & Galmiche, 1990; Singh, Dartois, & Kaur, 2010; Zou, Sissons, Gidley, Gilbert, & Warren, 2015). Applying shear to cooked porridges was demonstrated to increase the amount of starch digested (Pletsch, 2018) and was utilized to mimic a portion of the physical process of digestion (such as chewing and stomach grinding) due to the thick, viscous nature of starch-based porridges. Performing the *in vitro* α-amylase digestion without disrupting the gel prior to buffer addition resulted in large standard deviations and poor data quality (data not shown).

Rapidly digestible starch is defined by the Englyst method (Englyst, Kingman, & Cummings, 1992) as starch digested within 20 min, which would be absorbed in the proximal small intestine, and contributes to the early rise in postprandial glycemic response. The addition of apigeninidin to the yellow corn flour porridges prior to cooking decreased the initial starch digestion rate, slowing the release of maltose equivalents. However, the total release of reducing sugars from starch reached the same amount as untreated corn porridge by 20 min α-amylase digestion, resulting in no net change in digestion across the initial 20 min (Figure 5.1). Changing the redox environment of the cooking solution has been shown to alter starch digestion, by increasing digestion of sorghums with a reducing agent (Ezeogu, Duodu, Emmambux, & Taylor, 2008; G. Zhang & Hamaker, 1998) or decreasing digestion of corns by an oxidizing agent (Bugusu, 2004), with modifications to protein polymerization the main effect. Starch digestion is also affected by viscosity of the medium, as more viscous systems reduce the rate of starch hydrolysis (Kim & White, 2013). While phenolic compounds may alter the viscosity of starch gels and pastes, apigeninidin addition, at the levels utilized, was considered unlikely to cause a significant increase in viscosity, as phenolic extracts from white sorghum bran have demonstrated reduced pasting properties of corn starch porridges compared to a control (Lemlioglu-Austin, Turner, McDonough, & Rooney, 2012).

The blue corn porridge, though a whole grain product, exhibited an elevated reducing sugar release compared to the other porridges in the first minutes of *in vitro* digestion (Figure 5.2), indicating approximately 50% of the starch was highly available. Stone ground flours can have higher damaged starch content compared to other methods of flour production (Asmeda, Noorlaila, & Norziah, 2016), though the second milling (cyclone mill) performed to achieve an overall similar particle size compared to sorghum and yellow corn may have caused further damage to the starch granules, possibly increasing the α-amylase digestibility. Although viscous dietary fibers

can slow digestion rates (McRorie & McKeown, 2017), many carbohydrates undigestible by upper gastrointestinal enzymes, including arabinoxylans in corn bran, do not thicken the chyme and have little direct impact on nutrient digestion and absorption (Müller, Canfora, & Blaak, 2018).

Confocal microscopy has been utilized to examine microstructure and component interactions of cereal products (Bugusu, Hamaker, & Rajwa, 2002; Faltermaier, Zarnkow, Becker, Gastl, & Arendt, 2015; Hamaker & Bugusu, 2003). The observed zein matrices in the cooked blue corn porridge (Figures 5.12 and 5.13) were not sufficient to slow the initial starch digestion, but possibly contributed to the reduced total starch digested compared to the yellow corn porridges. As the protein matrix structure collapsed, it appeared to partially surround the starch remnants without forming large aggregative particles (Figures 5.25 and 5.40), possibly restricting access by α-amylase.

Adding apigeninidin to a yellow corn flour porridge prior to cooking increased the formation of protein matrices, which appeared at least partially resistant to collapse during α-amylase digestion (Figures 5.19, 5.22, 5.34, 5.37). Changes to the protein microstructure have previously been shown to alter digestion of other macronutrients (Ezeogu, Duodu, Emmambux, & Taylor, 2008; McClements, Decker, Park, & Weiss, 2008; Parada & Aguilera, 2007). Protein matrix stability seemed dose-dependent with apigeninidin, as APG2 samples retained more intact matrix formations (Figures 5.20, 5.35 compared to Figures 5.23, 5.38). The reduced starch digestion in the first 20 min of the *in vitro* assay may have been due to the increased matrix stability, as a change due to inhibition of the enzyme was unlikely because of the lack of α-amylase inhibition by apigeninidin (Figure 5.2). The presence of protein may constrain starch granules and hinder the access of α-amylase to starch (Xu, 2008; Zou, Sissons, Gidley, Gilbert, & Warren, 2015).

Sorghum flour porridge was utilized as a type of gold standard for protein matrix formation and observation of the microstructure. Outer portions of cooked particles exhibit less condensed protein structure compared to the core, which also experienced more limited granule swelling (Figures 5.14 and 5.15). The particulates which remained following α-amylase digestion for fluorescent staining compared more closely to the core material (Figures 5.28 and 5.43 vs Figures 5.14 and 5.15), which suggests constraining granule growth as well as entrapment within the protein matrix may be important to limiting starch digestion.

Changes in effective concentration due to viscosity and molecular crowding have been demonstrated and calculated (Rutgers, 1962) which apply to a variety of systems. With increased viscosity during granule swelling and gelatinization, 3-deoxyanthocyanidins leached from the sorghum particles may not experience free movement but rather more limited diffusion, increasing the effective concentration in the microenvironment and resulting in the higher degree of cross-linking observed in the particle core compared to the exterior.

5.7 Conclusions

The presence of anthocyanins increased the formation of cross-linked protein matrices in cereal porridges, however the stability of these structures may be dependent on the effective concentration present in a microenvironment. The presence of anthocyanin compounds in blue corn appeared to increase matrix formation and limit initial matrix protein aggregation compared to the untreated yellow corn. Yet, the stability of the resulting structures was less than that which resulted from apigeninidin addition to a non-anthocyanin-containing yellow corn, supporting the hypothesis that 3-deoxyanthocyanidin compounds are more effective at promoting non-aggregative, extensive protein polymerization to form the protein web-like matrix. In blue corn porridge, matrix collapse onto the starch remnants was observed, intimating that protein matrix without defined structure may also assist to constrain final starch digestion, though stable matrices may be required initially. Specific manipulation of food matrices may be a viable technique to produce foods designed with enhanced health benefits. By altering α-amylase access to starch, it may be possible to extend energy release and absorption, with implications for modulating blood glucose response and triggering ileal brake effects.

References

Altschul, S. F., Wootton, J. C., Gertz, E. M., Agarwala, R., Morgulis, A., Schäffer, A. A., & Yu, Y. K. (2005). Protein database searches using compositionally adjusted substitution matrices. FEBS Journal, 272(20), 5101-5109.

Asmeda, R., Noorlaila, A., & Norziah, M. H. (2016). Relationships of damaged starch granules and particle size distribution with pasting and thermal profiles of milled MR263 rice flour. Food Chemistry, 191, 45-51.

Awika, J. M., Rooney, L. W., & Waniska, R. D. (2004). Properties of 3-deoxyanthocyanins from sorghum. Journal of Agricultural and Food Chemistry, 52(14), 4388.

Badshah, H., Ullah, I., Kim, S. E., Kim, T.-h., Lee, H. Y., & Kim, M. O. (2013). Anthocyanins attenuate body weight gain via modulating neuropeptide Y and GABAB1 receptor in rats hypothalamus. Neuropeptides, 47(5), 347-353.

Bantan-Polak, T., Kassai, M., & Grant, K. B. (2001). A Comparison of Fluorescamine and Naphthalene-2,3-dicarboxaldehyde Fluorogenic Reagents for Microplate-Based Detection of Amino Acids - ScienceDirect. Analytical Biochemistry, 297(2), 128-136.

Bugusu, B. A. (2004). Understanding the basis of the slow starch digestion characteristic of sorghum porridges and how to manipulate starch digestion rate. Dissertation, Purdue University, West Lafayette, IN, USA.

Bugusu, B. A., Hamaker, B. R., & Rajwa, B. (2002). Interaction of maize zein with wheat gluten in composite dough and bread as determined by confocal laser scanning microscopy. Scanning, 24(1), 1-5.

Camelo-Méndez, G. A., Agama-Acevedo, E., Tovar, J., & Bello-Pérez, L. A. (2017). Functional study of raw and cooked blue maize flour: Starch digestibility, total phenolic content and antioxidant activity. Journal of Cereal Science, 76, 179-185.

Camelo-Méndez, G. A., Flores-Silva, P. C., Agama-Acevedo, E., Tovar, J., & Bello-Pérez, L. A. (2018). Incorporation of whole blue maize flour increases antioxidant capacity and reduces in vitro starch digestibility of gluten-free pasta. Starch - Stärke, 70(1-2), 1700126.

Castañeda-Ovando, A., Pacheco-Hernández, M. d. L., Páez-Hernández, M. E., Rodríguez, J. A., & Galán-Vidal, C. A. (2009). Chemical studies of anthocyanins: A review. Food Chemistry, 113(4), 859-871.

Colonna, P., Barry, J. L., Cloarec, D., Bornet, F., Gouilloud, S., & Galmiche, J. P. (1990). Enzymic susceptibility of starch from pasta. Journal of Cereal Science, 11(1), 59-70.

DeRose, R. T., Ma, D. P., Kwon, I. S., Hasnain, S. E., Klassy, R. C., & Hall, T. C. (1989). Characterization of the kafirin gene family from sorghum reveals extensive homology with zein from maize. Plant Molecular Biology, 12(3), 245-256. Duodu, K. G., Taylor, J. R. N., Belton, P. S., & Hamaker, B. R. (2003). Factors affecting sorghum protein digestibility. Journal of Cereal Science, 38(2), 117-131.

Englyst, H. N., Kingman, S. M., & Cummings, J. H. (1992). Classification and measurement of nutritionally important starch fractions. European Journal of Clinical Nutrition, 46(0954-3007 (Print)), S33-50.

Ezeogu, L. I., Duodu, K. G., Emmambux, M. N., & Taylor, J. R. N. (2008). Influence of Cooking Conditions on the Protein Matrix of Sorghum and Maize Endosperm Flours. Cereal Chemistry, 85(3), 397-402.

Faltermaier, A., Zarnkow, M., Becker, T., Gastl, M., & Arendt, E. K. (2015). Common wheat (Triticum aestivum L.): evaluating microstructural changes during the malting process by using confocal laser scanning microscopy and scanning electron microscopy. European Food Research and Technology, 241(2), 239-252.

Flores, F. P., Singh, R. K., Kerr, W. L., Pegg, R. B., & Kong, F. (2013). Antioxidant and Enzyme Inhibitory Activities of Blueberry Anthocyanins Prepared Using Different Solvents. Journal of Agricultural and Food Chemistry, 61(18), 4441-4447.

Friedman, M., & Jurgens, H. (2000). Effect of pH on the stability of plant phenolic compounds. Journal of Agricultural and Food Chemistry, 48(6), 2101-2110.

Hamaker, B. R., & Bugusu, B. A. (2003). Overview: Sorghum proteins and food quality. In P. S. Belton & J. R. N. Taylor (Eds.), Afripro Workshop on the Proteins of Sorghum and Millets). Pretoria, South Africa.

Hernández-Uribe, J. P., Agama-Acevedo, E., Islas-Hernández, J. J., Tovar, J., & Bello-Pérez, L. A. (2007). Chemical composition and in vitro starch digestibility of pigmented corn tortilla. Journal of the Science of Food and Agriculture, 87(13), 2482-2487.

Khoo, H. E., Azlan, A., Tang, S. T., & Lim, S. M. (2017). Anthocyanidins and anthocyanins: colored pigments as food, pharmaceutical ingredients, and the potential health benefits. Food & nutrition research, 61, 1361779.

Kähkönen, M. P., & Heinonen, M. (2003). Antioxidant Activity of Anthocyanins and Their Aglycons. Journal of Agricultural and Food Chemistry, 51(3), 628-633.

Kim, H. J., & White, P. J. (2013). Impact of the Molecular Weight, Viscosity, and Solubility of β-Glucan on in Vitro Oat Starch Digestibility. Journal of Agricultural and Food Chemistry, 61(13), 3270-3277.

Lemlioglu-Austin, D., Turner, N. D., McDonough, C. M., & Rooney, L. W. (2012). Effects of Sorghum [Sorghum bicolor (L.) Moench] Crude Extracts on Starch Digestibility, Estimated Glycemic Index (EGI), and Resistant Starch (RS) Contents of Porridges. Molecules, 17(9), 11124-11138.

Mazza, G., & Brouillard, R. (1987). Color stability and structural transformations of cyanidin 3,5-diglucoside and four 3-deoxyanthocyanins in aqueous solutions. Journal of Agricultural and Food Chemistry, 35(3), 422-426.

McClements, D. J., Decker, E. A., Park, Y., & Weiss, J. (2008). Designing Food Structure to Control Stability, Digestion, Release and Absorption of Lipophilic Food Components. Food Biophysics, 3(2), 219-228.

McDougall, G. J., & Stewart, D. (2005). The inhibitory effects of berry polyphenols on digestive enzymes. BioFactors, 23(4), 189-195.

McRorie, J. W., & McKeown, N. M. (2017). Understanding the Physics of Functional Fibers in the Gastrointestinal Tract: An Evidence-Based Approach to Resolving Enduring Misconceptions about Insoluble and Soluble Fiber. Journal of the Academy of Nutrition and Dietetics, 117(2), 251-264.

Müller, M., Canfora, E. E., & Blaak, E. E. (2018). Gastrointestinal Transit Time, Glucose Homeostasis and Metabolic Health: Modulation by Dietary Fibers. Nutrients, 10(3).

Ng, K., Gu, C., Zhang, H., Yusolf Putri, C., & Ng, K. (2015). Evaluation of α-Amylase and α-Glucosidase Inhibitory Activity of Flavonoids. International Journal of Food and Nutritional Science, 2(2), 174-179.

Oria, M. P., Hamaker, B. R., & Shull, J. M. (1995). Resistance of sorghum α-, β-, and γ-kafirins to pepsin digestion. Journal of Agricultural and Food Chemistry, 43(8), 2148-2153.

Parada, J., & Aguilera, J. M. (2007). Food Microstructure Affects the Bioavailability of Several Nutrients. Journal of Food Science, 72(2), R21-R32.

Pletsch, E. A. (2018). Investigating the Purported Slow Transit and Starch Digestion of Whole Grain Foods (Order No. 10748139). Purdue University, West Lafayette, IN., Dissertations & Theses @ CIC Institutions; ProQuest Dissertations & Theses Global.

Reichert, R. D., Tyler, R. T., York, A. E., Schwab, D. J., Tatarynovich, J. E., & Mwasaru, M. A. (1986). Description of a production model of the tangential abrasive dehulling device and its application to breeders' samples. Cereal Chemistry, (3), 201-207.

Rutgers, I. R. (1962). Relative viscosity and concentration. Rheologica Acta, 2(4), 305-348.

Scalbert, A., & Williamson, G. (2000). Dietary Intake and Bioavailability of Polyphenols. The Journal of Nutrition, 130(8), 2073S-2085S.

Schneider, C. A., Rasband, W. S., & Eliceiri, K. W. (2012). NIH Image to ImageJ: 25 years of image analysis. Nature Methods, 9, 671-675.

Singh, J., Dartois, A., & Kaur, L. (2010). Starch digestibility in food matrix: a review. Trends in Food Science & Technology, 21(4), 168-180.

Song, B. J., Sapper, T. N., Burtch, C. E., Brimmer, K., Goldschmidt, M., & Ferruzzi, M. G. (2013). Photo- and Thermodegradation of Anthocyanins from Grape and Purple Sweet Potato in Model Beverage Systems. Journal of Agricultural and Food Chemistry, 61(6), 1364-1372.

Tonner, T. (2018). Understanding the Effect of Extrusion Conditions on Melt Viscosity to Aid in Modeling of a Single Screw Extruder with Internal Restrictions for Scale-up Purposes. Unpublished Master's Thesis, Purdue University, West Lafayette, IN.

Vodovotz, Y., & Chinachoti, P. (1998). Confocal Microscopy of Bread. In T. M.H., P. S.A. & F. P.M. (Eds.), New Techniques in the Analysis of Foods, (pp. 9-17). Boston, MA: Springer.

Xu, X. (2008). In vitro digestibility of starch in sorghum differing in endosperm hardness and flour particle size. Kansas State University, Manhattan, KS.

Zhang, B., Dhital, S., Flanagan, B. M., Luckman, P., Halley, P. J., & Gidley, M. J. (2015). Extrusion induced low-order starch matrices: Enzymic hydrolysis and structure. Carbohydrate Polymers, 134, 485-496.

Zhang, G., & Hamaker, B. R. (1998). Low α-Amylase Starch Digestibility of Cooked Sorghum Flours and the Effect of Protein. Cereal Chemistry, 75(5), 710-713.

Zou, W., Sissons, M., Gidley, M. J., Gilbert, R. G., & Warren, F. J. (2015). Combined techniques for characterising pasta structure reveals how the gluten network slows enzymic digestion rate. Food Chemistry, 188, 559-568.

Table 5.1 Phenolic components identified from the acidified 80% methanol extraction of yellow and blue corn flours.

Identified Phenolic Compounds	R_t (min)	Yellow Corn	SD [1]	Blue Corn	SD [1]
Phenolic Acids					
Protocatechuic Acid	0.89	0.44	0.07	1.78	1.35
Caffeic Acid	1.61	0.19	0.02	0.13	0.08
Feruleyolquinic Acid	1.69	0.65	0.06	1.46	0.83
Syringic Acid	2.23	13.30	3.43	0.29	0.06
p-Coumaric Acid	2.36	5.14	0.30	5.29	1.46
Ferulic Acid	2.94	2.33	0.07	1.96	0.62
Sinapic Acid	3.12	0.49	0.02	0.35	0.06
Flavonoids					
Quercetin-3-glucoside	3.43	nd		0.20	0.05
Quercetin	4.17	nd		0.02	0.00
Anthocyanidins					
Cyanidin-3-Glucoside	1.55	nd		89.53	19.36
Peonidin-3-Glucoside	2.32	nd		0.56	0.16
Cyanidin-3-Arabinoside	2.33	nd		0.32	0.08
Peonidin-3-6(*p*-Coumaroyl-Glucoside)	2.55	nd		0.14	0.04
Peonidin-3-Arabinoside	3.06	nd		0.07	0.02
Cyanidin-3-6(*p*-Coumaroyl-Glucoside)	3.69	nd		0.12	0.03

[1] SD: standard deviation

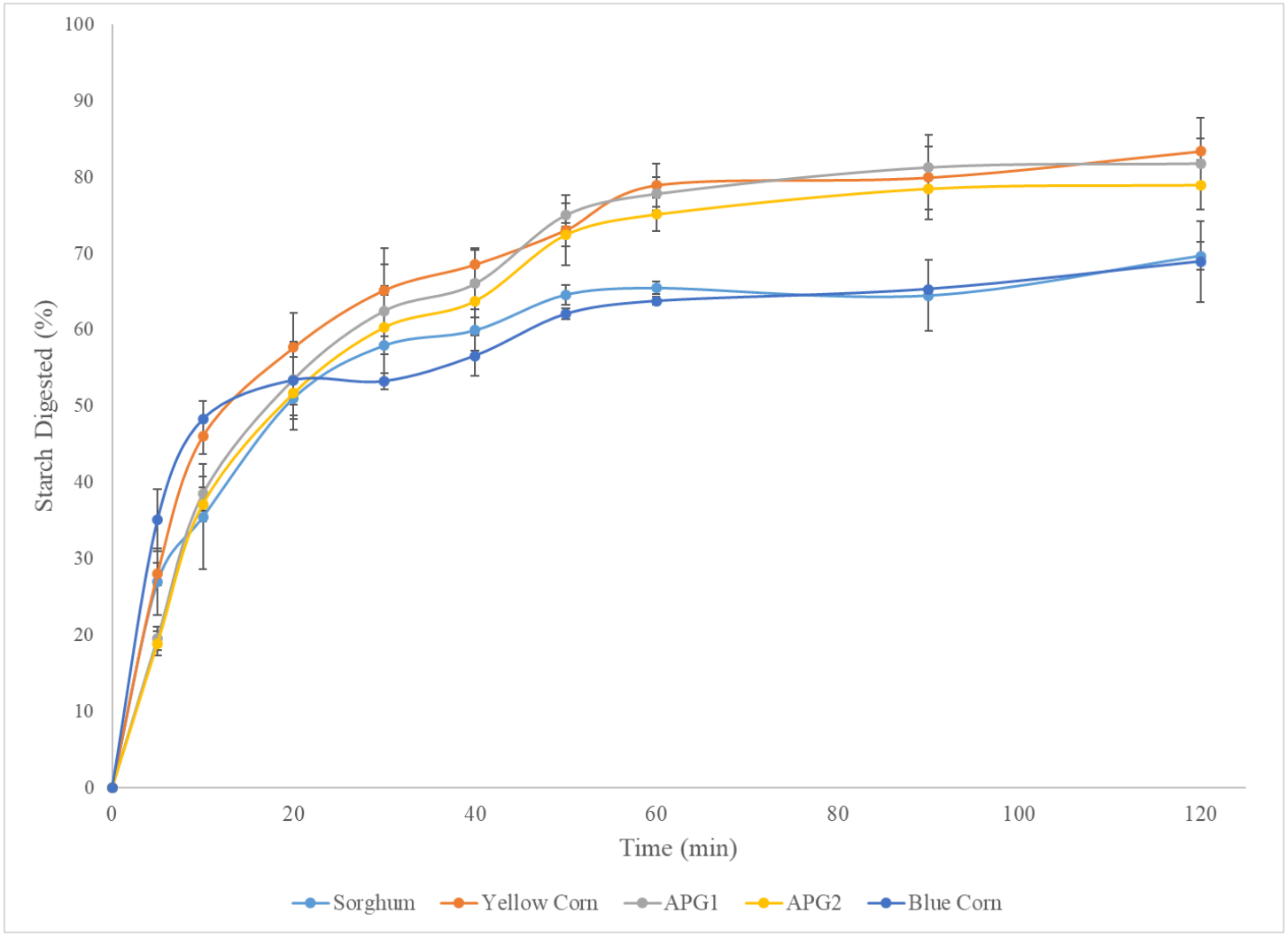

Figure 5.1 Progression of *in vitro* α-amylase digestion of starch from cereal flours.

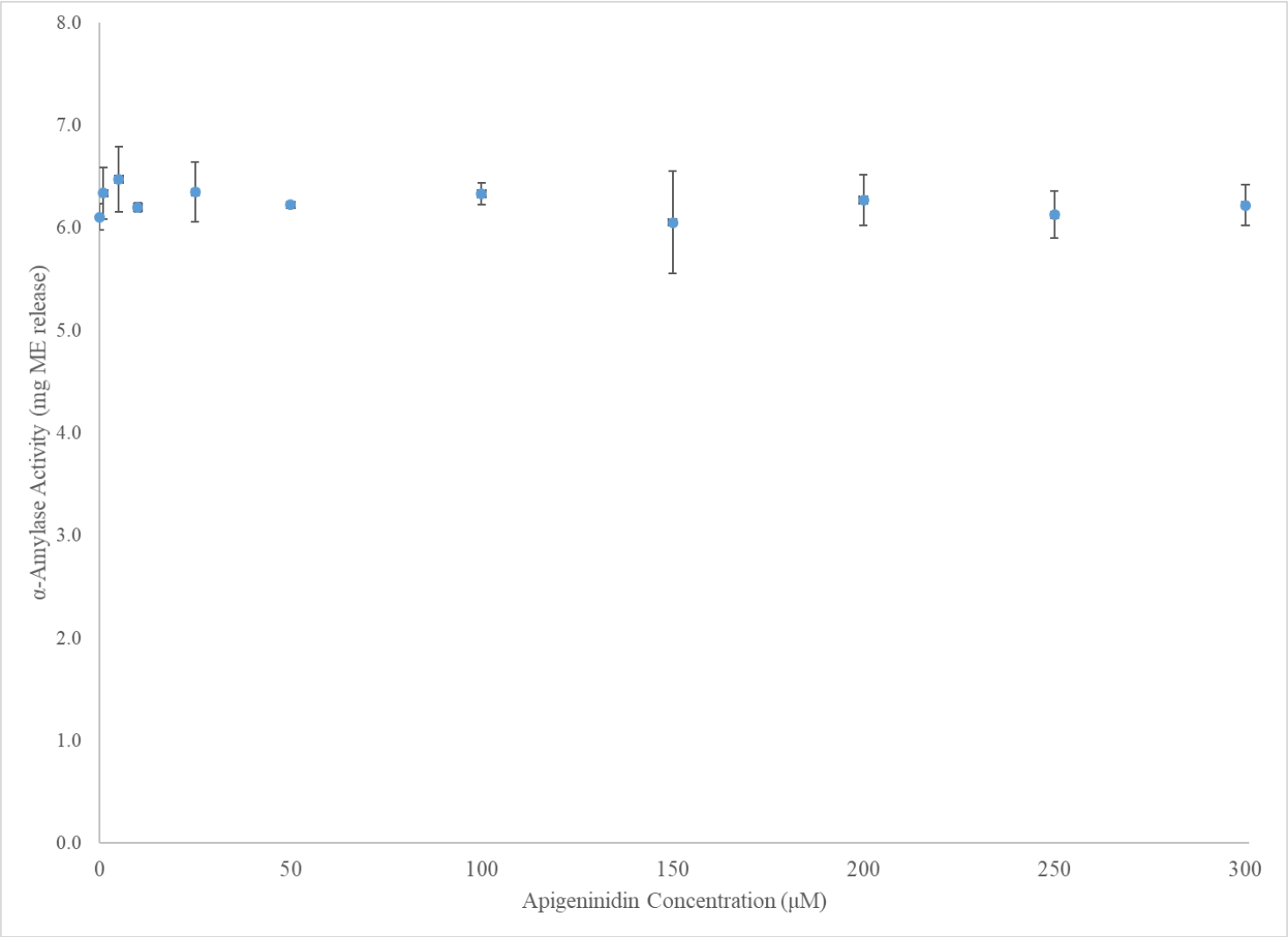

Figure 5.2 Change in apparent activity of α-amylase in the presence of apigeninidin.

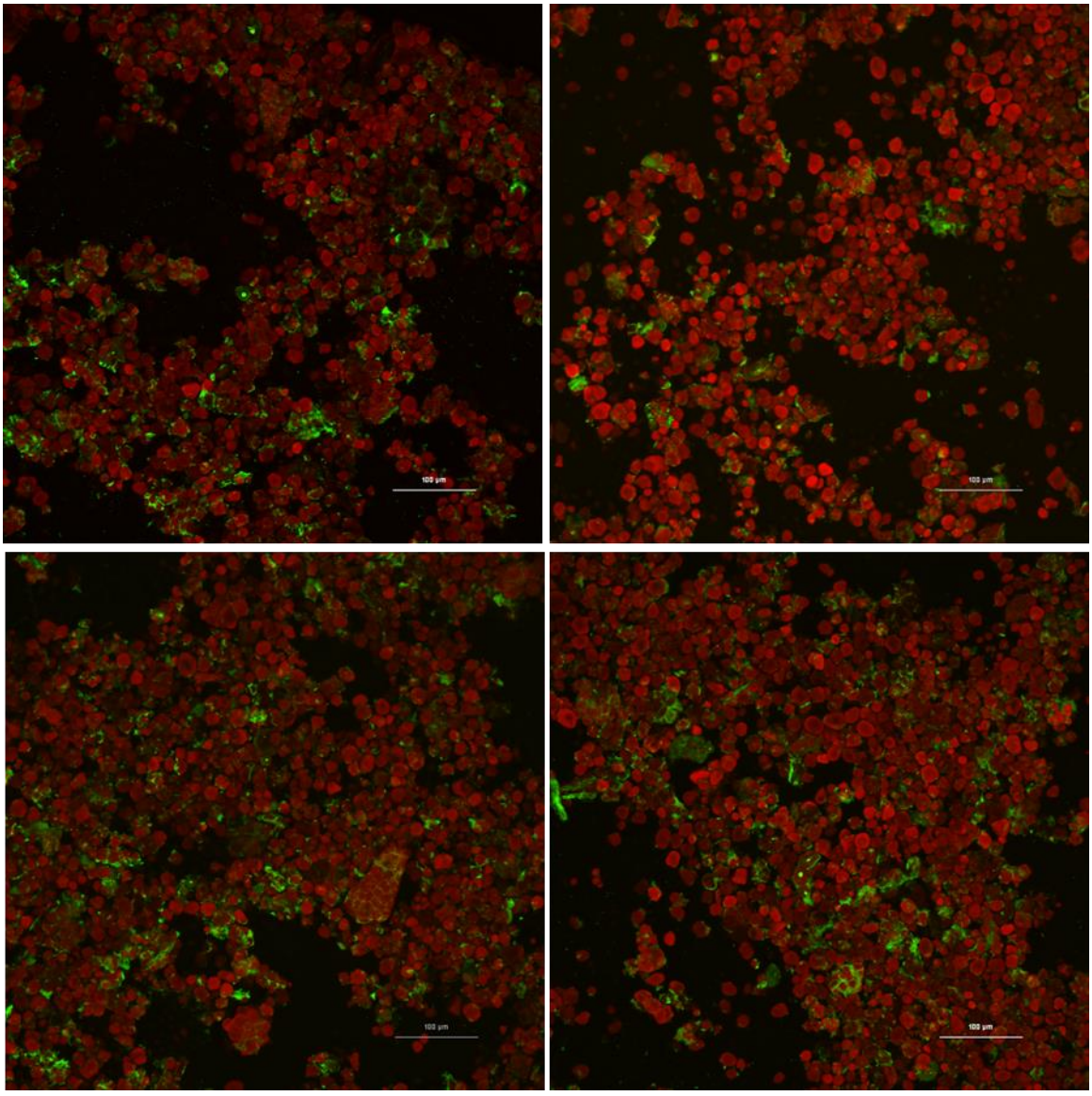

Figure 5.3 Raw yellow corn flour, combined Z-image double labeled with PAS for starch (red) and fluorescamine for protein (pseudo-colored green)

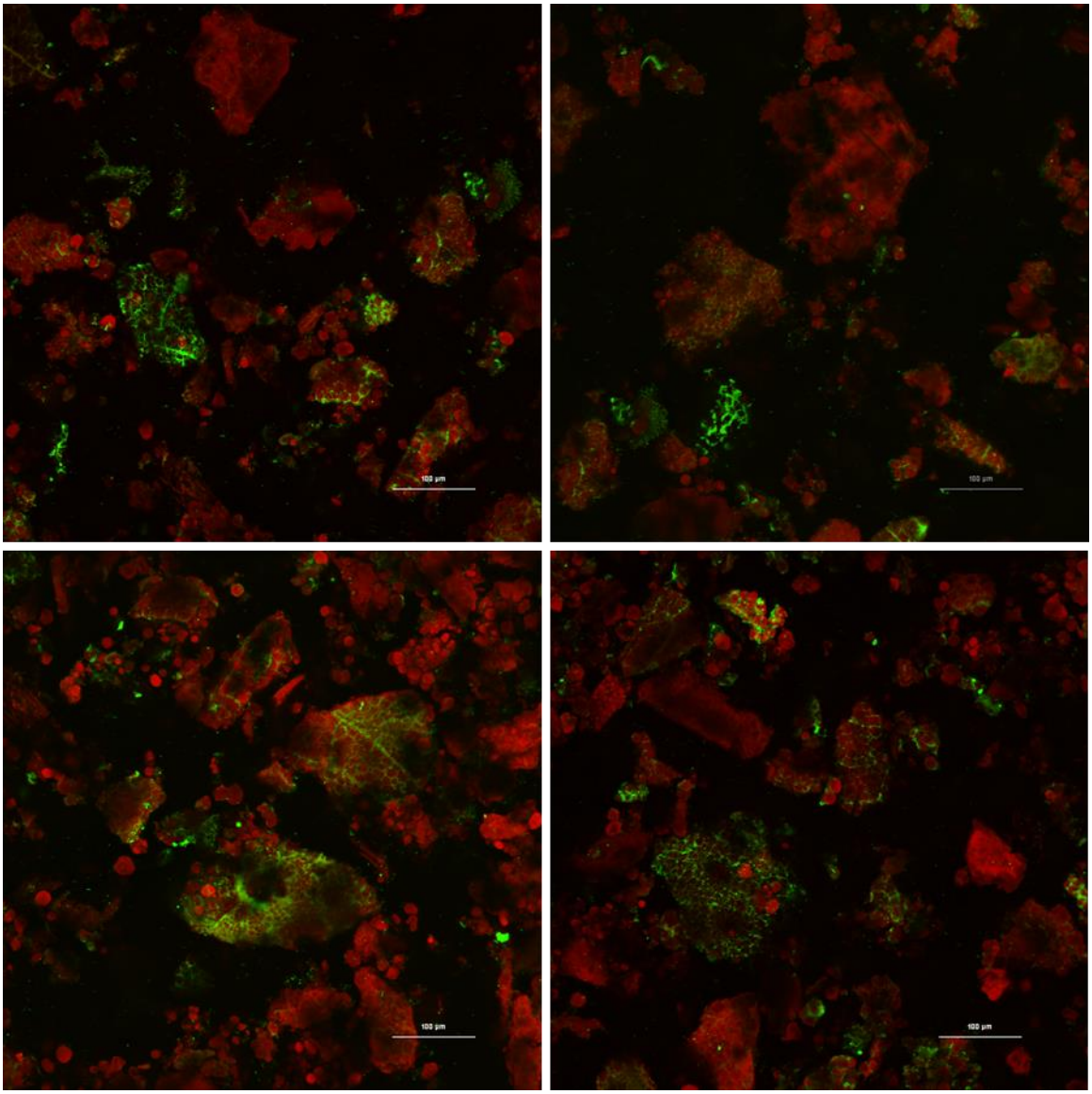

Figure 5.4 Raw blue corn flour, combined Z-image double labeled with PAS for starch (red) and fluorescamine for protein (pseudo-colored green)

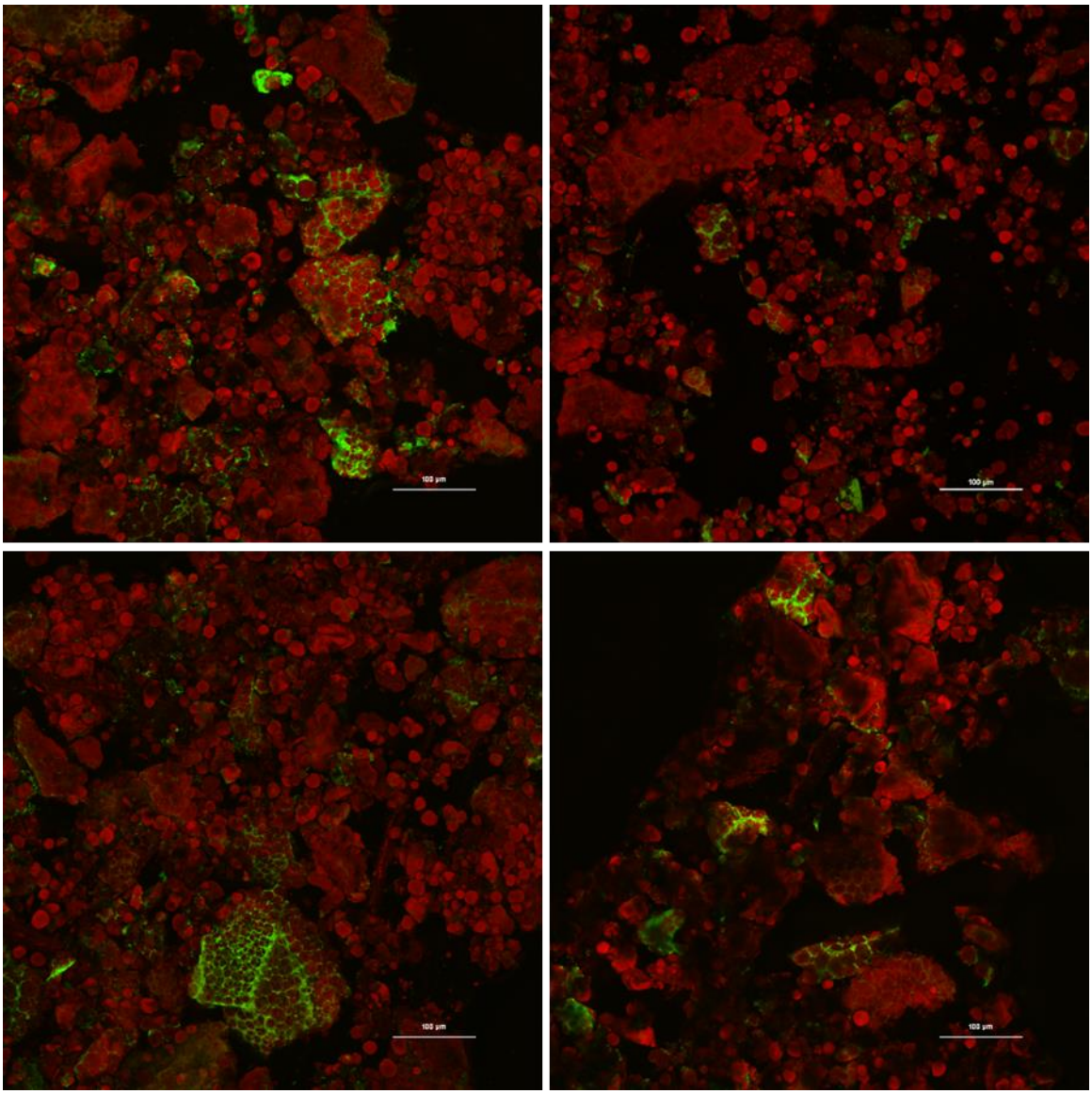

Figure 5.5 Raw decorticated white sorghum flour, combined Z-image double labeled with PAS for starch (red) and fluorescamine for protein (pseudo-colored green)

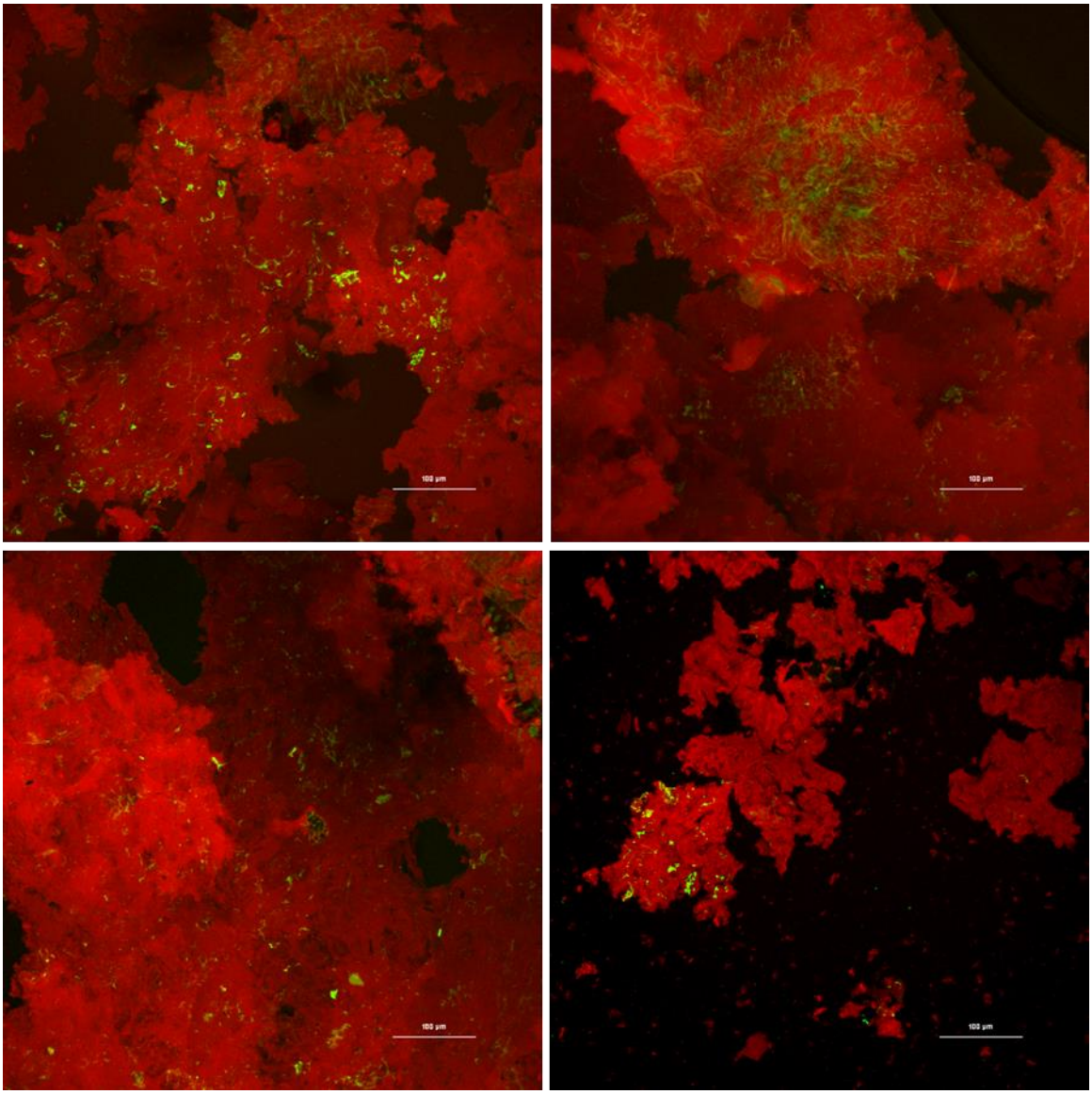

Figure 5.6 Cooked yellow corn porridge “control”, combined Z-image double labeled with PAS for starch (red) and fluorescamine for protein (pseudo-colored green)

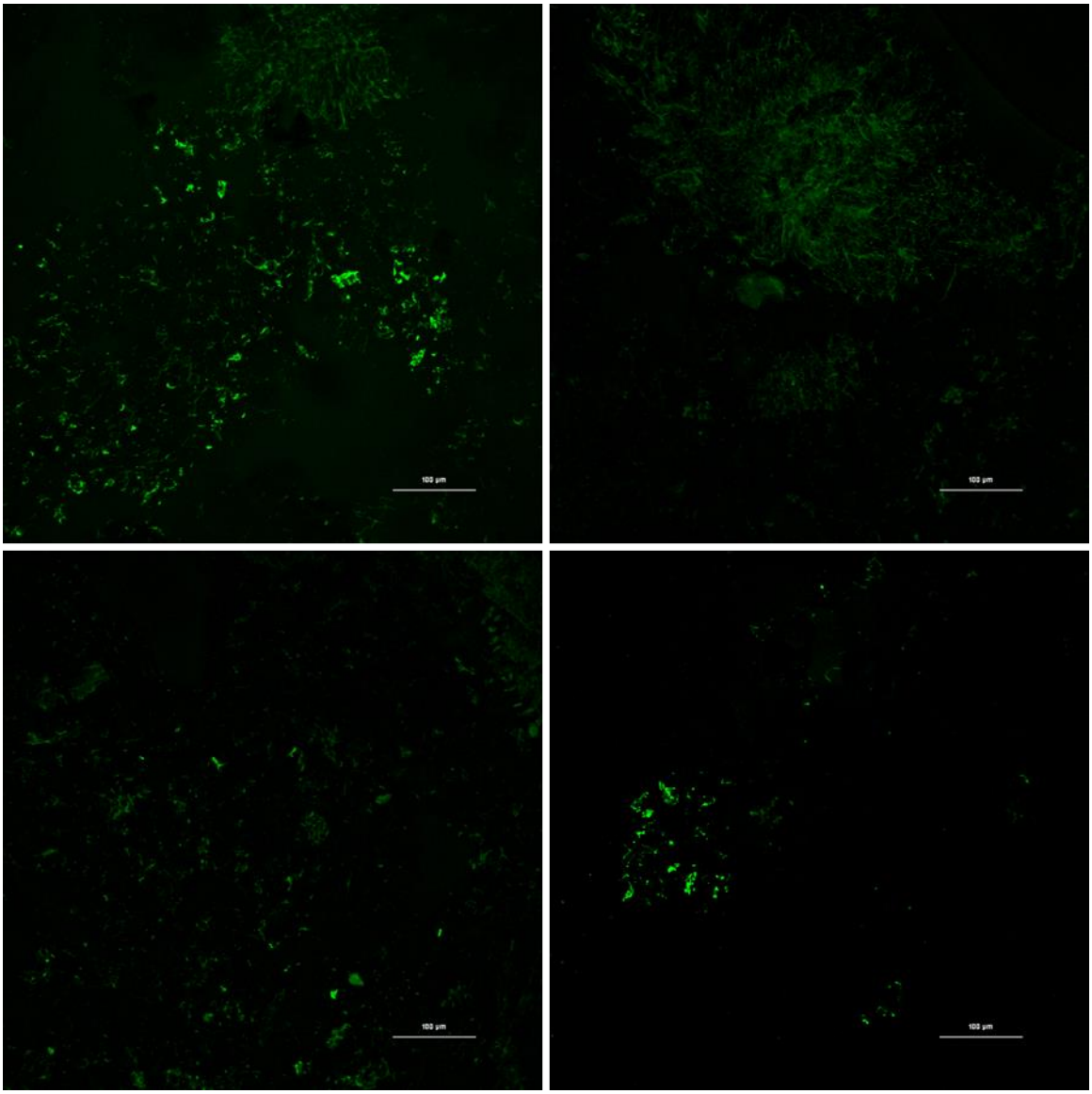

Figure 5.7 Cooked yellow corn porridge “control”, protein portion, combined Z-image (pseudo-colored green)

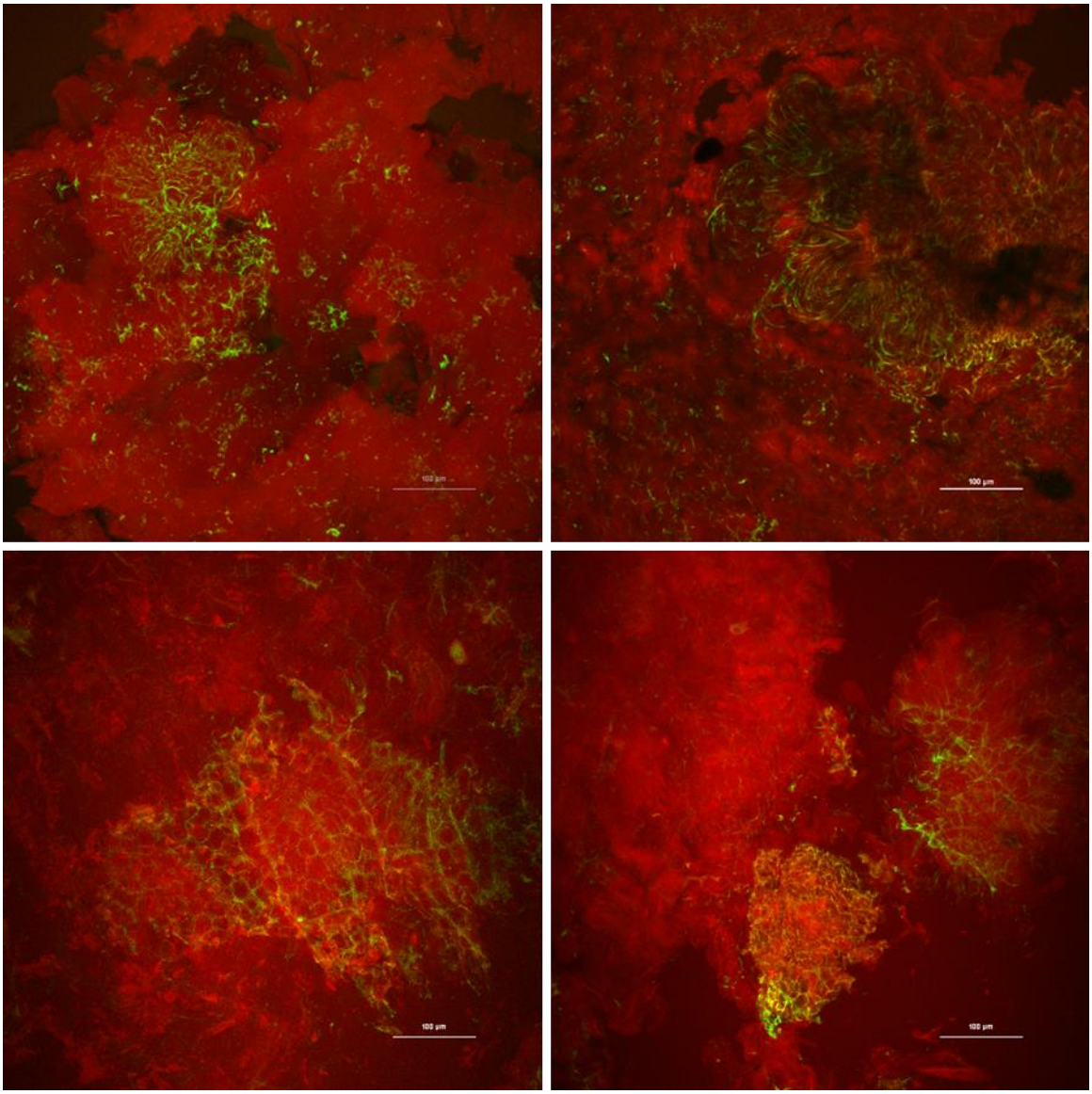

Figure 5.8 Cooked yellow corn porridge “APG1” treated with apigeninidin, combined Z-image double labeled with PAS for starch (red) and fluorescamine for protein (pseudo-colored green)

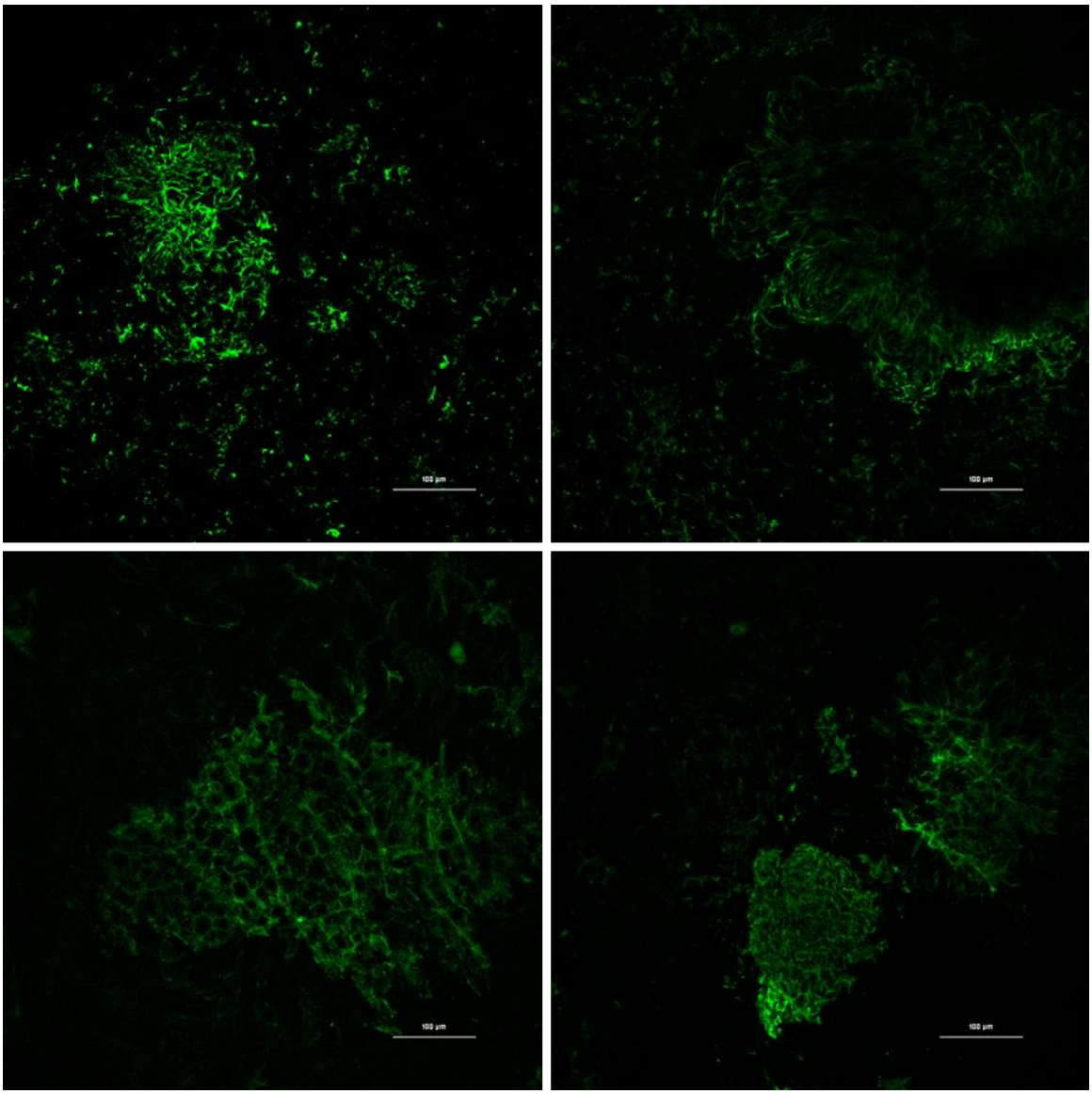

Figure 5.9 Cooked yellow corn porridge “APG1” treated with apigeninidin, protein portion, combined Z-image (pseudo-colored green)

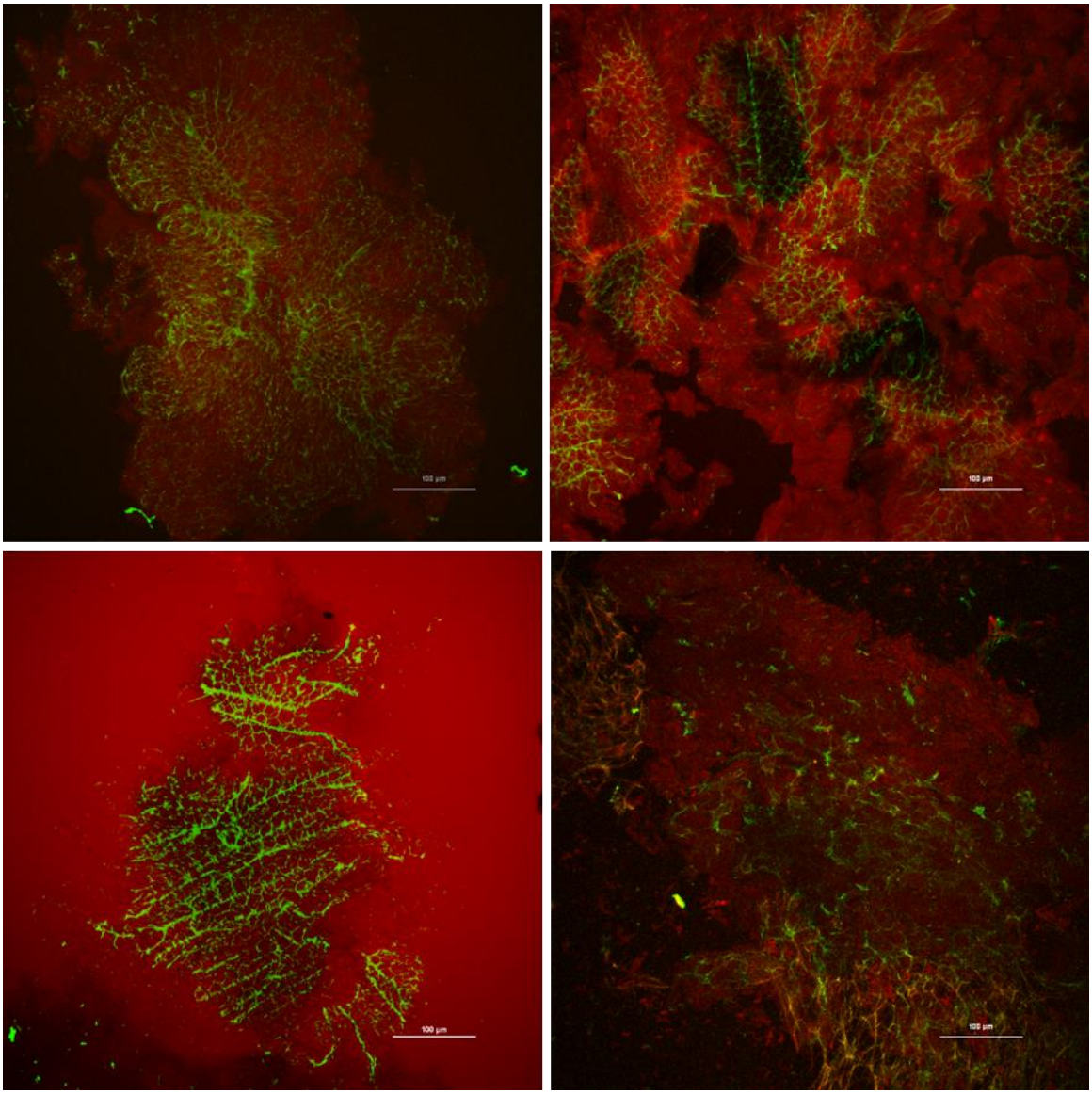

Figure 5.10 Cooked yellow corn porridge “APG2” treated with apigeninidin, combined Z-image double labeled with PAS for starch (red) and fluorescamine for protein (pseudo-colored green)

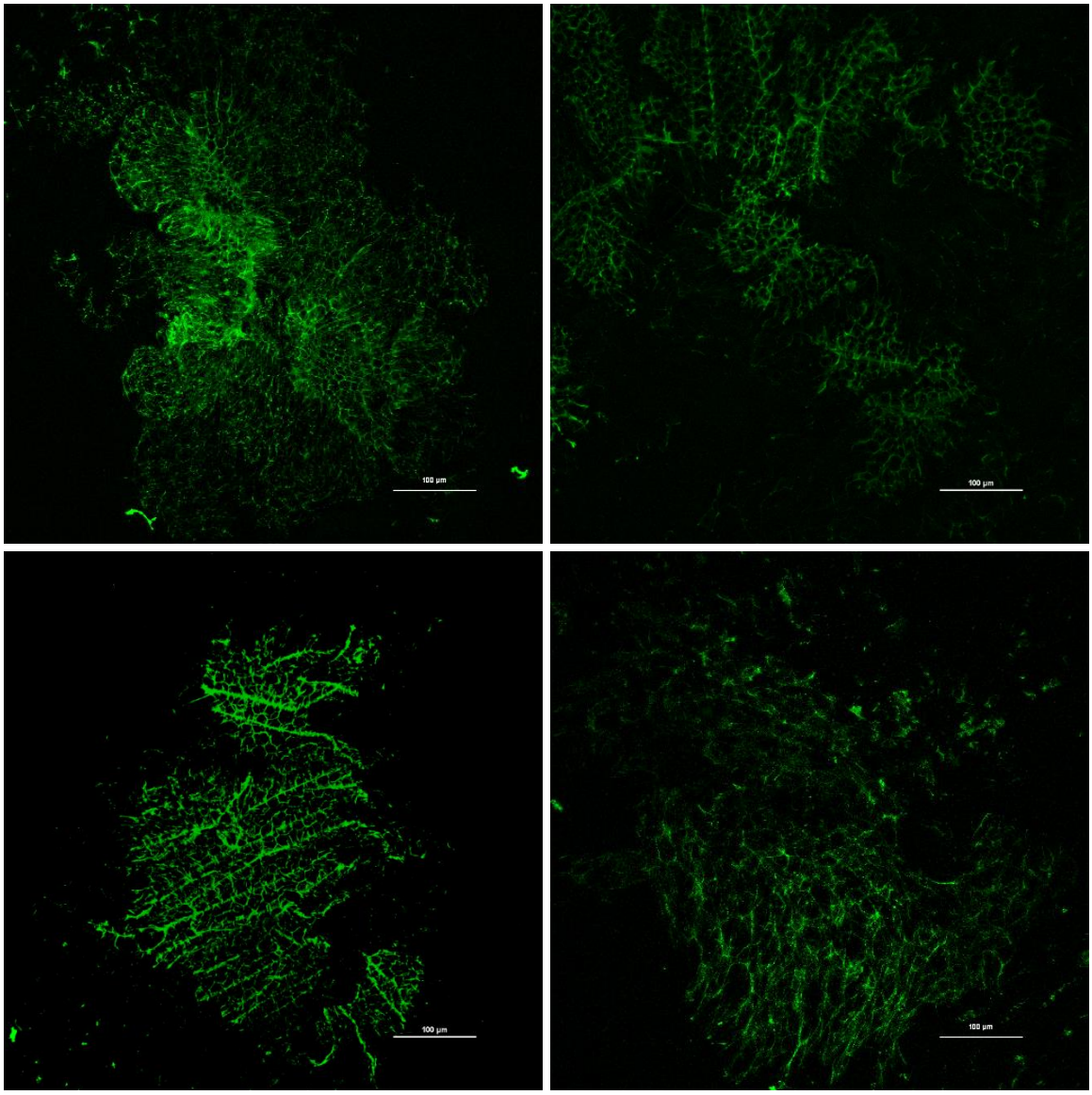

Figure 5.11 Cooked yellow corn porridge “APG2” treated with apigeninidin, protein portion, combined Z-image (pseudo-colored green)

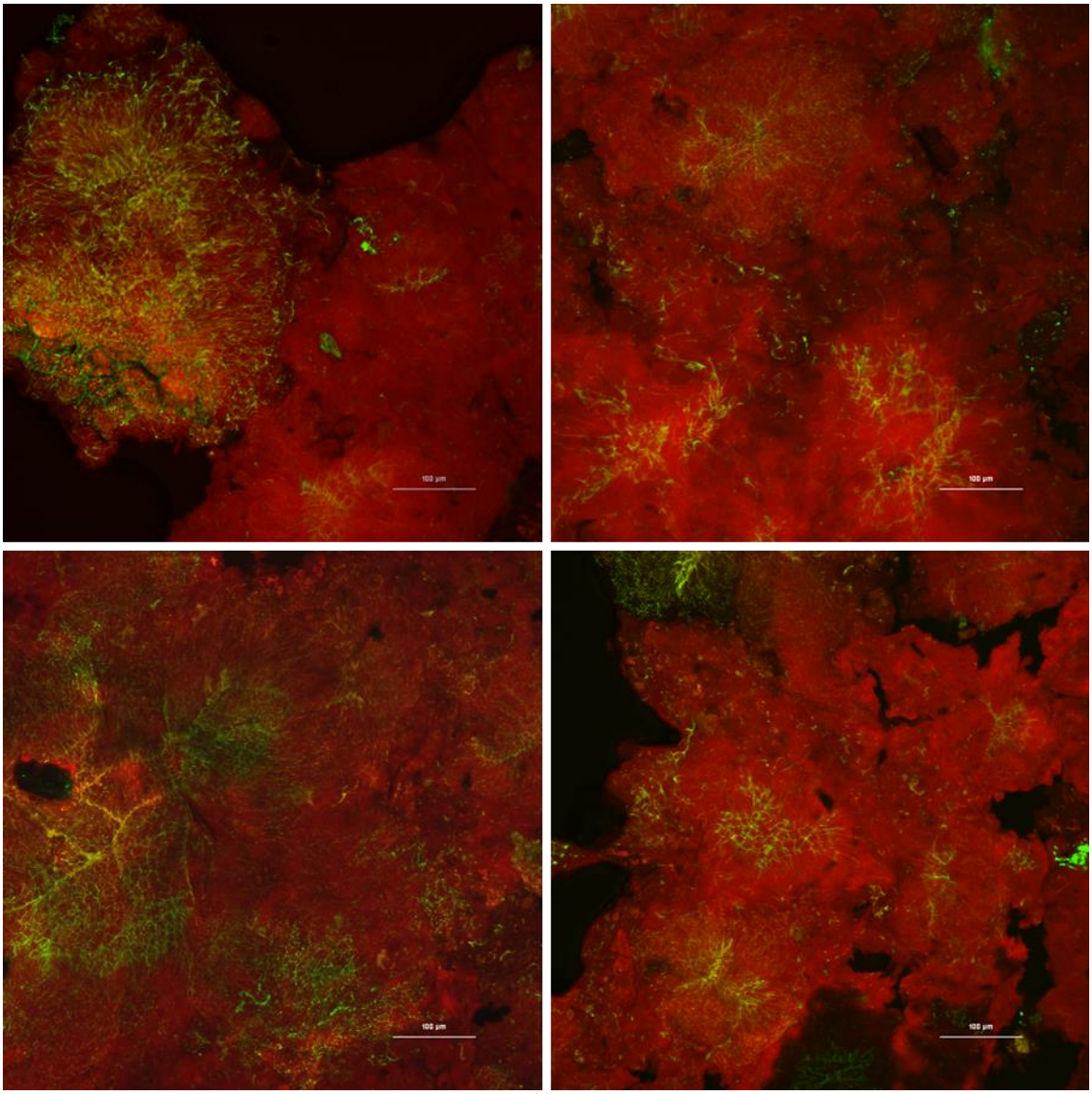

Figure 5.12 Cooked blue corn porridge, combined Z-image double labeled with PAS for starch (red) and fluorescamine for protein (pseudo-colored green)

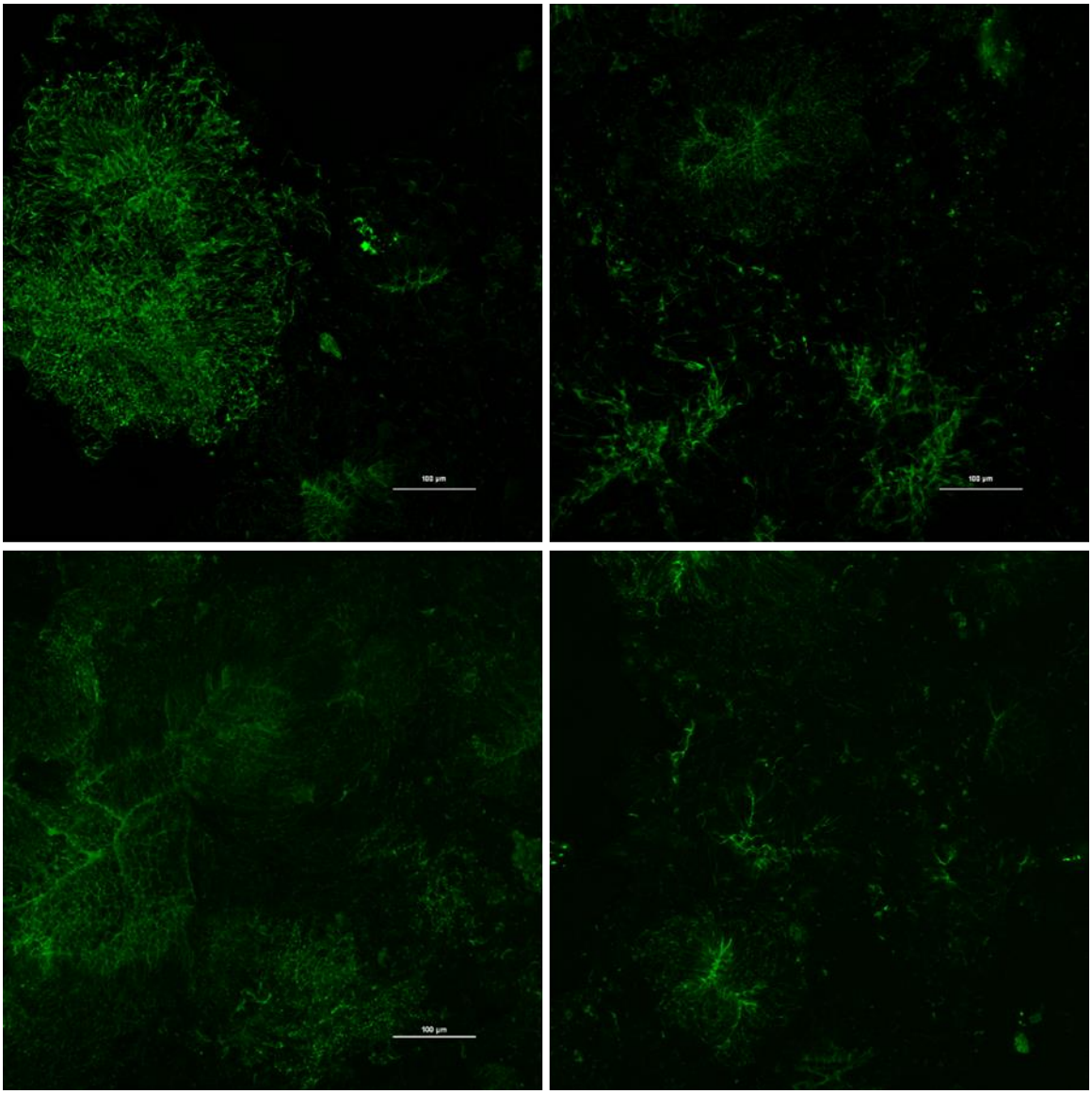

Figure 5.13 Cooked blue corn porridge, protein portion, combined Z-image (pseudo-colored green)

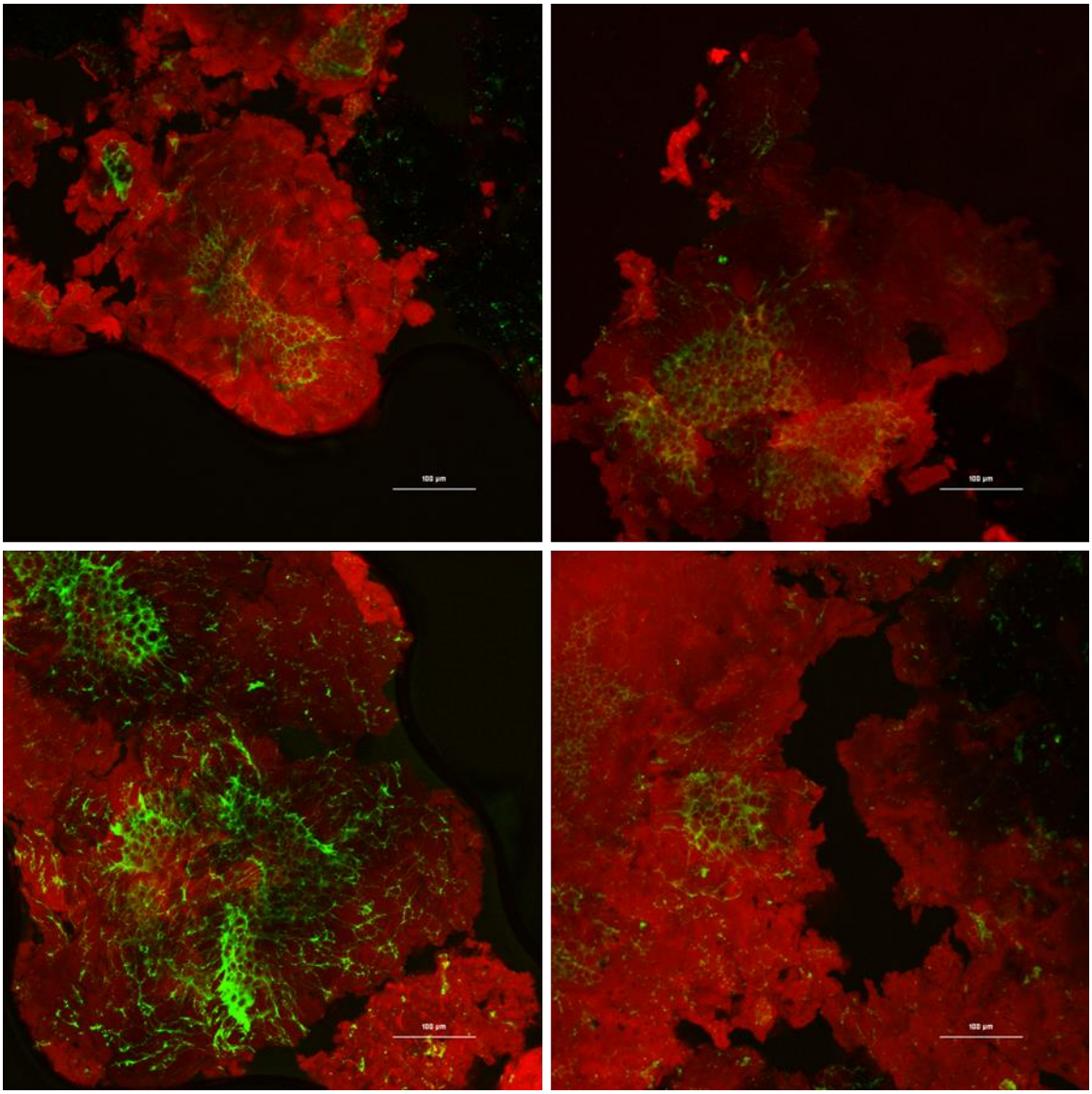

Figure 5.14 Cooked decorticated white sorghum porridge, combined Z-image double labeled with PAS for starch (red) and fluorescamine for protein (pseudo-colored green)

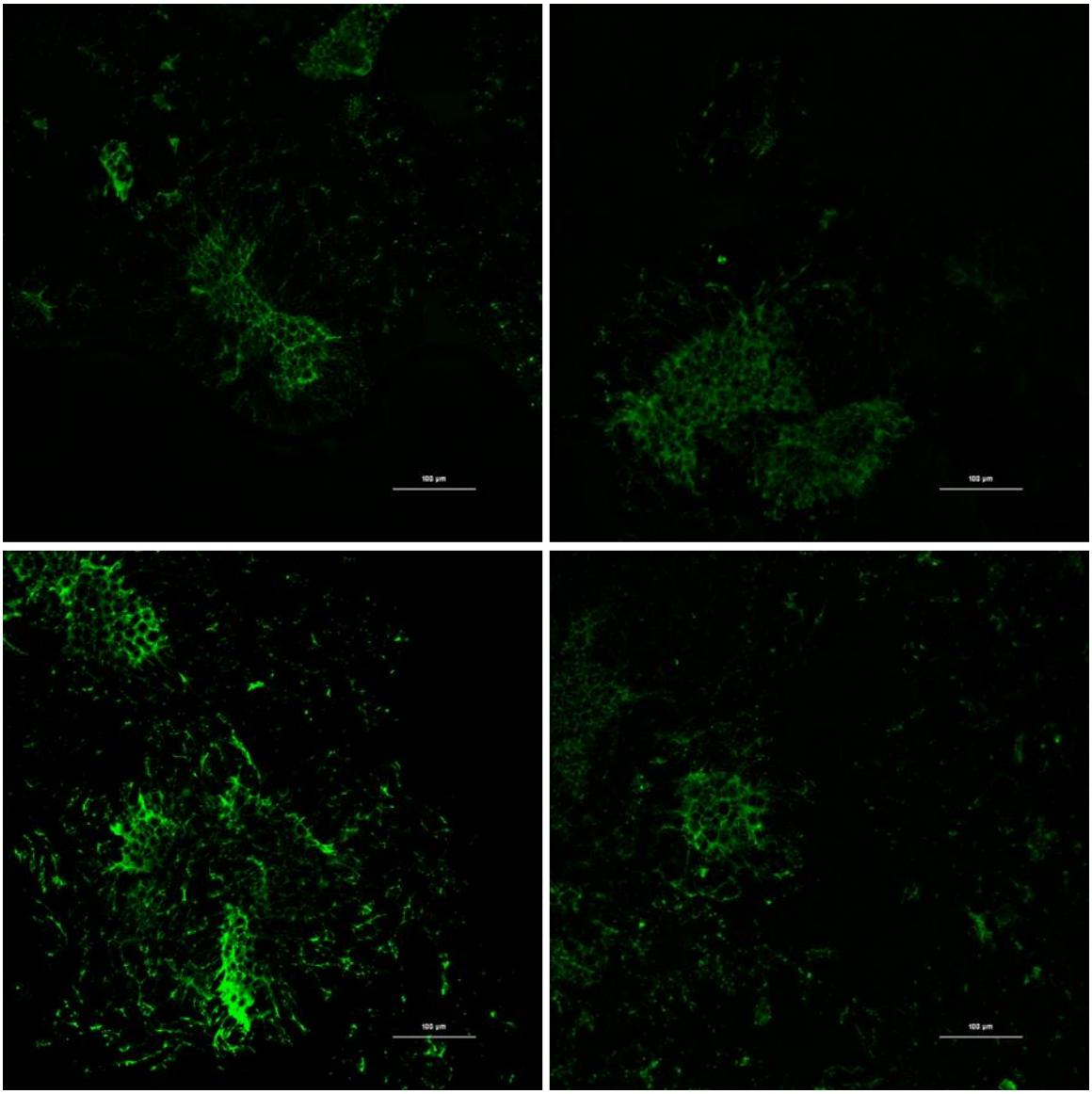

Figure 5.15 Cooked decorticated white sorghum porridge, protein portion, combined Z-image (pseudo-colored green)

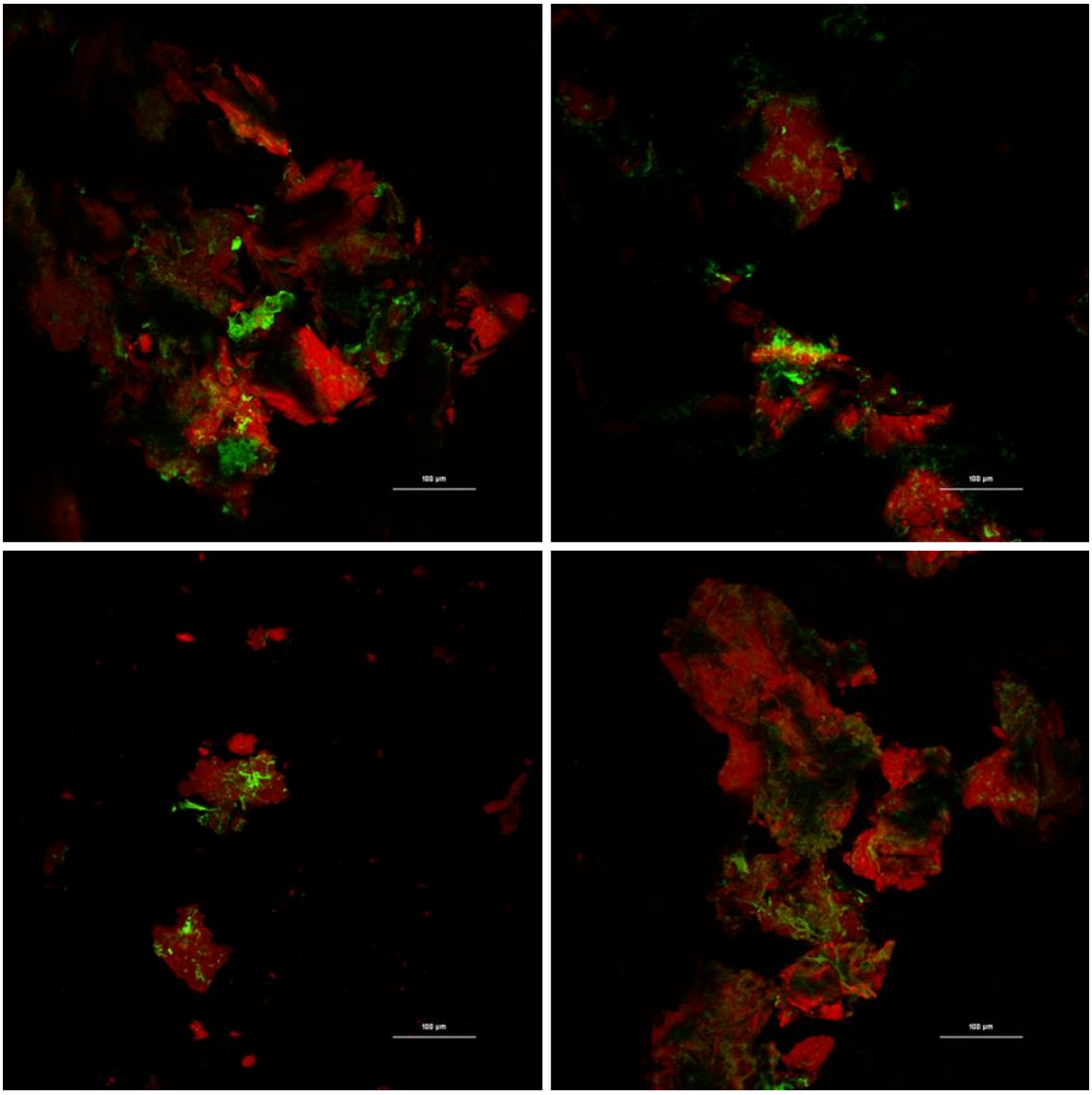

Figure 5.16 Yellow corn porridge “control” after 30 min α-amylase digestion, combined Z-image double labeled with PAS for starch (red) and fluorescamine for protein (pseudo-colored green)

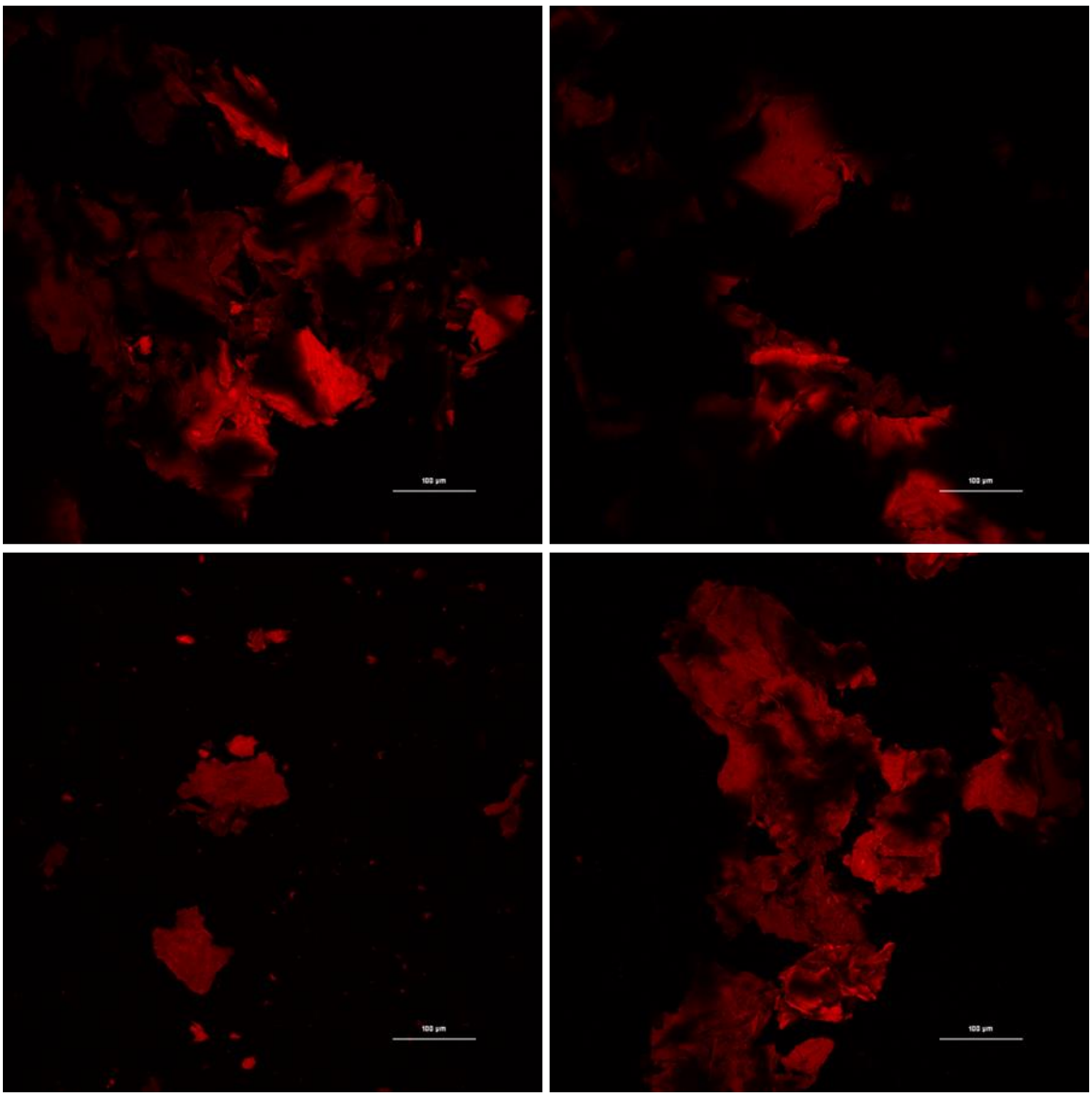

Figure 5.17 Yellow corn porridge “control” after 30 min α-amylase digestion, starch portion, combined Z-image

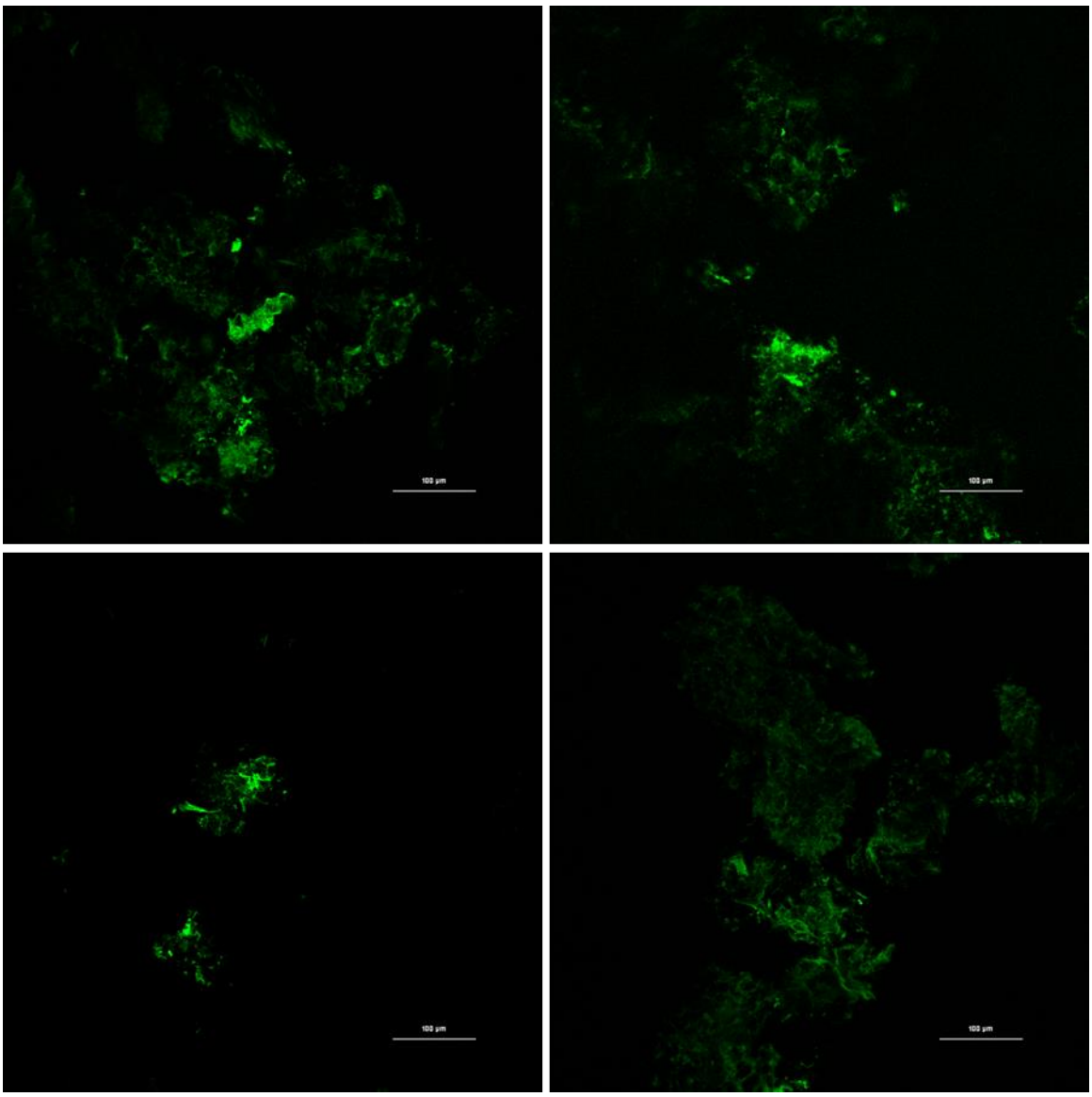

Figure 5.18 Yellow corn porridge “control” after 30 min α-amylase digestion, protein portion, combined Z-image (pseudo-colored green)

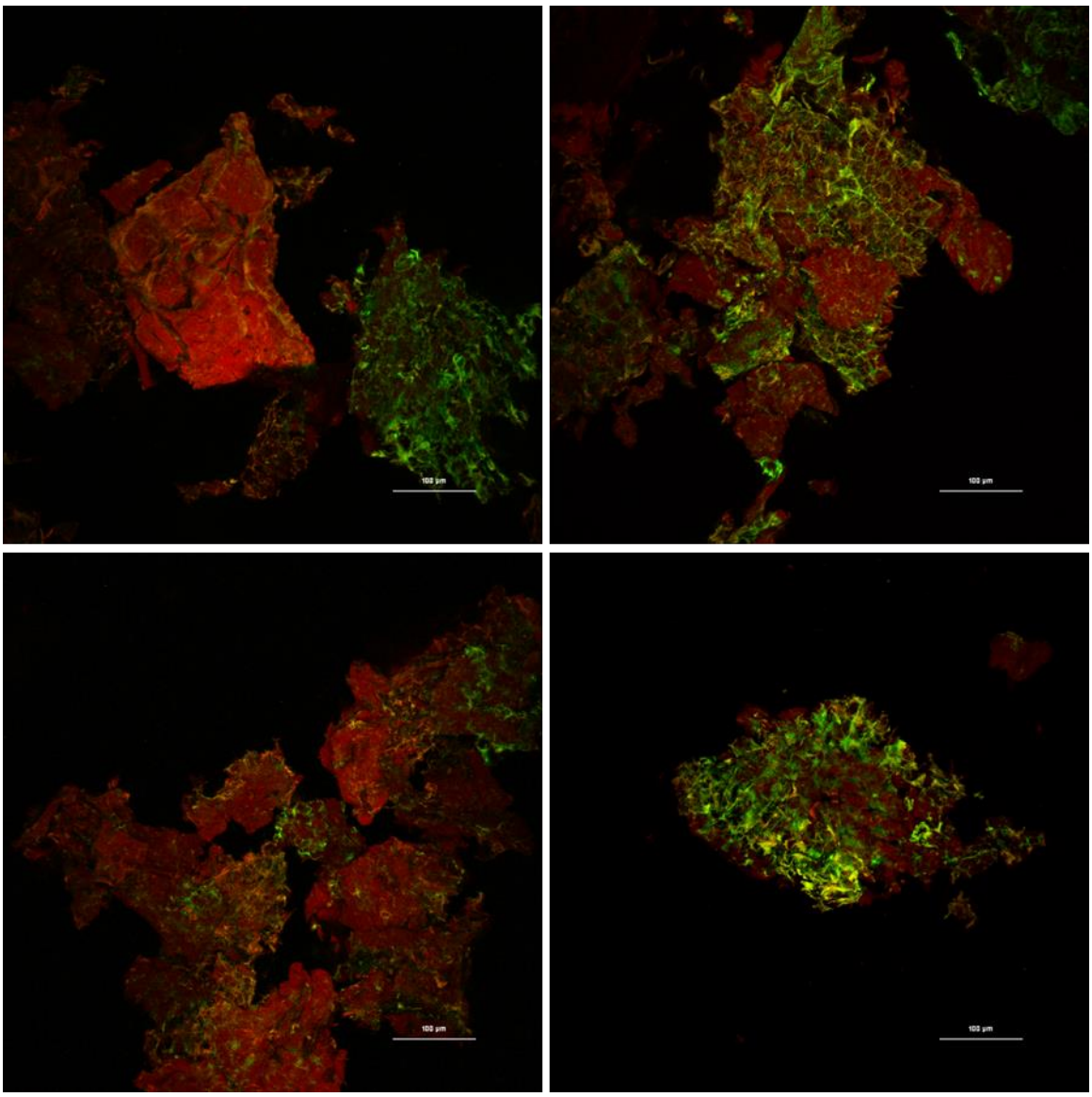

Figure 5.19 Yellow corn porridge “APG1” treated with apigeninidin after 30 min α-amylase digestion, combined Z-image double labeled with PAS for starch (red) and fluorescamine for protein (pseudo-colored green)

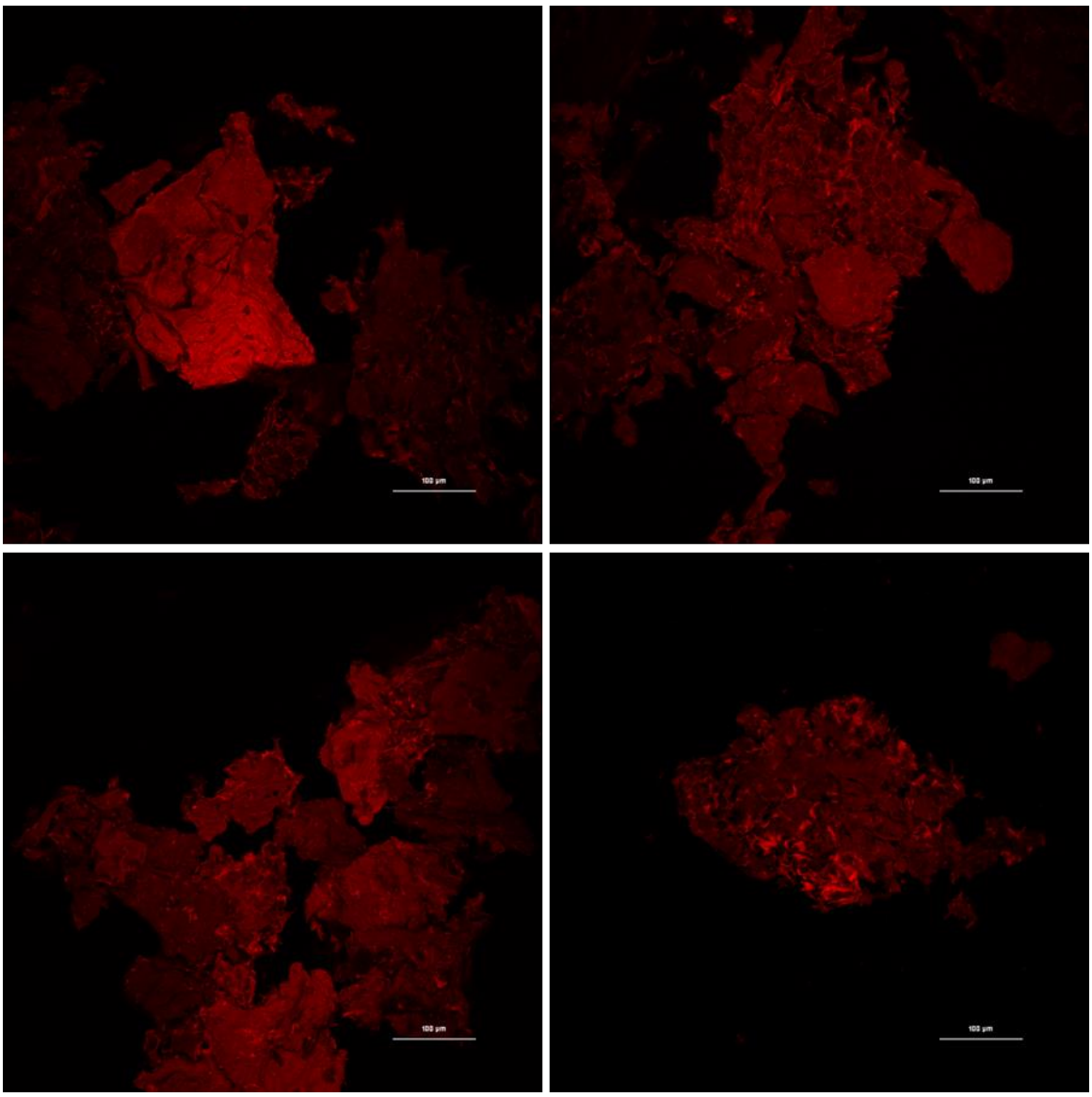

Figure 5.20 Yellow corn porridge “APG1” treated with apigeninidin after 30 min α-amylase digestion, starch portion, combined Z-image

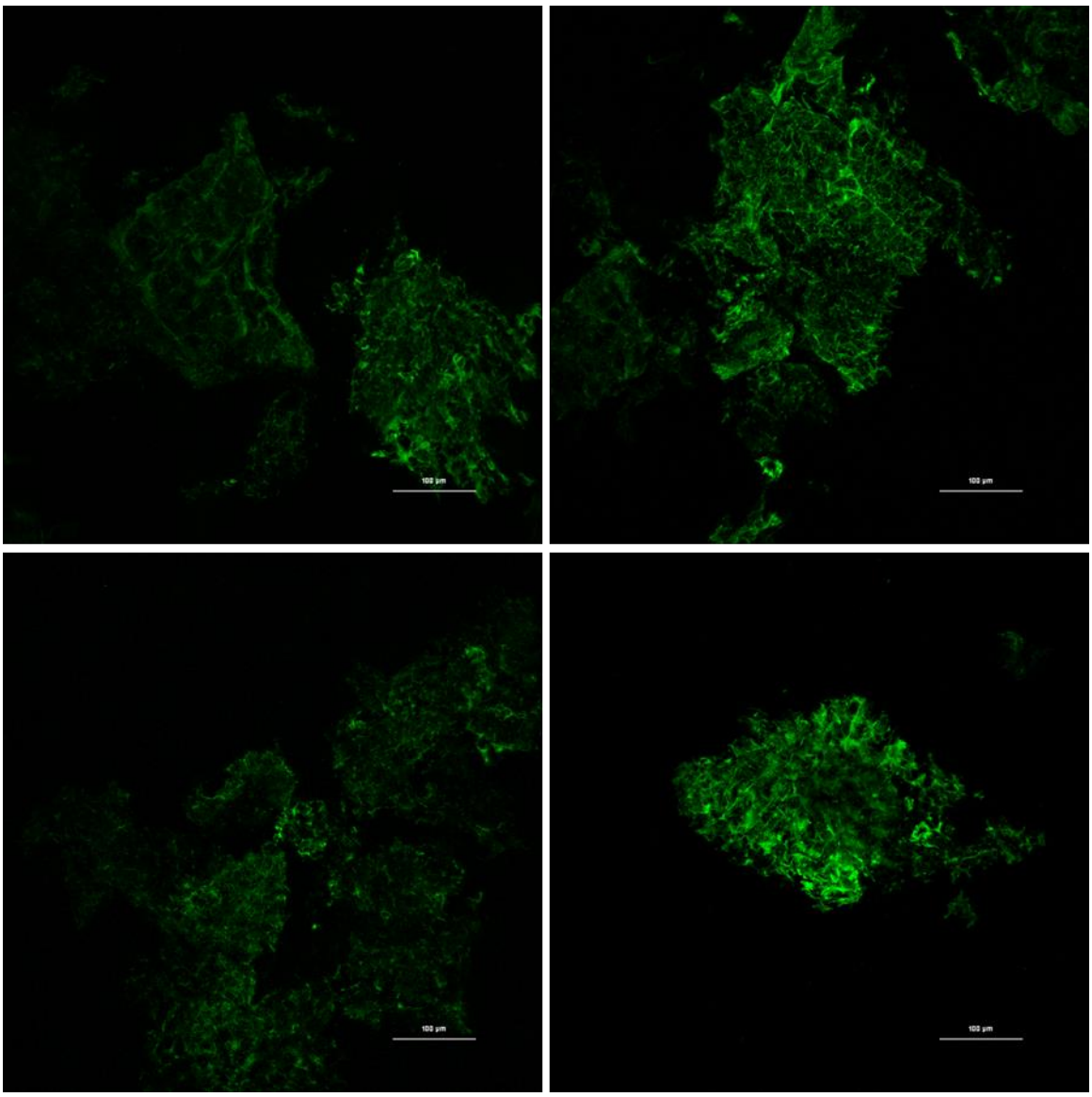

Figure 5.21 Yellow corn porridge “APG1” treated with apigeninidin after 30 min α-amylase digestion, protein portion, combined Z-image (pseudo-colored green)

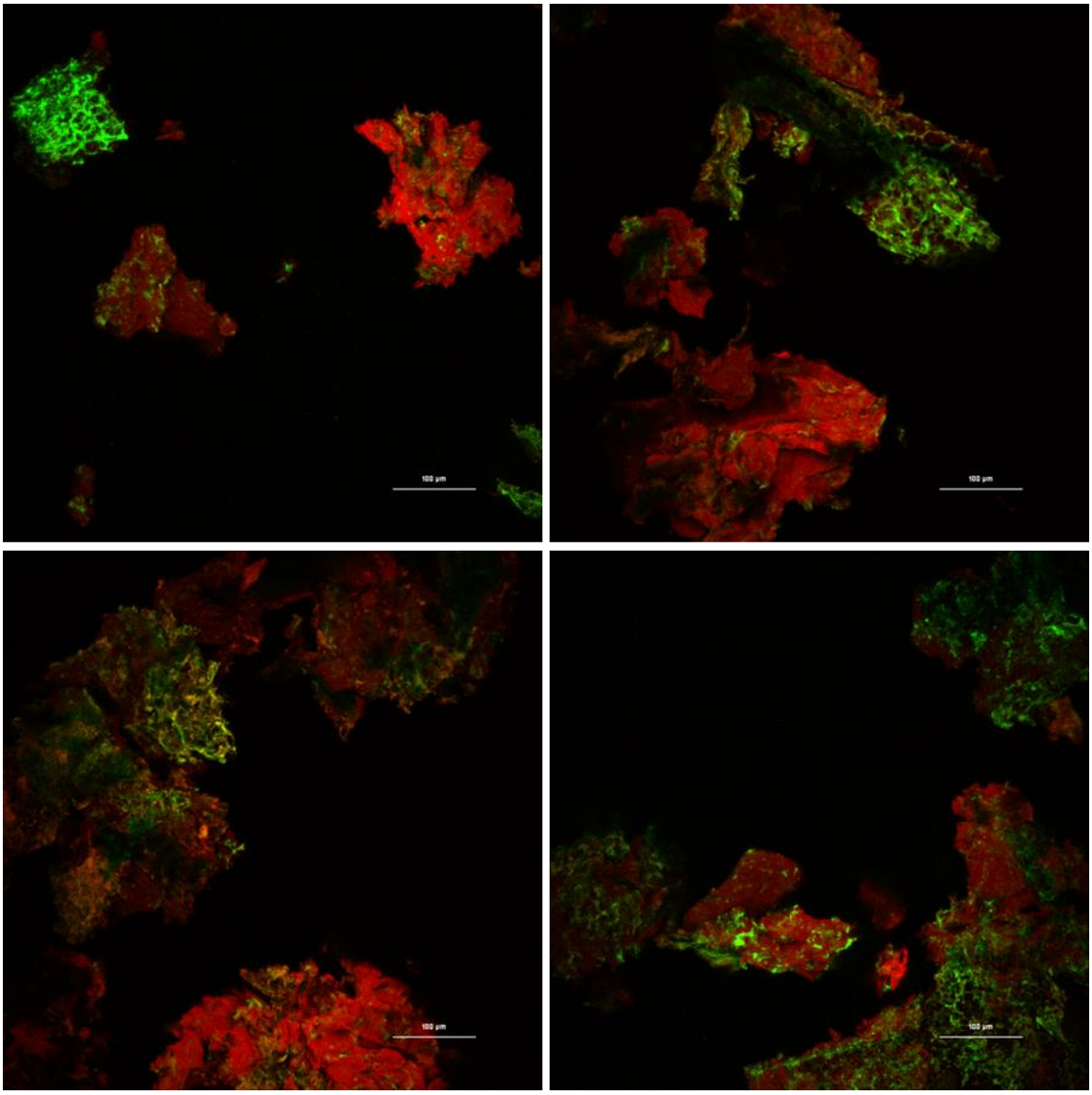

Figure 5.22 Yellow corn porridge “APG2” treated with apigeninidin after 30 min α-amylase digestion, combined Z-image double labeled with PAS for starch (red) and fluorescamine for protein (pseudo-colored green)

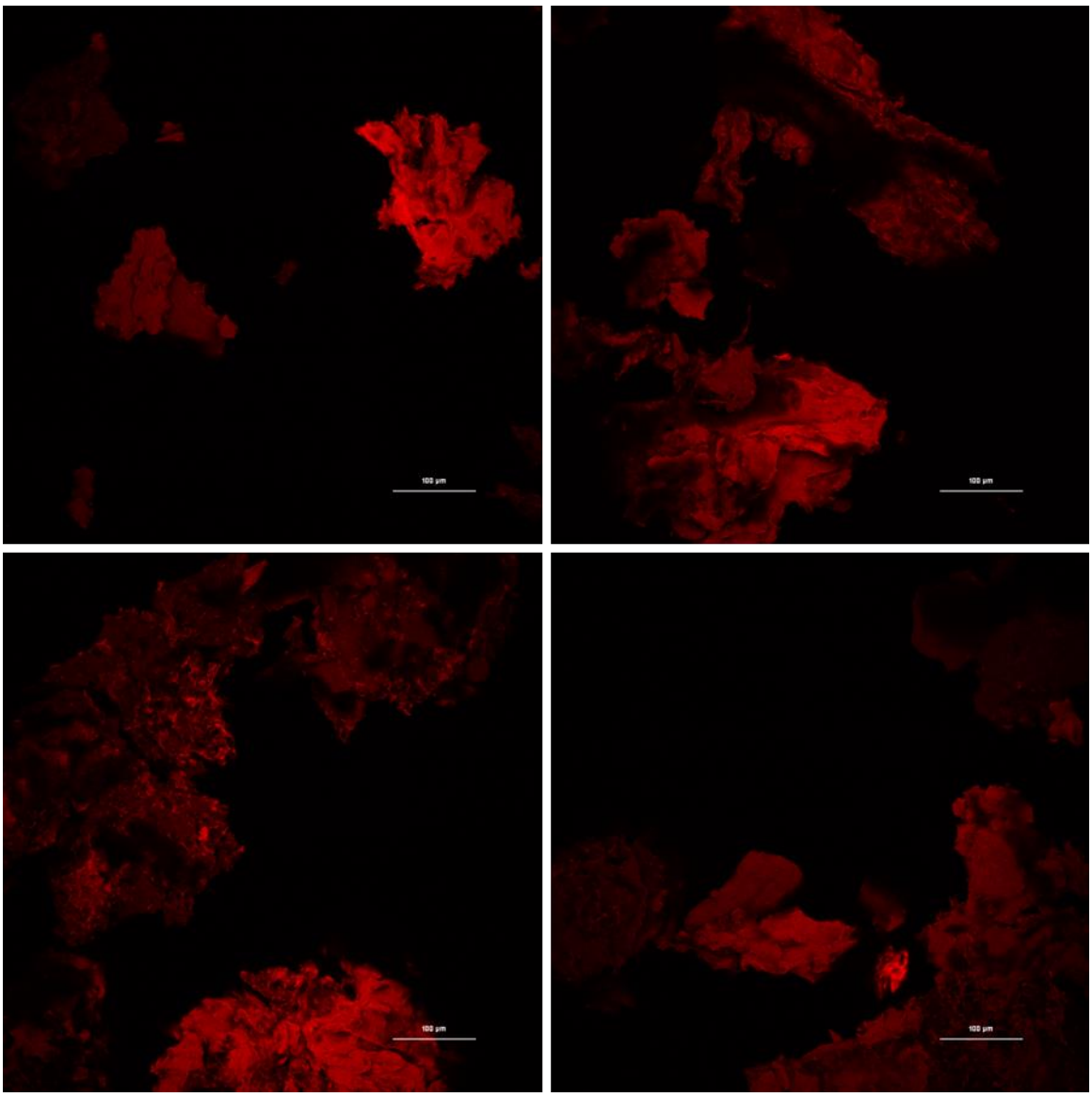

Figure 5.23 Yellow corn porridge “APG2” treated with apigeninidin after 30 min α-amylase digestion, starch portion, combined Z-image

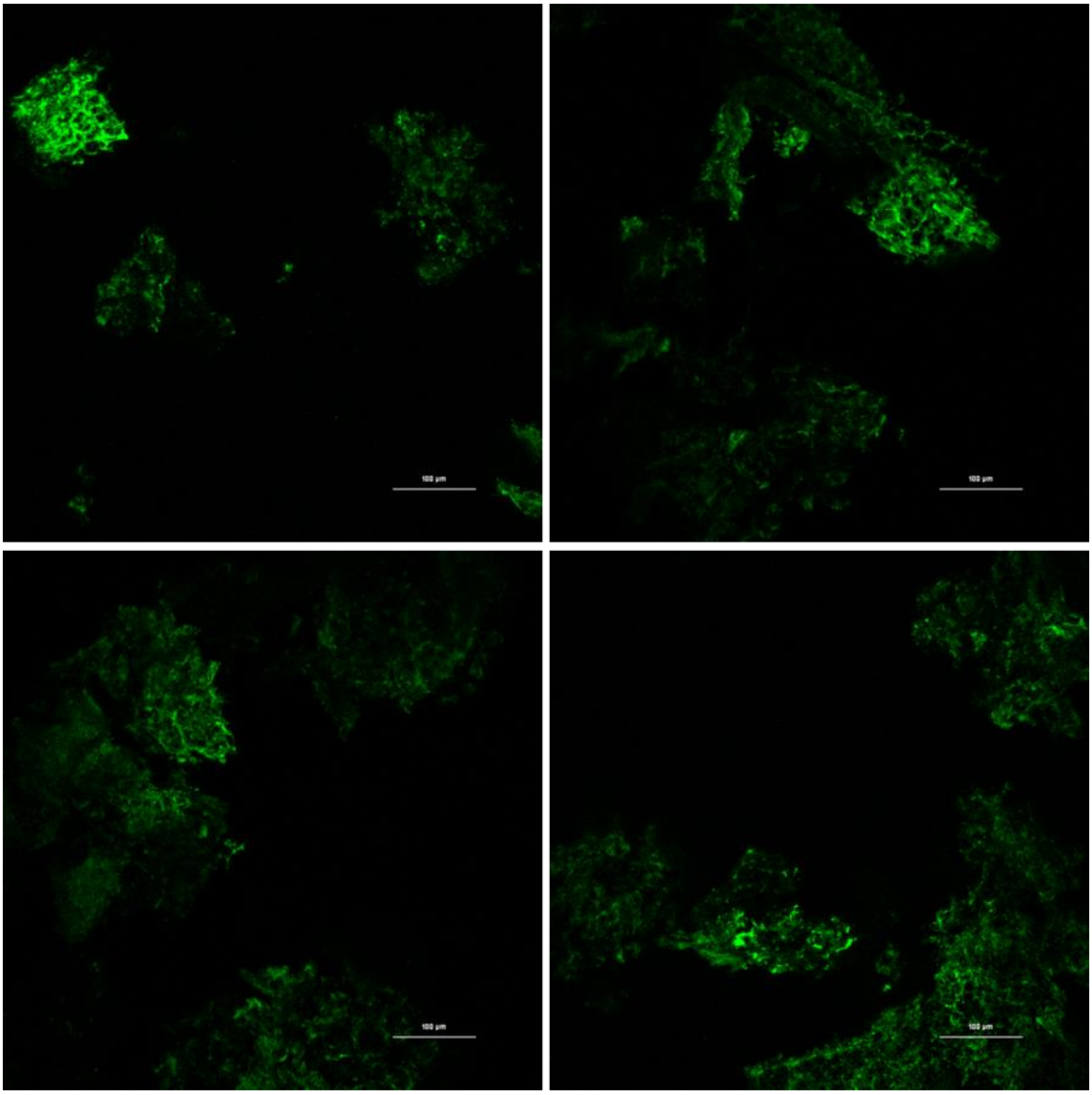

Figure 5.24 Yellow corn porridge “APG2” treated with apigeninidin after 30 min α-amylase digestion, protein portion, combined Z-image (pseudo-colored green)

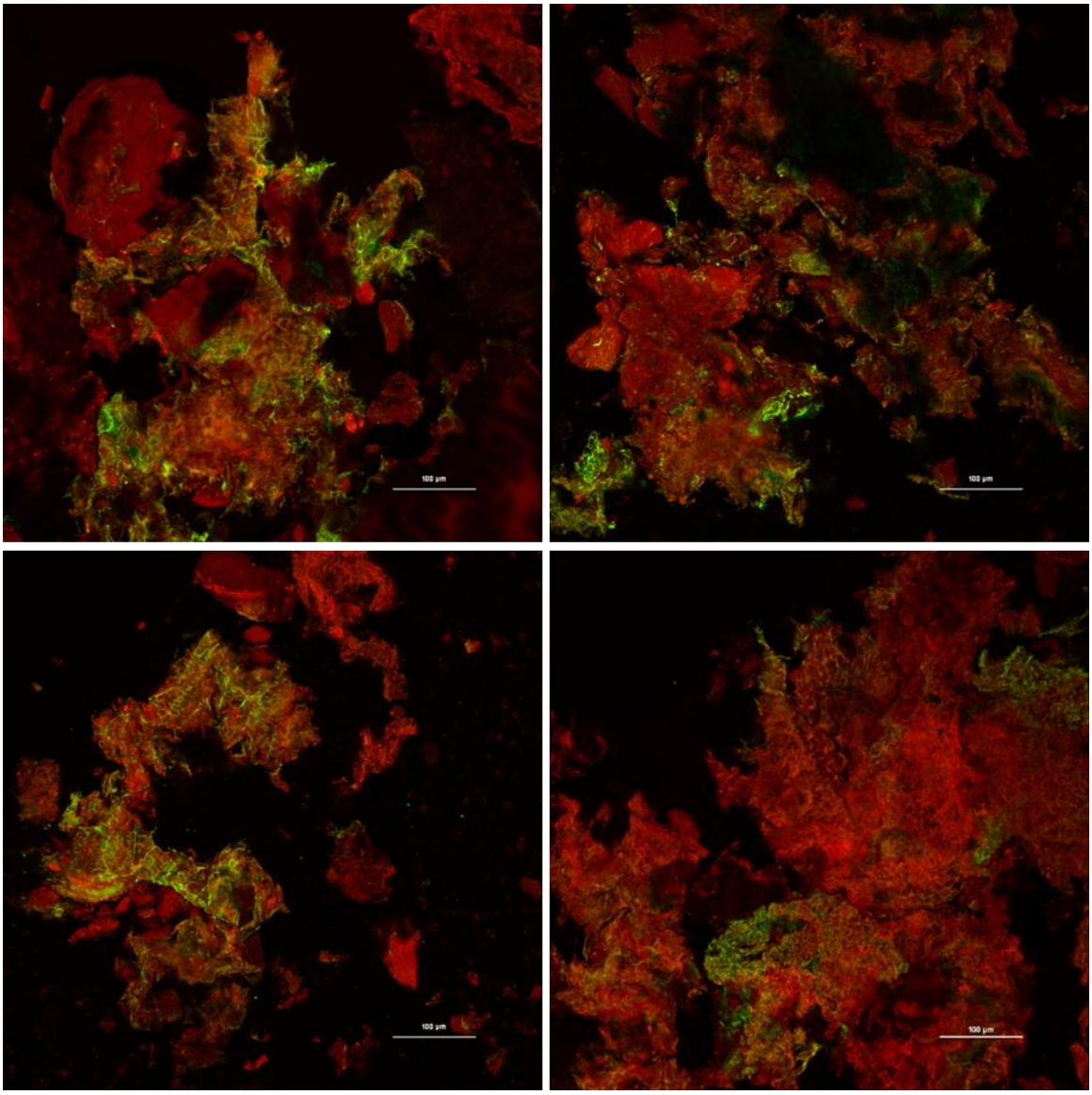

Figure 5.25 Blue corn porridge after 30 min α-amylase digestion, combined Z-image double labeled with PAS for starch (red) and fluorescamine for protein (pseudo-colored green)

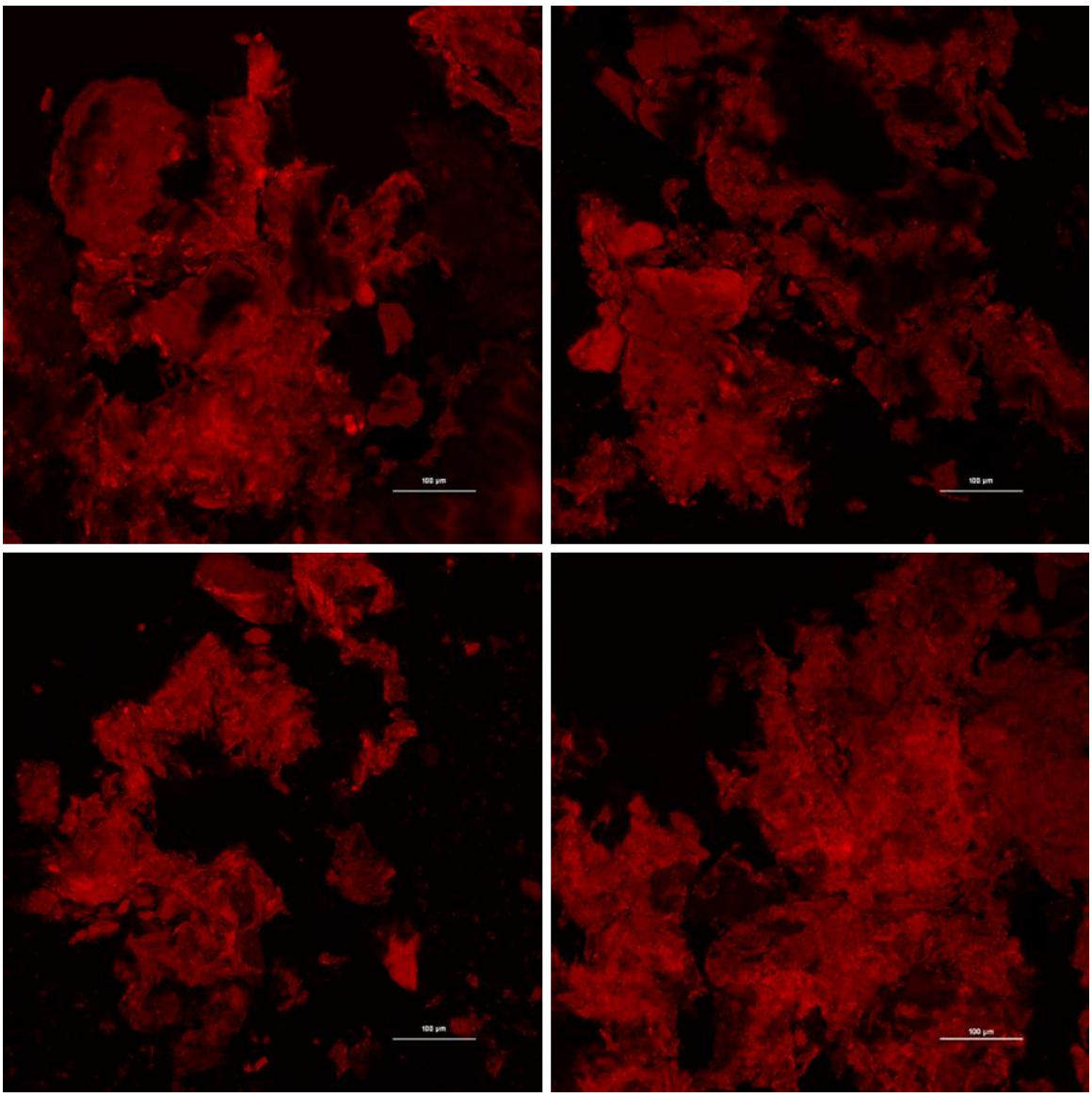

Figure 5.26 Blue corn porridge after 30 min α-amylase digestion, starch portion, combined Z-image

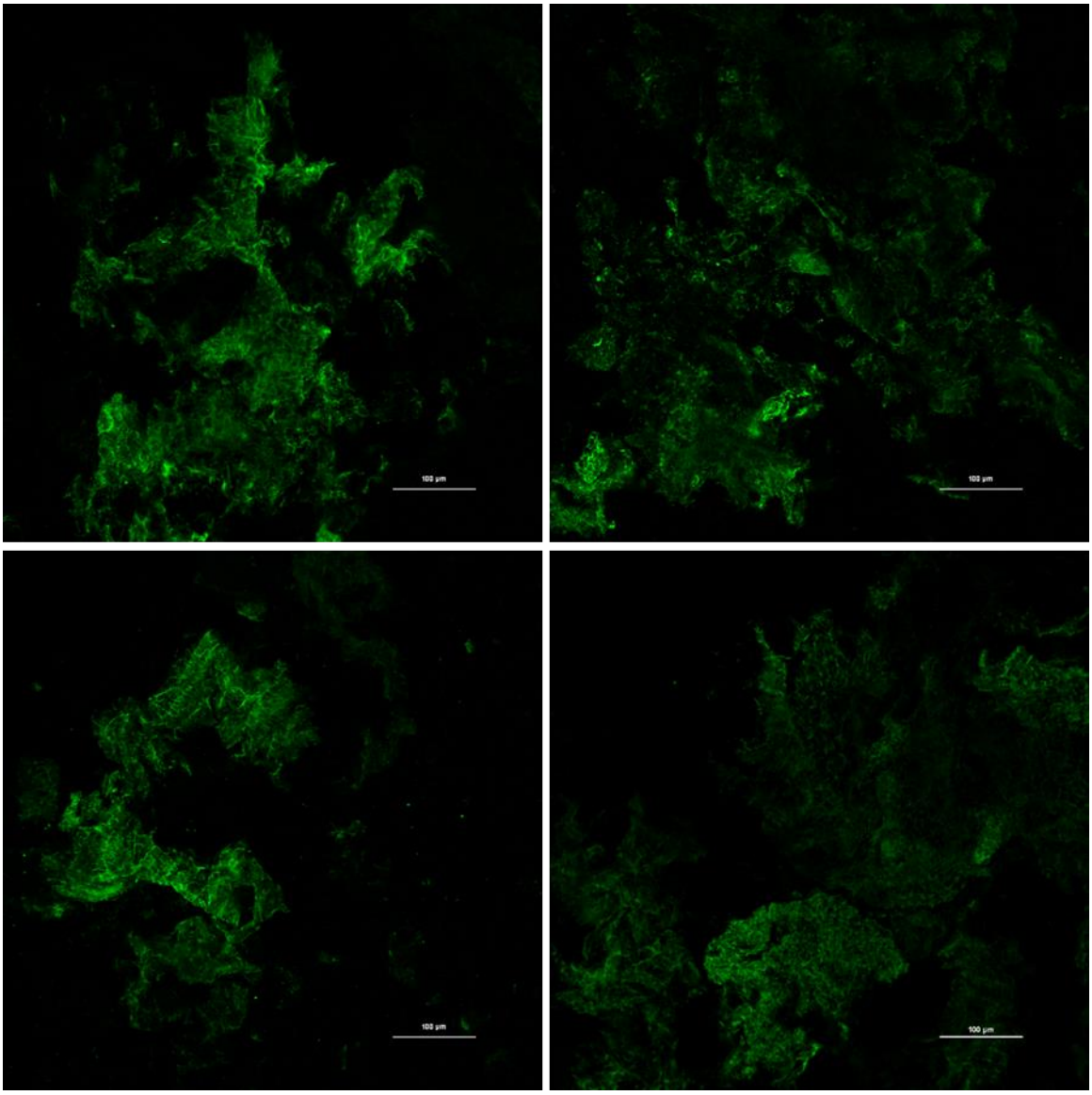

Figure 5.27 Blue corn porridge after 30 min α-amylase digestion, protein portion, combined Z-image (pseudo-colored green)

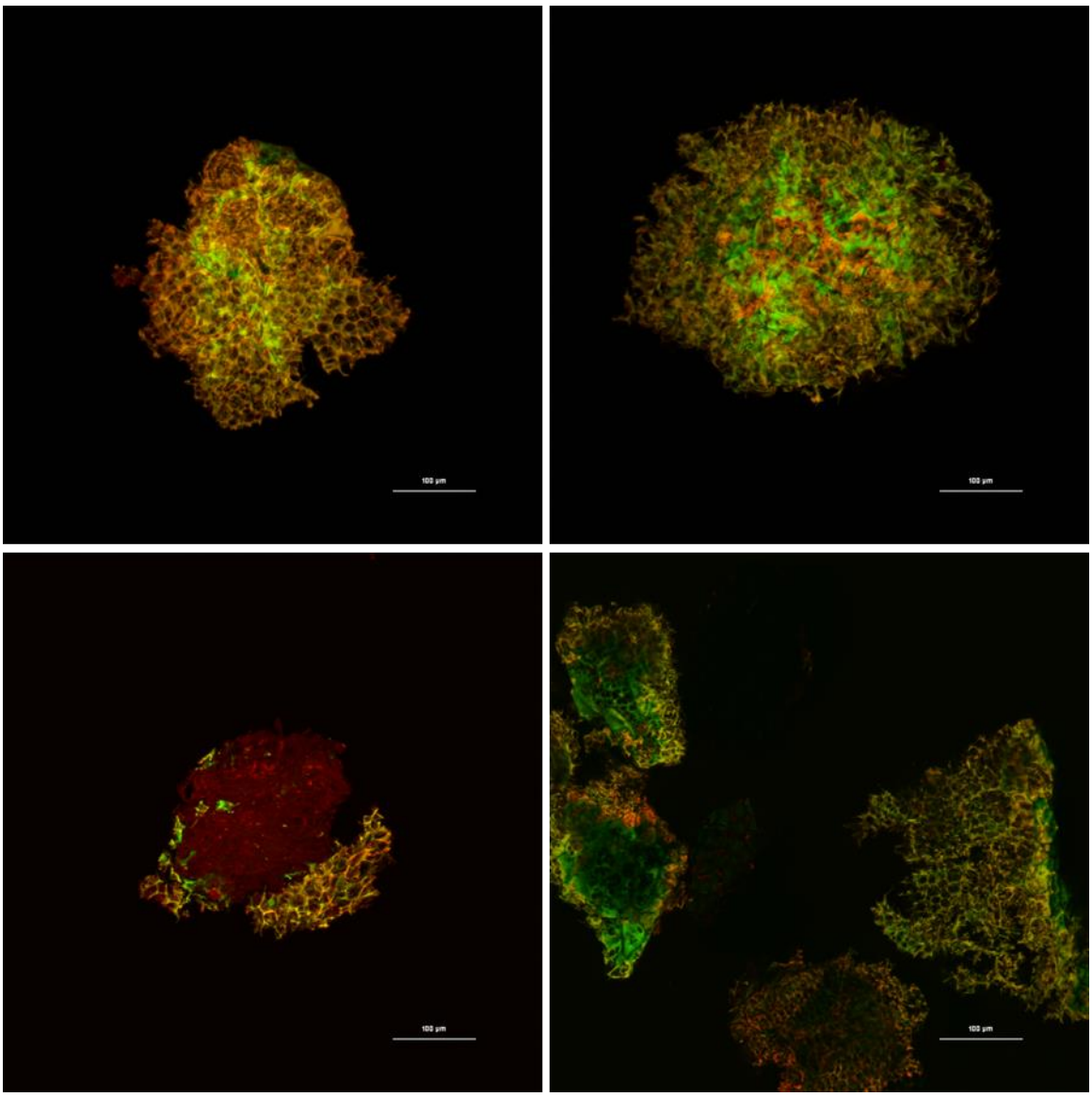

Figure 5.28 Decorticated white sorghum porridge after 30 min α-amylase digestion, combined Z-image double labeled with PAS for starch (red) and fluorescamine for protein (pseudo-colored green)

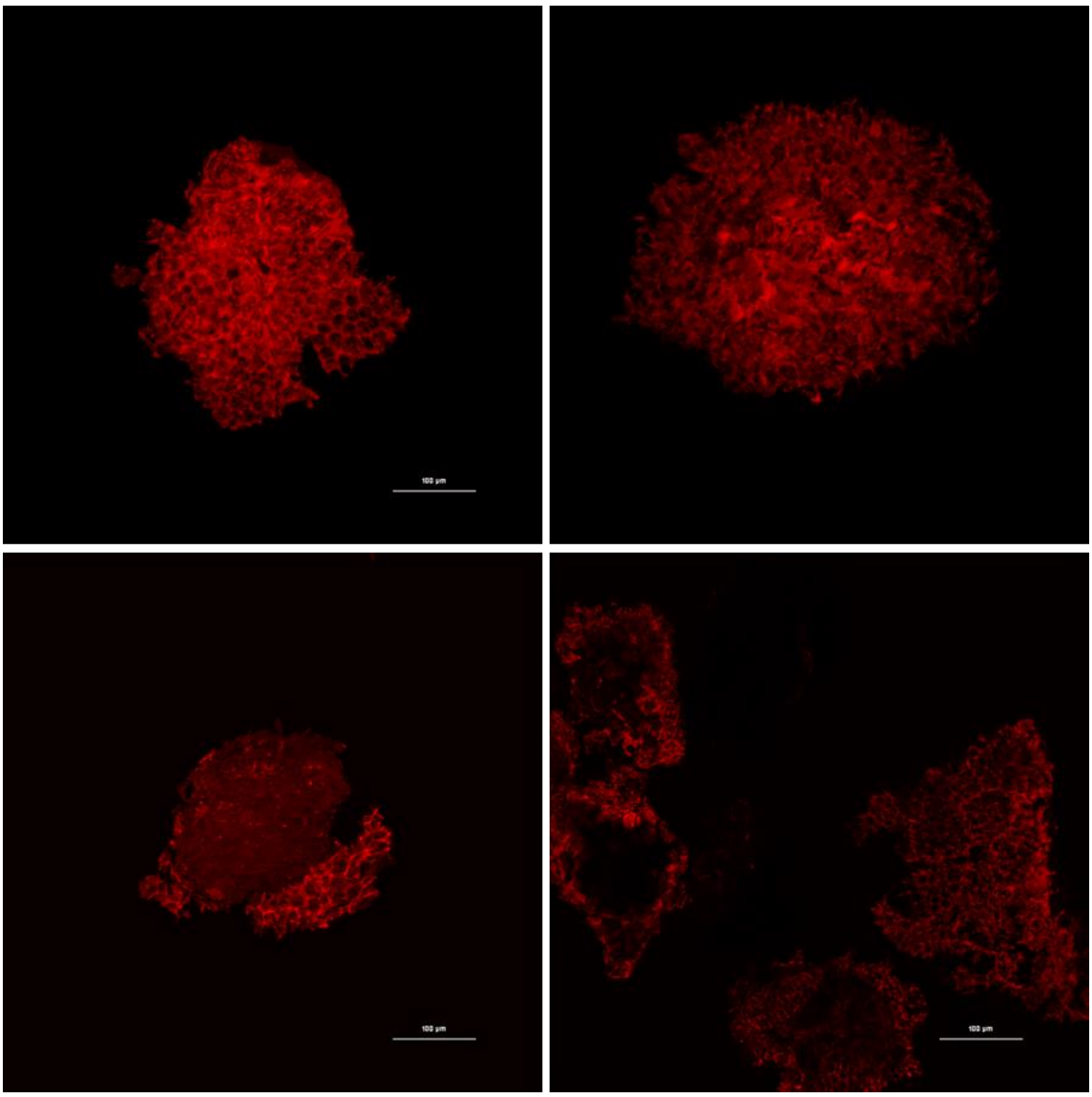

Figure 5.29 Decorticated white sorghum porridge after 30 min α-amylase digestion, starch portion, combined Z-image

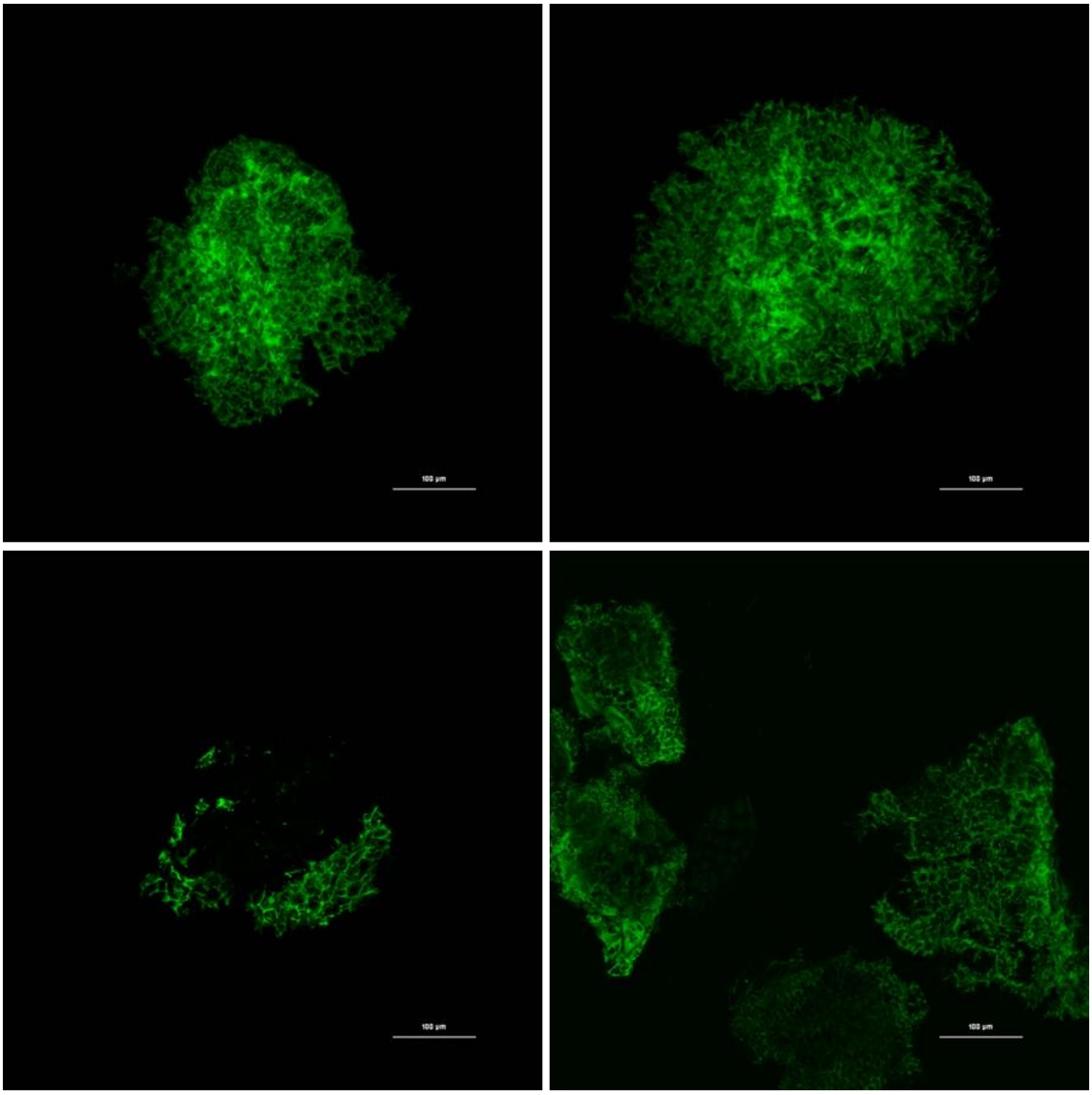

Figure 5.30 Decorticated white sorghum porridge after 30 min α-amylase digestion, protein portion, combined Z-image (pseudo-colored green)

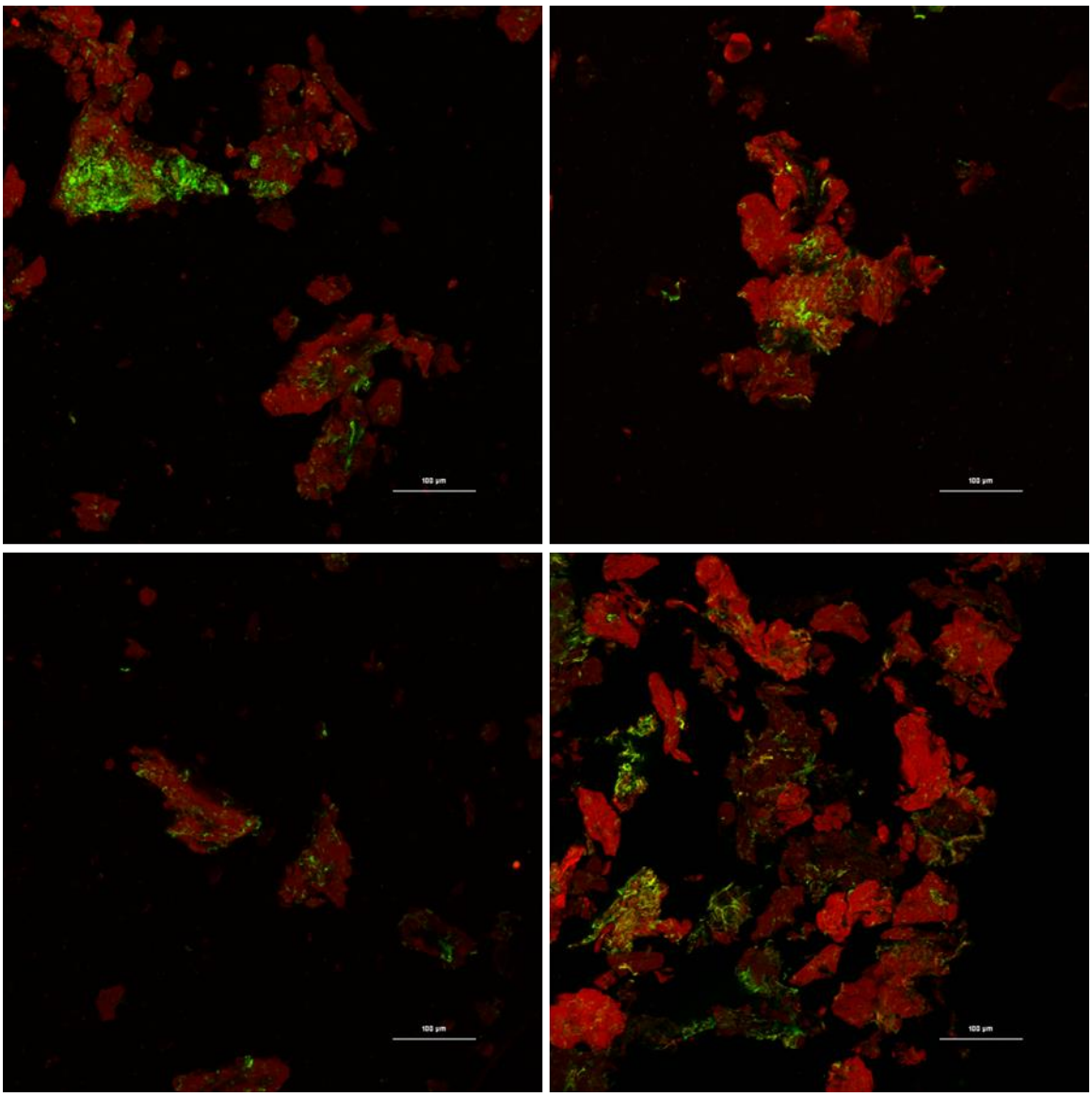

Figure 5.31 Yellow corn porridge “control” after 60 min α-amylase digestion, combined Z-image double labeled with PAS for starch (red) and fluorescamine for protein (pseudo-colored green)

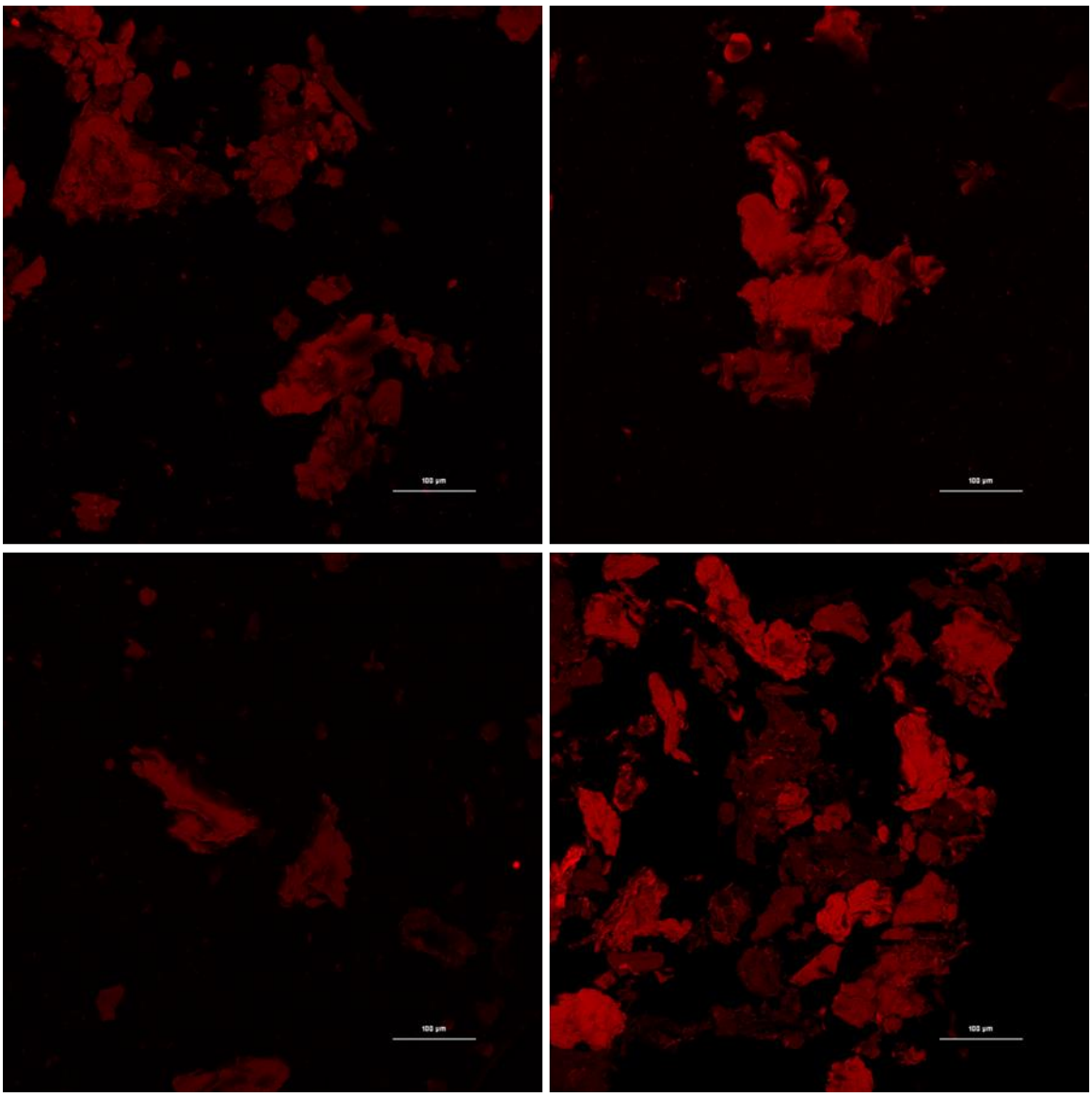

Figure 5.32 Yellow corn porridge “control” after 60 min α-amylase digestion, starch portion, combined Z-image

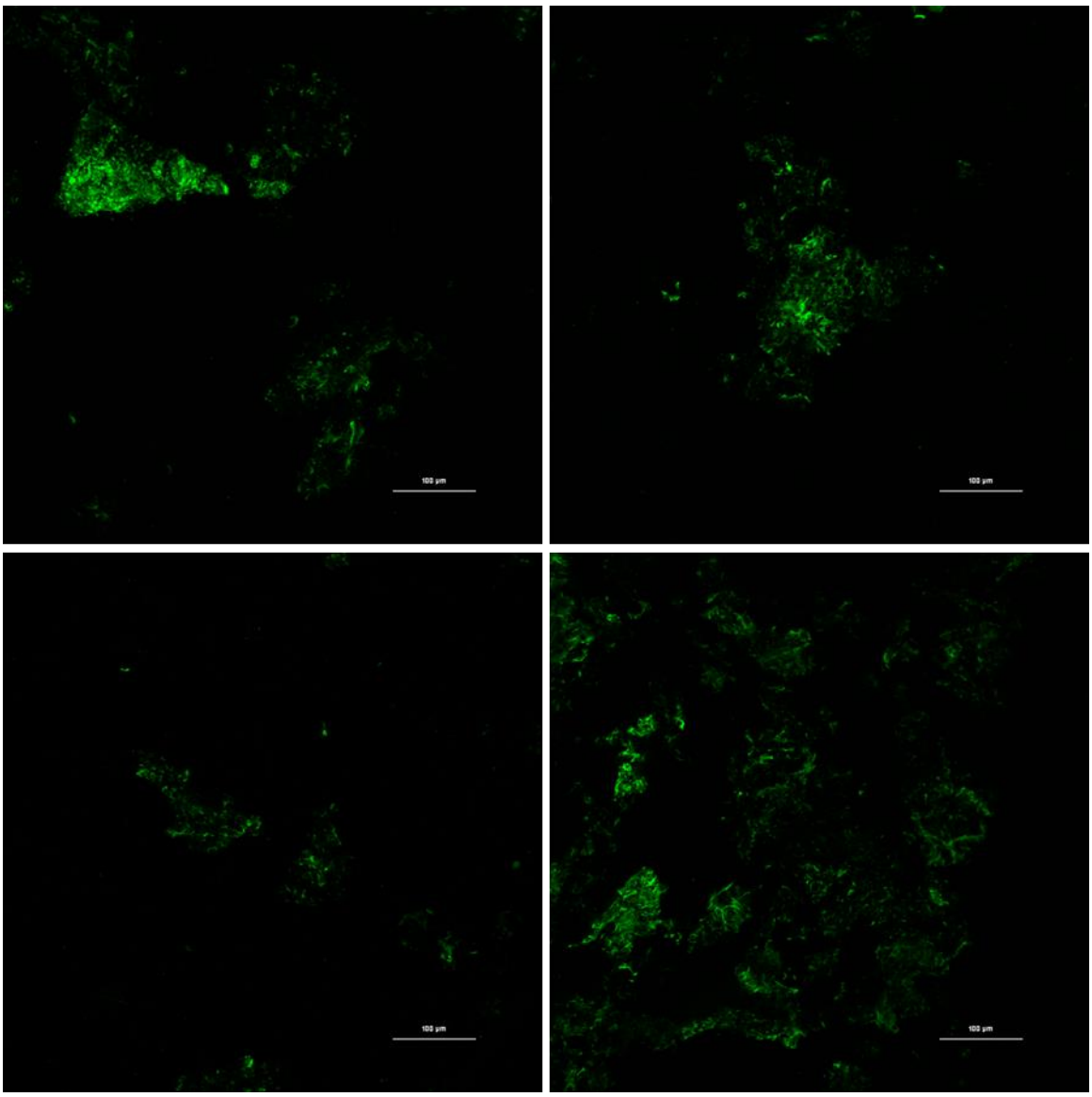

Figure 5.33 Yellow corn porridge “control” after 60 min α-amylase digestion, protein portion, combined Z-image (pseudo-colored green)

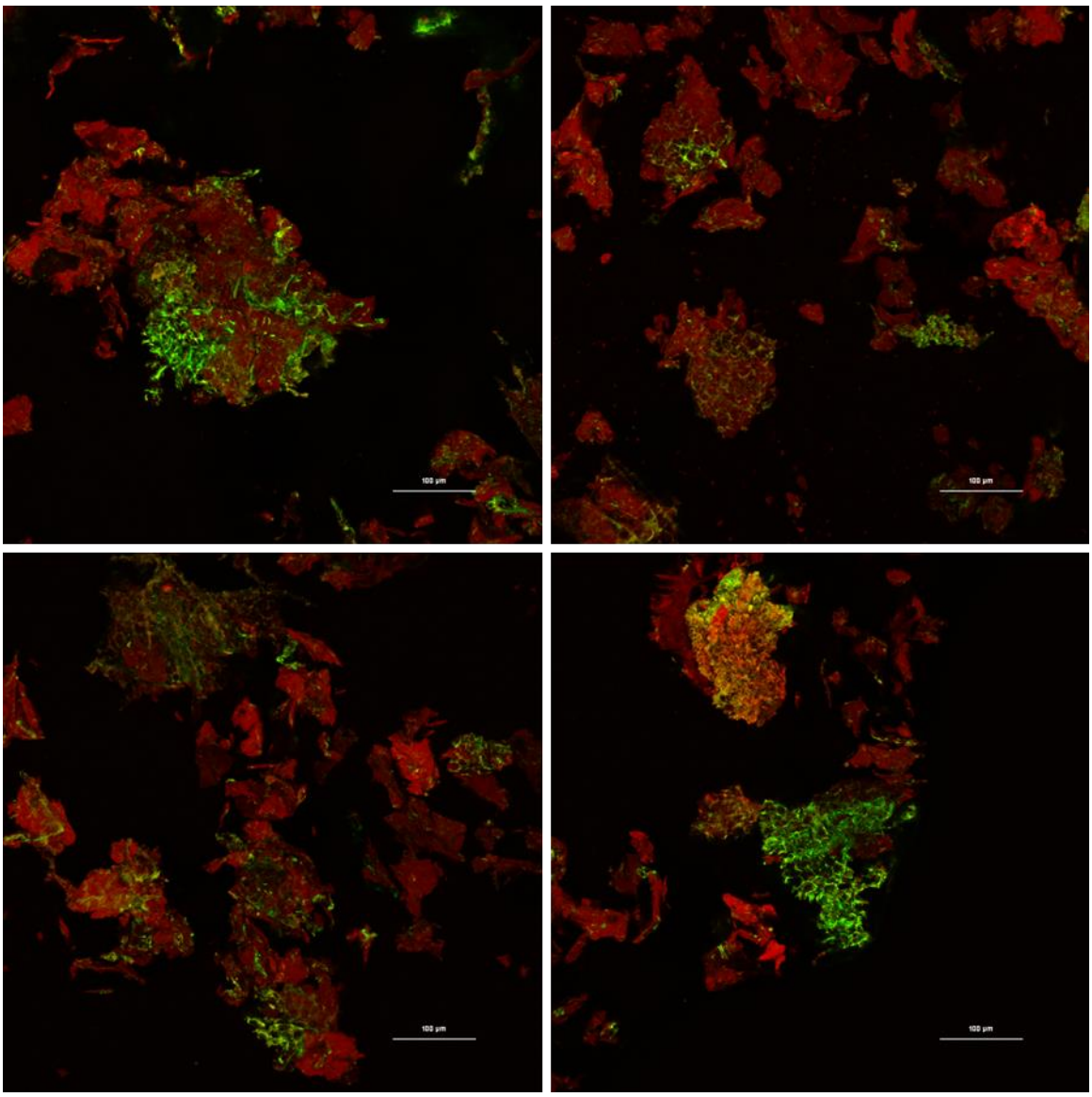

Figure 5.34 Yellow corn porridge “APG1” treated with apigeninidin after 60 min α-amylase digestion, combined Z-image double labeled with PAS for starch (red) and fluorescamine for protein (pseudo-colored green)

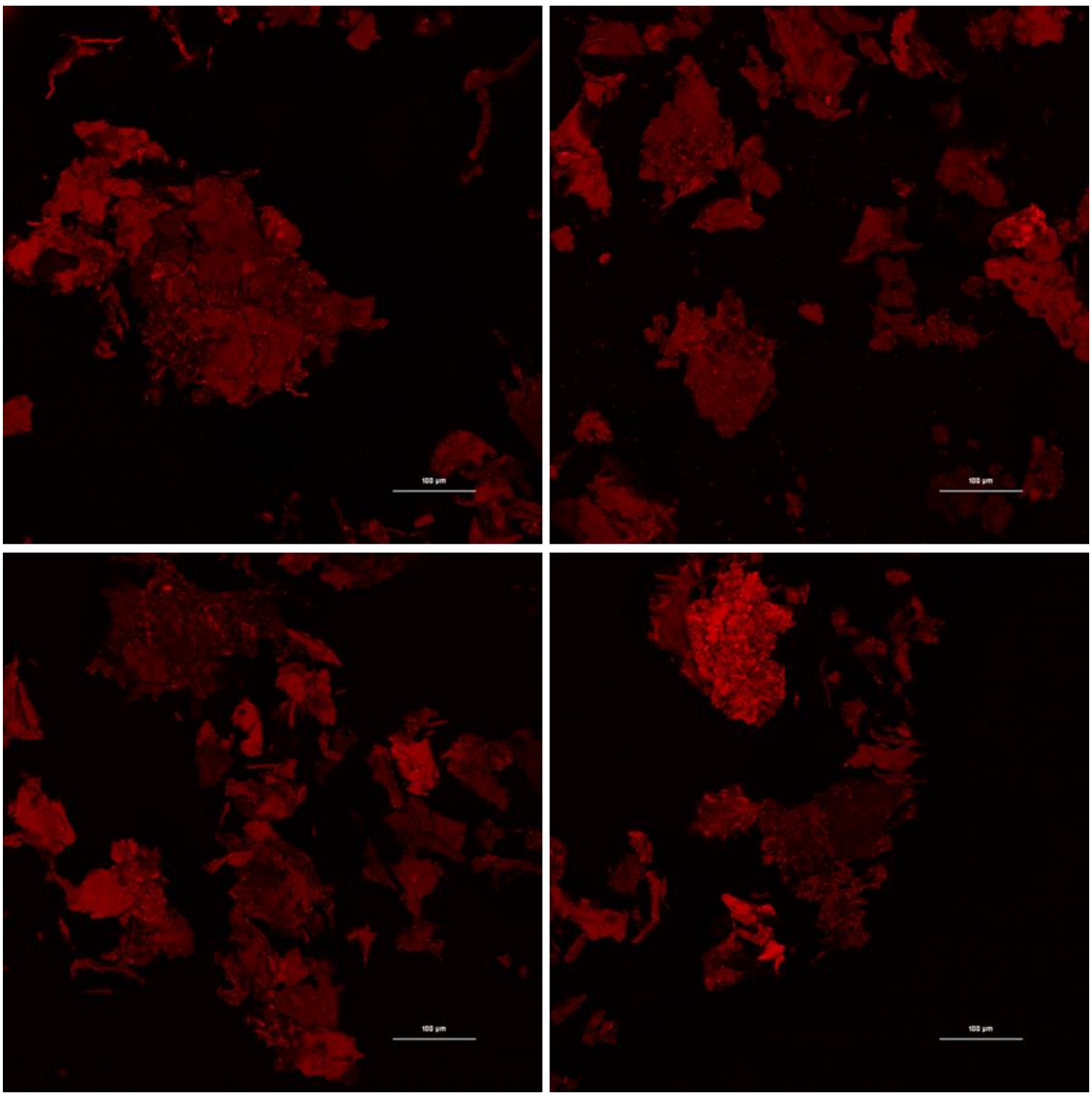

Figure 5.35 Yellow corn porridge “APG1” treated with apigeninidin after 60 min α-amylase digestion, starch portion, combined Z-image

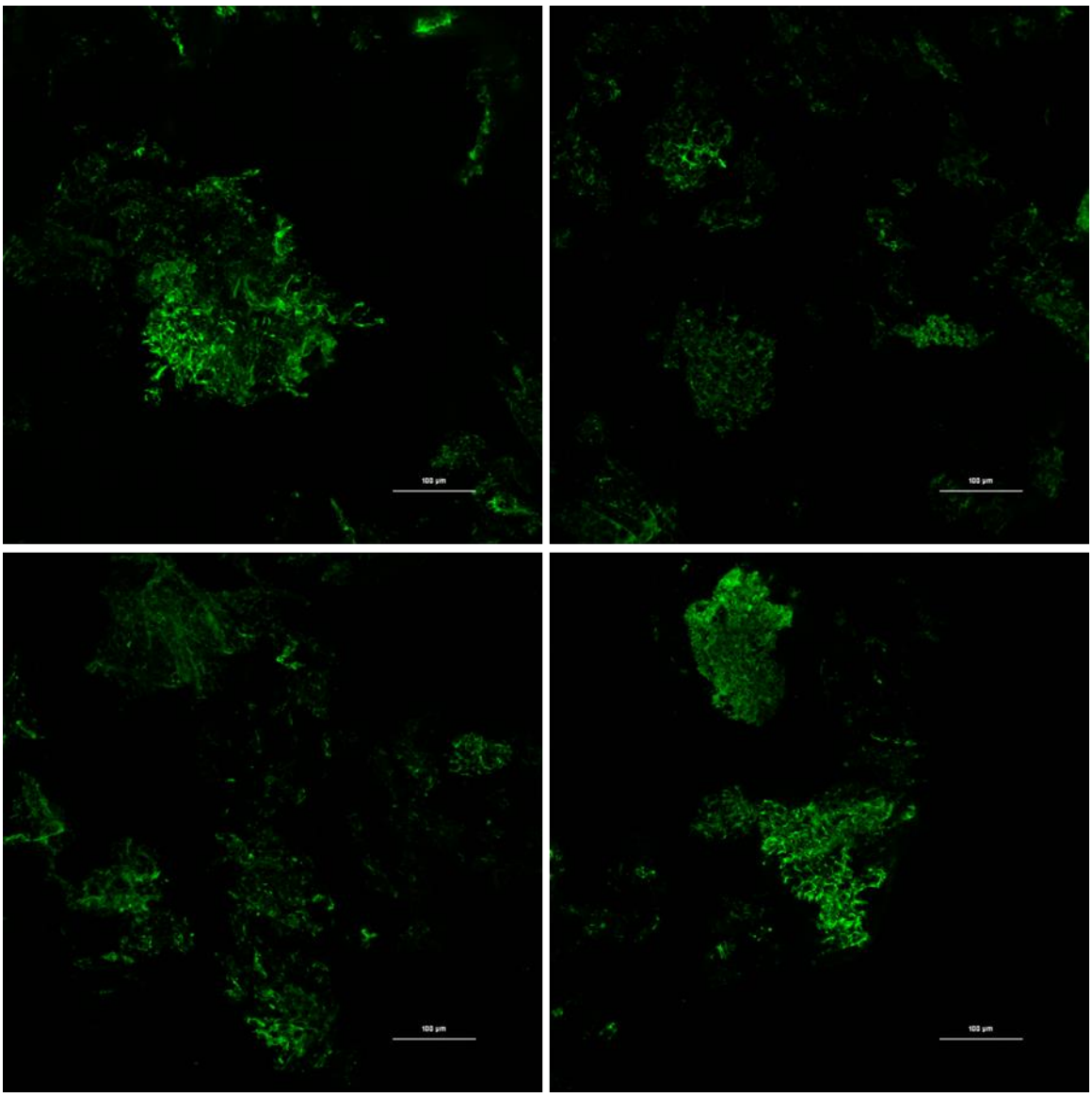

Figure 5.36 Yellow corn porridge “APG1” treated with apigeninidin after 60 min α-amylase digestion, protein portion, combined Z-image (pseudo-colored green)

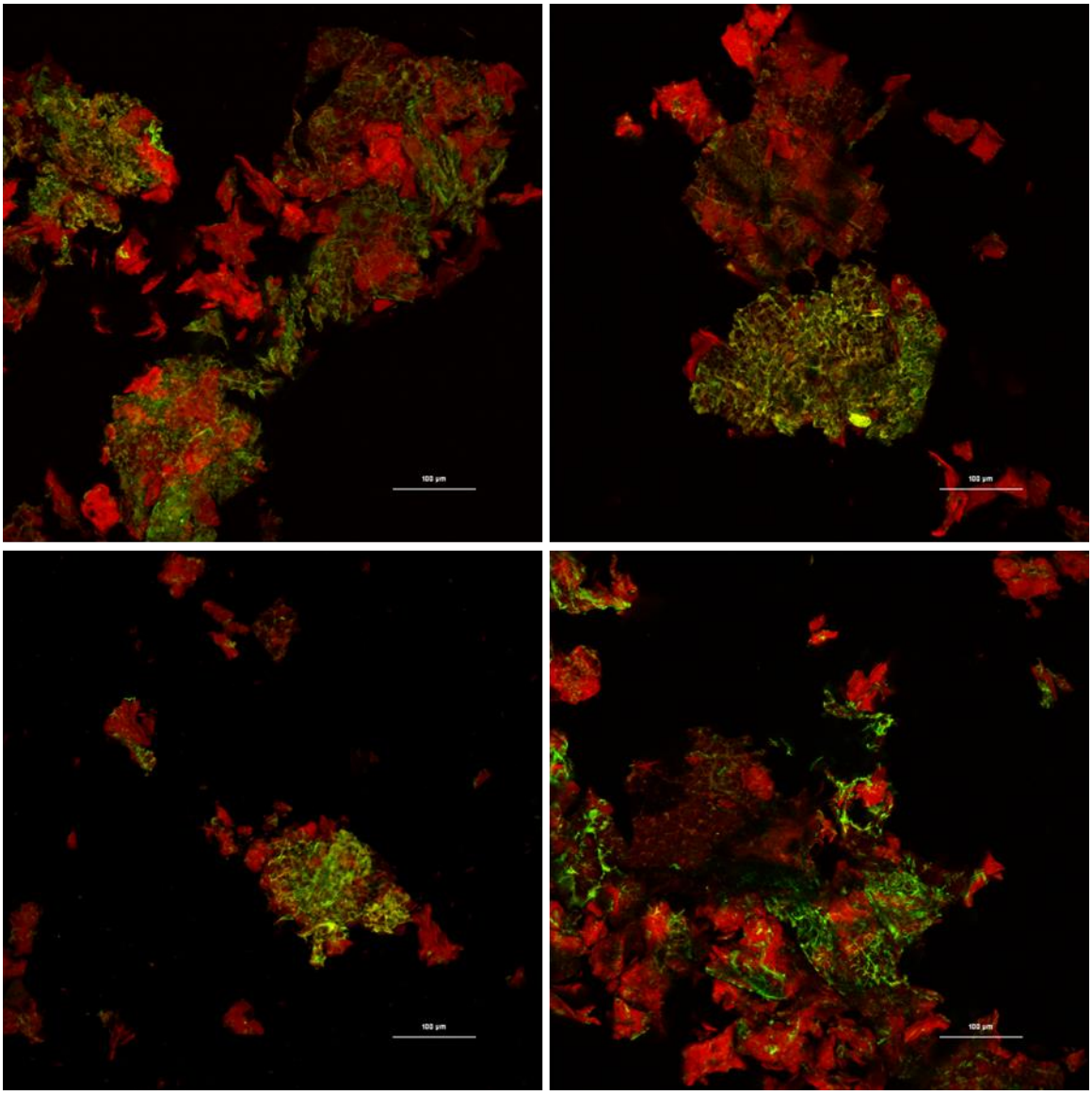

Figure 5.37 Yellow corn porridge “APG2” treated with apigeninidin after 60 min α-amylase digestion, combined Z-image double labeled with PAS for starch (red) and fluorescamine for protein (pseudo-colored green)

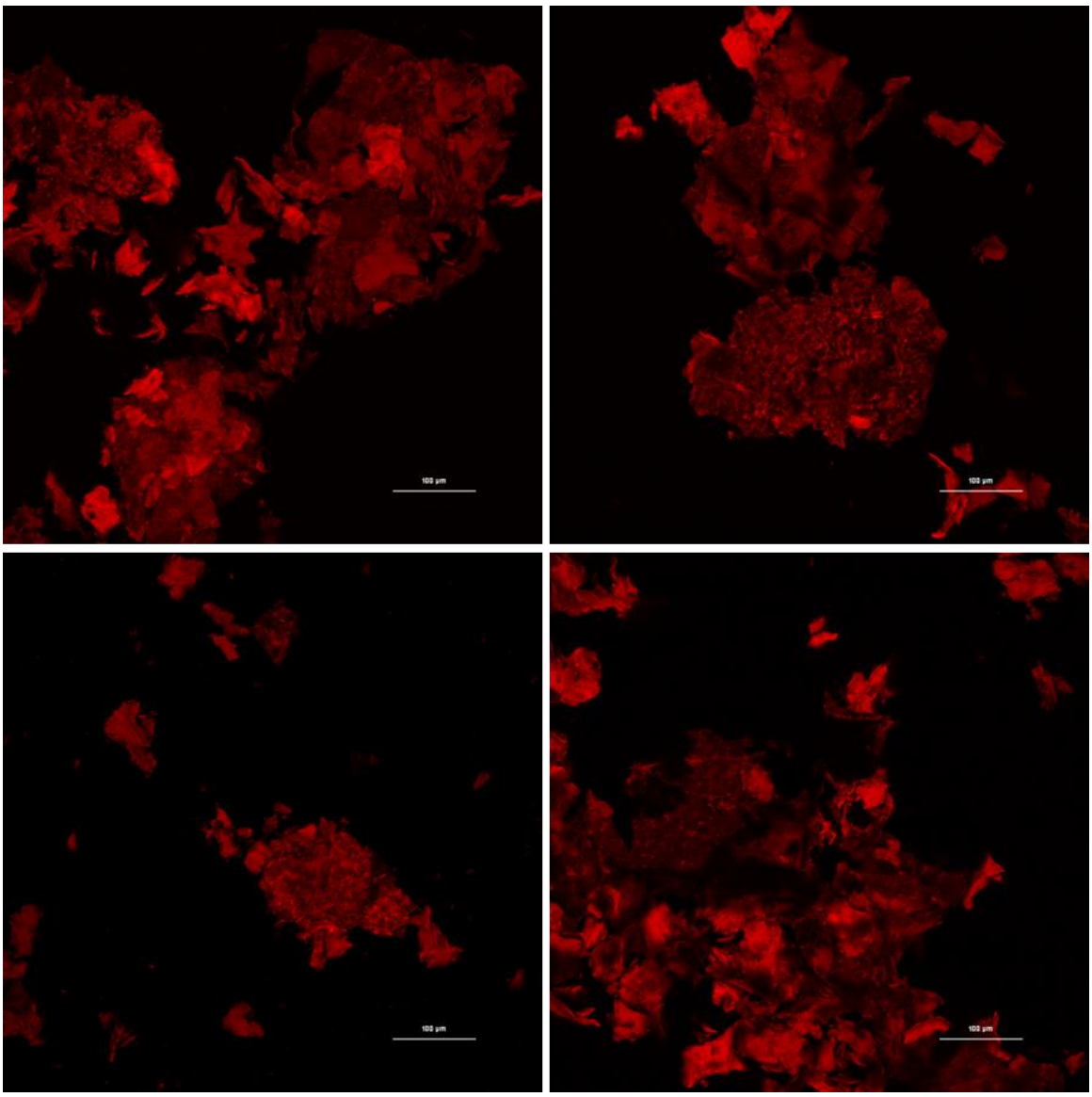

Figure 5.38 Yellow corn porridge “APG2” treated with apigeninidin after 60 min α-amylase digestion, starch portion, combined Z-image

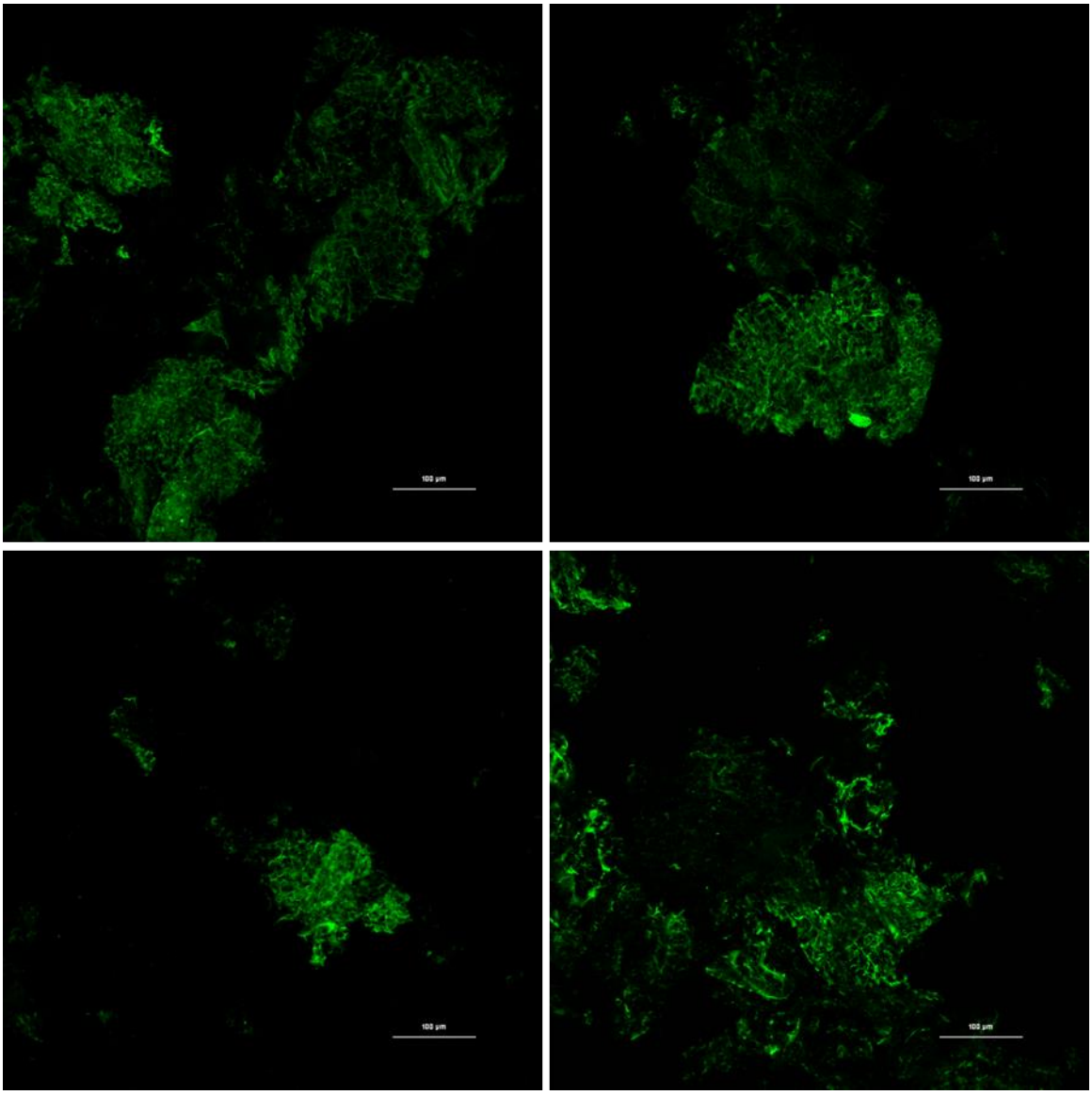

Figure 5.39 Yellow corn porridge “APG2” treated with apigeninidin after 60 min α-amylase digestion, protein portion, combined Z-image (pseudo-colored green)

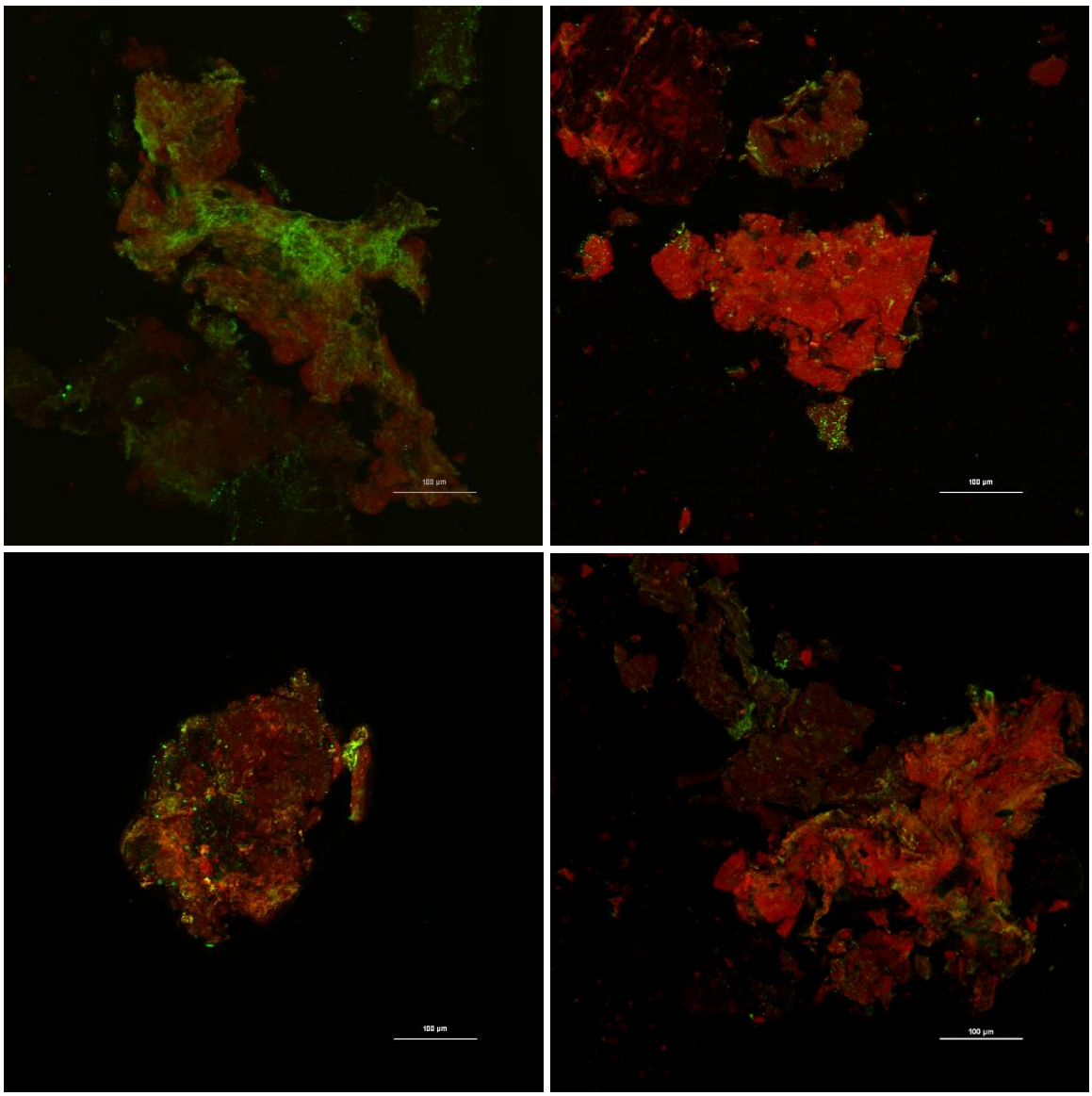

Figure 5.40 Blue corn porridge after 60 min α-amylase digestion, combined Z-image double labeled with PAS for starch (red) and fluorescamine for protein (pseudo-colored green)

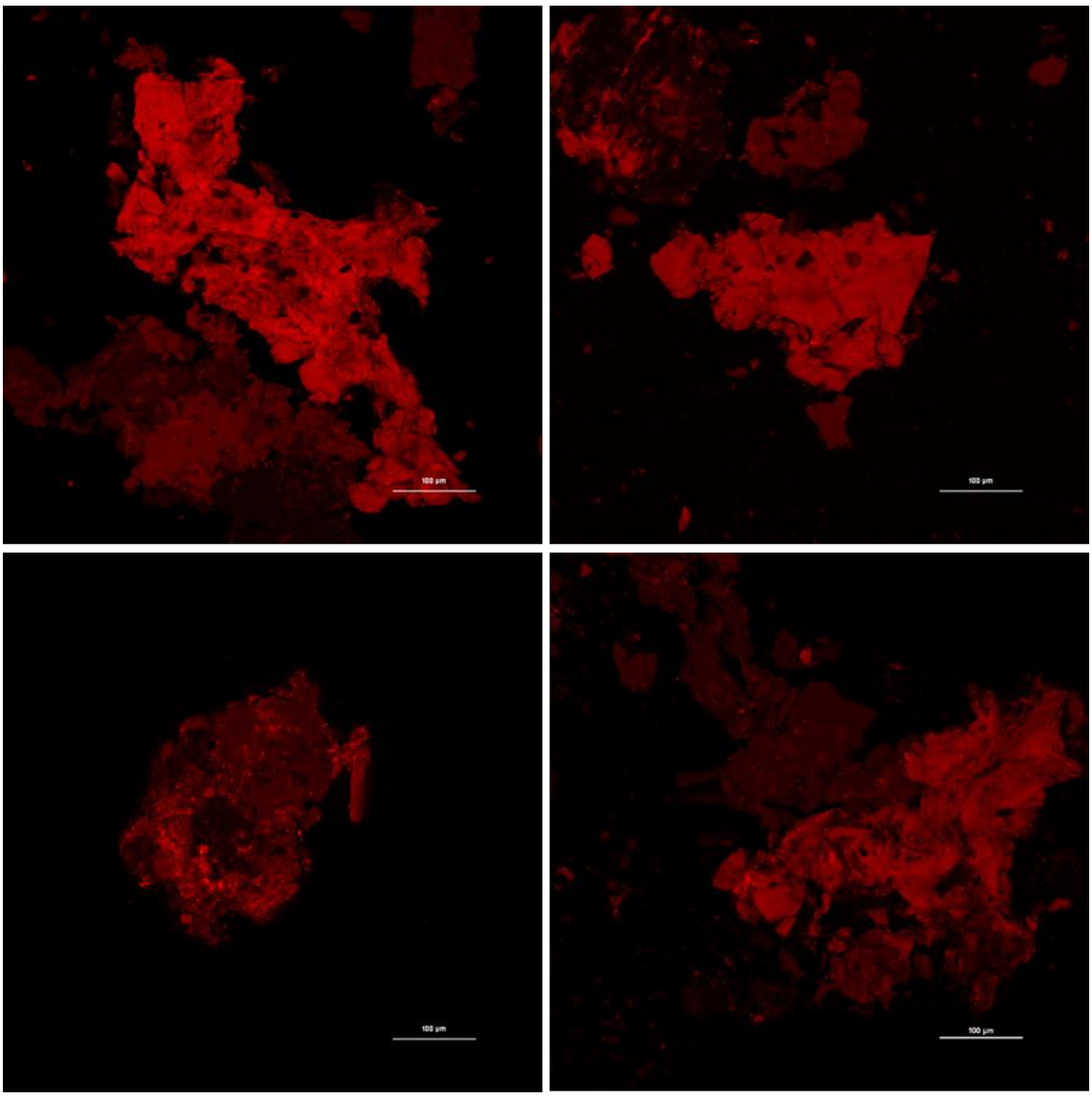

Figure 5.41 Blue corn porridge after 60 min α-amylase digestion, starch portion, combined Z-image

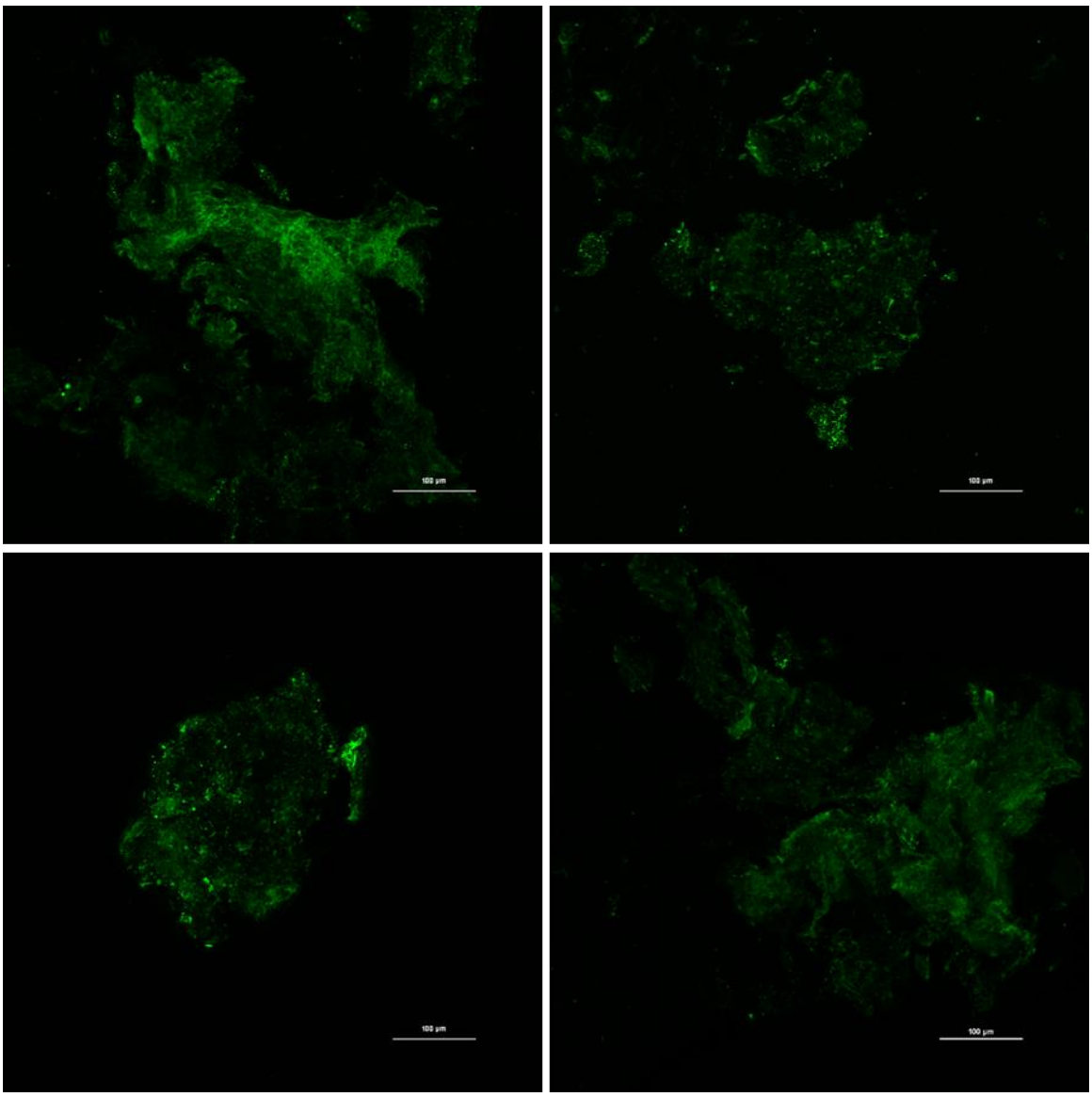

Figure 5.42 Blue corn porridge after 60 min α-amylase digestion, protein portion, combined Z-image (pseudo-colored green)

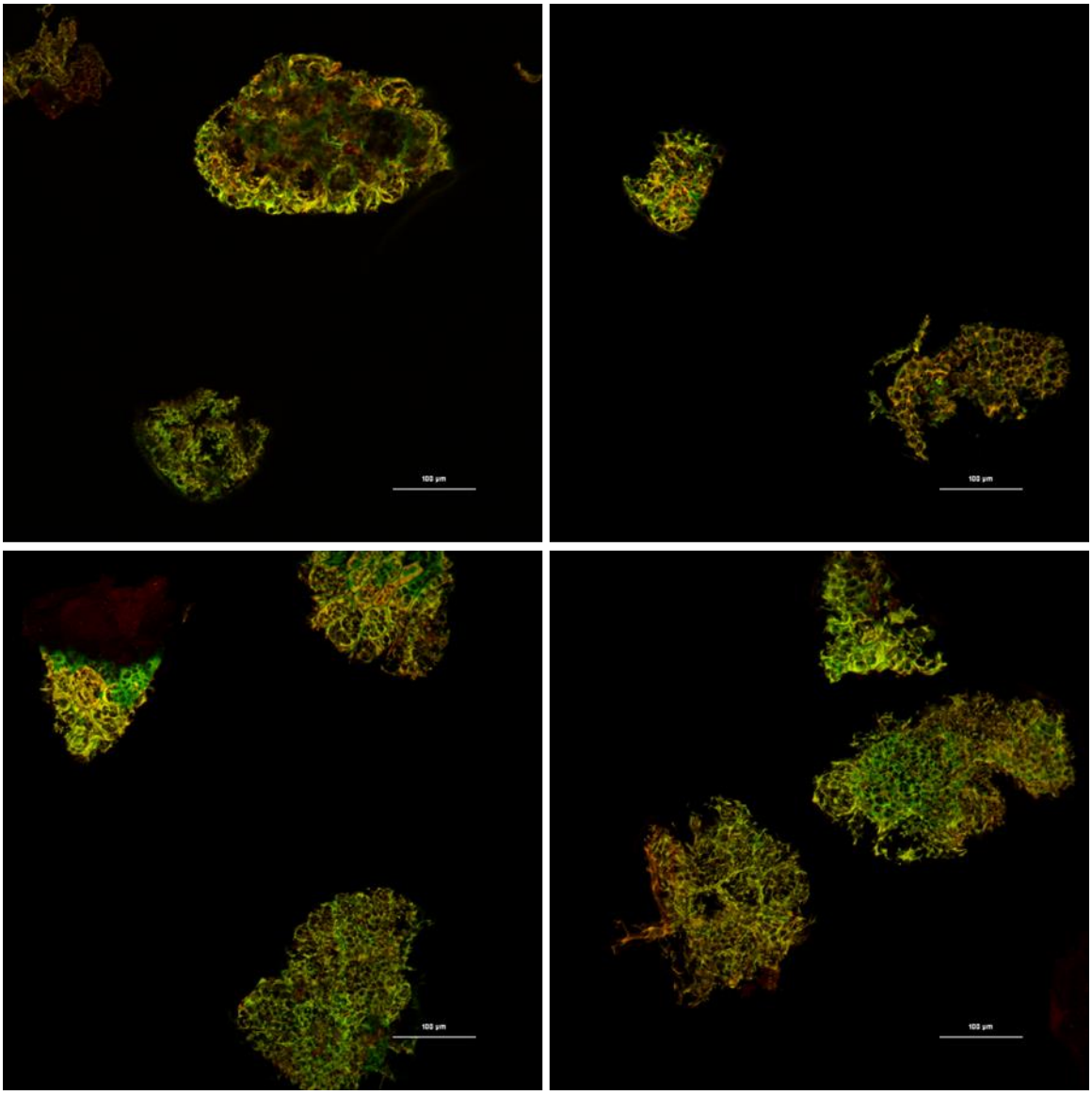

Figure 5.43 Decorticated white sorghum porridge after 60 min α-amylase digestion, combined Z-image double labeled with PAS for starch (red) and fluorescamine for protein (pseudo-colored green)

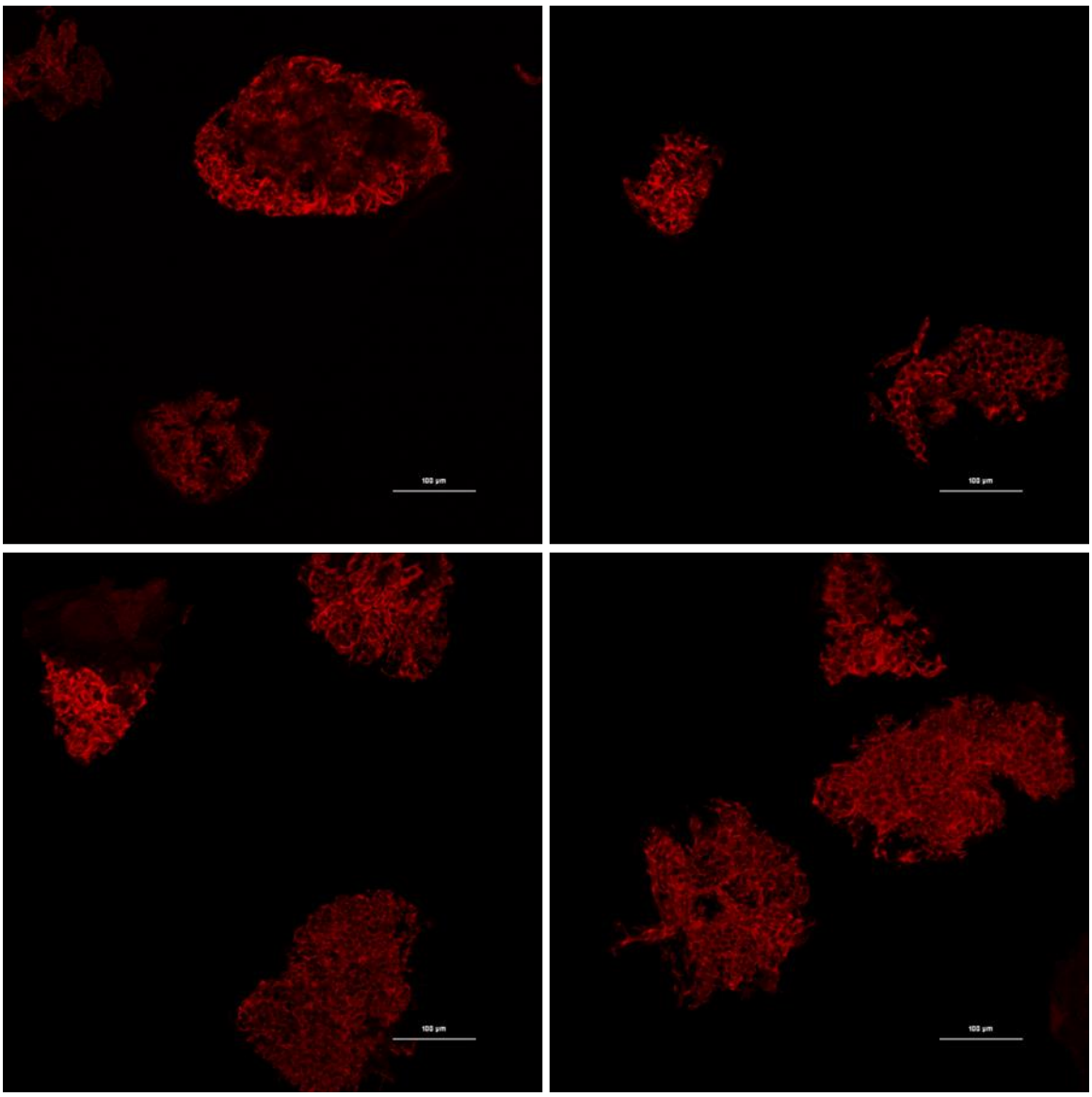

Figure 5.44 Decorticated white sorghum porridge after 60 min α-amylase digestion, starch portion, combined Z-image

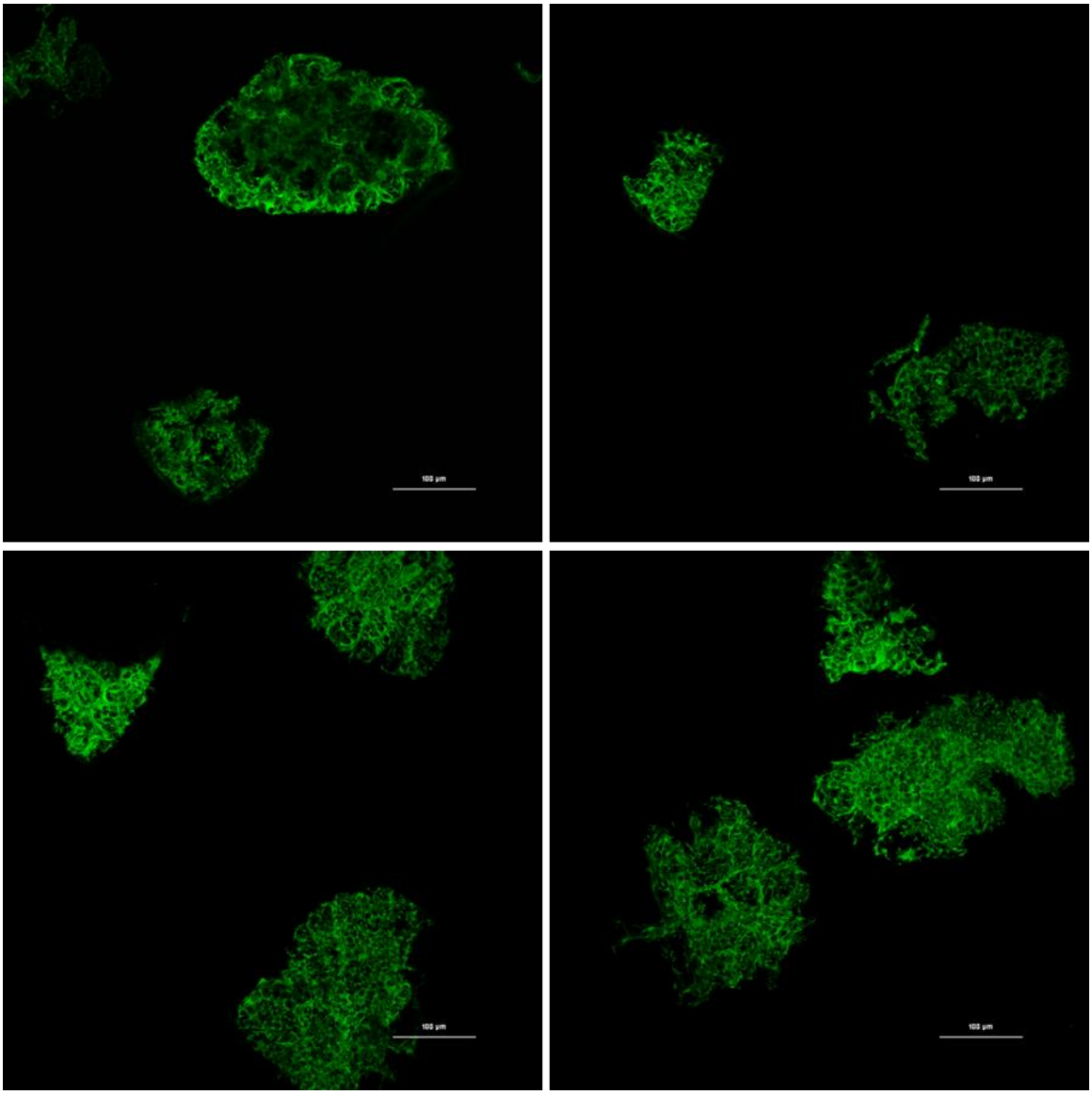

Figure 5.45 Decorticated white sorghum porridge after 60 min α-amylase digestion, protein portion, combined Z-image (pseudo-colored green)

CHAPTER 6. CONCLUSIONS AND FUTURE DIRECTION

6.1 Summary and Overall Conclusions

Through the work performed and presented in this thesis, a depiction has emerged highlighting apigeninidin as an alternative food oxidizing agent which promotes inter-protein sulfhydryl-disulfide interchanges, leading to diverse MW products. The work presented aimed to understand the factors affecting the formation of food matrices and how stability of a food matrix impacted starch digestion. A model system allowed for examination of protein polymerization due to protein-phenolic interactions while *in vitro* starch digestion and confocal microscopy facilitated discovering the relationship between anthocyanin compounds and starch digestion based on microstructural changes. A summary of the main conclusions and considerations for future work and direction pertaining to matrices designed for altering digestive properties is outlined below.

Chapter 3 examined the characteristics of grain-based phenolic extracts and their ability to polymerize a model protein (ovalbumin) system. Neither phenolic content nor antioxidant activity were sufficient to predict protein polymerization, and phenolic analysis determined several components were present in all the extracts. Corn masa and white rice extracts tended to form high MW protein products of similar size rather than more disparate products, as occurred with sorghum extracts, in the model system. Although the 3-deoxyanthocyanidins present in sorghum flour was likely responsible for the dynamic polymerization, other phenolic components may have a role in matrix formation.

Several phenolics were investigated utilizing the ovalbumin model protein system for the ability of specific compounds to polymerize ovalbumin, and the nature of polymer formation, in Chapter 4. The pH of the system (6.8) was above the pK_A of the phenolic acids (*p*-coumaric, sinapic, and gallic). Consequently, the acids would be present in deprotonated (negatively charged) forms, affecting their ability to interact with ovalbumin due to ionic repulsions from the overall negative charge on the protein molecules in an environment above its pI. For gallic acid, this was overcome. Radical formation was speculated to occur, leading to extensive oxidation-driven polymerization by both disulfide formation and non-amide peptide formation (suspected as tyrosine-tyrosine and similar cross-links). Catechin interacts with ovalbumin, as shown through fluorescence quenching spectroscopy, but the interactions did not lead to an increase in soluble

polymers with concentration for SDS-PAGE separation. Apigeninidin had the greatest effect on opening protein structure (based on peak shift), which should increase cysteine access for sulfhydryl-disulfide interchanges. Additionally, a wide range of high MW polymers was generated, indicating apigeninidin had the highest potential to increase protein matrix formation of the phenolics studied.

In Chapter 5, the effects of apigeninidin addition and naturally-occurring anthocyanin were explored with regard to starch digestion and protein matrix formation and stability. Apigeninidin appeared to increase the tendency for protein matrix formation, decrease aggregation, and enhance stability, leading to a reduction of initial starch digestion rate. Although the starch digestion of whole blue corn was unexpectedly high initially, the development of protein matrix filaments through the cooked porridge confirmed (non 3-deoxy)anthocyanin-containing cereals were capable of forming matrices which survived processing, though collapsed upon digestion. However, protein collapse onto starch remnants without forming large aggregative particles may have reduced α-amylase access after removal of rapidly digestible starch and may frame a portion of the reason anthocyanin-containing grains tend to digest starch more slowly than similar non-anthocyanin products.

6.2 Future Direction

While a 3-deoxyanthocyanidin compound can improve protein matrix formation and attenuate *in vitro* starch digestion in a corn porridge, it is yet unknown whether this yields a physiologically different outcome with regard to postprandial glucose response. Currently there is no source of food-grade purified 3-deoxyanthocyanidins, though preparations of natural colors exist which could potentially be utilized for future human studies to examine changes to satiety and glucose response. Alternatively (or in addition), providing a prepared feed to ileostomized pigs may provide improved data on particle degradation.

Although not common to foods apart from sorghums, the 3-deoxyanthocyanidins have been found throughout the sorghum plant, and harvest waste may prove a viable source of naturally-occurring 3-deoxyanthocyanidins. Bioengineering cereals to express the gene responsible for removal of the C-3 hydroxyl group may also prove useful in designing grain-based starchy foods to modify food matrices for reducing glucose response.

Further research is also needed to determine the efficacy of 3-deoxyanthocyanidin addition to other starchy cereal food products and other food processing techniques for matrix formation and starch digestion, in order to determine if the applications may be limited to corn-based foods. Challenges also exist for studying matrix effects in foods, as microscopic techniques are currently required. In this work, a periodic acid-Schiff reaction was utilized to produce a fluorescent marker for starch, however it is a method which stains all carbohydrates, including cellulose and hydrocolloids. Addition of non-glycemic carbohydrates to alter microstructure and digestion would require a different staining technique. Calcofluor-white and other dyes could be utilized for β-linked polysaccharides, but while studies have compared staining agents, literature searches for co-staining techniques to distinguish carbohydrates were unclear.

Overall, efforts should continue to examine the properties affecting food matrix construction and stability, as well as the effects of matrix manipulation on digestive properties of the food, to decrease rates and consequences of metabolic diseases.

VITA

Leigh C. R. Schmidt

EDUCATION

Ph.D. Food Science, Summer 2019, Purdue University, West Lafayette, IN 47907
Emphasis: Foods for Health

M.S. Food Science 2009, University of California Davis, Davis, CA 95616
Emphasis: Food Chemistry & Biochemistry
Research Focus: Nutritional & quality changes in romaine lettuce stored in air or controlled atmosphere

B.S. Food Science 2003, Purdue University, West Lafayette, IN 47907

INDUSTRY EXPERIENCE

Product Developer, Cache Creek Foods, Woodland, CA, May 2010 – July 2013
Matt Morehart, President

R&D Technician, Cunningham Business Consulting, Folsom, CA, May–September 2010
Dr. Sam Cunningham, Owner.

Lab Technician, Simi Winery, Healdsburg, CA, September 2004 – September 2005

Lab Technician, Berkeley Farms, Hayward, CA, March – September 2004

Traffic Office Administrative Assistant, Frito Lay, Inc., Frankfort, IN, May – July 2001

INTERNSHIP EXPERIENCE

Product Development Intern, Frito Lay North America, Plano, TX, May – August 2008
Dr. Mary Carunchia, Technical Mentor
Determination of physico-chemical changes occurring during tortilla chip processing

TEACHING EXPERIENCE

Teaching Assistant, Department of Food Science, Purdue University, Jan – May 2017
FS 44300 Food Product Design, Spring semester 2017
Drs. Brian Farkas and Dharmendra Mishra, professors

Teaching Assistant, Department of Food Science & Technology, UC Davis
FS 160, Product Development, Winter Quarters 2007-2009
Drs. Robert Martin, Jr.; Michael McCarthy; & Maria Giovanni, professors
FS 101A, Food Chemistry Lab, Fall Quarter 2006; Dr. David Reid, professor
FS 101B, Food Properties Lab, Winter Quarter 2006; Dr. Elisabeth Garcia, professor

MEMBERSHIPS & INVOLVEMENT

Institute of Food Technologists, IFTSA, Northern California Section, Hoosier Section
- Carbohydrate Division Leadership, 2016-present
  - Mentorship Project Lead 2018-19, Student Outreach Lead 2017-18, Student Representative 2016-17
- Division Champion Team, student representative, 2017-18
- IFTSA Leadership Development Workgroup 2015-16
- Purdue College Bowl team 2013-16
- IFT15-17 AMSP track team reviewer (Foods & Health)
- Product Development Division poster abstract reviewer 2012-14
- IFT Award Jury member 2011-14
- UC Davis College Bowl team 2007-09, Product Development team 2009
- IFTSA Pacific West Area Representative 2007-08

Cereals & Grains Association / AACC International, AACCI Student Association
- Board of Directors Student Representative to the Board 2016, 2017
- AACCISA Online Communicator 2015

Phi Tau Sigma Honor Society, Life Member
- Hoosier Chapter, Purdue University President 2016-17
  - President-Elect / Treasurer 2015-16

Purdue University FSGSA (2013-19) and Food Science Club (1999-2003)

UC Davis FSGSA President 2008-09, Vice President 2007-08, Social Chair 2006-07

VOLUNTEER ACTIVITIES

National FFA Organization
- Product Development Competition national-level judge 2016, 2017
- Food Science Demonstrations judge for Indiana District V 2017

AWARDS & RECOGNITIONS

3rd Place, AACC International Best Student Research Paper Competition, 2018

1st Place, IFT Protein Division Poster Competition, 2018

IFT Carbohydrate Division Outstanding Volunteer, 2018

Phi Tau Sigma Student Achievement Scholarship, 2017

1st Place, AACC International Protein Division Poster Competition, 2017

2nd Place, IFT Protein Division Poster Competition, 2016

USDA National Needs Fellowship for Foods & Health, 2013-2016

UC Davis Frank & Grace Benedix Fellowship, 2008

UC Davis Jastro-Shields Award, 2007

Purdue Alumni Association Ice Cream Dessert Contest Winner, 2006

PUBLICATION

Carreiro AL, Dhillon J, Gordon S, Higgins KA, Jacobs AG, McArthur BM, Redan BW, Rivera RL, Schmidt LR, Mattes RD. The Macronutrients, Appetite, and Energy Intake. Annu Rev Nutr 2016; 36:73-103. doi: 10.1146/annurev-nutr-121415-112624.